

MULTICOMPONENT CONTINUOUS FLOW
KINETIC ANALYSIS

by

David J. Hooley

Dissertation submitted to the Graduate Faculty of the
Virginia Polytechnic Institute and State University
in partial fulfillment of the requirements for the degree of

DOCTOR OF PHILOSOPHY

in

Chemistry

APPROVED:

R. E. Derry, Chairman

J. D. Graybeal

J. G. Mason

H. M. McNair

G. Sanzone

May, 1981

Blacksburg, Virginia

ACKNOWLEDGMENTS

I would like to thank my parents for their encouragement and dedication to education. Their support has been valuable in a number of ways.

and have been largely successful in their attempt to provide an environment conducive to learning and research. I would like to thank them, along with all the past and present members of the research group, for their contributions to this effort. of USDA has provided many questions of a practical and thought provoking nature, as well as valuable suggestions.

supplied several of the indicators needed for the test reactions as well as suggestions and information about the kinetics of several reactions.

TABLE OF CONTENTS

	Page
ACKNOWLEDGEMENTS.....	ii
TABLE OF CONTENTS.....	iii
TABLE OF FIGURES.....	v
TABLE OF TABLES.....	viii
I. INTRODUCTION.....	1
II. HISTORICAL DEVELOPMENTS.....	3
III. ENHANCEMENTS AND POTENTIAL APPLICATIONS.....	7
IV. INSTRUMENTATION.....	10
A. Transport System.....	15
1. Flow Controller.....	20
2. Flowmeter.....	24
3. Electronic Balance.....	68
4. Flowmeter and Controller Performance..	79
B. Mixer.....	89
C. Reaction-Observation Tube and Detectors...	102
1. Colorimeter.....	107
2. Colorimeter Electronics.....	111
3. Colorimeter Performance.....	125
D. Data Acquisition and Processing System...	134
1. Forth Programming System.....	135
2. Operator Interaction.....	142
IV. INSTRUMENT EVALUATION.....	150

A.	Dilution Stability.....	150
B.	Flow Injection Analysis.....	160
C.	Flow Injection with a Reaction.....	173
D.	Single Component Continuous Flow Kinetics.	193
E.	Flow Injection Kinetics.....	205
F.	Multicomponent Continuous Flow Kinetics.,,	211
V.	DISCUSSION.....	229
VI.	SUMMARY.....	242
	BIBLIOGRAPHY.....	246
	APPENDIX A: Software Source Listings.....	249
	APPENDIX B: Documentation Dictionaries.....	272
	APPENDIX C: Hardware Block Diagrams.....	302
	APPENDIX D: Calculation of the KMnO ₄ - KI Rate Constant at 25 C.....	306
	VITA.....	309
	ABSTRACT	

TABLE OF FIGURES

Figure	Page
1. Instrument Block Diagram.....	14
2. Valve Controller Electronics.....	22
3. Capillary Valve Controller.....	23
4. Electromagnetic Flow Meter.....	28
5. Voltage Induced in a Wire.....	33
6. Flow Sensor Cell.....	35
7. Unbalanced Magnetic Field Signals.....	37
8. Flowmeter Control Signals.....	38
9. Flowmeter Signals with a 50 cm Head of .05 M NaCl	40
10. Input Instrumentation Amplifier.....	42
11. Flowmeter Signals with no flow of .01 M NaCl....	46
12. 60 Hz Notch Filter.....	47
13. Flowmeter Signals with no flow of .01 M NaCl....	49
14. Flowmeter Signals with a 50 cm Head of .01 M NaCl	50
15. Flowmeter Signals with no flow of .1 M NaCl....	51
16. Flowmeter Signals with a 50 cm Head of .1 M NaCl.	52
17. Flowmeter Signals with no flow of 1.0 M NaCl....	53
18. Flowmeter Signals with a 50 cm Head of 1.0 M....	54
19. Flowmeter Response vs. Time with .01 M NaCl....	55
20. Flowmeter Response vs. Time with .1 M NaCl....	56
21. Flowmeter Response vs. Time with 1.0 M NaCl....	57
22. Baseline Signal vs. M NaCl.....	58

Figure	Page
23. Standard Deviation of Baseline Signal vs. M NaCl.	59
24. Flow Minus Baseline Signal vs. M NaCl.....	60
25. Low Pass Filters and Amplifier.....	62
26. Voltage to Frequency Converter and Logic.....	64
27. Balance Buffer.....	70
28. Flowmeter Calibration Curve, 0.1 M NaCl.....	84
29. Flowmeter #1 Response, 0.1 M NaCl.....	85
30. Flowmeter #2 Response, 0.1 M NaCl.....	86
31. Balance Flowmeter Response, 0.1 M NaCl.....	87
32. Mixers.....	91
33. Time - Flow Calibration Curve.....	106
34. Colorimeter Head.....	109
35. Colorimeter Front End Signal Processor.....	112
36. Colorimeter Signal Processing Electronics.....	117
37. Colorimeter Error Amplifier and Modulator.....	119
38. Colorimeter Auxilliary Circuits.....	121
39. Colorimeter Block Diagram.....	122
40. Colorimeter Light Beam Interruption.....	124
41. Colorimeter Calibration Curve, KMnO4.....	132
42. Dilution Stability Colorimeter Response.....	156
43. Dilution Stability Flowmeter Response.....	157
44. Colorimeter Response to KMnO4, 9 ml/min.....	163
45. Colorimeter Response to KMnO4, 6 ml/min.....	164

Figure	Page
46. Colorimeter Response to KMnO ₄ , 3 ml/min.....	165
47. FIA Mode Calibration Curve, Flow Rate.....	169
48. FIA Mode Calibration Curve, Peak Area.....	172
49. FIA Mode Calibration Curve, Methyl Red Area....	177
50. FIA Mode Calibration Curve, Methyl Red Height... .	179
51. FIA Mode Calibration Curve, KMnO ₄ Peak Height... .	181
52. FIA Diffusion Rate.....	184
53. Multiple Colorimeter Response to KMnO ₄	188
54. FIA Mode Calibration Curve, KMnO ₄ - Fe(oo)++... .	190
55. Colorimeter Response vs. Time for KMnO ₄ - KI... .	198
56. Single Component Kinetic Plot for KMnO ₄ - KI... .	199
57. Multicomponent Kinetic Plot.....	219

TABLE OF TABLES

Table	Page
I. Initial Balance Flowmeter Error.....	75
II. Corrected Balance Flowmeter Error.....	77
III. Flowmeter Calibration Run Results for .1 M NaCl	82
IV. Flowmeter Calibration Run Summary Report.....	88
V. Mixing Efficiency with a .031" Jet.....	95
VI. Mixing Efficiency with a .014" T-Jet Mixer.....	97
VII. Mixing Efficiency, KMnO ₄ Dilution.....	99
VIII. Mixing Efficiency, KMnO ₄ - Fe(II) Reaction....	101
IX. Colorimeter Time Intervals Observed at 10 to..	105
X. Colorimeter Stability Studies.....	129
XI. Instrument Stability Evaluation.....	152
XII. Dilution Accuracy Evaluation.....	159
XIII. Peak Area, 100 ul injections of 500 uM KMnO ₄ ..	166
XIV. Peak Area, 100 ul injections into 2 ml/min....	170
XV. Peak Area, 100 ul injections of indicator.....	175
XVI. Peak Area, 100 ul injections of KMnO ₄	182
XVII. Peak Area, 100 ul injections of Fe(aq) ⁺⁺	191
XVIII. KMnO ₄ - KI Reaction Summary.....	200
XIX. Time Interval Data Treatment Results.....	203
XX. Flow Injection Kinetic Results, Swinbourne's..	207
XXI. Flow Injection Kinetic Results, Predicted A _∞ ..	209
XXII. Colorimeter Specimens and Time Intervals.....	216

Table		Page
XXIII.	Single Component Calibration Runs with Hg & Zn	223
XXIV.	Multicomponent Test Runs with Hg and Zn.....	226

I. INTRODUCTION

A large number of analytical methods are based on the rate of reaction of a sample with a reagent. In other words, the kinetics of a reaction can be used to obtain information, such as the concentration of an unknown, which is of analytical interest. These methods are found to be particularly useful in clinical and biological analysis. In selected cases kinetic methods are preferred to equilibrium methods because of one or more of the advantages listed below (1).

1. Differences in reaction rates of similar compounds are often sufficiently large to allow simultaneous determinations. Time consuming or difficult separations may be avoided.
2. Chemical reactions which are not well behaved in equilibrium techniques may be used.
3. Adequate kinetic measurements may be made before side reactions become significant, or when an equilibrium reaction is not sufficiently quantitative.
4. Catalyzed reactions have great potential for trace analysis.
5. Reaction rates may be adjusted to select a reactant of interest or to match instrumental

limitations by varying reaction conditions.

6. Extremely specific enzymatic methods may be used.

7. Kinetic measurements use the relation of one measurement to another rather than requiring an absolute response from the detector system.

Automation of the measurement process is necessary to allow the determination to proceed rapidly and economically. Other benefits of automation include increased reproducibility, greater sample throughput, and easier integration of the results of the analytical technique into a laboratory data system. The data system allows rapid recall of specific information from an ever increasing data base of all types of information, an important feature when dealing with even moderate sized laboratory data requirements. The ready availability of data eases the use of more sophisticated quality control procedures in the laboratory.

II. HISTORICAL DEVELOPMENTS

Established analytical techniques which can be used for kinetic analysis or which are easily adapted to kinetic analysis include the following:

1. Classical manual methods may be used if the reaction rates are slow enough. Aliquots of the reaction mixture may be periodically sampled, quenched if necessary, and determined by nearly any applicable method. If the determination method is continuous, it may be possible to place the reaction vessel in the sample compartment of the measuring instrument and follow the reaction from the time of mixing until enough data is collected for calculation of the results. Problems with classical manual methods are low sample throughput, high cost, skilled technicians are required, and relatively large amounts of reagents and solutions may be required.

2. Segmented flow apparatus, such as that developed by Technicon, essentially automates the manual techniques (2). Segmented flow techniques use a multichannel peristaltic pump to propel samples and reagents through the analyzer system. To assure complete mixing, turbulent flow is maintained by passing the reaction stream, which is segmented by injected air bubbles, through helical mixing coils. A number of reagents may be added to the reaction

stream in this manner. After debubbling the stream, it is passed through a detector, typically a colorimeter. Often, elaborate calibrations are necessary to correct the resulting signal since waiting for the occurrence of a steady state would reduce the sample throughput to unacceptable rates (3). The instrumentation, reagents, and maintenance for segmented flow methods are relatively expensive. Throughput is generally lower than flow injection techniques.

3. Flow Injection Analysis was developed to solve the expense and throughput problems of segmented flow methods for specific determinations. As it is a relatively new technique, many possibilities for further development exist. In contrast to segmented flow, flow injection does not separate samples by air bubbles. The sample is injected into a reagent carrier stream and a process, analogous to chromatography without partitioning and without a stationary phase to disturb the flow pattern, occurs. Instrumentation can be very simple; a wide range of detectors are available for use; excessive quantities of reagents are not required; and continuous streams may be easily sampled (2).

4. Stopped flow analysis is an inherent kinetic method and is designed for following rapid reactions. Reagents and samples are held in two syringes which are

rapidly driven to force the solutions through a mixer and into an observation cell. A stoppers syringe, attached to the cell outlet, fills to a predetermined point after which flow is no longer possible. As soon as conditions in the observation cell stabilize, the progress of the reaction can be followed, generally by optical means. Common instrumentation allows useful observations to begin as soon as four milliseconds after mixing (4). Instrumentation is moderately expensive; flowing streams must be sampled; and sample handling is a problem because of the need to fill and empty the syringes which force the solutions through the instrument.

5. Continuous flow kinetics was the first method developed for studying fast reactions. Initial instrumentation was primitive and consumed large amounts of reagents (5). With modern instrumentation, considerable amounts of reagents are still consumed for true continuous flow methods; however, techniques such as accelerated and pulsed flow can minimize this problem. Unfortunately, accelerated and pulsed flow methods result in more complicated sample handling procedures due to the necessity of widely varying the flow rates of the reagents. In this aspect, they have little advantage over stopped flow techniques.

Typical continuous flow instrumentation consists of

sample sources, a mixer, and an observation tube with a detector which can be positioned at several places along the tube. The placement of the detector determines the time between mixing and observation of the extent of reaction.

III. ENHANCEMENTS AND POTENTIAL APPLICATIONS

The addition of multiple detectors spaced along the observation tube allow the nearly simultaneous acquisition of a large number of data points which define the extent of reaction. Fitting these points to the expected equation of the reaction via a least squares procedure will give improved results over the conventional single or dual point measurements. This is because errors in the individual measurements due to random instrumental noise or instability are minimized by the least squares procedure using a large number of data points. The use of multiple detectors makes available the data which is required to solve the set of simultaneous equations resulting from several unknowns reacting at different rates with a common reagent. Thus it is possible to calculate the concentrations of the components of an appropriate binary or ternary mixture using this instrumental technique. The use of detectors with varying characteristics, i.e., different wavelength sensitivity in light absorption systems, is also possible, and may contribute to the selectivity and resolution of the overall detection system.

Concentrations of the components of an appropriate mixture at intervals of a fraction of a second are obtainable with this instrumentation. It could be used as

a sensor in process control applications where rapid adjustment or monitoring of a system parameter is needed.

The instrument would be particularly useful when the other methods required a separation step before good determinations of the species of interest were possible.

A similar application is a selective detector for liquid chromatography. Several modes of operation are possible. The first takes advantage of the selectivity of kinetic methods, allowing the component of interest to be determined to the exclusion of other components. Various post-column reactions have been extensively used to improve the detectability of otherwise difficult or impossible to detect species. As an example, amino acids are separated chromatographically and then reacted with ninhydrin to form a derivative which is easily detectable colorimetrically. The reaction proceeds to completion before the measurement is made in this case; however, given a computer system which could rapidly calculate concentrations from initial reaction rates, there is no reason why kinetic methods could not be used with this or other reactions to improve sensitivity. Resolution of mixtures incompletely resolved by the chromatographic process is possible if the rates of reaction of the unresolved components with the reagent are sufficiently different.

Adding a chromatographic sampling valve to the sample

stream results in a continuous flow kinetic detector for flow injection analysis. A small plus of sample is injected into an inert sample stream which reacts with the reagent at the mixer. Rather than observing steady state conditions in the reaction tube, the sample plus will appear, with changing physical characteristics according to the reaction kinetics, at successive detectors. This mode of operation promises to reduce the sample requirements of continuous flow kinetics to reasonable amounts.

IV. INSTRUMENTATION

The goal of designing an instrument capable of continuous kinetic analysis which is relatively simple and inexpensive is a considerable challenge. Furthermore, the development of the instrument must advance the state of the art of analytical chemistry in some aspect to justify itself as a topic of research. Areas of investigation requiring expensive equipment, areas which are well developed and areas which do not immediately show a need for improved instrumentation should be avoided. Thus the area of multicomponent continuous flow kinetic analysis is a prime candidate for development.

The instrumental development is intended to advance the state of the art of analytical chemistry by applying the latest in rapidly evolving electronic technology to a combination of chemical techniques to enhance their usefulness. Due to the synergistic effects of knowledge of developments in both chemistry and electronics, a greater advancement is possible than if cross-fertilized development is avoided.

The success of the project will be assured if it shows that the techniques and improvements investigated are feasible. Fulfilling the obvious goals of any instrumental design, improvements in sensitivity, reduction

in required sample size, improvements in precision and accuracy, improvements in sample throughput, or decreases in expense are desirable but not necessarily the primary goal of the project. Neither is the instrument intended to be generally applicable.

Experience at the Nutrition Institute of the United States Department of Agriculture's Agricultural Research Service in Beltsville, Maryland, the Food and Drug Administration in Washington, D. C., and the analytical laboratories of the Chemicals and Plastics Group of Dart Industries in Paramus, New Jersey, indicates that current requirements in instrumentation are for devices which need as few preliminary separation and sample work-up steps as possible. Wilks (6) indicates that demand today is for repetitive quantitative measurements. Dedicated instruments with minimal controls lower costs and improve reliability by eliminating operator errors. Minimal sample handling, minimal sensitivity to ambient conditions, high signal to noise ratios, and output of data directly in composition units are additional requirements of the new generation of analytical instruments. Therefore, the potential specificity and possible multicomponent determination of the multicomponent continuous flow kinetic analysis technique are possible partial solutions to the problem.

Often hundreds or thousands of samples will be determined by a method over a period of years. It is therefore economically feasible to configure or develop an instrument from a group of instrumental building blocks to perform a single, specific determination rapidly and efficiently. One of the prime characteristics of the resulting instrument is high specificity for the species of interest, and again kinetic methods may be of value.

Computerization is necessary to handle this volume of samples and the mass of resultant data in an organized and efficient manner. Because the instrument will require computerization to handle the additional data of the improvements to the traditional continuous flow kinetic methods discussed in the introduction, careful planning of the computer system so that it can handle both the instrument control and the data base management and reporting tasks would be advantageous.

When considering long term projects with large numbers of samples, quality assurance becomes a very real problem. To assure consistent determinations, standards will have to be developed and determined periodically. The data system will need to prepare and check calibration curves, calculate final results based on the calibration curves, and keep statistical records over the lifetime of the project. Should significant deviations from expected

values occur, the instrument operator must be notified so that he can take corrective action.

The instrument, developed to explore these characteristics, consists of four major subsections as indicated in Figure 1. The samples and reagents are handled by the transport system which is responsible for sampling and providing a consistent, known flow of material. The mixer assures complete and uniform mixing of the sample and reagents. The reaction-observation chamber provides the time delay required for the reaction in addition to providing mechanical mounting points for the detectors. Finally, the data acquisition and processing system controls the other components of the apparatus and makes the needed calculations.

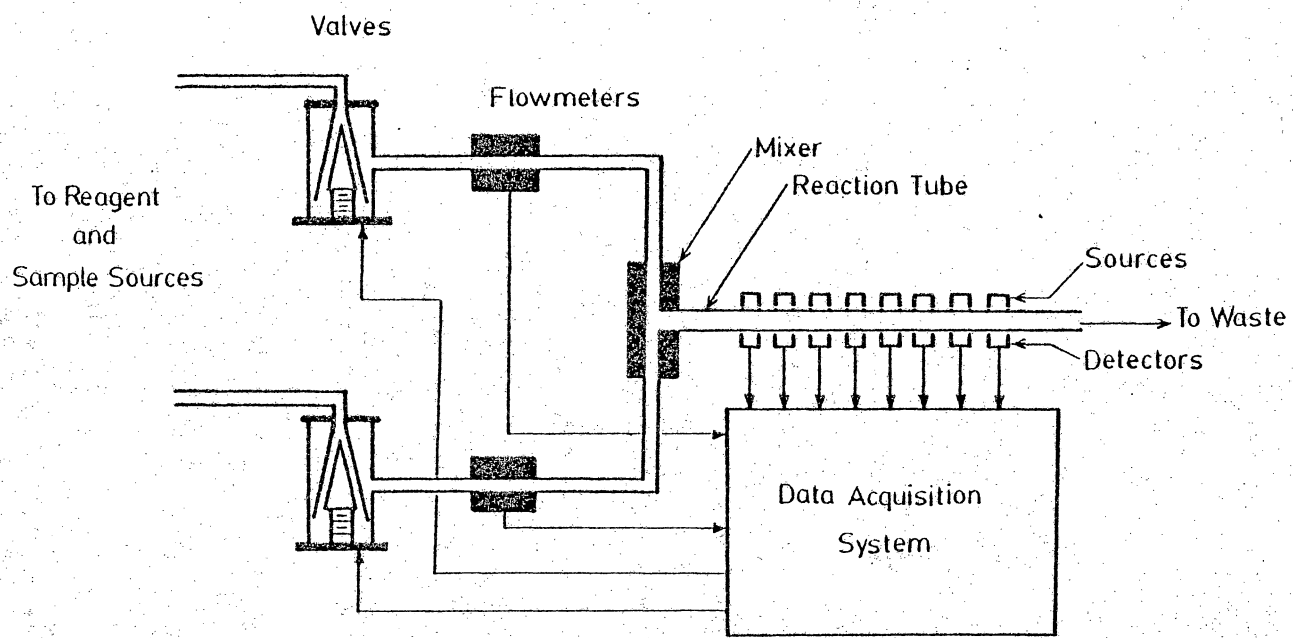


Figure 1. Instrument Block Diagram

A. Transport System

Continuous flow transport systems offer the advantage of minimal sample manipulation because flowing streams are utilized rather than physical movement of containers. The operations associated with continuous flow transport systems are inherently simple. For the purposes of this instrument, a motive force, flow sensor and controller, and reagent containment apparatus constitute the transport system.

The containment apparatus is constructed of common laboratory materials. Glass reagent reservoirs are fitted with adapters for the Cheminert TFE[®] tubing used to connect individual pieces of apparatus. On the opposite end of the reservoirs, connections are made to a source of pressurized inert gas by closely fitting glass-plastic connectors. This arrangement is easily constructed and can withstand low pressures. If excessive gas pressure builds up, these connections will separate rapidly, thus releasing the pressure without damage to the apparatus or operating personnel. Typically, a pressure of a few pounds per square inch is maintained in the reagent reservoir which assures the ability of the flow controller to deliver an adequate amount of reagent.

As previously indicated, the force propelling the

reagents through the system is pressure from an inert gas. In contrast to many types of pumps, this apparatus is relatively inexpensive, very simple, pulseless, requires little maintenance and can easily be constructed of inert materials. Inexpensive peristaltic pumps exhibit significant pulsation as well as requiring tubing replacement due to degradation. Chromatographic pumps are more reliable but exhibit more pulsation, are relatively expensive and are sensitive to air bubbles and abrasive particles. These pumps also require metal construction materials because they are designed for higher pressures than will be encountered in this instrument. It is possible that some potential reagents would react with the metal parts of the chromatographic pumps with undesirable results.

As with any analytical technique, it is necessary to know precisely the amount of reagent and sample involved in the reaction. It was soon discovered that an assumption of equal flows in both the reagent and sample transport system through the mixer could not be relied upon. Minor irregularities in the construction of the mixer resulted in greater flow in one or the other channels, even when the reservoirs were at equal levels and pressurized from the same source. Reservoir balance was rapidly lost, adding to the differences in flow rates. Therefore, in the absence

of positive displacement provided by the syringes of stopped flow apparatus or various types of pumps, a means for measuring and controlling the flow of reagents is necessary.

Implied in controlling the flow is the ability to measure it. It would be convenient, but not necessary, to have constant flows in this instrument as long as the flow rate is accurately known. Given a good flowmeter, it is not difficult to generate a feedback mechanism which will result in constant flow through the use of techniques well known to process control engineers and designers of circuits involving operational amplifiers (7). Including the computer, which is which is controlling other aspects of the instrumentation, in the feedback loop considerably expands the range of reaction rates observable by the instrument. For example, it is possible to vary the flow of the reagent, under computer control, to change the observed reaction rate so that optimum measurement conditions are maintained in the reaction-observation tube. This allows a single concentration of reagent to be used over a much wider range of concentrations of sample than if the extent of reaction in the observation tube was the only variable observed. In other words, the sensitivity of the detector can be varied to obtain optimum measurements.

Another advantage of this flexibility is that the

reagent flow can be varied to maintain constant conditions in the reaction-observation tube. This is commonly referred to as the "stat" technique (3). Potentiostats and pHstats are examples of the use of this technique. An outstanding characteristic of the "stat" technique is that the detector need not be linear for good results. All that is important is that the inputs to the system can be varied in such a manner that the detector output is essentially constant. This is just another application of the feedback principle previously applied to the problem of maintaining a constant flow of reagent and sample. In practice, perfect consistency of the detector output is not possible because the method requires an error in the positive or negative response direction to allow it to determine in which direction to change the input parameters. However, if this error is sufficiently small, the small oscillations around the desired value will not be objectionable.

A consequence of this type of control is that the instrument can easily be adapted to perform titrations on flowing streams. Flow may be adjusted so that the product of the flow and concentration in the reagent side matches that of the sample side.

$$Fr * Cr = Fs * Cs$$

Solving for the sample concentration:

$$Cs = Fr * Cr / Fs$$

Thus, the sample concentration is easily calculated from the flow or ratio of the flows in both sample and reagent sides, and the reagent concentration.

1. Flow Controller

The flow controlling element is a micrometer capillary valve (Model M7100, Gilmont Instruments, Great Neck, NY). The valve is constructed of glass and Teflon which are inert with respect to most potential reagents.

Glass to Cheminert® adapters provide a simple means of connecting the valve to the other components of the system.

A modified high torque digital proportional servo (Model GDA-1205-B, Heath Co., Benton Harbor, MI) is mechanically coupled to the valve, thus allowing the computer to control the flow through the valve by rotating the micrometer in one direction or the other. The control range of the valve is from .1% to 100% of maximum flow. The range of .5% to 50%, a 100-fold change, is easily achievable. In the range of 1% to 10% of maximum flow the regulation of the valve is semi-logarithmic. The flow is directly proportional to the pressure drop across the valve and inversely proportional to the viscosity of the fluid.

Flow regulation in the semi-logarithmic region requires 14 of the 20 possible turns of the micrometer, allowing precise control of the fluid flow. The best closed loop control of the flow by the complete system, flowmeter, computer control algorithm, and controlling valve was experienced in this region. The valve was

between one-eighth and three-quarters open under these conditions.

The direction and rotation of the motor is under direct computer control according to the schematic diagram in Figure 2. To prevent rotation past the limits of the capillary valve, infrared emitters and sensors are positioned at the desired end points of the micrometer's movement as indicated in Figure 3. Before starting any movement, the computer must check these sensors to determine if the requested movement is allowable. If not, activation of the motor does not occur, avoiding damage to the valve.

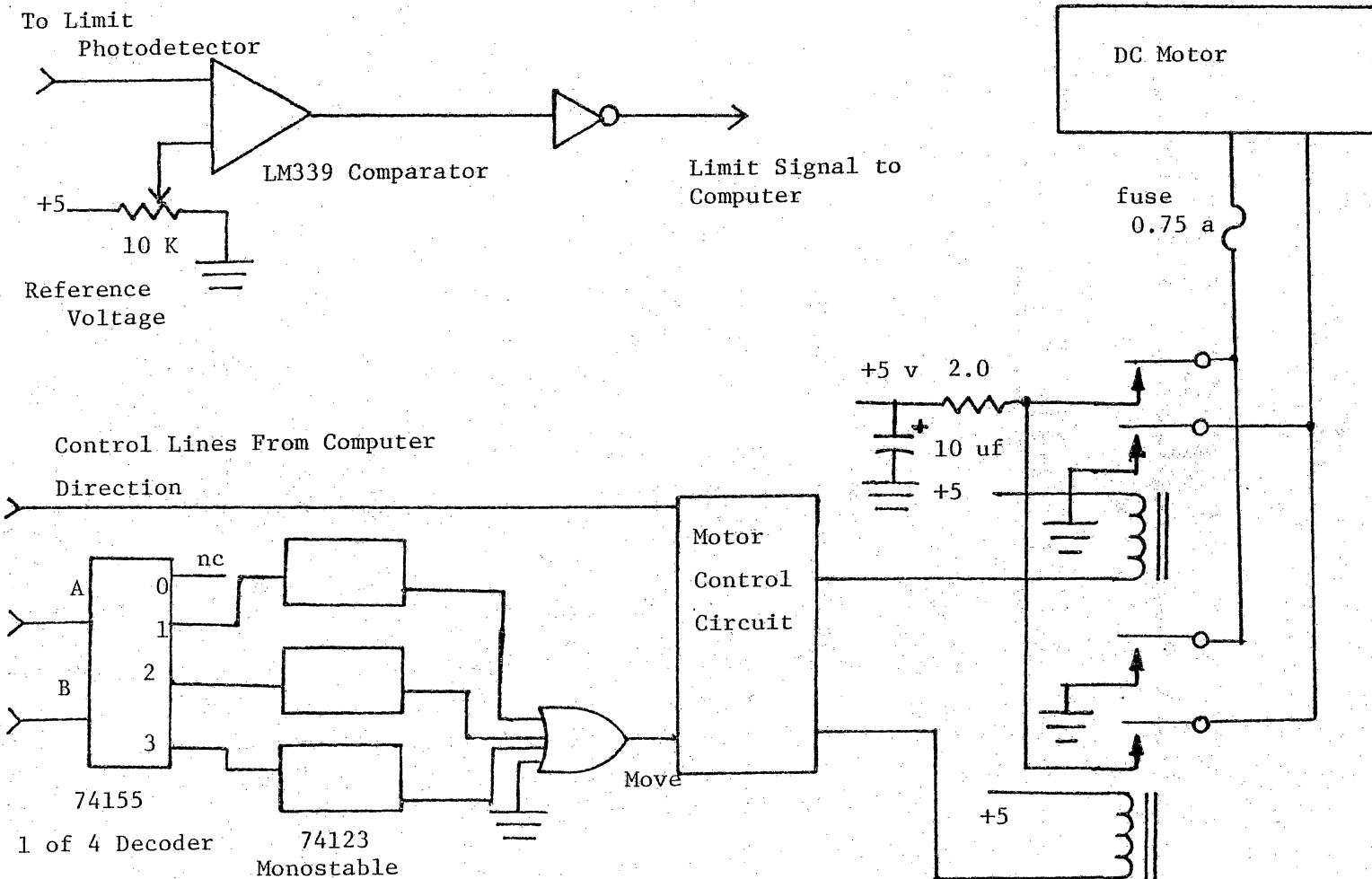


Figure 2. Valve Controller Electronics

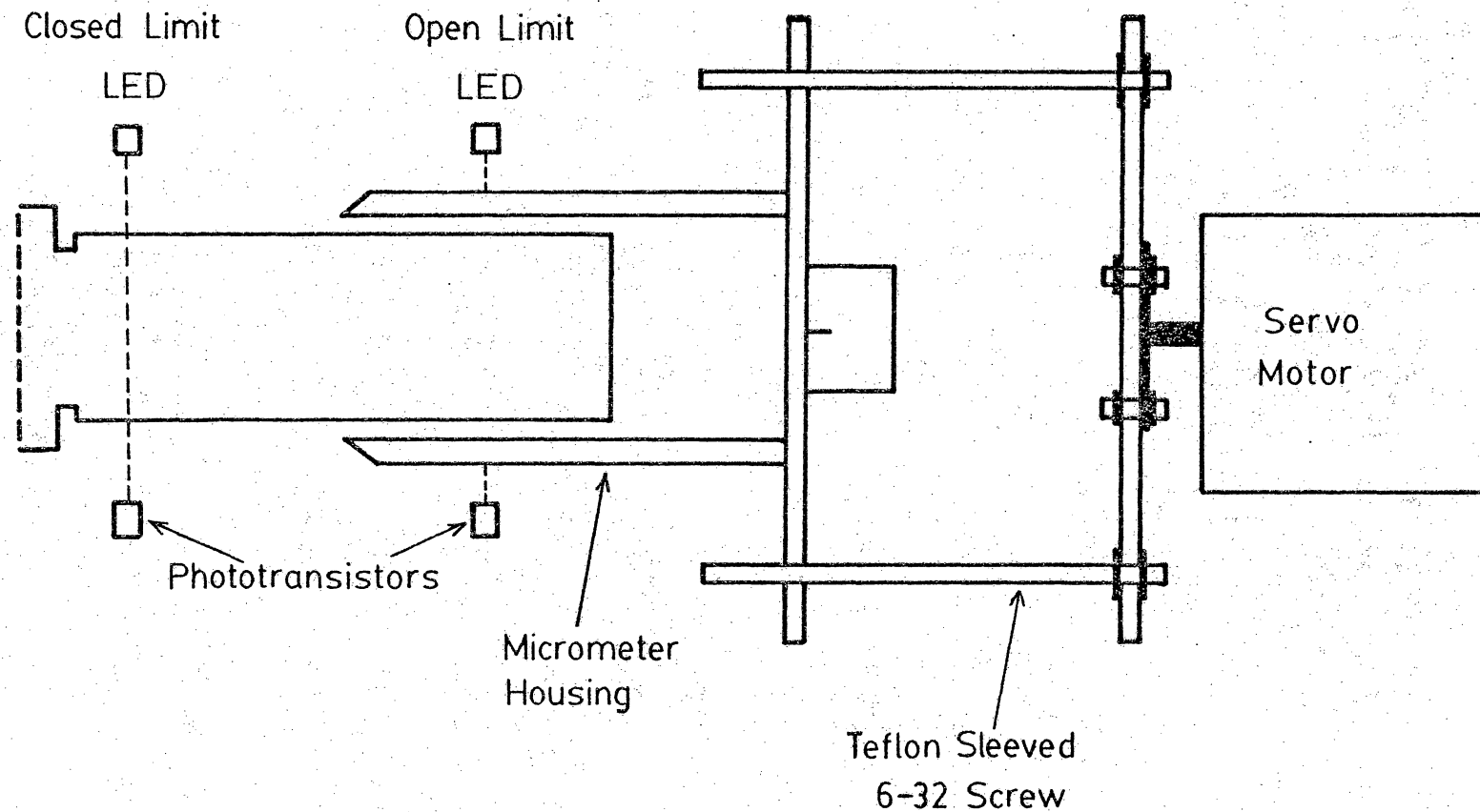


Figure 3. Capillary Valve Controller

2. Flowmeter

Measuring low flow rates of a liquid accurately and in a closed system is not a simple matter if computer compatible signals are required. In a system where the flow measurement can be made at the end of a tube open to the atmosphere, such as the eluent of a liquid chromatograph, the liquid can be collected over a period of time and the flow determined gravimetrically. An automatic approach to this method collects the liquid in a container placed on an electronic balance which periodically reports the measured weight to a computer system. The flow can be determined from the change in weight and the density of the liquid being measured. Measurements can be made as often as every 2 or 3 seconds, allowing observation of relatively short permutations of the flow. This method of flow measurement can easily be used to calibrate flowmeters which will subsequently be used in closed systems.

Characteristics necessary for the flowmeters to be used in the transport system of this instrument are the following:

1. Operable in a closed system.
2. Provide computer compatible output.
3. Small size - The flowmeter must operate with low volume cells, less than the 2 millimeter diameter.

of the connecting tubing in the system.

4. Rapid response - Reactions of less than a second duration are anticipated. The flowmeter must respond to changes in flow on approximately this scale. It is unlikely that flow changes of shorter duration, given a constant average flow, will affect the instrument's determinations since multiple rapid determinations can be averaged over an appropriate period of time. Rapid response will enable better feedback to the flow controller also.
5. Accurate - The total error of the determination is a function of all the measurements and the subsequent processing of the measurements. Consequently, minimum error is desired in a measurement as fundamental as the flow rate to avoid excessive propagation of error.
6. Inexpensive - Several units are required.
7. Constructed of inert materials to avoid contamination of reagents.

A variety of flow measuring techniques exist. The common rotameter flowmeters consist of a precision tube through which the fluid flows. The tube is positioned vertically and the fluid pushes a small ball higher in the tube according to its flow rate when passing from the

entrance at the bottom of the tube to the exit at the top. The flow rate is read from a scale engraved on the tube. Although this type of flowmeter could be made computer compatible, the adaptation would be makeshift, to say the least, and would degrade the already insufficient accuracy. The rotameter is also sensitive to air bubbles which are often difficult to remove.

Any type of flow meter relying on rotating mechanical sensors is unsatisfactory because of size restraints. The measurement of a small pressure difference across an orifice is not linear and would require very sensitive pressure transducers with low dead volume to avoid dispersing small sample pluss. The construction of a pressure transducer of completely inert materials is difficult.

Exotic devices based on the time between some perturbation of the fluid and subsequent detection of the perturbation some distance downstream are generally expensive and complex. Devices using this technique include the nuclear magnetic resonance flowmeter which flips the spin of a proton in the fluid and later detects the flipped spins (8). Ultrasonic doppler effects (9) and laser interferometers have been used in larger diameter pipes when particles are present in the fluid. It is also possible to add heat pulses to the fluid and detect

temperature changes downstream (10). This procedure could trigger unwanted reactions in the fluid. An instrument employing this method is available for liquid chromatography, but is excessively expensive. Fisher & Porter's oscillating bell flowmeter, based on an improved rotameter, is likewise excessively expensive (11).

The electromagnetic flowmeter remains as a potentially satisfactory flow measuring device (12). It is based on the principle of elementary physics which indicates that a current is induced when a medium passes through a magnetic field. Flowmeters based on this principle are used to measure fluid flow in large pipes in industrial plants, liquid metals in nuclear reactors and in blood vessels. Improved apparatus is required to obtain the accuracy desired at the low flow encountered in the continuous flow instrument.

Referring to Figure 4, a potential difference, e , is observed between the electrodes which is proportional to the velocity of the fluid at right angles to the magnetic field as expressed in Equation 1 (12).

$$e = k * H * d * v * 10^{-8} \text{ volt} \quad (1)$$

H is the magnetic field in oersteds, d the diameter of the tube in centimeters, v the average velocity of the fluid cross section. The sensitivity of the flowmeter, k , is 1 under ideal conditions.

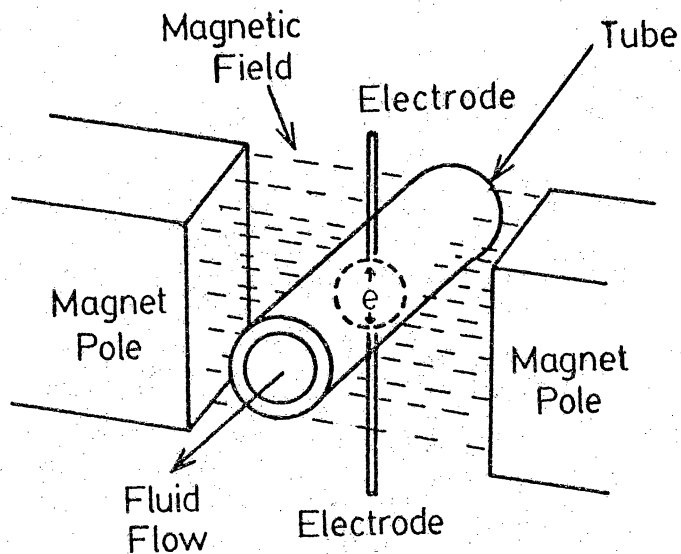


Figure 4. Electromagnetic Flow Meter

As a consequence of the low flow rates encountered in this instrument, the observed potential is very low and direct current amplification using a permanent magnet as a source of the magnetic field is impossible. The use of a solenoid excited by an alternating current as a magnetic field generator allows the use of AC coupled amplifiers and has the further advantage of avoiding polarization of the electrodes. Unfortunately, use of an alternating magnetic field introduces additional components to the potential, e, measured in Figure 4, due to the effects of magnetic induction. A multitude of disturbing effects occur at the electrodes and contribute to the noise in the flowmeter signal. The design, construction, and evaluation of the flowmeter is presented in detail in the following section. In summary, a linear response of about 1×10^{-7} volts per milliliter per minute over a range of 2 to 30 milliliters per minute was obtained. The noise level corresponds to a flow of ± 0.2 milliliters per minute.

The magnetically induced flow signal, on the order of 1×10^{-7} volts per milliliter per minute, must be amplified to a level which can be digitized with adequate resolution. The current implementation of the flowmeter electronics has a sensitivity of 3 millivolts per unit at the voltage to frequency converter input, thus the gain of 320,000 in the rest of the flowmeter circuit results in a

sensitivity of about 1×10^{-8} volts per response unit at the flow cell. This corresponds to a flow of 0.1 milliliters per minute.

Amplifications of the order of 0.1 to 1 million (100 to 120 db) will be required to obtain the desired flow resolution. It is not practical to obtain this extremely large gain with DC coupled amplifiers, therefore AC coupled amplifiers will be required. The lack of a DC reference level in the system requires that the applied excitation be chopped, i.e., turned on and off so that the difference between the on and off states can be used as a measure of the system's response. It will be seen subsequently that a number of other advantages are obtained from chopping the excitation source. Flicker or 1/f noise will be a significant problem with large gains at low frequencies, thus shifting the bandpass of the amplifier to higher frequencies by chopping will help solve this problem. The "lock-in amplifier" uses this technique to limit the bandpass of the system to a narrow frequency region, thus rejecting some of the noise which exists at all frequencies. Because the signal occupies the bandpass of the amplifier, and noise outside of the the bandpass is not integrated into the output signal, the signal to noise ratio of the system is improved by this technique. The term "lock-in" arises from the fact that as the bandpass is

made narrow to reject the maximum amount of noise, minor changes in the frequency of the chopper could place the signal outside of the amplifier bandpass. To remedy this problem the amplifier is synchronized or "locked-in" to the chopper.

It is well known that electrodes rapidly become polarized if a DC potential is allowed to exist for a significant amount of time, thus rapidly making the measurements worthless. To counteract polarization in electromagnetic flow meters, nonpolarizable electrodes have been used. Unfortunately, these electrodes result in high cell resistances and are subject to disturbances, perhaps due to flow over their surfaces. A much more satisfactory solution is to alternate the polarity of the excitation field, thus keeping polarization at an average value of zero. The chopping process, required because of AC couplings, can be easily modified to remedy the polarization problem.

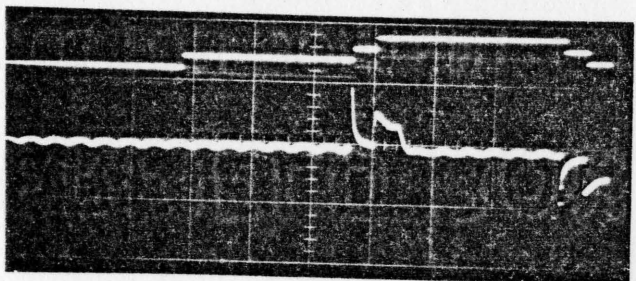
The simplest way to chop the flow cell excitation is to turn an electromagnet, which is supplying the magnetic field to the flow cell, on and off. In addition, alternating the direction of the current in the magnet coil will eliminate the effects of polarization.

Initial flowmeters used sine wave excitation, easily obtainable from AC power supplies or oscillators (13).

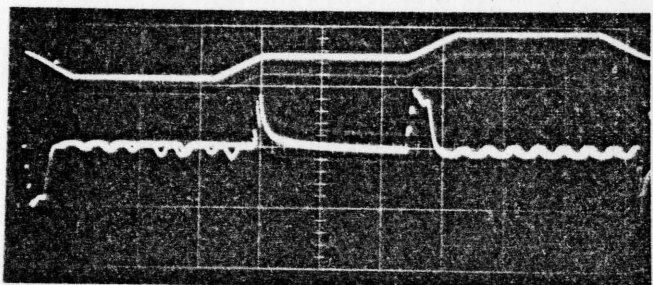
Amplitude and phase detection methods were used to extract the flow signal from a number of spurious signals induced by this system. In an effort to reduce the effect of these spurious signals, square and pulsed excitation waveforms were used (14). The semi-square wave magnet excitation, shown in Figure 5, results in very large spikes in the observed waveform. The spikes are orders of magnitude larger than signal due to flow. This is because the current induced in a stationary conductor by a magnetic field is proportional to the time rate of change of the magnetic field. The magnetic field is changing very rapidly at the edges of the square wave, producing pulses which require the amplification system to have fast response and a very large dynamic range if the flow signal is to be undistorted. With square wave excitation, measurements are made after the system has reached an equilibrium point and the spurious signals have decayed to insignificance. This is a form of phase sensitive detection and may be achieved by setting an amplifier "on" at the proper time in the excitation cycle. The square wave method is superior to sine wave methods because the amplifier may be on for a larger portion of the cycle, allowing more noise to be averaged out.

Advancing a step further, applying a trapezoidal excitation waveform (15) reduces spurious signals

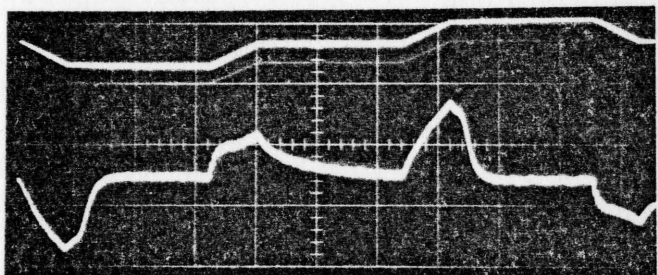
SEMI-SQUARE WAVE
MAGNET EXCITATION
10 V/DIV



TRAPEZOIDAL WAVE
MAGNET EXCITATION
5 V/DIV



FILTERED TRAPEZOIDAL
WAVE EXCITATION
1 V/DIV



TOP TRACES - MAGNET EXCITATION 10 V/DIV

HORIZONTAL SWEEP 20 MS/DIV

FIGURE 5. VOLTAGE INDUCED IN A WIRE BY VARIOUS
MAGNET EXCITATION WAVEFORMS

considerably because the time rate of change of the magnetic field is greatly reduced by rounding the sharp edges of the square wave as shown in Figure 5. Filtering the waveform generator output further reduces rapid excitation changes and results in the bottom trace of Figure 5, where it can be seen that the induced signals are significantly attenuated. Signals of this magnitude do not present problems of response and dynamic range in the subsequent circuits.

The signals represented in Figure 5 are those induced in a wire by the excitation magnetic field. A similar signal is also induced in the electrodes of the flow cell. Because this induced signal is not related to flow, it is desirable to eliminate it. Referring to Figure 6, a wire passes along the top of the flow cell parallel to the electrodes in the cell. The magnetic field will induce equal currents in both wires; however, because the induced flow of current is in opposite directions in the parallel wires making up the loop, the currents resulting at the amplifier input contain only the components induced in the flow cell. The components induced in the electrodes and return wire cancel each other. It is necessary to position the excitation magnet, the flow cell, and the return wire very precisely to achieve the complete cancellation of non-flow signals. The effect of improper positioning is

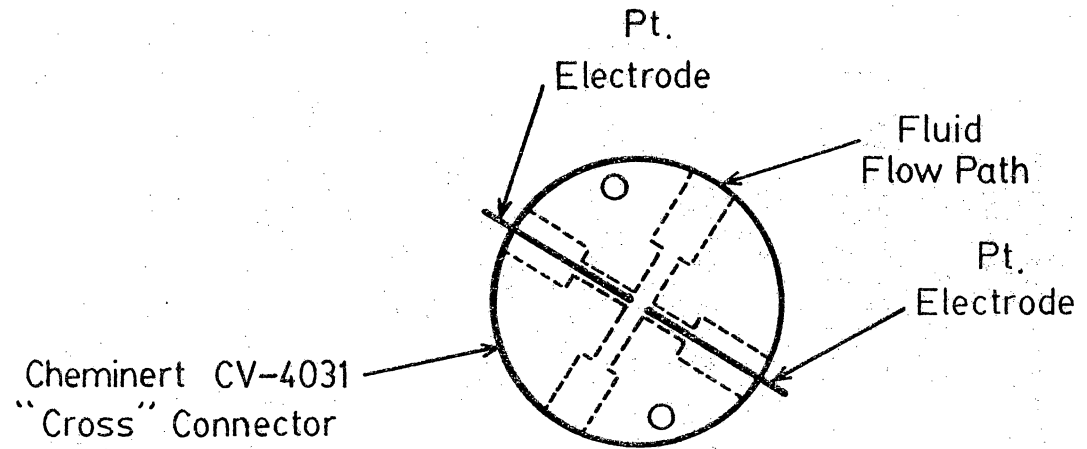


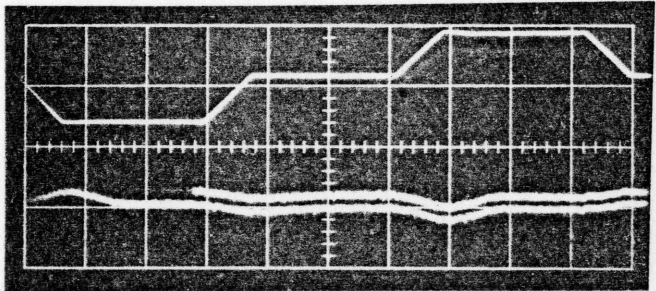
Figure 6. Flow Sensor Cell

illustrated in Figure 7. Poorly cancelled induced signals result in significantly higher baseline levels.

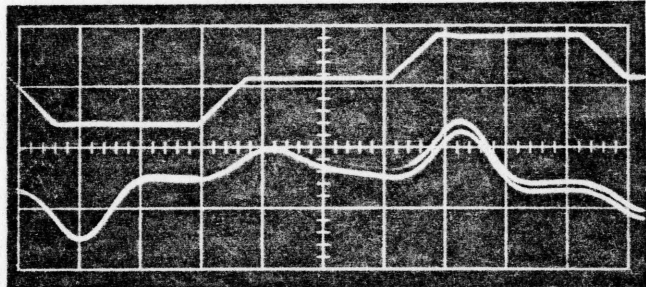
In addition to the positive and negative trapezoidal pulses shown in the magnet excitation waveform of Figure 8, a period of time without excitation has been left after every pulse. Because of a large number of errors, the signal observed when no excitation is applied may not be zero. Thus, if it were possible to subtract the no excitation signal from the signal in the presence of excitation, these errors would be cancelled (16).

To achieve this cancellation of errors by subtracting the no excitation signal, to reduce the effect of 60 Hz power line noise by integrating the signal over a multiple of the period of the power cycle, and to digitize the signal, a voltage to frequency converter followed by a up/down counter was used in the current implementation. The VFC produces a train of pulses whose frequency is proportional to the input voltage. Referring to Figure 8, the counter accumulates the pulses from the VFC during the period when the count up line is low. When the count down line is low, pulses from the VFC decrement the counter, effectively subtracting the no excitation value. The read counter pulses, occurring just after each of these count up and count down cycles, interrupt the computer which then obtains the value in the counter and resets the counter.

NOTCH FILTER
OUTPUT
.5 V/DIV



VFC INPUT
1 V/DIV



TOP TRACES - MAGNET EXCITATION 10 V/DIV

HORIZONTAL SWEEP 20 MS/DIV

FIGURE 7. UNBALANCED MAGNETIC FIELD SIGNALS
WITH NO FLOW OF 1.0 M NaCl

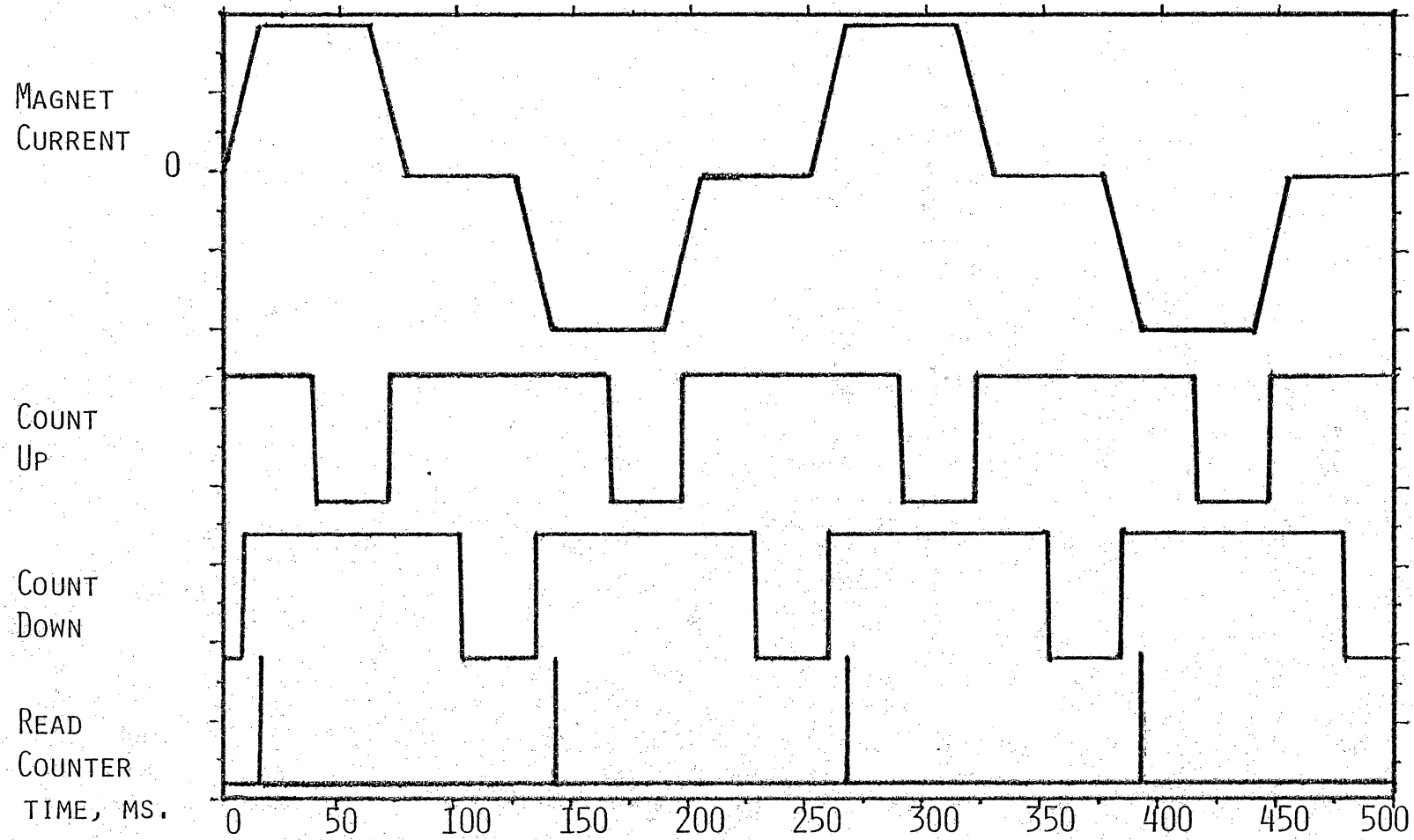
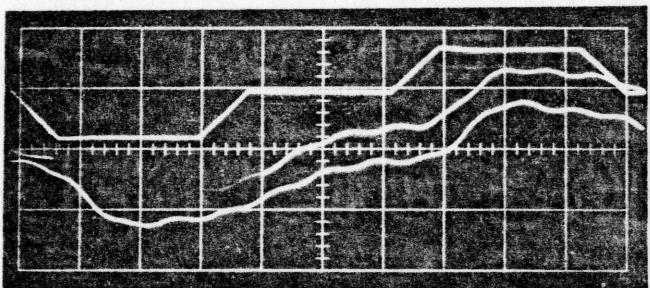


FIGURE 8. FLOWMETER CONTROL SIGNALS

readying it for another cycle. The count up and count down pulses are positioned so that they are active during the steady state condition of the amplified flow signal, which is delayed slightly in comparison to the excitation signal because of the heavy filtering in the flowmeter amplifier. The pulses are approximately twice as long the period of the 60 Hz power line frequency, thus 60 Hz sine waves superimposed on the flow signal should be integrated out.

An additional advantage of the no excitation subtraction feature of this flowmeter is that slow shifts in DC level of the VFC input signal are compensated for as long as significant shifts do not occur during one excitation cycle. Referring to Figure 9, where the camera shutter was open long enough to capture portions of two succeeding cycles, it can be seen that the DC level shifts between cycles, but is relatively constant within a cycle. If absolute level detection was used, these DC level shifts would result in noise levels above commonly encountered flow signals, thus making the flowmeter useless. These DC level shifts probably originate at the electrodes in the flow cell. It appears that changes in flow rate rapidly shift the 80 to 100 millivolt potential observed across the electrodes in some unpredictable manner. Even under no flow conditions, this potential slowly drifts in one direction or another. This characteristic necessitated

VFC INPUT
1 V/DIV



TOP TRACE - MAGNET EXCITATION 10 V/DIV

HORIZONTAL SWEEP 20 MS/DIV

FIGURE 9. FLOWMETER SIGNALS WITH A 50 CM HEAD OF .05 M NaCl

capacitive coupling of the inputs to the instrumentation amplifier indicated in Figure 10. Because of the amplifier's gain (4000), even a small change in the difference between the plus and minus inputs results in amplifier saturation, incapacitating the flowmeter. The coupling capacitors block this DC potential, allowing the higher frequency AC flow dependent potentials to pass. The capacitors must be large to assure the low frequency (4 Hz) flow signals pass undistorted, thus the charging and discharging of the capacitors is slow, contributing to the slow shifts in DC levels observed in subsequent sections of the circuit.

Construction of the electromagnetic flow sensing cell appears to be somewhat of an art. A number of designs and configurations were tried before adequate results were consistently obtained.

The flow sensing cell is constructed by enlarging one of the paths in a Cheminert[®] CJ-4031 "cross" connector to a 1/16th inch bore. Although these connectors are specified with 1/16th inch bores, it appears that those received had bores of about half of that specified. Equation iv, on Page 27, indicates a flowmeter response proportional to the diameter and velocity; thus, the small diameter bore should exhibit reduced response. A significant increase in velocity is required to maintain a constant delivery of

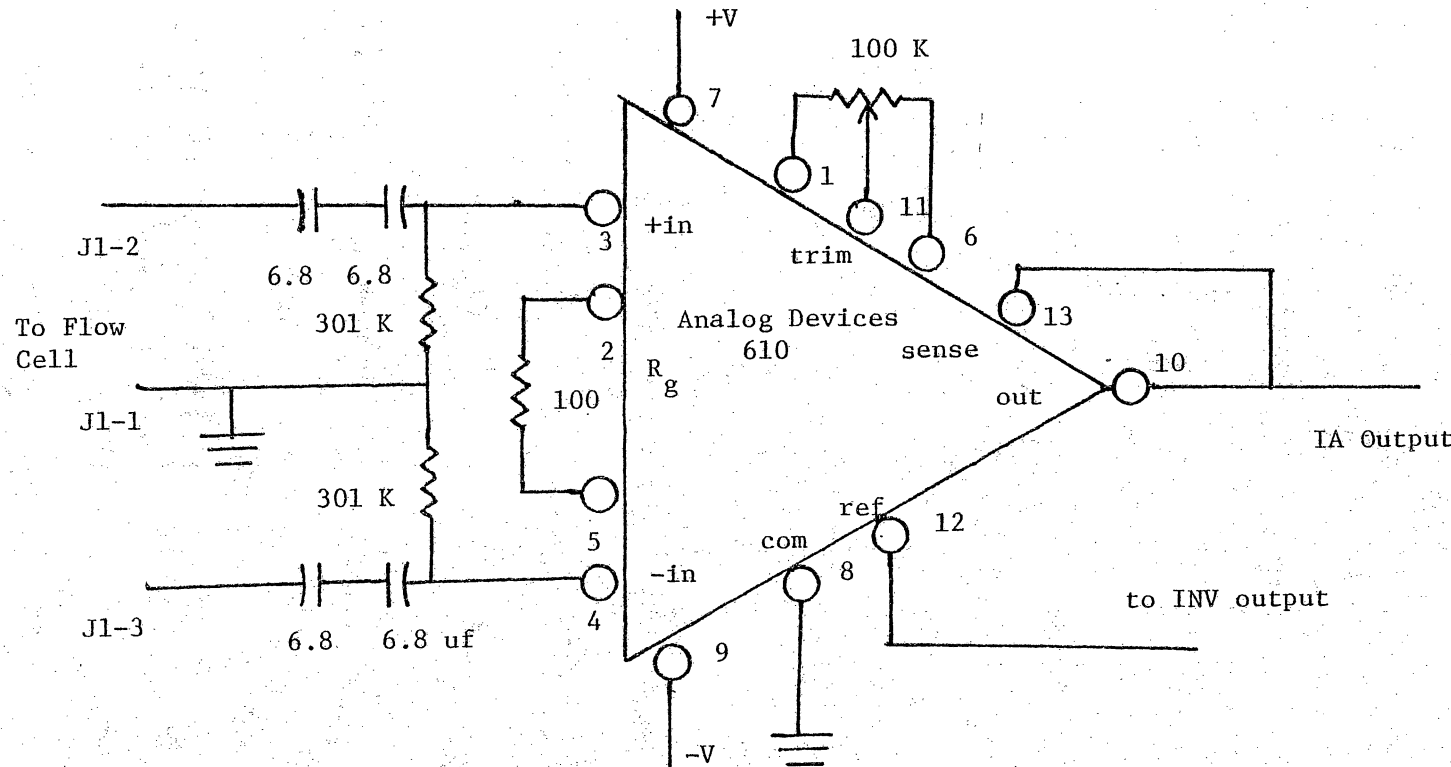


Figure 10. Input Instrumentation Amplifier

liquid so one would expect to see a net increase in response with smaller bores. Apparently other effects are more important under very small diameter conditions, and no flow related response was obtained at all. Larger diameters were tried, and a 1/16th inch bore was selected as a convenient compromise. Good response characteristics were obtained with this design.

The electrode surfaces are very important contributors to the cell resistance, which should be low to reduce noise. The smaller surface areas of polished metals are much less satisfactory than electrodes with large surface areas. Platinized platinum electrodes appear to be one of the best choices (17).

The electrodes in use are platinum wires which have been platinized by passing a current of 50 microamperes between the electrodes after constructing the flow detector cell. The platinizing solution was 2 percent by weight of platinic chloride in 2 N HCl. The direction of the current was alternated periodically during the several hour platinization period. The platinized electrodes worked well in comparison to others tried. A silver coated copper wire worked poorly until corrosion of the exposed copper at the tip of the wire occurred, confirming the fact that large surface area electrodes are result in lower noise levels. Good platinization of the electrodes is very

important to minimize the low frequency noise of the cell. An even coating of platinum black over the very slightly protruding tips of the platinum wire is necessary. If discolorizations or bare spots are present, poor noise performance is very likely to result.

The electrodes are made of approximately 1 cm lengths of 22 gauge platinum wire. Connecting wires are soldered to the platinum wire, after which it is inserted into the remaining two holes in the "cross" connector. These holes are at 90 degree angles to the enlarged flow path. The 22 gauge wire is just slightly larger than the existing holes in the slightly deformable plastic connector, resulting in a tight fit and no liquid leakage. Glue may be used to further attach the wires, but it is not necessary.

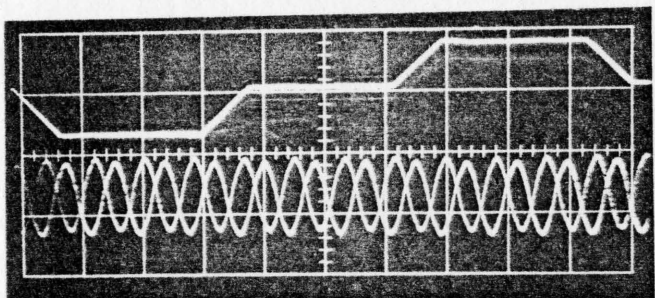
The current induced in the electrodes by the changing magnetic field is nulled by an equal current induced in the 30 gauge wire which is used to connect the far platinum electrode to the shielded twisted pair cable connecting the flow sensor to the flowmeter electronics. This wire is folded over the top of the flow cell and its position carefully adjusted for minimum deviation from a straight line at the VFC input under stopped flow conditions.

The ground reference for the input instrumentation amplifier is also important in reducing noise. Cheminert® CJ-3031 "tee" connectors, constructed in the same way as

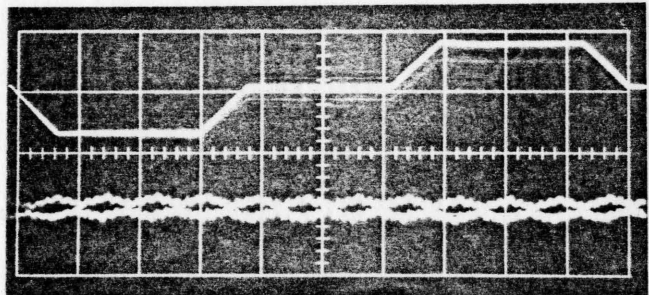
the flow sensor "cross" connectors, are used upstream and downstream from the flow sensor to make the ground connection. This arrangement minimizes the possibility that currents might flow through the liquid due to some external influence. Problems due to such current flows are often encountered in industrial systems where metal pipes are used. External current flow should not be a problem in this totally non-metallic system. Adequate groundings is still necessary to minimize the effects of 60 Hz line noise which is easily induced into any conductor by building wirings.

The instrumentation amplifier is responsible for the initial amplification of the signal and for rejecting as much noise as possible, primarily the 60 Hz power line induced signal which is common to both electrodes of the flow cell. The Analog Devices model 610 has a common mode rejection ratio of 110 db, a 300,000 fold voltage reduction in signals common to both inputs. It can be seen that this is not adequate with solutions of low conductivity as indicated in Figure 11. To improve the rejection of 60 Hz noise, a very selective bandreject filter was constructed using a Burr-Brown universal active filter, UAF-31 (see Figure 12). The output of this filter is acceptable for most solutions. Since this filter rejects only 60 Hz frequency components, it is followed by a low pass filter

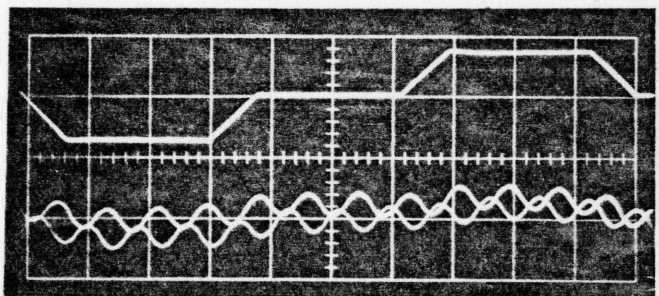
INSTRUMENTATION
AMPLIFIER OUTPUT
1 V/DIV



NOTCH FILTER
OUTPUT
1 V/DIV



VFC INPUT
1 V/DIV



TOP TRACES - MAGNET EXCITATION 10 V/DIV

HORIZONTAL SWEEP 20 MS/DIV

FIGURE 11. FLOWMETER SIGNALS WITH NO FLOW
OF .01 M NaCl

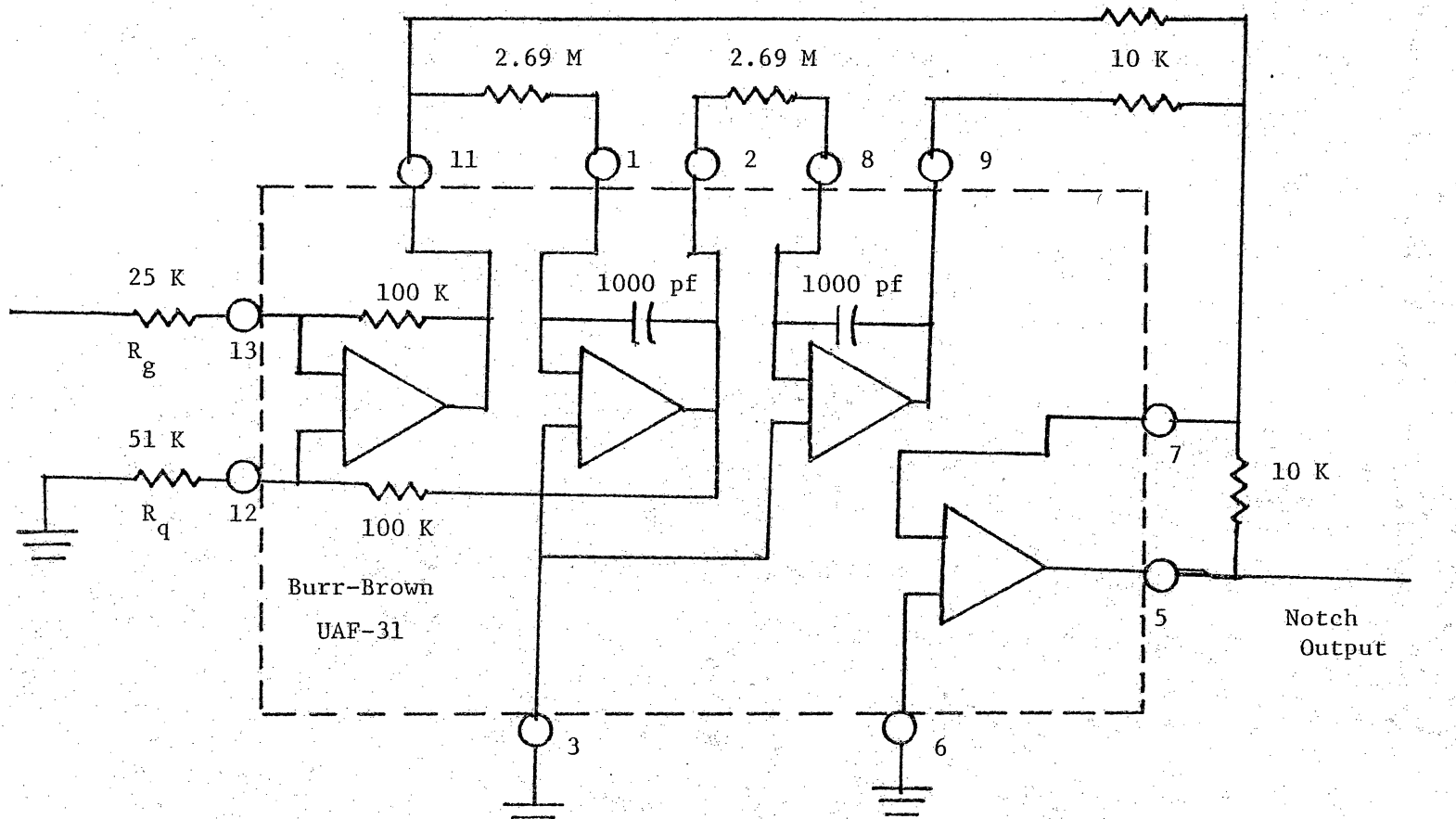


Figure 12. 60 Hz Notch Filter

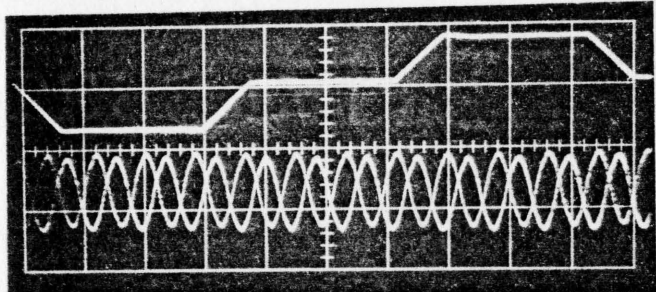
with a 3 db cutoff frequency of about 40 Hz.

It was found that the noise level of the system is heavily influenced by the conductivity of the solution in the flow cell. The experimental data of Figures 13 through 21 are summarized in Figures 22 and 23 where baseline levels and noise levels as the standard deviation of the observed signal are plotted vs. concentration of NaCl. It can be seen that low concentration results in high noise and high baseline levels. A possible reason for this characteristic is that the noise signals, seen to be primarily 60 Hz line interference, have a higher source impedance than the induced flow signals and thus are attenuated more by increased cell conductivity. Notice that the flow signal amplitude in Figure 24 is also attenuated at high concentration, which also supports this theory.

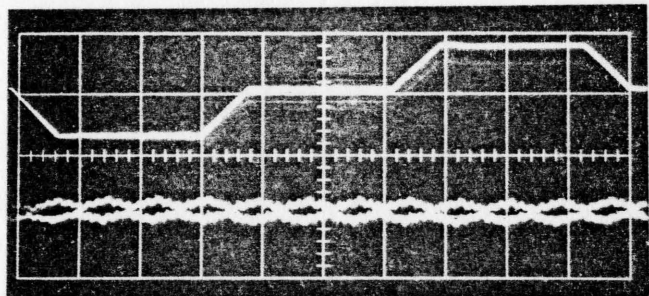
Conductivity of the solution does not appear in Equation 1 on page 27, which describes the flowmeter transducer. More detailed investigations show that conductivity dependent terms are not significant (18). Experiments have shown little conductivity dependence over a wide range of values (12). Conductivity determines the noise level of the system; thus, high conductivity improves the results.

The present results indicate that adequate

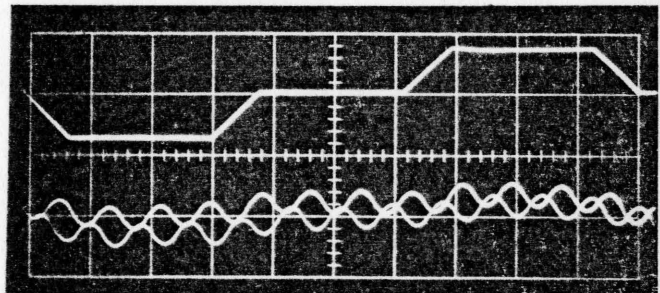
INSTRUMENTATION
AMPLIFIER OUTPUT
1 V/DIV



NOTCH FILTER
OUTPUT
1 V/DIV



VFC INPUT
1 V/DIV

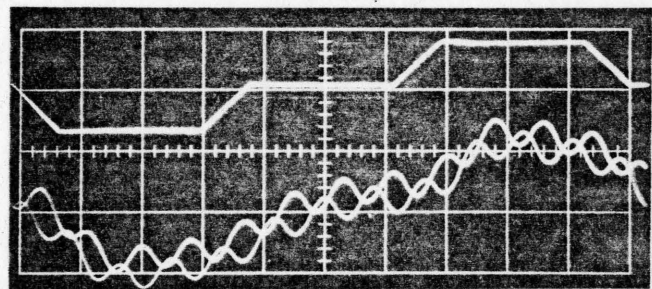


TOP TRACES - MAGNET EXCITATION 10 V/DIV

HORIZONTAL SWEEP 20 MS/DIV

FIGURE 13. FLOWMETER SIGNALS WITH NO FLOW
OF .01 M NaCl

VFC INPUT
1 V/DIV

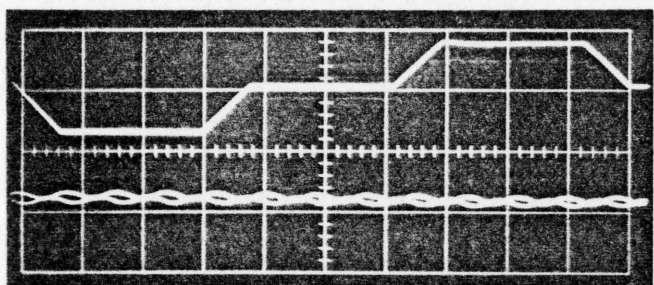


TOP TRACE - MAGNET EXCITATION 10 V/DIV

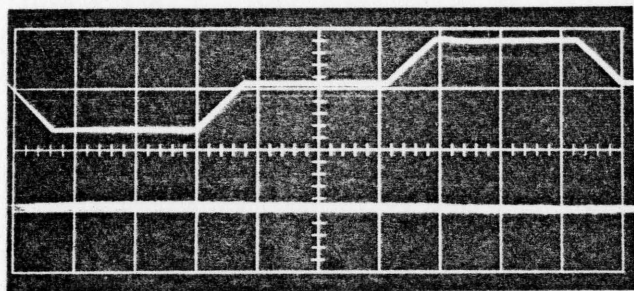
HORIZONTAL SWEEP 20 MS/DIV

FIGURE 14. FLOWMETER SIGNALS WITH A 50 CM
HEAD OF .01 M NaCl

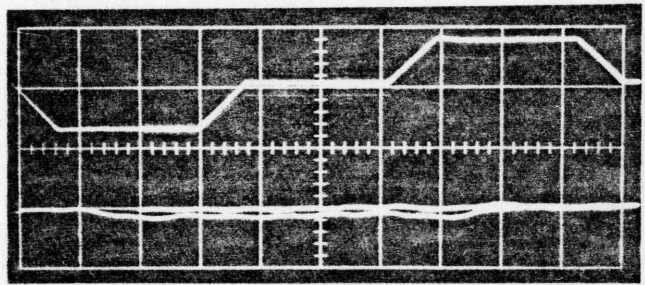
INSTRUMENTATION
AMPLIFIER OUTPUT
1 V/DIV



NOTCH FILTER
OUTPUT
1 V/DIV



VFC INPUT
1 V/DIV

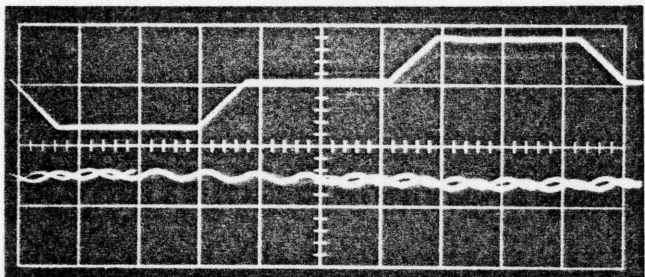


TOP TRACES - MAGNET EXCITATION 10 V/DIV

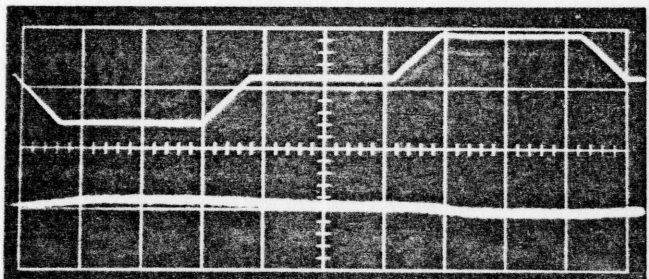
HORIZONTAL SWEEP 20 MS/DIV

FIGURE 15. FLOWMETER SIGNALS WITH NO FLOW
OF .1 M NaCl

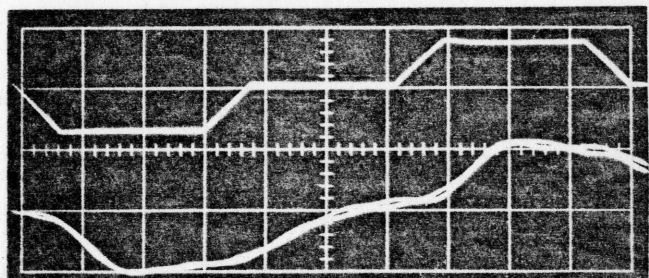
INSTRUMENTATION
AMPLIFIER OUTPUT
1 V/DIV



NOTCH FILTER
OUTPUT
1 V/DIV



VFC INPUT
1 V/DIV

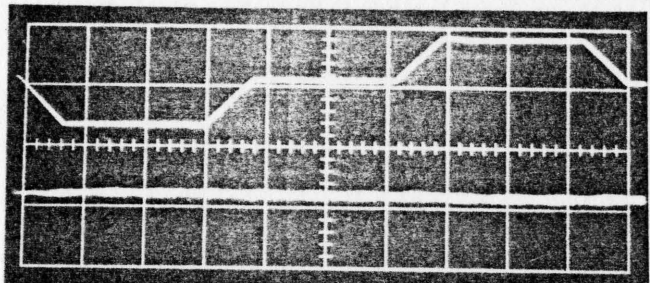


TOP TRACES - MAGNET EXCITATION 10 V/DIV

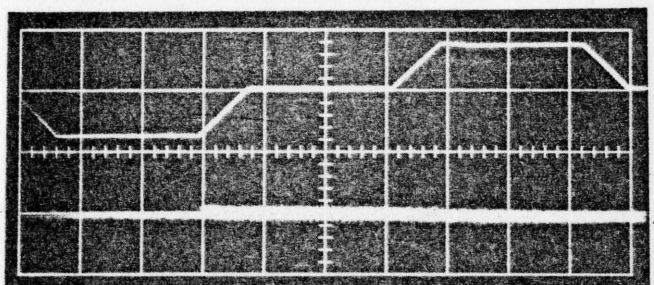
HORIZONTAL SWEEP 20 MS/DIV

FIGURE 16. FLOWMETER SIGNALS WITH A 50 CM HEAD OF .1 M NaCl

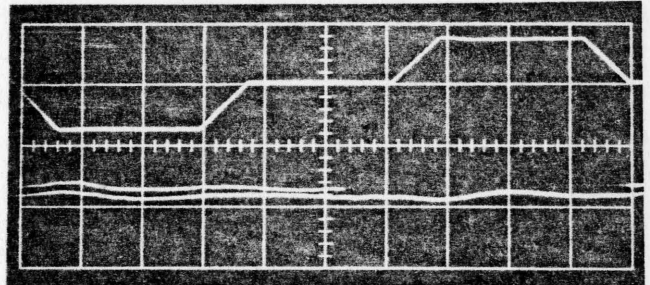
INSTRUMENTATION
AMPLIFIER OUTPUT
.5 V/DIV



NOTCH FILTER
OUTPUT
.5 V/DIV



VFC INPUT
.5 V/DIV

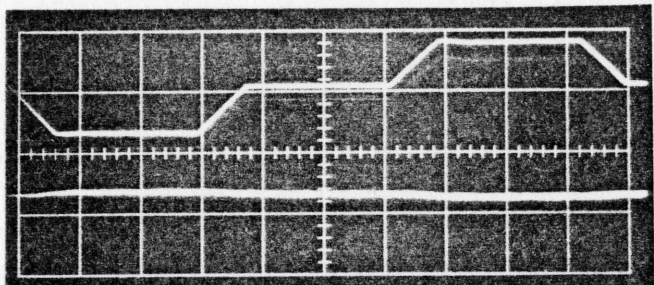


TOP TRACES - MAGNET EXCITATION 10 V/DIV

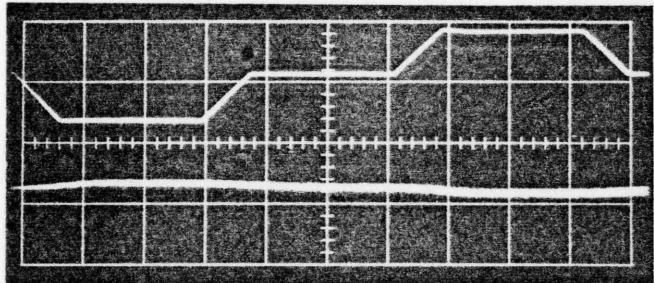
HORIZONTAL SWEEP 20 MS/DIV

FIGURE 17. FLOWMETER SIGNALS WITH NO FLOW
OF 1.0 M NaCl

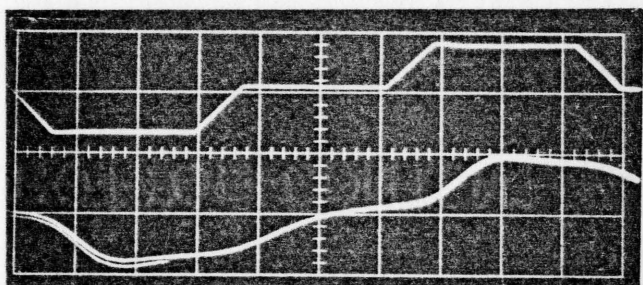
INSTRUMENTATION
AMPLIFIER OUTPUT
1 V/DIV



NOTCH FILTER
OUTPUT
1 V/DIV



VFC INPUT
1 V/DIV



TOP TRACES - MAGNET EXCITATION 10 V/DIV

HORIZONTAL SWEEP 20 MS/DIV

FIGURE 18. FLOWMETER SIGNALS WITH A 50 CM
HEAD OF 1.0 M NaCl

448

ARBITRARY
FLOWMETER
RESPONSE
UNITS

0

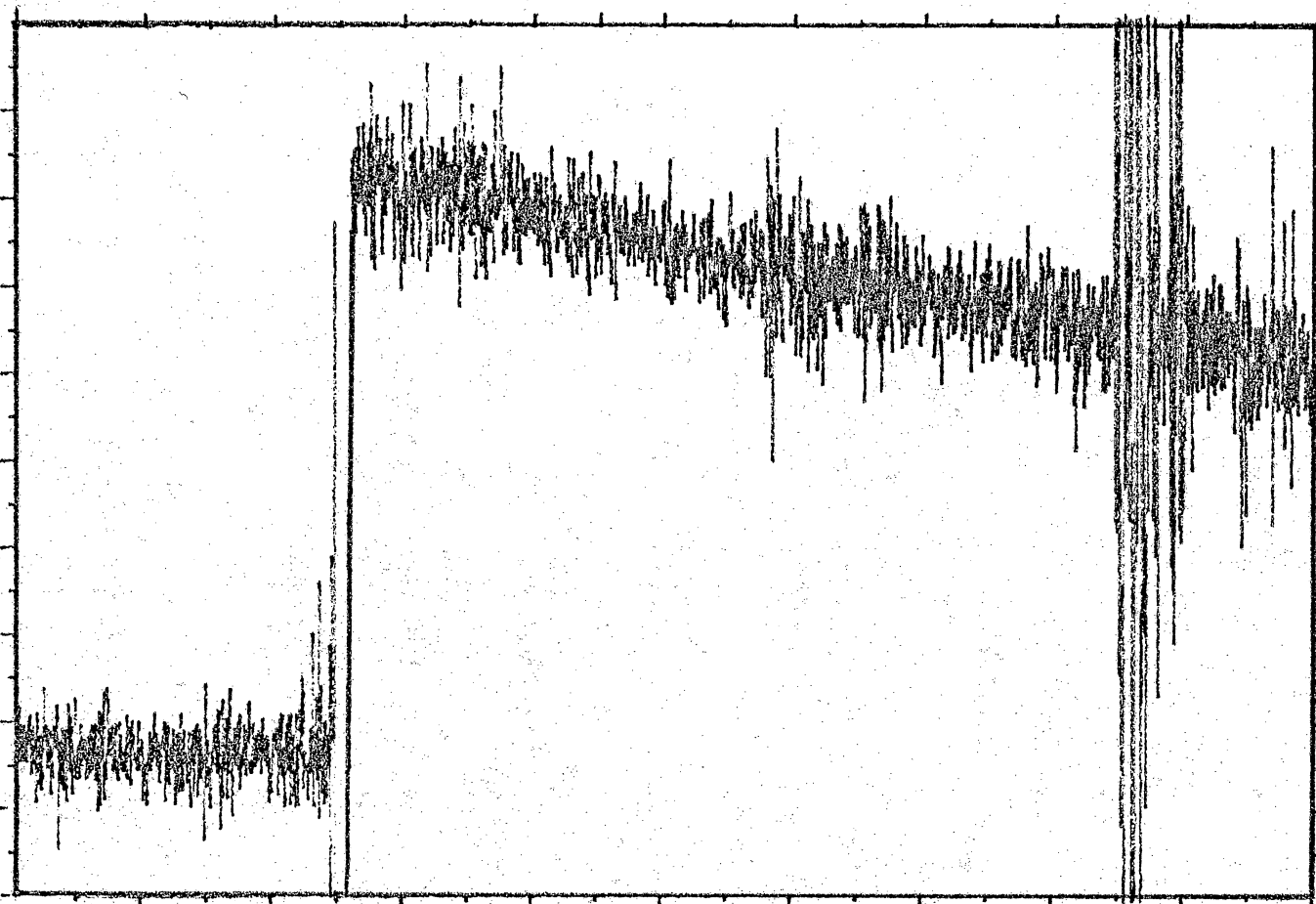


FIGURE 19. FLOWMETER RESPONSE VS TIME WITH .01 M NaCl

448

ARBITRARY
FLOWMETER
RESPONSE
UNITS

0

95

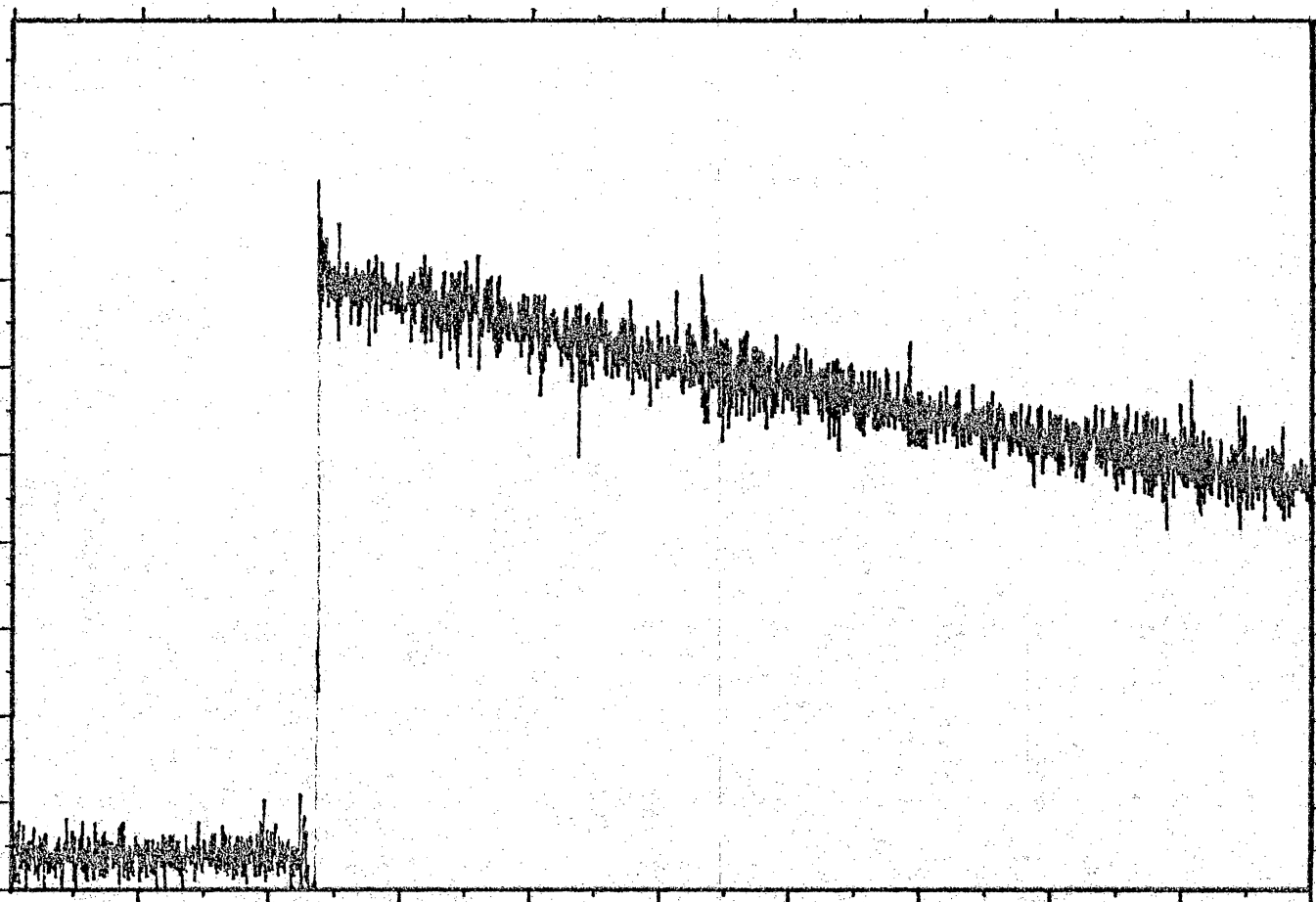


FIGURE 20. FLOWMETER RESPONSE VS. TIME WITH .1 M NaCl

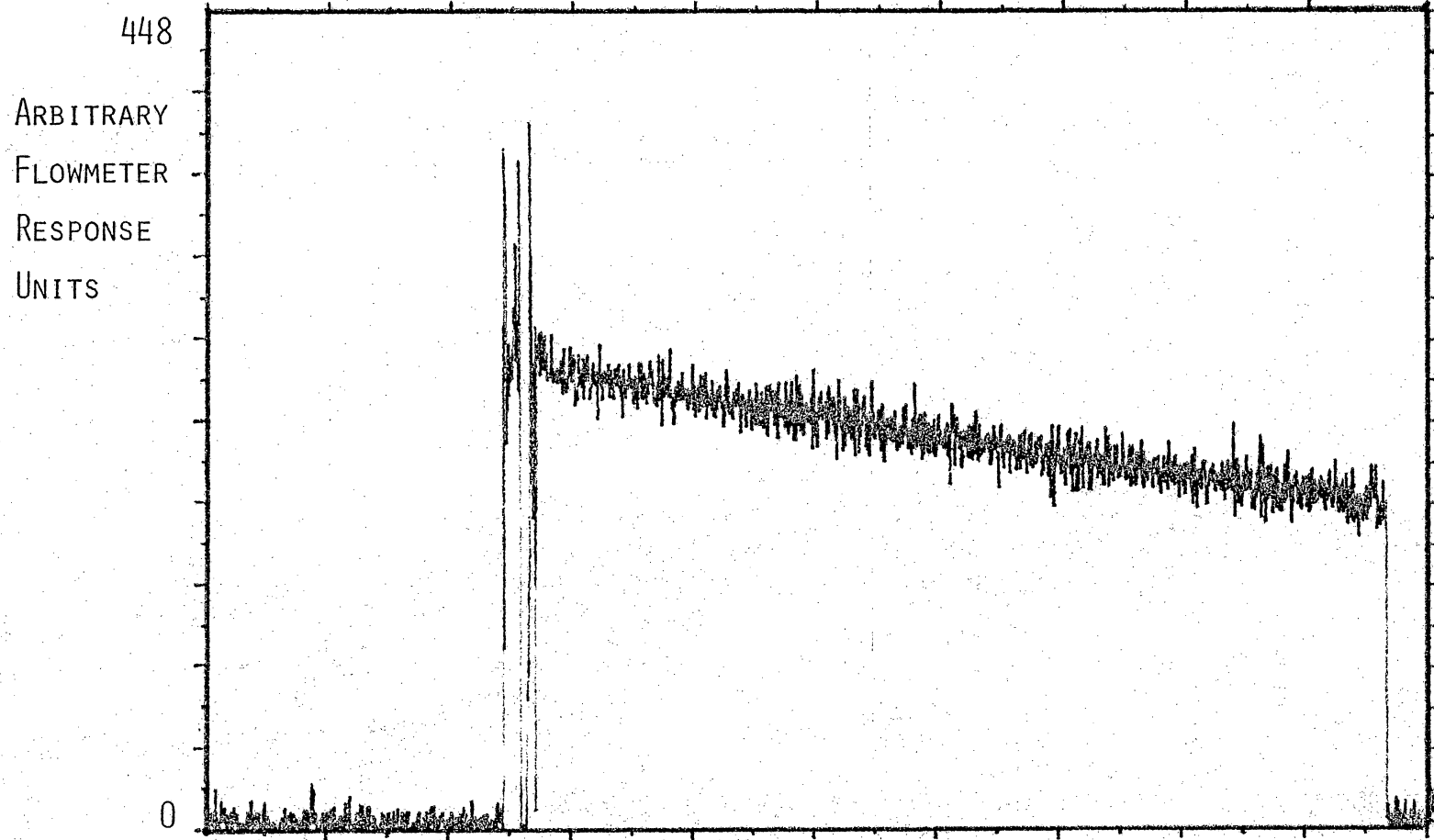


FIGURE 21. FLOWMETER RESPONSE VS. TIME WITH 1.0 M NaCl

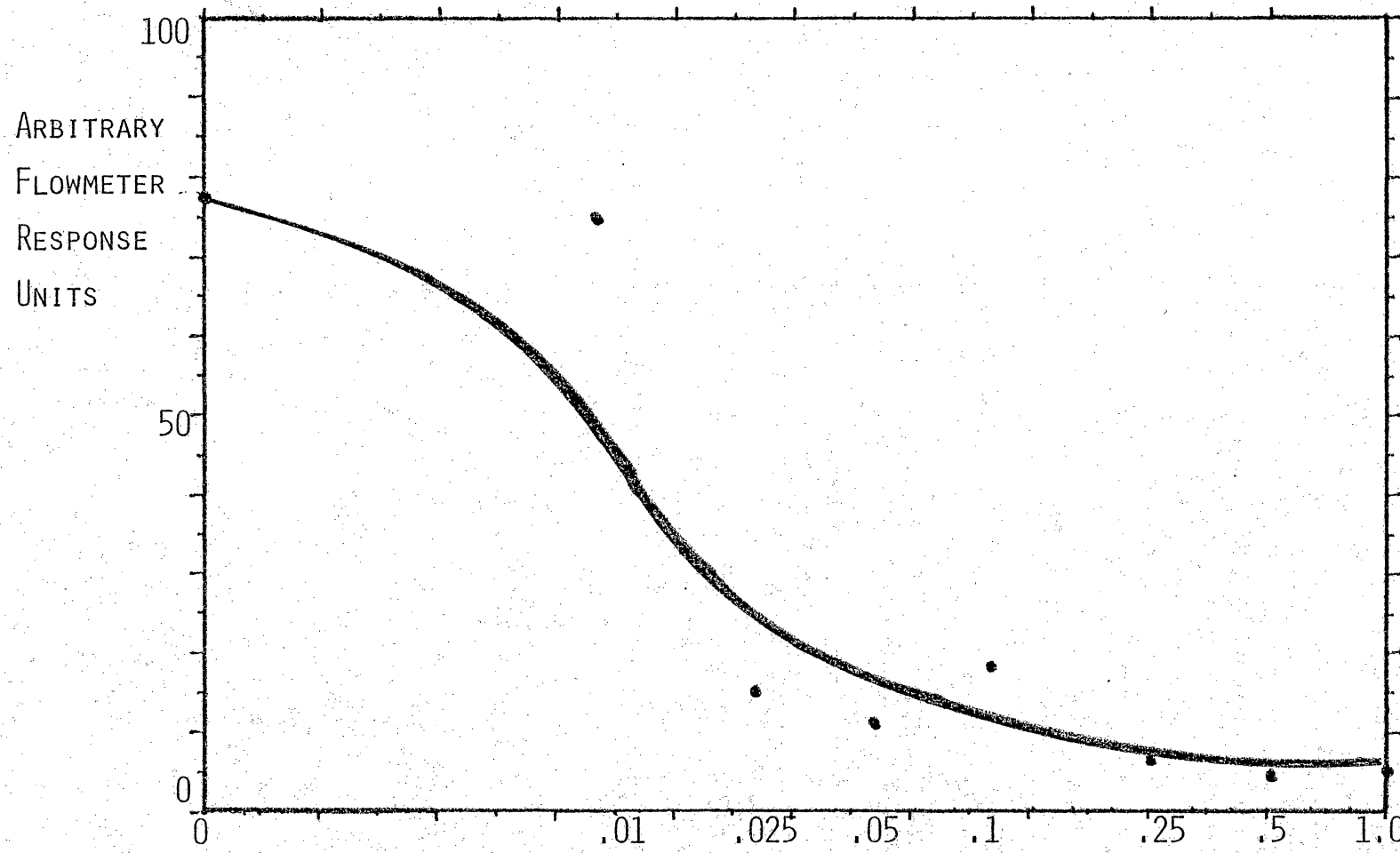


FIGURE 22. BASELINE SIGNAL VS. M NaCl

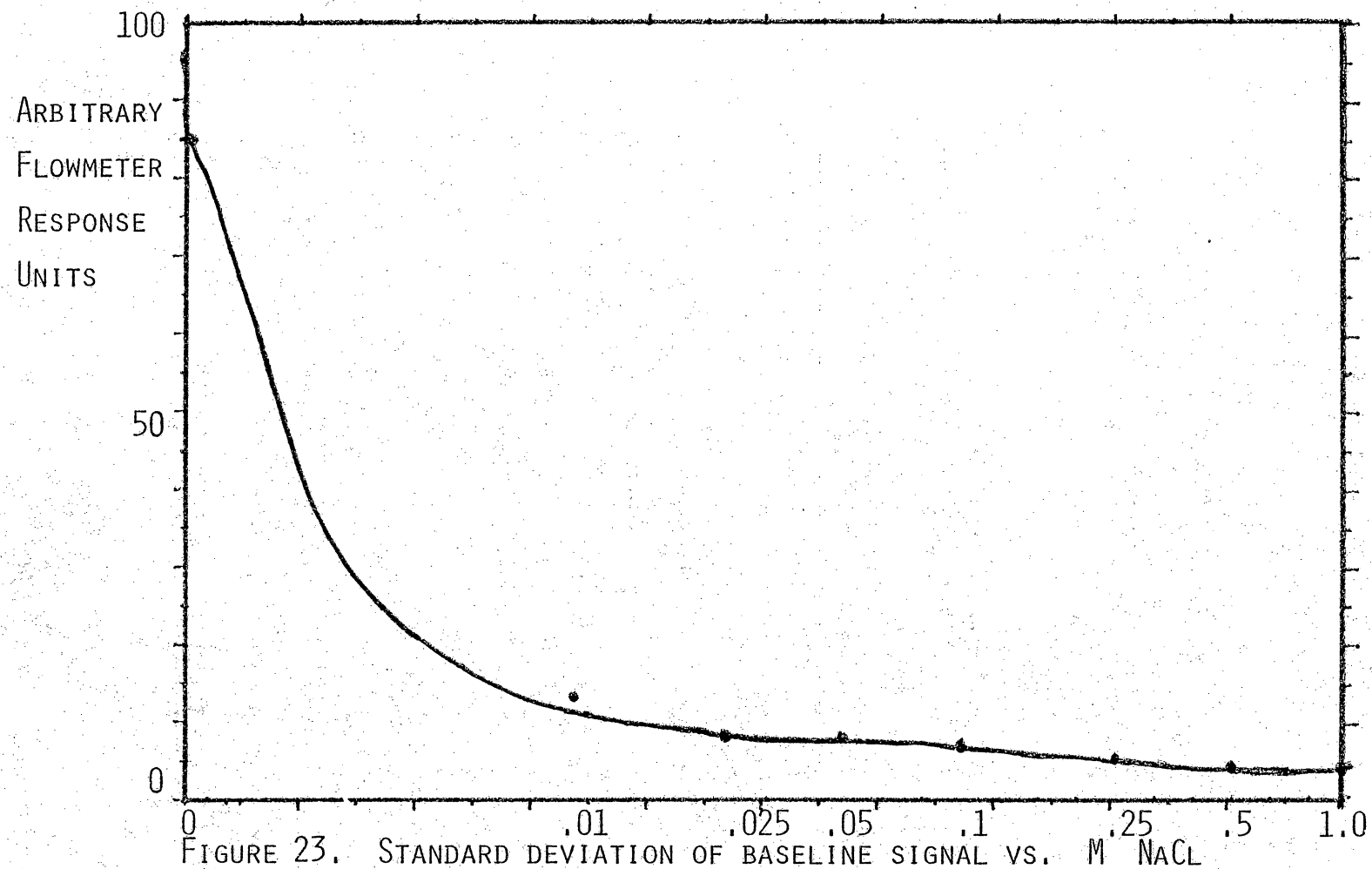


FIGURE 23. STANDARD DEVIATION OF BASELINE SIGNAL VS. M NaCl

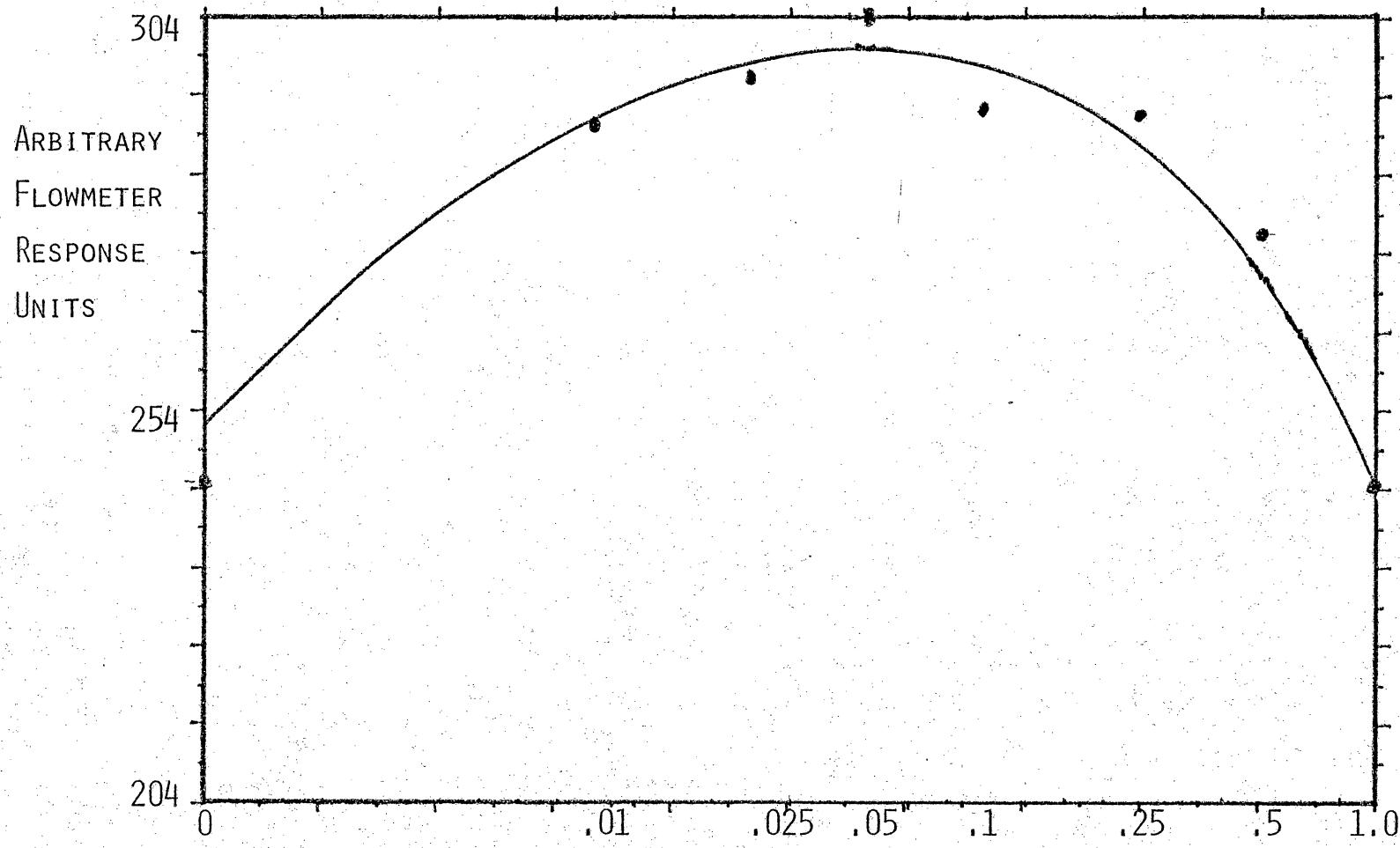


FIGURE 24. FLOW MINUS BASELINE SIGNAL VS. M NaCl

Performance is obtainable at concentrations greater than .002 M NaCl, and that the flowmeter may require recalibration if the concentration varies greatly. Notice that in Figure 24 the flow minus baseline signal is not constant with concentration. These limitations are not serious in practice since most reactions take place in buffered solutions with relatively constant conductivities which are in the range which result in low noise levels.

A possible reason for the less than optimum performance of the current flowmeter amplifier is that the input impedance of about 300 kilohms is much lower than previous designs which had impedances of 20 to 50 megohms. Unfortunately, this low impedance was necessary to supply the input bias current for the instrumentation amplifier.

At the output of the notch filter, the signal has been amplified by a factor of about 16,000, and has a widely varying DC component which results in amplifier saturation if further amplification is attempted. A high pass filter with a sharp cutoff around 2 or 3 Hz is needed. Construction of another low pass filter with a very long time constant (3 db down at 0.5 Hz), the output of which is subsequently subtracted from the shorter time constant low pass filter (3 db down at 40 Hz) resulted in the much more satisfactory circuit shown in Figure 25. The long term DC component of the signal is now subtracted, but the more

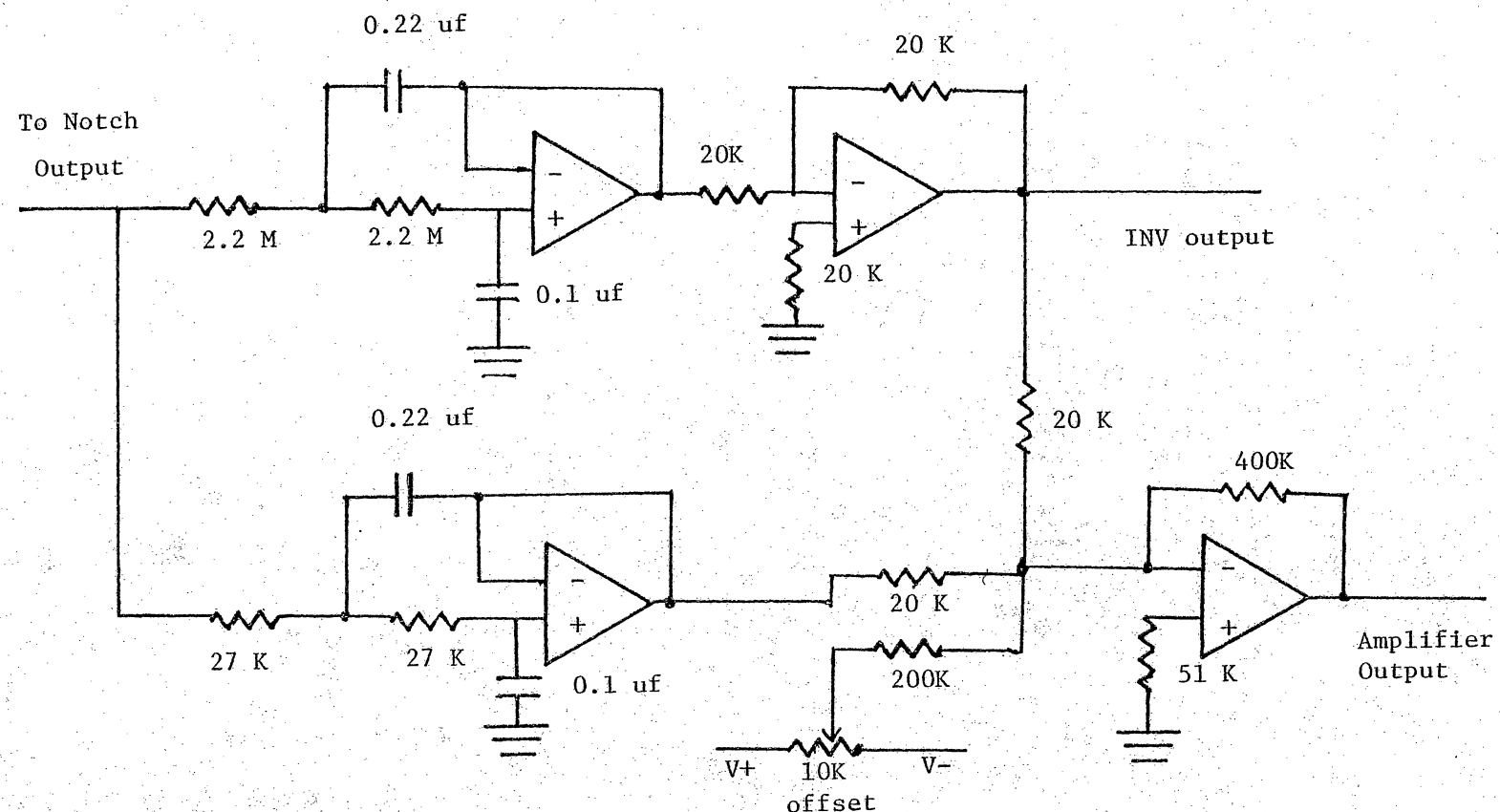


Figure 25. Low Pas Filters and Amplifier

quickly varying components due to the flow signals at about 4 Hz are not significantly affected, and further amplification is possible without saturation. The DC level of the VFC input signal is adjusted, by the offset potentiometer of Figure 25, to be above one volt and below six volts to accommodate the VFC's positive voltage input requirement and assure that momentary DC level transitions do not cause negative VFC inputs.

As indicated earlier, the waveform generator also provides signals to control the direction of counting by the real time clock counters and to interrupt the computer when one flowmeter excitation cycle has occurred. The generation of the count up and count down pulses from the VFC output are illustrated in Figure 26. The resultant counter value is stored in the processor's memory, after which the counter is cleared in preparation for the next excitation cycle.

A very substantial amount of noise, primarily due to the remaining DC level shifts in the flowmeter signal which were not removed by the analog signal processing electronics, is removed by averaging the flowmeter signal over a period of 16 seconds. This is accomplished by entering each successive value obtained at interrupt time into a 64 point circular buffer, overwriting the value obtained 65 points previously. To further improve the

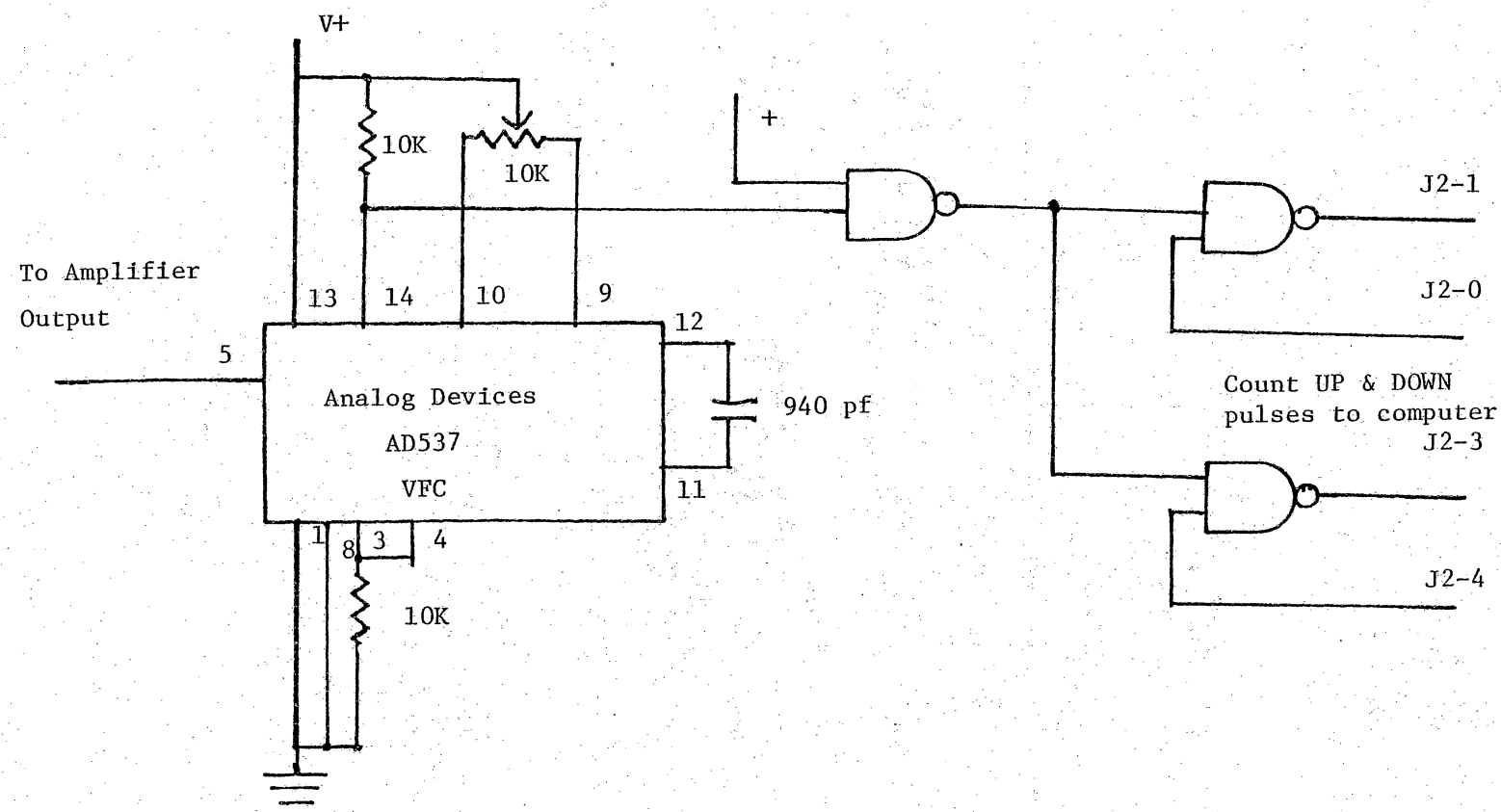


Figure 26. Voltage to Frequency Converter and Logic

stability of this average, the value entered into the buffer is never allowed to differ from the average value by more than 32 units. This restriction causes response to rapid changes to be very slow, but rapid changes in fluid supply conditions are not encountered under normal circumstances. In addition, large, rapid changes in the desired flow rate are not essential for adequate performance of the instrument. This limitation is necessary because the DC level of the flowmeter signal occasionally shifts violently in response to external noise pulses. If entered into the circular buffer, these large noise values would influence the average value for the next 16 seconds before they would be replaced by a new value, resulting in very poor flowmeter performance because the noise values are often many times the amplitude of the normal values encountered.

The circular buffer is summed after entering each limited difference value and the double precision result is stored in memory for use by other sections of the software.

In addition to generating the average flow related signal at each cycle completed interrupt, a valve control signal is developed every fourth excitation cycle, approximately once each second. The control signal is the sum of the difference between the averaged flowmeter signal and the goal or setpoint value and a negative multiple of

the derivative of the averaged flowmeter signal. This causes the valve to be driven in a direction which will reduce the error term. The total flow regulation system has a considerable time constant, ie., the effect of the control signal is not apparent for several seconds. Because of this, the derivative signal is subtracted from the error signal, producing less corrective action when the averaged flowmeter signal is changing toward the desired value and more if it is going in the opposite direction. This procedure results in a more stable system with greatly reduced overshoots of the goal or set point. It operates in much the same manner as the damping control of many chart recorders.

One of four different valve movement values is selected each second by the controller software. If the accumulated error control value is small, no movement of the valve is made. Movements of approximately 2, 8, or 30 degrees of rotation are selected as the error value increases.

The control algorithm was developed empirically by observing the effects of changing the parameters of the algorithm. It falls into the class of PID (Proportional Integral Derivative) algorithms, common in engineering and process control applications (7). A theoretical and mathematical optimization of the algorithm is not necessary

because the common sense, empirically derived algorithm produced satisfactory control and avoided the excessive effort required to translate the mathematically obscured theory of process control textbooks into practical programs.

3. Electronic Balance

An Ohaus model 300 electronic balance was employed to calibrate and evaluate the operation of the flowmeter. Basically, the computer reads the balance periodically and calculates the difference in weight between readings, resulting in the flow rate which is stored for later comparison with values simultaneously obtained from the flowmeter. In practice, this simple procedure results in an excessive amount of noise because differences of less than 0.1 grams in 100 grams are being observed. In addition, it was found that the update rate of the balance's BCD interface varied between 0.5 and 2.5 seconds, depending on the total weight on the balance and other unknown factors. This variability contributes largely to the error. For example, if measurements were taken at 30 second intervals, it is possible that the first value represents the weight 2.5 seconds earlier than intended. If the final measurement reflected the current weight value, the flow rate determined would be in error by $2.5/30.0$ or 8 percent. This represents the maximum error because the final measurement is also likely to be late by a similar amount. These problems were significantly reduced by averaging the weight values over 6 second periods before taking the differences, as explained later.

Ohaus's optional BCD interface for their balance consists of 5 four bit latches and some control logic which stores the information presented on the balance display bus and makes it available to external devices. In addition, a balance done line signals the completion of loading of new data into the latches. This results in 21 output lines from the balance. A balance buffer, shown in Figure 27, was constructed to conserve parallel interface lines. The buffer consists of eight four-bit registers which can be loaded by the balance. The computer reads the registers sequentially selecting one of the eight, which then presents its data on four bits of a parallel input port, until all digits stored in the registers are obtained. The inputs of the balance buffer registers are connected to the balance display bus by replacing one of the latches of the Ohaus BCD interface by an integrated circuit socket with jumpers from the input pins to the output pins. The addresses of the balance buffer registers are selected by a 74148 priority encoder whose inputs are connected to the load latch signals of the Ohaus BCD interface. Thus, the balance buffer latches are loaded under control of the balance whenever a new weight value is available. After the balance done signal interrupts the computer, the balance buffer may be read by the computer at any time. Naturally, this reading should be done as soon as possible.

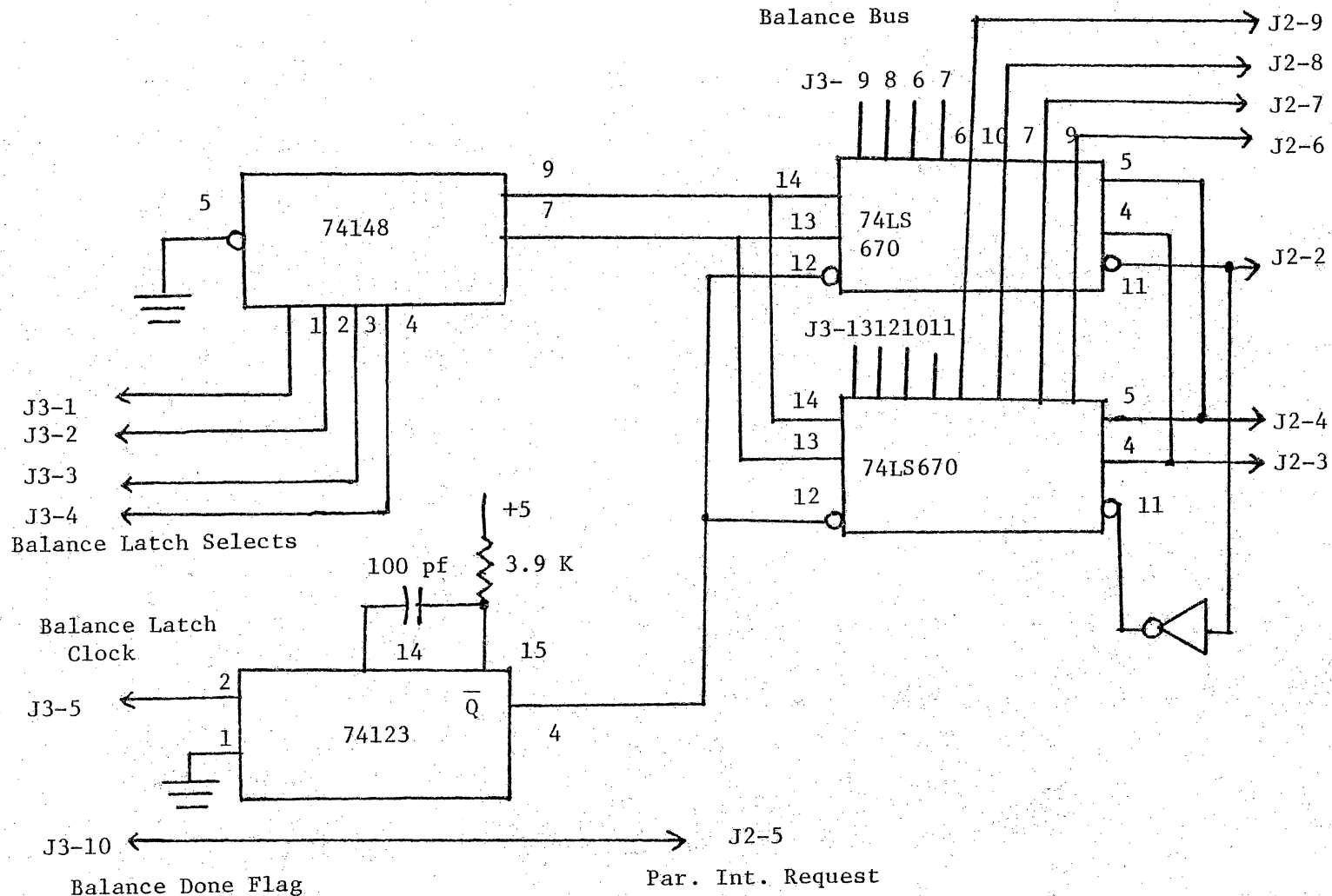


Figure 27. Balance Buffer

to avoid the possibility that the balance may update the balance buffer registers during the reading process, resulting in erroneous values. Because the balance buffers are updated at a maximum rate of 2 Hz, no problems in reading the balance buffer values before they are changed are anticipated.

The balance software is organized as a Forth task for minimum effect on the rest of the software operation. A task is a self contained software construct which supervises a specific operation. Tasks are discussed in the data acquisition section. The interrupt service routine, when activated by the balance done interrupt from the balance interface, transfers the information in the balance buffer to an eight byte buffer in the balance task table before re-enabling the processor interrupts. This assures that the information is read by the computer before the balance updates the values in the balance buffer registers, even if the computer is busy with another high level task. The interrupt service routine also clears the balance task status word so that the high level code of the task will be executed when the microprogrammer loop reaches the balance task.

When execution of the balance task is enabled, the BCD digits stored by the interrupt service routine are multiplied by the power of ten corresponding to their

significance. The resultant values are then summed, leaving the binary representation of the weight on the balance pan on the stack. This value is then stored in the balance task table, making it easily available for use by other tasks. The balance task is then deactivated by setting its status word to -1 via the STOP definition. Whenever the interrupt service routine clears the balance status word following another balance done interrupt, the complete process is repeated. In this manner, a variable is always available in the balance task table which represents the current weight on the balance pan.

Because determination of the flow rate requires accurately timed observations, the balance task, with its variable report rate, cannot be used to perform this function. Consequently, the operations required have been incorporated in one of the flowmeter tasks. Flowmeter interrupts occur at a rate very close to 4 Hertz, under control of a stable crystal oscillator, providing the accurate time base required. Two operations are involved, the first being the maintenance of an average weight as reported by the balance over the last six seconds. This involves picking up the balance value from balance task four times a second and inserting it into a circular buffer of 24 points. The average value of this buffer is then calculated and stored in the balance task table for use by

other tasks. This value does not represent the current value of the weight on the balance, but that of about four seconds earlier. The circular buffer contains values from at least two balance updates and perhaps up to ten updates. When the balance value is not changing rapidly, the average is a good indicator of the current weight. When the weight is changing, the average value of the last six seconds will be obtained, keeping in mind that even the balance output is slightly behind in reporting the true weight. Thus, considerable noise is to be expected in the flow rate values.

To achieve a more current value of the flow rate than would be obtained by taking the difference in weights every 30 seconds, another circular buffer with a length corresponding to 30 seconds can be maintained. Every time a new weight value is added to the buffer, the value it replaces can be subtracted from the new value, resulting in the change in weight, or flow rate for the last 30 seconds. Thus, every second or so, a new flow rate value may be obtained which represents the average flow rate of the last 30 seconds. The 30 second period was chosen to minimize the noise due to the balance update period uncertainty and provide a reasonable difference in weights. Much smaller intervals are subject to quantization errors due to the digital nature of the process. Much longer intervals would

not be sensitive to short term variations. Fifteen second periods could have been chosen to match the averaging period of the electromagnetic flowmeter, however more noise in the balance flow rate would be observed and quantization errors would be larger than those experienced by use of the 30 second interval.

The 30 second flowrate value is then multiplied by two and stored in the balance task table, making the flow rate in one-hundredths of a milliliter per minute available to other tasks. The buffers required to calculate the averages and differences are maintained in the unused dictionary area of the balance task.

Practical considerations make it impossible to check the short term accuracy of the balance flowmeter. The average flow rate over a period of minutes can easily be determined by the weight difference between the beginning and end of the period. Assuming a constant flow rate, the short term and long term flow rates should match. Table I presents the results of several runs at different flow rates as maintained by the electromagnetic flowmeter. Runs 1 through 7 show a consistent error of about one-half of one percent. Part of the error can be attributed to the fact that the flowmeter time base, which controls the balance reading interval, is fast by about 3.3 ms per second because the waveform generator uses binary rather

Table I. Initial Balance Flowmeter Error

Run#	Wt. Flow gm/min	Bal. Flow gm/min	Fractional Error
1	3.155	3.135	-.0063
3	8.064	8.021	-.0053
4	5.483	5.448	-.0064
5	10.157	10.104	-.0052
6	12.662	12.591	-.0056
7	14.918	14.839	-.0053

than decimal counters. This means that a second for the balance flowmeter is only about 99.67 percent of a real second, accounting for about half of the observed error. This error is corrected by adding 0.33 percent to the output flow value. Note that at flow rates of less than 3 ml/min, nothing is added to the flow value because the correction is less than one unit (one-hundredth of a ml/min) in which values are reported. Approximately 2 to 3 tenths of a percent of error are left unaccounted for.

Evaporation of the liquid in the collection container is a source of error which affects both the long term and short term flow rate measurements equally. An evaporation rate of 0.017 sm/min was observed at a room temperature of 24 degrees Celsius using a beaker as a collection vessel. Therefore, all flow rates measured by the balance are about 2 units or 2 hundredths of milliliter per minute low. A correction for this would need to be determined empirically because the evaporation rate is dependent on temperature, humidity, liquid surface area and local air movement. The evaporation problem was solved by substituting a narrow mouth collection vessel for the beaker. No weight loss was observed during a 20-minute test period.

A subsequent test run is reported in Table II using a narrow mouth collection vessel and employing correction of the time base error. Note that the error observed is about

Table II. Corrected Balance Flowmeter Error

Run#	Wt. Flow sm/min	Bal. Flow sm/min	Fractional Error
1	0.003	0.001	-
2	1.623	1.617	-.0037
3	4.038	4.025	-.0032
4	6.355	6.343	-.0019
5	8.560	8.553	-.0008
6	10.949	10.927	-.0020
7	13.456	13.428	-.0021
8	13.366	13.335	-.0023
9	15.687	15.628	-.0038

two tenths of a percent except where the correction's fractional part is significant, but is not added because integer arithmetic is being used. This occurs below 3 ml/min.

The linearity of the average values is excellent over the flow range observed. It was observed that some runs exhibited poorer control than others. The factor common to these runs was that the capillary valve was near its extreme open position where small changes in position make large changes in flow. To avoid this problem, the driving gas pressure should be adjusted so that the flow rate desired occurs when the valve is approximately one eighth to one half open. In this range, flow control is much better.

4. Flowmeter and Controller Performance

The performance of the complete flowmeter and controller system, including the controller algorithm, was evaluated by executing 18 flowmeter calibration runs over a period of several days with several salt water concentrations and experimental configurations. Each calibration run consisted of a sequence of ten goals or flow setpoints. After each flow goal was achieved, flowmeter and balance readings were obtained every second for five minutes, resulting in information from which calibration curves for the flowmeters could be constructed. In addition, the effectiveness of the flow control at various rates can be obtained, as well as information about the precision of the calibration curves and their day-to-day reproducibility.

Frequent calibration of the current system will be necessary because of its many analog components. Adjustments are required to compensate for component tolerances. Temperature coefficients may be expected to be significant since many components are being operated at high gain or near their performance limits. The magnet excitation requires a moderately high power amplifier which is inherently not as stable or insensitive to temperature changes as lower power devices. The flowmeter is pushing

the state of the art, generally achieving flow control of better than ± 0.25 ml/min over the range of 2.5 to 25 ml/min. In the probable operational range of the instrument, 10 to 25 ml/min, a better than one percent relative standard deviation of the controlled flow was achieved. Most of the previous electromagnetic flowmeters were designed for biological applications where flow was measured in liters per minute. This flow level produces much greater signals, consequently random noise is not such a significant matter although other noise sources, such as physiological potentials, are significant. The acceptable noise level of these devices, 1 or 2 percent of full scale, is in the 10 to 25 ml/min range which is nearly full scale on the current flowmeter system.

James (13) reports the best flowmeter performance values found in the literature. A stability of ± 0.5 ml/min a linearity of ± 0.25 ml/min was observed using his design. Very carefully designed vacuum tube equipment was used at flow rates less than 50 ml/min. Thirty years later, with the benefit of vastly improved electronic technology but minimal resources for design and construction, the much more difficult task of controlling the flow achieved a maximum deviation from the desired flow rate of ± 0.5 ml/min at half the earlier flow rate (± 0.2 ml/min calculated from the relative standard deviation) and

a typical deviation of the individual flow values from a least squares line of ± 0.1 ml/min over a range of 2.5 to 25 ml/min. The flow response exhibited a slight decrease in amplitude and reduced noise levels with increasing conductivity of the fluid being measured. The slope of the flowmeter calibration curve deviated a maximum of 2 percent from the average value over 10 calibration runs of 0.1 M NaCl, as reported in Table III. The relative standard deviation of the observed slopes is 1.0 percent for flowmeter 1 which was controlling the flow and 2.1 percent for flowmeter 2 which exhibited more noise than flowmeter 1.

This good reproducibility of the flowmeter calibration parameters indicates that calibration of the flowmeter is necessary only when major changes in conditions are encountered. Until more repeatability data is obtained, calibrations should be done at least once per day and every time the apparatus is turned on. Naturally, each reagent will require its own calibration curve.

After some experience with the flowmeter system, it became apparent that even greater sensitivity was required because lower flow rates were to be used. A doubling of the flowmeter sensitivity was achieved by adding a second solenoid on the opposite side of the flowmeter cell from the original. This doubled the field experienced by the

Table III. Flowmeter Calibration Run results for
0.1 M NaCl

Run I. D.		FM1 Slope	Coeff.	FM2 Slope	Coeff.
30 20	3 SEP	.0980	.9998	.1177	.9999
48 21	3 SEP	.0984	.9999	.1163	.9992
9 23	3 SEP	.0983	.9999	.1162	.9999
56 17	4 SEP	.0984	.9999	.1203	.9989
40 20	4 SEP	.0980	.9999	.1131	.9997
7 22	4 SEP	.0987	.9999	.1141	.9999
29 17	5 SEP	.0991	.9999	.1139	.9998
56 20	5 SEP	.1004	.9997	.1199	.9997
49 21	5 SEP	.0966	.9997	.1155	.9997
8 0	6 SEP	.0973	.9999	.1159	.9999

charges in the flowing stream, thus doubling the detected potential. The noise level remained the same since it is not proportional to the applied field. The performance discussed earlier is now obtained at flow rates of 1 to 10 ml/min.

Figure 28 shows the resultant calibration curve. The flowmeter slopes are approximately twice those reported in Table III. Figures 29 to 31 show the response of flowmeter #1, flowmeter #2, and the balance to various flow rates over a 5 minute period. Table IV summarizes this information, giving the minimum and maximum flow rates detected by the balance during the observation period as well as the relative standard deviations of the balance and flowmeter signals. At flow rates greater than 3.0 ml/min, typical relative standard deviations are less than two percent and the maximum deviation from the average flow rate is rarely greater than ± 0.2 ml/min.

Flowmeter Calibration Run of 118 35 28 16 13 DEC 1980
+ - Flowmeter # 1 * - Flowmeter # 2

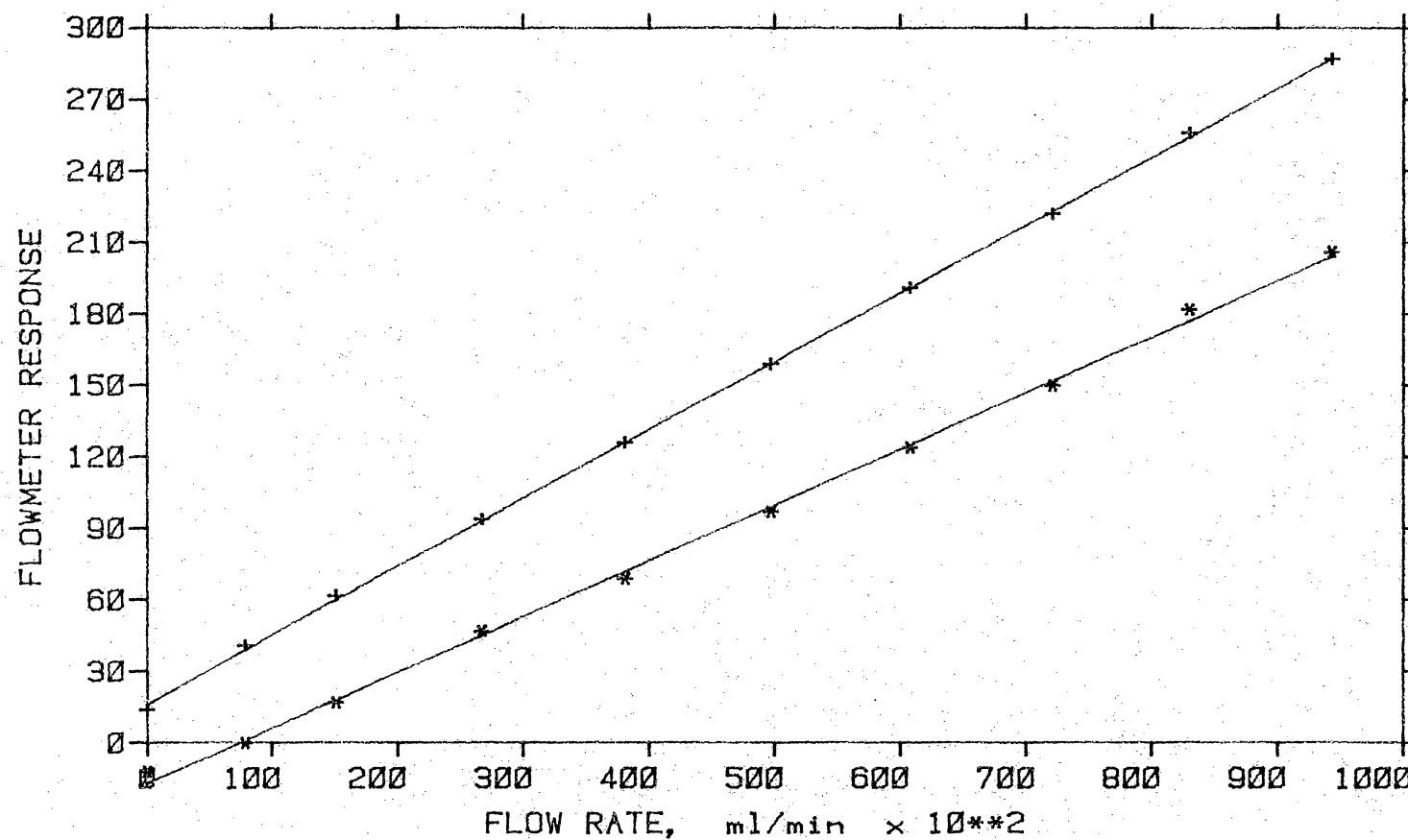


Figure 28. Flowmeter Calibration Curve, 0.1 M NaCl

Flowmeter Calibration Run of 118 35 28 16 13 DEC 1980
Flowmeter # 1

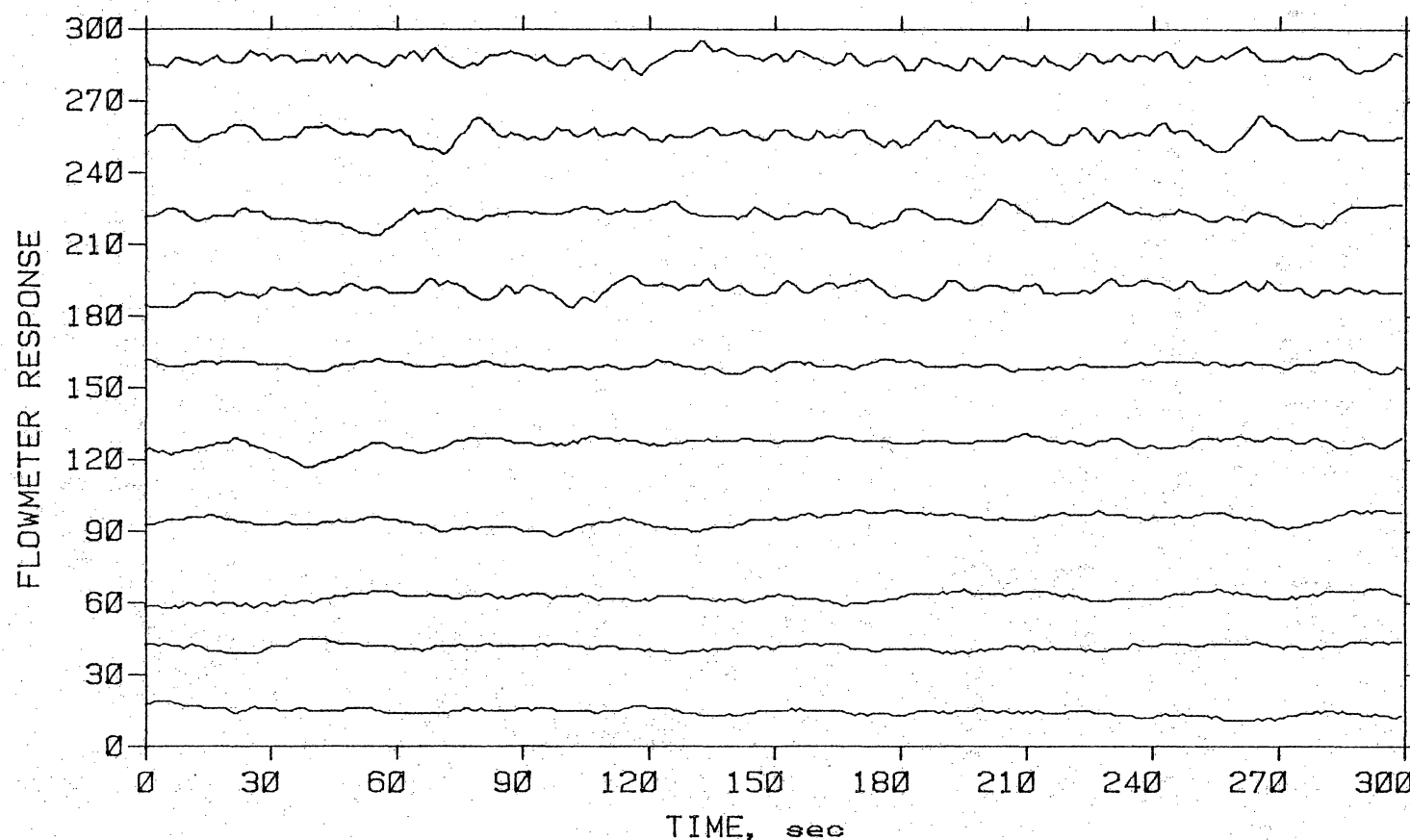


Figure 29. Flowmeter #1 Response, 0.1 M NaCl

Flowmeter Calibration Run of 131 35 28 16 13 DEC 1980
Flowmeter # 2

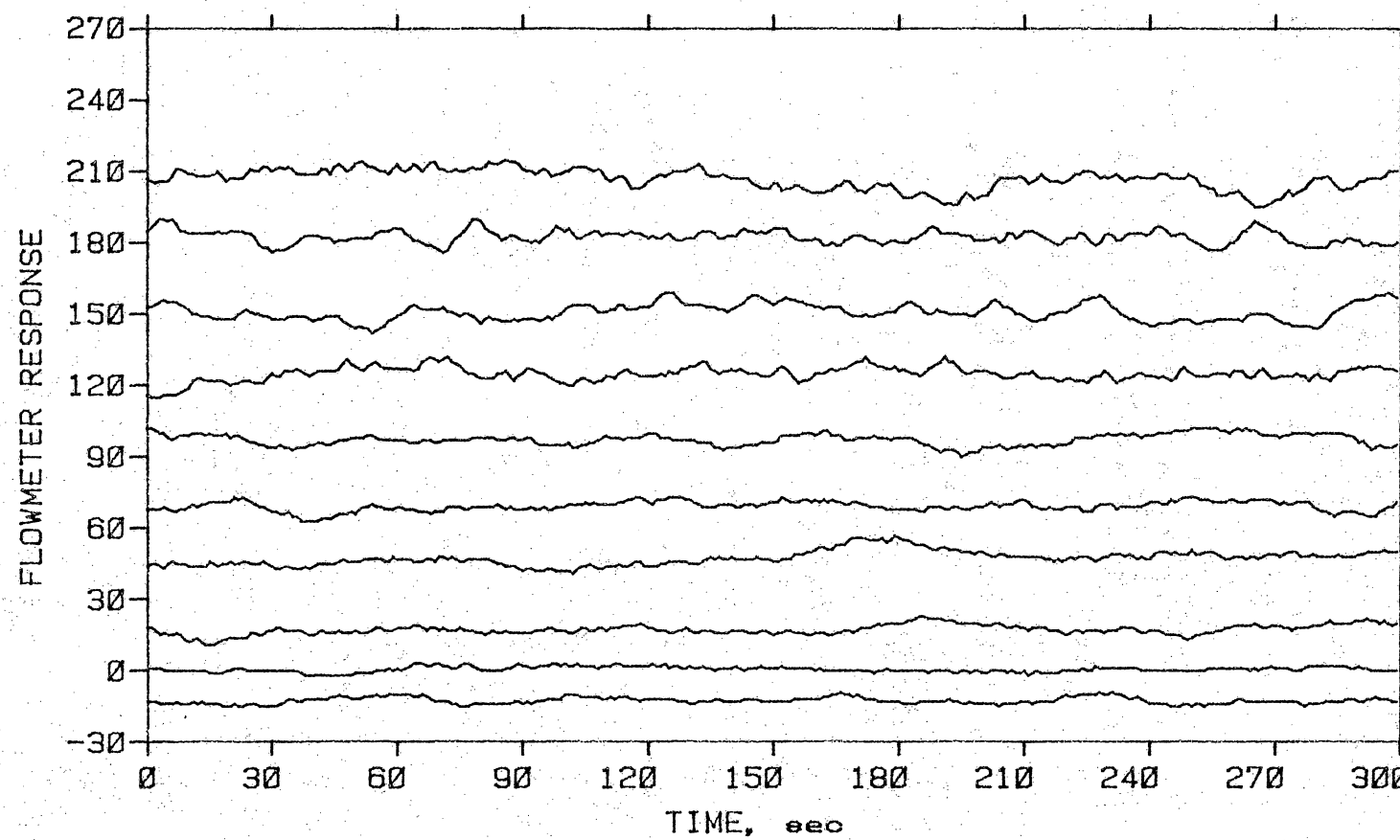


Figure 30. Flowmeter #2 Response, 0.1 M NaCl

Flowmeter Calibration Run of 142 35 28 16 13 DEC 1980
Balance Response

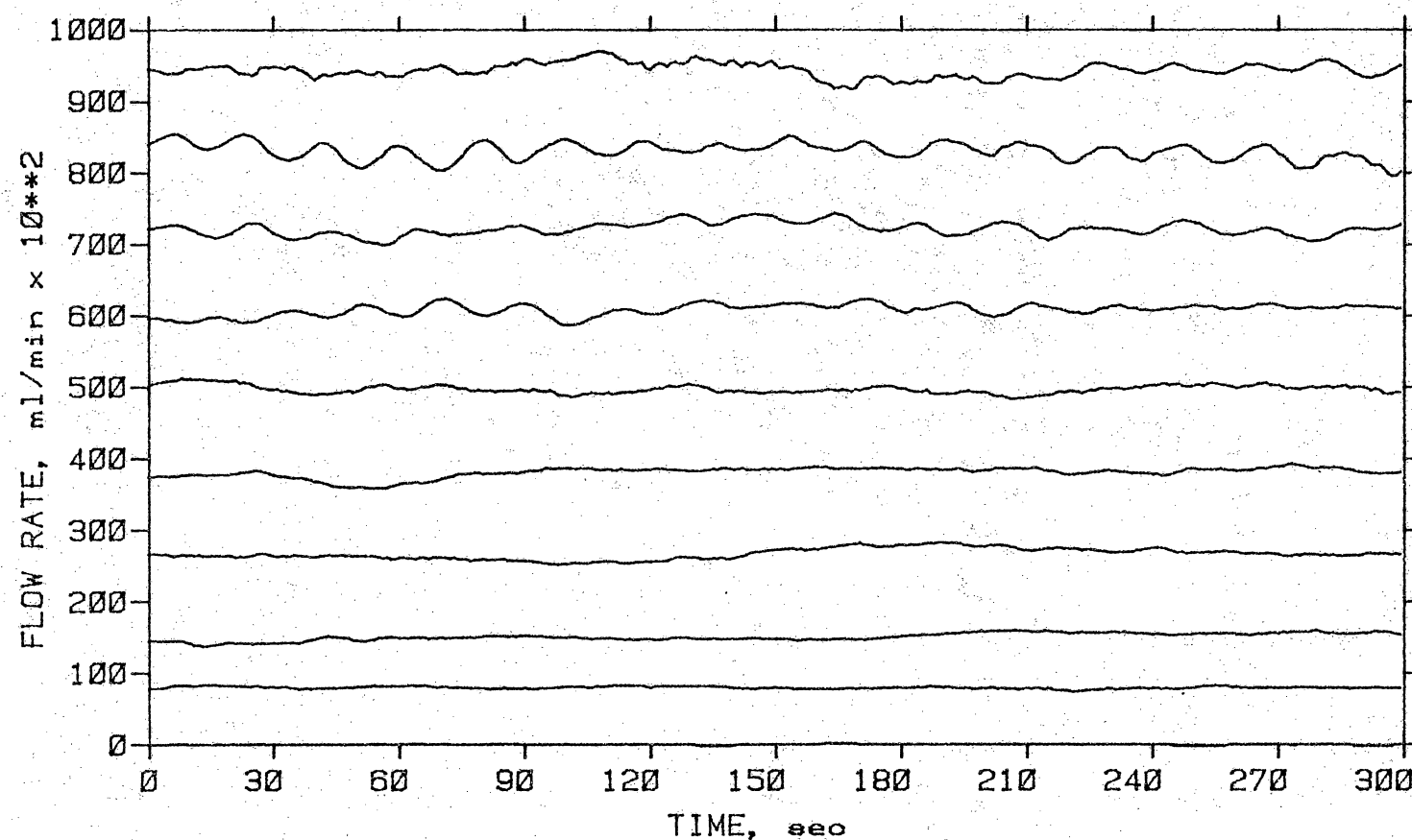


Figure 31. Balance Flowmeter Response, 0.1 M NaCl

Table IV. Flowmeter Calibration Run Summary Report

TEST OF		118 35 28 16				13 DEC 1980			
RUN	GOAL	BALANCE, 0.01 gm/min				FLOWMETER # 1			
		MEAN	MIN	MAX	RSD	MEAN	MIN	MAX	RSD
0	0	0	-2	2	.4.37	14	11	19	.102
1	32	79	74	84	.0229	41	39	45	.0315
2	64	151	138	160	.0335	62	58	66	.0293
3	96	267	252	284	.0283	94	88	99	.0266
4	128	381	359	393	.0188	126	117	131	.0196
5	160	497	484	513	.0115	159	156	162	.0084
6	192	608	587	625	.0134	191	184	197	.0135
7	224	721	699	744	.0129	222	214	229	.0123
8	256	830	795	855	.0145	256	248	264	.0106
9	288	943	917	970	.0109	287	281	295	.0083

300 SEC. OBSV. PERIODS

CORR. COEF. INTERCEPT SLOPE STD. ERR. ESTM.
.9998 16.86 .02866 10.82

TEST OF		118 35 28 16				13 DEC 1980			
RUN	GOAL	BALANCE, 0.01 gm/min				FLOWMETER # 2			
		MEAN	MIN	MAX	RSD	MEAN	MIN	MAX	RSD
0	0	0	-2	2	.4.37	-12	-15	-9	.111
1	32	79	74	84	.0229	0	-2	3	.94
2	64	151	138	160	.0335	17	11	23	.118
3	96	267	252	284	.0283	47	41	57	.0649
4	128	381	359	393	.0188	69	63	73	.0301
5	160	497	484	513	.0115	97	90	102	.0250
6	192	608	587	625	.0134	124	115	132	.0238
7	224	721	699	744	.0129	150	142	159	.0238
8	256	830	795	855	.0145	182	176	190	.0150
9	288	943	917	970	.0109	206	195	215	.0212

300 SEC. OBSV. PERIODS

CORR. COEF. INTERCEPT SLOPE STD. ERR. ESTM.
.9992 -17.15 .02348 11.33

B. Mixer

It is essential that the reagent and sample streams are thoroughly and rapidly mixed before flowing through the reaction tube, assuring that the detectors observe consistent conditions. A number of very complex multi-jet mixers have been employed in stopped and pulsed flow studies where very rapid mixing is necessary because reaction times on the order of milliseconds are being observed. In contrast, reaction times of tens to hundreds of milliseconds will be observed by this instrument. Also, flow rates are orders of magnitude less than those encountered in stopped flow studies. Typically, 10 ml/min flow rates are encountered, rather than the 10-20 ml/sec of stopped flow.

Ballou (19) has shown that simple T-Jet mixers provide adequate mixing in 10 milliseconds or less at flow rates of 1 ml/sec or less. His results indicate that mixing efficiency is improved by increasing the flow velocity or by decreasing the mixing jet diameter, which causes an increase in velocity if flow rates are held constant. Little difference in mixing efficiency is observed when the ratio of flow rates is changed from 1:1 to 10:1. As expected, a large increase in viscosity of the solutions decreases mixing efficiency considerably.

Ballou attributed mixing to the collision of the solution streams, causing them to break up into small interspersed blocks. The mixing jet produces turbulent eddies when forcing these blocks to move at high velocities. Turbulence causes dispersion of the fluid until a homogeneous mixture is obtained. Therefore, anything which increases turbulence is likely to increase mixing efficiency. Thus, increasing the flow rate, either by actually increasing the flow rate or by decreasing the jet diameter, with the flow rate held constant, is likely to improve mixing.

The first mixer considered was a Cheminert[®] CJ-3031 tee connector, shown in Figure 32. The actual connector used has flow channels of 1/32" (.031") diameter which fall between the largest (.040") and second largest (.021") jet sizes Ballou tested. At flow rates greater than 1 ml/sec, Ballou observed good mixing in less than 10 ms. This connector is also used successfully in flow injection analysis where flow rates are 1 to 6 ml/min. Anticipated flow rates are 5 to 10 ml/min for the multicomponent continuous flow kinetic method; thus, the tee connector is potentially useful as a mixing device. It is particularly convenient because it is commercially available.

Careful testing of the mixing efficiency is necessary because the anticipated flow rates are much lower than

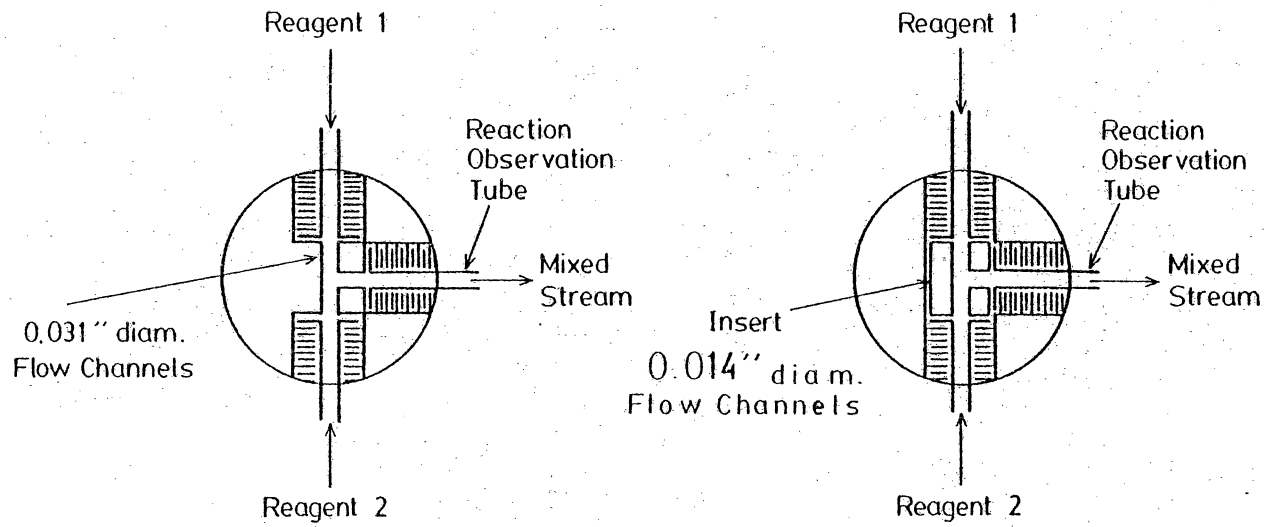


Figure 32. Mixers

those employed by Ballou. His results indicate that incomplete mixing is a possibility, even though problems are not reported at the even lower flow rates encountered in flow injection analysis.

Although it may be possible to include a mixing rate constant (19) in the overall rate equation for some reactions, much simpler and more satisfactory conditions exist when mixing is known to occur in a period much shorter than the half life of the reaction to be observed. To investigate the mixing characteristics of a system, a very fast reaction may be carried out. Choosing an acid-base neutralization and indicator reaction which is diffusion controlled allows any observed reaction rate to be treated as the rate of mixing. A convenient reaction for this purpose is the neutralization of HCl by NaOH using Methyl Red as an indicator. The extent of reaction, i.e., the appearance of the red color of acidic Methyl Red, can be observed at 565 nm by the colorimeters along the reaction-observation tube, as shown in Figure 1 (20).

At a total flow rate of 20 ml/min in the 1 mm diameter reaction-observation tube and a 3 cm distance between the mixer and the observation point of the first colorimeter, a time period of about 70 ms is required for fluid transit. Subsequently, the 8 cm distance between colorimeters results in a transit time of about 190 ms.

between colorimeters. Due to the fact that these flow rates are in the laminar flow region, the actual detection of the beginning of a plus of sample injected into the flowing stream often occurs at about 0.6 the time calculated above on the basis the volume of the tube. This is because the velocity of the liquid in the center of the tube is greater than at the sides, causing the originally cylindrical plus to spread out along the tube. Even with this phenomenon occurring, 35 ms or more elapses before the first colorimeter detects the results of the mixing operation. Experience indicates, and Ballou's results, imply, that mixing will be completed in less than 10 or 15 ms if it is to be completed. Certainly, mixing will not be improved in the observation-reaction tube if turbulent conditions are not experienced.

The preceding observations indicate that a reasonable criteris for adequate mixing in the multicomponent continuous flow kinetic instrument is that all colorimeters are in agreement when observing a rapid reaction. More specifically, the relative standard deviation of the eight colorimeter output values, for a given absorbance, should be roughly equivalent when a fast reaction is occurring, a dilution is being performed, or the reaction-observation tube is filled with a non-flowing reagent. Any trends or significant variations in the colorimeter output values

which are greater than the noise level of the measurement are sure signs that inadequate mixing has occurred.

Table V shows the results of eight runs which test the mixing efficiency of a .031" Jet Cheminert[®] connector. Runs 30 to 32 were conducted under static, or no flow, conditions to determine what value the standard deviation of the eight colorimeter values should be under completely mixed conditions at full scale, blank, and half scale absorbance values. Runs 41 to 45 were then conducted by adjusting the flow rates until the pink color of acidic Methyl Red appears. The reaction occurring was the neutralization of NaOH by HCl. The NaOH contained Methyl red in its basic yellow form which doesn't absorb at 565 nm. At the equivalence point the Methyl Red is rapidly converted to its acidic form, which absorbs 565 nm. Because indicators are binary in nature, it was necessary to have the acid in slight excess, otherwise slight variations in the flow rates of the reagents would cause very unstable colorimeter responses due to changes in the form of the indicator. As the resulting colored segments travel down the reaction-observation tube over a period of about one second, large variations in absorbance at successive colorimeters would be expected unless this slight excess of acid is maintained.

Mixing with the Cheminert[®] connector is not very

Table V. Mixing Efficiency with a .031" Jet Cheminert® Connector

Run#	Chan 1	Chan 2	Flow Rate, ml/min	Ave.*	SDV	RSDV
30	Static, Neutralized Base		990	16.2	.016	
31	Static, Acid Blank		23	13.1	.562	
32	Static, #30 diluted 1:1		419	8.8	.021	
41	3.69	6.28		414	80.8	.195
42	6.11	7.28		370	76.8	.208
43	8.16	9.01		409	67.7	.166
44	11.44	12.60		563	44.3	.079
45	14.80	17.38		621	31.0	.050

* - Arbitrary colorimeter response units

complete; thus, it was difficult to determine the exact appearance of the pink color. Therefore, the average values observed vary because of the varying dilutions experienced when varying excesses of acid are employed. Clearly, mixing improves with higher flow rates; however, even Run 45 has a relative standard deviation of several times that of the static measurements. The Cheminert® connector, with its .031" jets, does not supply adequate mixing under any practical conditions experienced with the Multicomponent Continuous Flow Kinetic Instrument.

Obviously, improved mixing is necessary. Ballou has shown that mixing, at a constant flow rate, can be improved by reducing the mixer jet sizes. A T-jet mixer with .014" jets was constructed, as shown in Figure 32, by drilling out a Cheminert connector and constructing an insert, with smaller jets, to be contained in the drilled out portion of the connector. Greatly improved mixing was observed. Unfortunately, the small jets of this mixer easily become clogged by small dirt particles in the reagents; thus, care in excluding dirt is required.

Table VI gives the result of 26 mixer test runs under a wide variety of conditions, similar to those of Table V. It is clear that relative standard deviations, comparable to those under static conditions, are obtained when flow rates in both channels are greater than 5 ml/min. Flow

Table VI. Mixing Efficiency with a ".014" T-jet Mixer

Run#	Chan 1	Chan 2	Flow Rate, ml/min	Ave.*	SDV	RSDV
1	Static, Base Blank			1	12.1	.16.2
2	Static, Acid Blank			20	31.9	.1.57
3	Static, Neutralized F. S.			996	11.6	.012
4	Static, #3 diluted 1:1			416	10.4	.025
5	5.56	6.66		897	18.9	.021
6	5.41	6.85		842	14.5	.017
7	5.40	6.36		939	16.4	.018
9	6.15	7.94		817	11.4	.014
12	6.44	7.33		902	13.6	.015
13	3.77	5.23		692	29.4	.043
14	3.24	3.48		800	83.9	.105
15	3.44	4.30		747	26.5	.036
16	3.97	4.49		838	29.7	.035
17	3.65	5.89		583	16.9	.029
18	3.55	6.66		515	11.8	.023
20	2.32	3.59		565	17.9	.032
21	2.20	2.95		575	56.0	.098
34	5.77	5.37		918	14.7	.016
35	5.79	5.23		1006	18.0	.018
36	5.03	4.87		896	19.7	.022
37	4.97	4.93		892	22.6	.025
38	4.14	4.06		735	37.8	.052
39	3.58	3.80		753	72.9	.097
40	3.24	3.54		641	82.7	.129

* - Arbitrarily colorimeter response units

rates in the 3.5 to 4.5 ml/min resin do not produce adequate mixins and are comparable to the best results obtained with the .031" jets in Table V.

Reactions with KMnO₄ are of particular interest because both fast and moderate reaction rates have been observed with complexes of Fe(II). These reactions provide excellent test systems for evalution of the instrument, particularly since KMnO₄ absorbs intensely at 565 nm. The colorimeters observe the absorbance of KMnO₄ directly at 565 nm, rather than observing the absorbance of an indicator which is responding to reaction conditions.

The absorbance of KMnO₄ is on a continuous scale rather than the two discrete values of absorbance expected of an indicator system, when dilution is not a factor. Therefore, discontinuities around the equivalence point are not expected, and are not observed. The KMnO₄ reactions are also different in that the disappearance, rather than the appearance, of absorption is being observed. It is thus important that some absorbance remain, after the dilution or reaction, so that valid observations can be made. This is particularly necessary because instrumental relative error increases as the detection limits are approached.

Table VII shows the results of 10 runs which diluted 500 uM KMnO₄ solutions by a non-absorbins buffer. It is

Table VII. Mixing Efficiency, KMnO₄ Dilution

Run#	Chan 1	Chan 2	Flow Rate, ml/min	Ave.*	SDV	RSDV
50	2.98	3.00		259	8.67	.034
51	3.93	3.96		254	2.07	.008
52	4.95	4.95		252	1.07	.004
53	6.12	5.98		257	.84	.003
54	7.48	7.51		255	1.17	.005
55	5.06	7.99		196	1.36	.007
56	7.99	5.26		307	2.38	.008
57	--	6.70	Blank	1	1.63	1.55
58	5.38	--	KMnO ₄ F.S.	501	2.88	.006
59	Static		KMnO ₄ F.S.	501	3.08	.006

* - Colorimeter response units equal to 1 uM KMnO₄

clear that good mixing under dilution conditions occurs at flow rates greater than 4 ml/min and that lower rates, such as 3 ml/min, still produce acceptable results.

The reaction of KMnO₄ with Fe(II) under acidic conditions is fast, occurring in 1 to 2 ms or approximately the dead time of stopped flow instrumentation (21). This system provides another good test for the performance of the mixer. Table VIII shows the results of 10 test runs. Again, as in the previous test reactions, adequate mixing is observed at flow rates greater than 5 ml/min in both channels.

Table VIII. Mixing Efficiency, KMnO₄ - Fe(II) Reaction

Run#	Chan 1	Chan 2	Flow Rate, Ave.* ml/min	SDV	RSDV
60	3.78	3.91		98	.15.6 .160
61	4.90	5.09		103	.1.91 .018
62	5.99	5.97		95	.1.92 .020
63	6.28	4.93		143	.5.23 .037
64	5.29	--	KMnO ₄ F. S.	499	.1.10 .022
65	5.43	4.94		113	.1.54 .014
66	9.26	5.29		200	.2.23 .011
67	8.71	8.22		93	.1.43 .015
68	9.29	5.07		210	.2.07 .010
69	10.21	4.93		222	.6.77 .031

* - Colorimeter response units equal to 1 uM KMnO₄

C. Reaction-Observation Tube and Detectors

The reaction-observation tube consists of a 50 cm length of 1 millimeter inside diameter Suprasil[®] quartz tubing. The use of quartz allows passage of ultraviolet light, extending the wavelength range of observation to include the ultraviolet region of the spectrum if necessary.

Absorption measurements can be made in this system by positioning a source and detector directly opposite each other, with the tube between them. A wide range of sources and detectors are possible, with sensitivity and cost considerations being the primary factors affecting their selection. Because of the 1 mm path length in this configuration, low sensitivity in comparison to longer path length is to be expected. The maximum time for which a given kinetic reaction may be followed is dependent on the length of the observation-reaction tube and the velocity of the flowing liquid. For example, a flow velocity of two meters per second, required to maintain turbulent flow conditions, results in a .25 second residence time in a 50 cm tube. This velocity corresponds to a flow of 96 ml/min. At a velocity of .5 meters per second, a 1 second residence time with a flow of 23 ml/min is obtained. This is below the turbulent flow conditions long thought to be required

to avoid excessive dispersion of the sample. Flow injection studies have shown that dispersion and convection can be controlled by selection of tubing diameter and fluid flow rate. Excellent results have been obtained under "non-turbulent" conditions (2,22). Therefore, it is possible that the anticipated flow rates of 10 to 20 ml/min will produce good results.

The time interval between the colorimeters in Figure 1 is a very important parameter because it is required for calculation of reaction rates. The time interval was determined experimentally by acquiring colorimeter values at a 100 Hz rate. The reaction-observation tube is initially filled with a blank solution flowing at the desired rate. After initializing the storage pointer, a chromatographic sampling valve, which selects the reagent or carrier stream, is switched to an absorbins solution of 500 μM KMnO₄, also flowing at the desired rate. The time between colorimeters is determined by counting the number of data points taken between the detection of absorbance by one colorimeter and the next colorimeter along the tube. Because the transition is not very distinct, the beginning of the absorbance was identified when the colorimeter value changed by a specified amount. To improve the resolution of the measurement, the interval between the first and last colorimeters was measured and divided by one less than the

number of colorimeters involved. The resulting uncertainty in the observed time per colorimeter is less than 4 ms.

The resulting values are listed in Table IX. Also included in Table IX is a calculated time which is based on the flow rate and volume between colorimeters. A one millimeter cylinder of the one millimeter tube has a volume of 0.785 cubic millimeters, resulting in a volume of 62.8 cubic millimeters between the colorimeters which are at intervals of about 80 millimeters. The observed time values are almost uniformly less than the calculated values by a factor of about 0.58. This is because the flow velocity in the center of a tube is greater than the velocity near the walls under the laminar conditions employed in this instrument. The calculated volume of the 61 cm tube is 0.48 cc, agreeing well with values of 0.45 cc obtained by filling the tube with water from a syringe. Similarly, the weight of water contained in the tube is 0.45 grams.

Figure 33 shows a plot of the colorimeter interval observed vs. flow rate. The plot is linear and inversely related to the flow rate, as expected. Equation 2 is the resulting calibration curve.

$$\text{Interval, ms} = \text{Flow rate, ml/min.} \times -14.09 + 352.9 \quad (2)$$

Table IX. Colorimeter Time Intervals Observed at
10 to 16 ml/min

Flow Rate ml/min	Observed Time, ms	Calculated Time, ms	Ratio
10	213	377	.56
12	183	314	.58
13	166	290	.57
14	159	269	.59
15	143	251	.57
16	126	236	.53

Slope -1.409 E -1 Intercept 3.529 E 2 Corr. Coef. -9.966 E -1

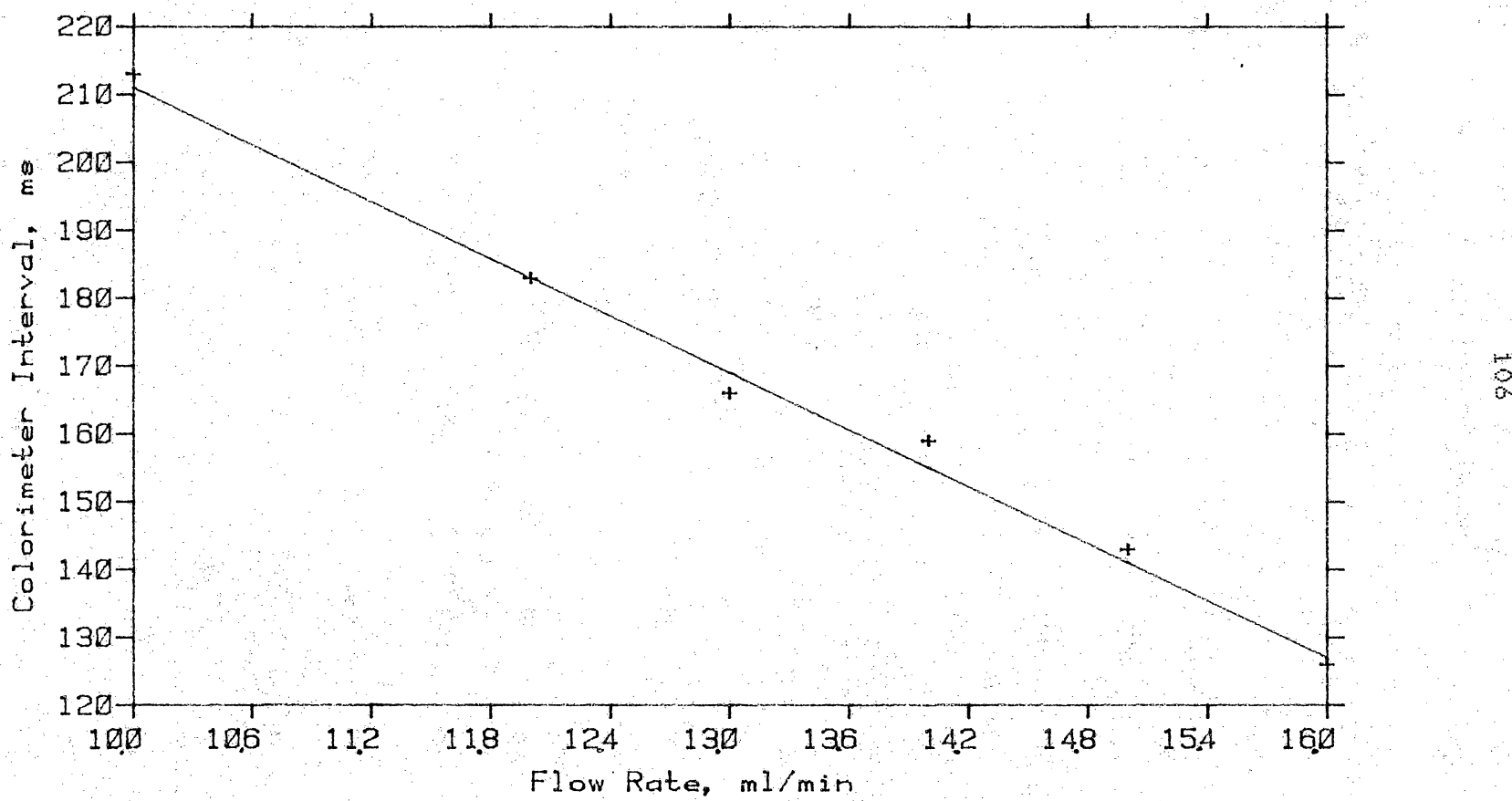


Figure 33. Time - Flow Calibration Curve

1. Colorimeter

One of the most convenient methods of monitoring the extent of a kinetic reaction is by measurement of the optical absorption of one of the species involved in the reaction. This method of detection is particularly convenient when a visible color, due to one of the reactants or products, appears or disappears during the reaction. If colorless species are being used, it may be possible to find an indicator to yield detectable color changes in a convenient region of the spectrum.

A typical colorimeter consists of a radiation source, a wavelength selection mechanism, a sample cell and detector. Should the absorption maximum of the species of interest fall in the green to red region of the spectrum, a light emitting diode (LED) may provide the desired narrow-band radiation source. It has been shown that a LED can deliver up to 5 times the radiant energy to a sample cell than does a 40 watt tungsten lamp and monochromator under similar bandpass conditions (23). Therefore, light emitting diodes are able to deliver more than adequate power to the sample cell.

LED sources are limited by the fact that only four major visible emission wavelengths are available. Green light emitting diodes have a peak emission wavelength at

565 nm, yellow at 585 nm, orange at 630, and red at 660 nm. The emission bandpass of a light emitting diode is quite narrow, typically less than ± 30 nm at 20 percent of peak output and ± 15 nm at 50 percent of peak output, comparable with the bandpass of interference filters.

As a consequence of the small size, narrow bandpass and high intensity of the light emitting diode source, a very compact measuring apparatus is possible. This enables the use of a number of source-detector pairs along the reaction-observation tube, making the measurement of the kinetic response of the system possible.

The colorimeter head consists of the narrow band light emitting diode radiation source, sample cell, and photodetector shown in Figure 34. The colorimeter head can be positioned at any point along the reaction-observation tube to allow observation of the extent of reaction at the desired time after mixing.

The components of the colorimeter head are mounted in a piece of black plastic as indicated in Figure 34. The black plastic blocks ambient light and provides a mechanically rigid mounting structure for the light source and detectors. Ambient light exclusion is very efficient; practically no change is observed in the detector output signal when normal room lighting and the absence of ambient light is compared.

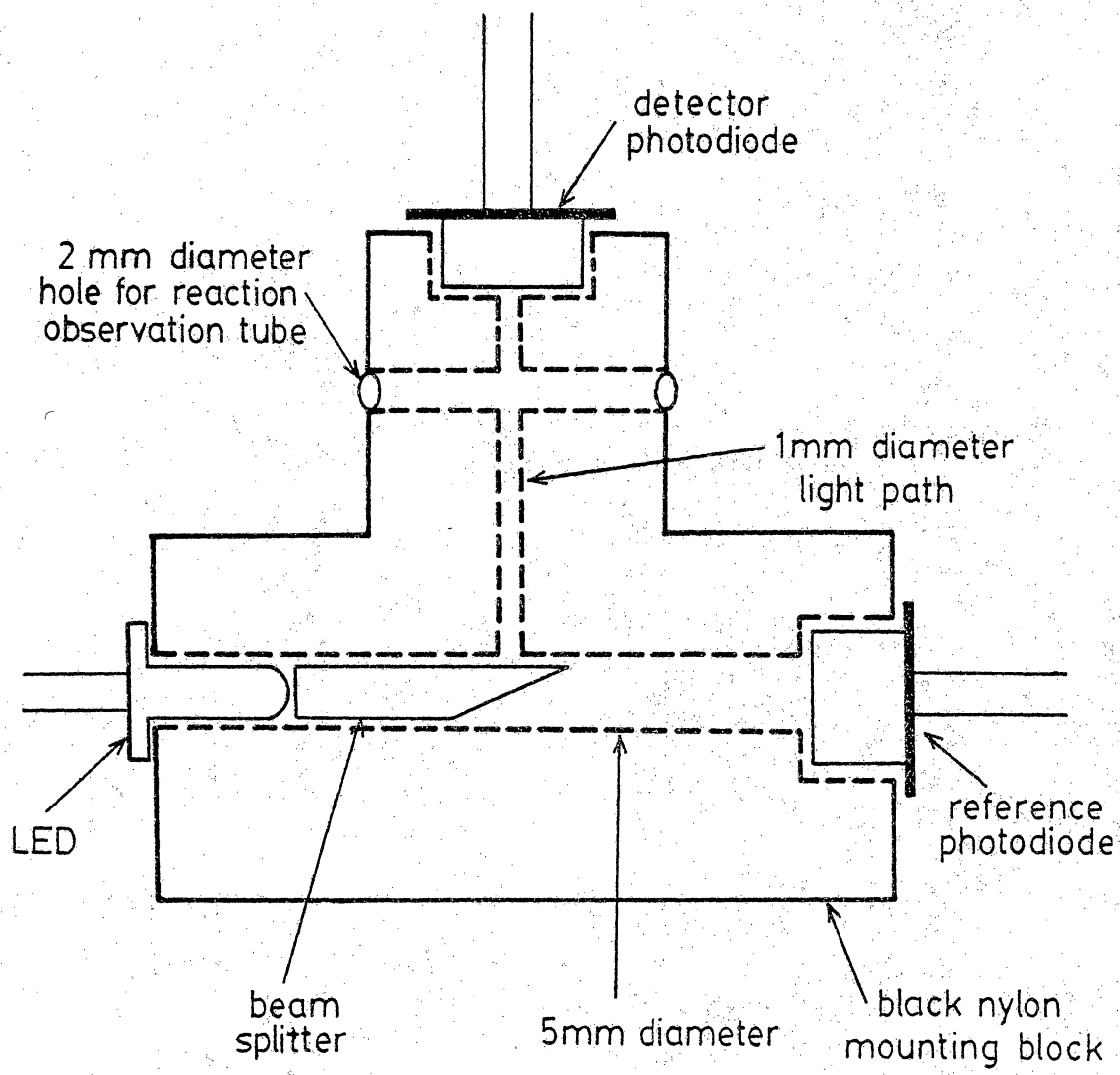


Figure 34. Colorimeter Head

The colorimeter head consists of light source and detector sections. The light source section is responsible for providing a stabilized light output to the detector section. Light originates in the light emitting diode and is directed into the beam splitter which consists of a short section of 5 mm diameter glass rod with one 45 degree face. More than half the light is reflected into the detector area with most of the rest passing through the 45 degree face to the LED reference photodiode. The reference photodiode monitors the light output of the LED and provides a signal to the colorimeter electronics which then adjusts the current to the light emitting diode to produce a constant light output. General Instrument MV50152 series (24) light emitting diodes were used.

The reflected light travels through a 1 mm light path to the reaction-observation tube where varying amounts of light may be absorbed by the molecules in the 1 mm inside diameter of the tube. The detector photodiode monitors the light passing through the tube and generates a signal which is processed by the colorimeter electronics to produce the final output signal. Vactec (St. Louis, MO) model VTB5050 blue enhanced photodiodes were employed.

2. Colorimeter Electronics

The photodetectors selected for the colorimeter are silicon photovoltaic diodes. These devices are characterized by low noise levels, linearity over a wide dynamic range, low temperature coefficients, and no hysteresis or memory effects. Their frequency response is good and they do not require expensive regulated high voltage power supplies as do photomultipliers or PIN and avalanche photodiodes (25).

A linear response to incident radiation over a wide dynamic range is obtained when the photodiode load resistance is very low. The measurement of this response is facilitated by using an operational amplifier in a current to voltage converter configuration. The photodiode is connected between ground and the inverting input of the amplifier. The noninverting input is connected to ground and a large value feedback resistor is used between the output and inverting input as shown in Figure 35. Because the operational amplifier tries to maintain the difference between the inverting and non-inverting inputs at the lowest value possible, this configuration results in the inverting input being at nearly ground potential. This is referred to as a "virtual ground" and is possible because the current flowing into the junction at the inverting

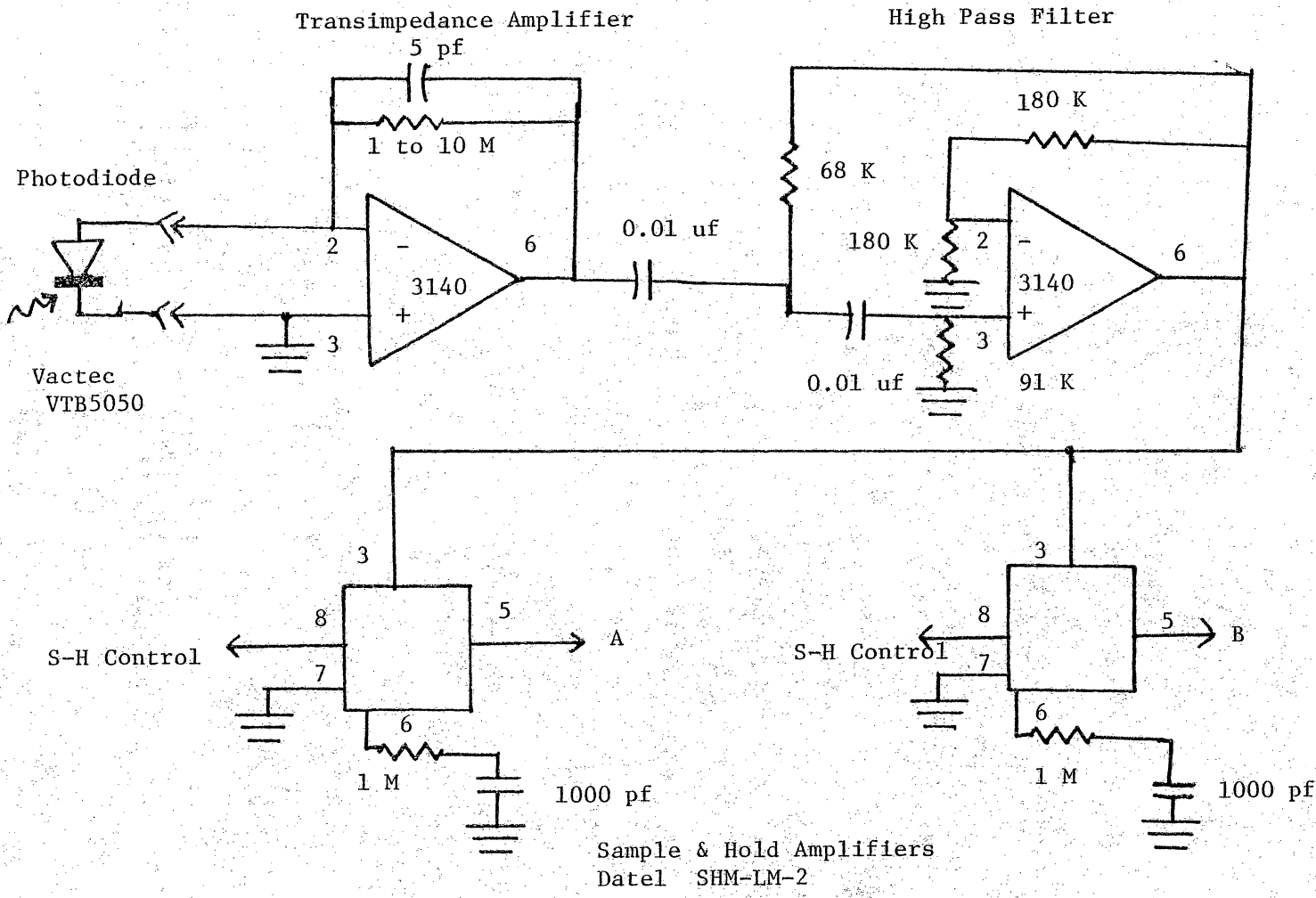


Figure 35. Colorimeter Front End Signal Processor

input from the photodiode is balanced by that flowing out through the feedback resistor to the output of the amplifier. The amplifier adjusts its output to achieve this balance at the inputs, resulting in a voltage proportional to the current flowing in the photodiode. This current is proportional to the light incident on the photodiode. The inverting input, with its virtual ground characteristics, appears to the photodiode as a very low load resistance, resulting the widest possible linear dynamic range.

The photodiode data sheet (25) indicates that the diode's noise spectrum is nearly flat. However, low frequency noise and drift is introduced by the operational amplifier and its feedback resistor. Therefore, best results are obtained when the operating frequency of the system is shifted to higher frequencies by "chopping" or turning the source on and off at a rapid rate. The output signal is then derived from the difference between the photodiode output when the source is on and when it is off. Noise performance is improved by this process because the low frequency noise and drift changes only slightly between these measurements while the difference due to the source is relatively large. Over a longer period of time, the low frequency noise may be considerably greater than the lowest light level detectable. If chopping was not used, the

lowest light level detectable would be set by the noise level, leaving much of the potential of the system unutilized. An additional advantage of chopping the source is that interference from light at frequencies far removed from the chopping frequency is greatly reduced. For example, if a high pass filter is used to remove DC and low frequency components from the chopped photodiode signal, little effect on the difference signal at the output is observed with varying levels of ambient sunlight, assuming the photodetector is not saturated. Light derived from the AC power network is more difficult to reject because of its higher frequency, 60 to 120 Hz. Even with a 1000 Hz chopping frequency, a sharp cut off high pass filter is required, resulting in considerable distortion of the chopping waveform. To improve the performance of the high pass filter, a 1500 Hz chopping frequency was used. This allows greater attenuation of the very low frequencies while maintaining more faithful reproduction of the chopping waveform.

The high pass filter output is stored, in analog form, by the sample and hold capacitors. One sample and hold capacitor is charged when the source is off, providing the no light reference level. The other is charged when the source is on, and the difference between the two is then continuously available at the difference amplifier.

output. The sample and hold amplifiers act as an analog latch. The value on the capacitor is rapidly charged to the input value when the amplifier is in sample mode. In hold mode, the value on the capacitor when the control signal changes from sample to hold is continuously available at the amplifier output. This characteristic produces a significant problem if noise is present on the input to the sample and hold. If the end of the sampling period occurs just as a noise pulse appears, the sample and hold output will be significantly effected by the noise. The incorrect output value will be held until the next sample period, possibly producing large output errors. The reason this occurs is that the sample and hold does not really integrate the input signal during the sample period. High speed operation is often required; thus, the capacitor is charged to very near the input value in several microseconds. Therefore, even though the sample period may be many microseconds, only the last few microseconds determine the value which will be held until the next sample period. The first approach to reducing this sample and hold noise problem is to reduce the noise at the amplifier input through use of an appropriate filter. Consistent phase delays in the filter and low sample control signal jitter are necessary to avoid introduction of additional noise, particularly if the end of the

sampling period occurs when the input voltage is changing rapidly. The effect of these problems can be reduced by sampling on a plateau rather than on the side of a sine wave where the change in voltage with time is great. Another approach to sample and hold noise reduction is to reduce the changing rate of the capacitor by inserting a resistance in series with the capacitor. Proper selection of the resistance should result in the effect of integrating the input signal over most of the sample period. Under these conditions, short noise pulses produce only a very small effect on the output level. This modification has the undesirable effect of limiting the large signal response of the sample and hold if significant integration over a sampling period is to be obtained. In the case of the colorimeter, this is not a problem because changes in input should be occurring slowly in comparison to sampling times of approximately twenty microseconds.

The final stage of the photodetector signal processing circuit is a low pass filter which smooths the output of the difference amplifier as shown in Figure 36. This is necessary to provide a steady output signal which does not require computer data acquisition at specific times to avoid slight shifts in the output due to updating of one of the sample and hold values.

Light emitting diodes are ideal chopped radiation

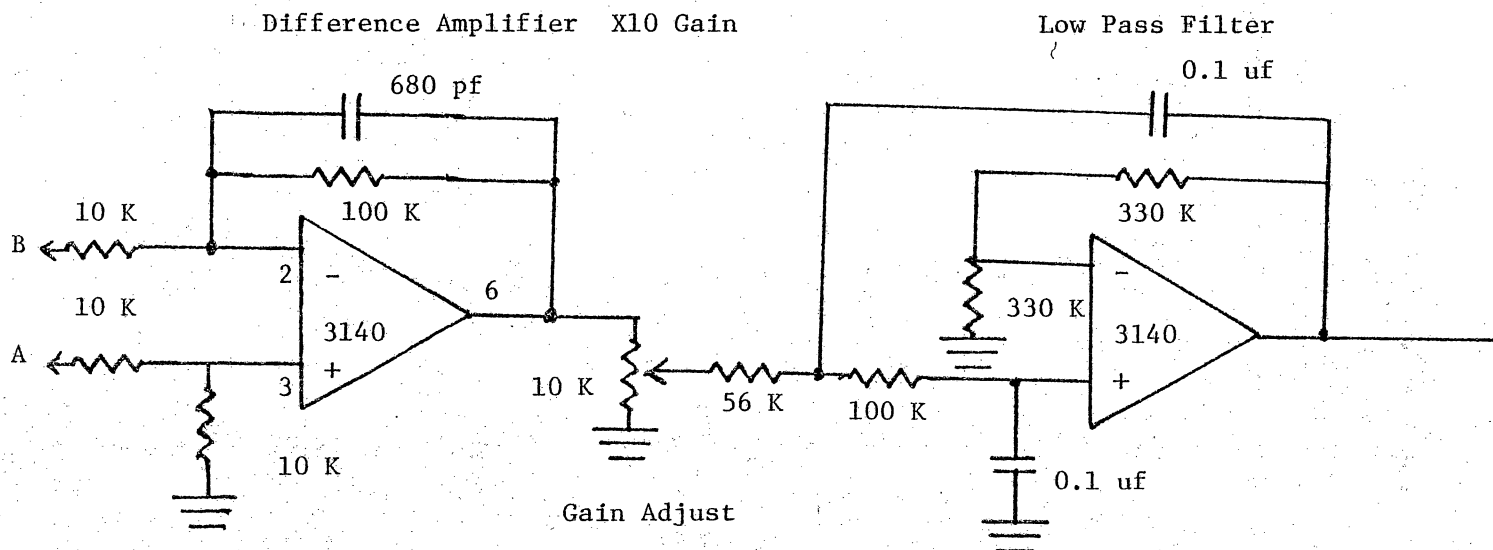


Figure 36. Colorimeter Signal Processing Electronics

sources because they have fast rise and fall times, are easily switched on and off, and require low current levels.

Many light emitting diodes are specified at an average current of twenty milliamperes, allowing peak currents of forty milliamperes when a 50 percent duty cycle is employed. This is easily supplied by a small signal switching transistor driven by an operational amplifier.

Most light emitting diodes exhibit a large variation in light output with temperature and are subject to aging effects (23,26). A dual channel operational mode is employed to compensate for these undesirable effects. A photodiode directly monitors the light output of the emitting diode. This photodiode is of the same type as the detector photodiode and its signal is processed in the same manner. The photodiodes typically have low temperature coefficients and do not age significantly. In addition, both photodiodes are in similar thermal environments. The output of the reference channel is compared to a very stable reference voltage by the error amplifier in Figure 37, and the error signal developed is applied to the modulator amplifier. The error causes the LED intensity to be changed to minimize the error signal, thus maintaining a very stable light output. This output can be considered as stable as the reference beam monitoring circuit over long time periods.

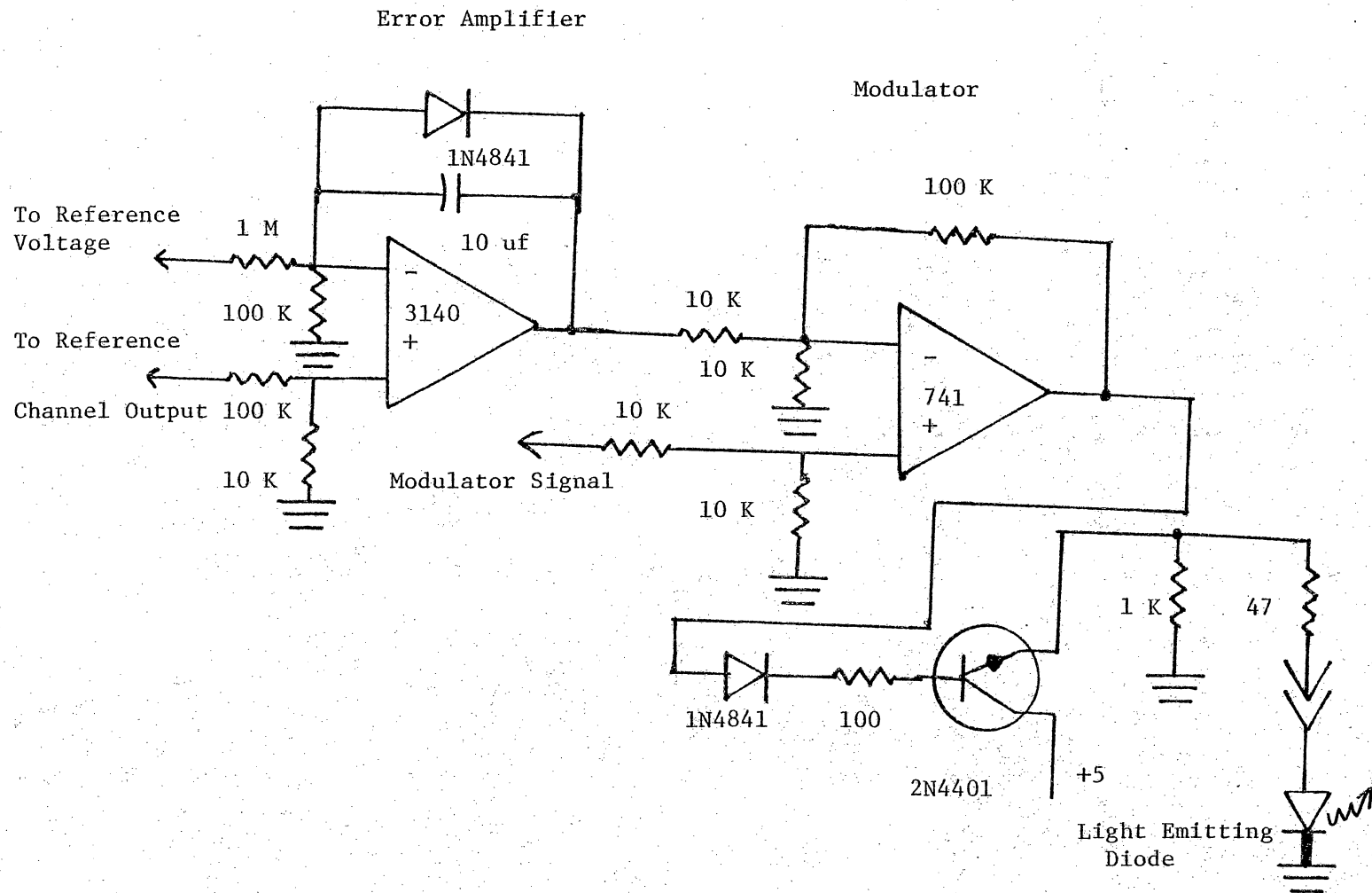


Figure 37. Colorimeter Error Amplifier and Modulator

The chopping waveform is inserted in the LED excitation circuit at the non-inverting input of the modulator amplifier. Component values were chosen to cause the LED to be completely off when the modulation waveform is low. The TTL circuits divide an externally generated 100 KHz waveform by 16, resulting in a precise, 50 percent duty cycle square wave. This is then divided by four, resulting in the modulation waveform. The other circuits generate the sample and hold amplifier's sample control signals for the source on and source off conditions. These auxiliary circuits, along with the optical isolators which are used to reduce noise couplings between analog and digital grounds, are shown in Figure 38.

Figure 39 shows a general block diagram of a single colorimeter channel. Each subsection, discussed earlier, is shown in relation to the other subsections of a complete colorimeter channel. Up to eight of these channels are available to monitor the reaction-observation tube conditions at up to eight different points.

The colorimeter will be used to measure several signals which have different rates of change with time. The steady state signal observed under continuous flow kinetic conditions is relatively constant and thus does not require rapid detector response. Rapid response is required to detect accurately the sample pluss injected

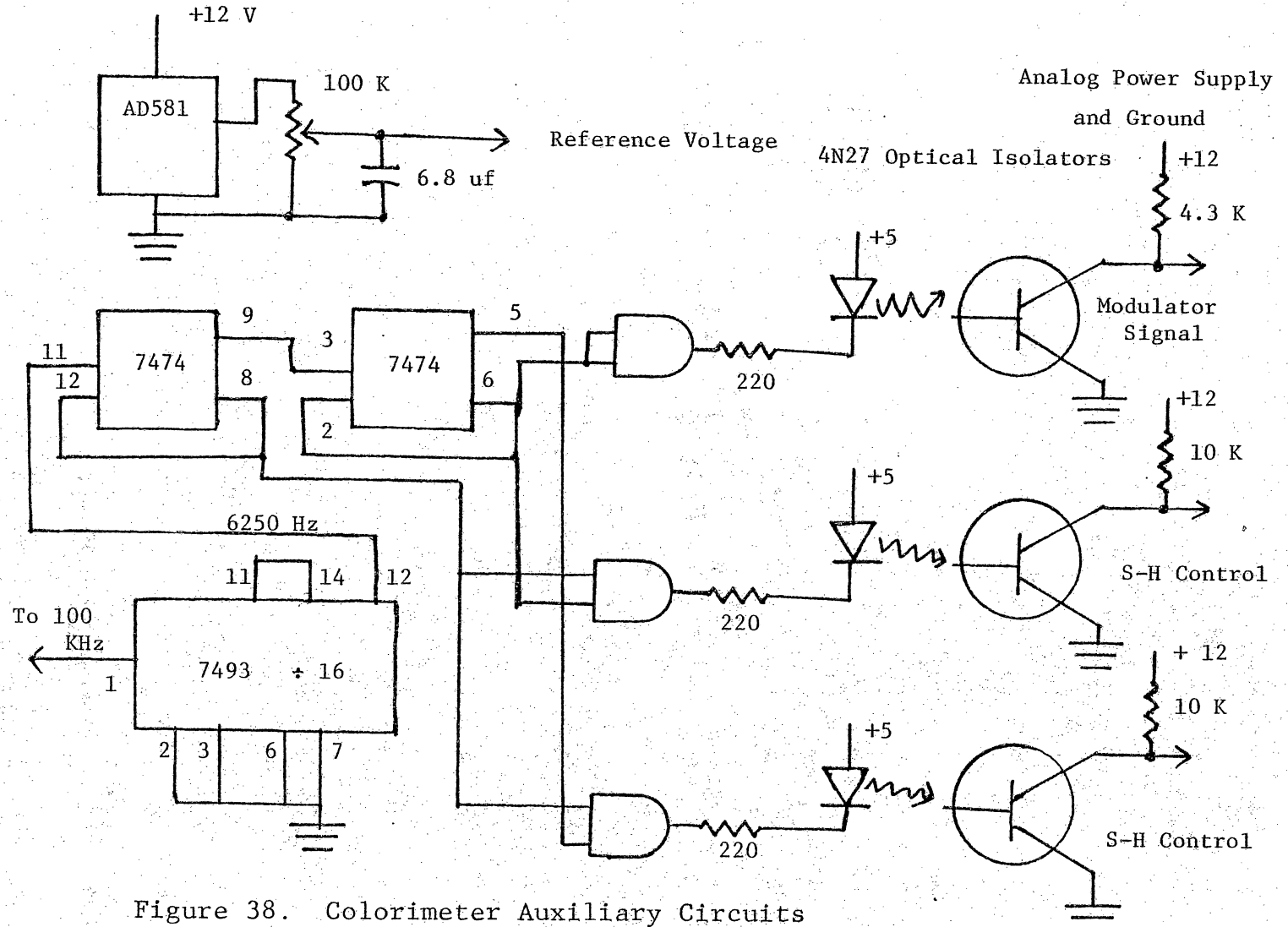


Figure 38. Colorimeter Auxiliary Circuits

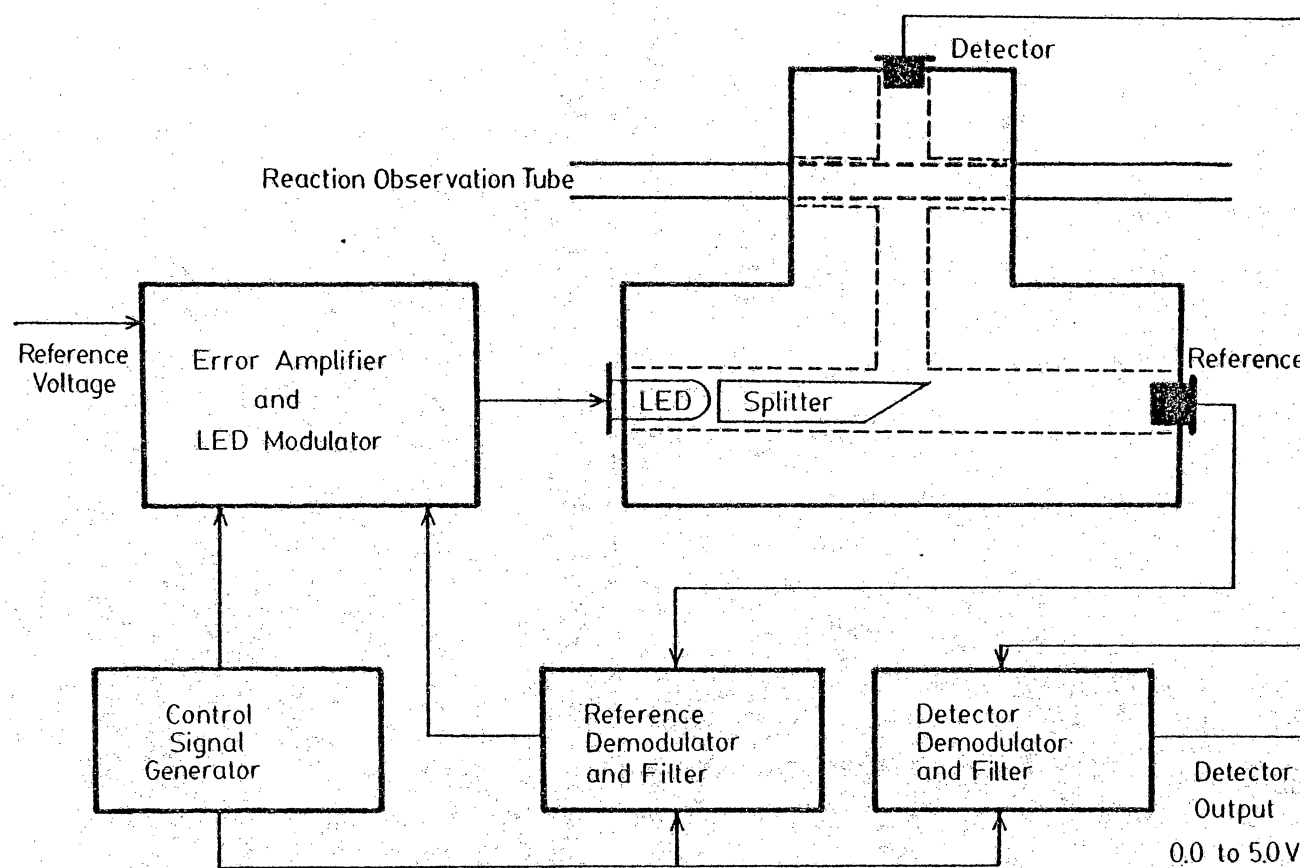


Figure 39. Colorimeter Block Diagram

into a carrier stream by flow injection analysis techniques. Detecting the endpoint of a titration while varying the flow rate of one of the reagents requires an intermediate response rate.

The frequency response of the total colorimeter system is therefore a very important characteristic. A number of filters are encountered in the signal processing electronics which could have a significant distortion effect on the observed output. The final low pass filter determines the highest frequency signal the colorimeter can respond to, or in other words, the rise and fall time of the output signal. Should physical or chemical changes in the observation cell take place faster than this time, the colorimeter would produce deceptive results. Ideally, the colorimeter should respond in a much shorter time period than any chemical or physical changes require. Filter design calculations indicate that the low pass filter 3 db point (70 percent of maximum) occurs at 20 Hz. This means that a peak 50 ms wide would have an amplitude of 70 percent of a much longer peak, say 1 second wide.

Figure 40 illustrates the response of the colorimeter in a more practical manner. An opaque wire was set up to interrupt the detector beam at a rate of about 6 Hz. The colorimeter response was observed every millisecond and later plotted. The plot indicates that the rise and fall

Block 3411 Data, New Filter Out

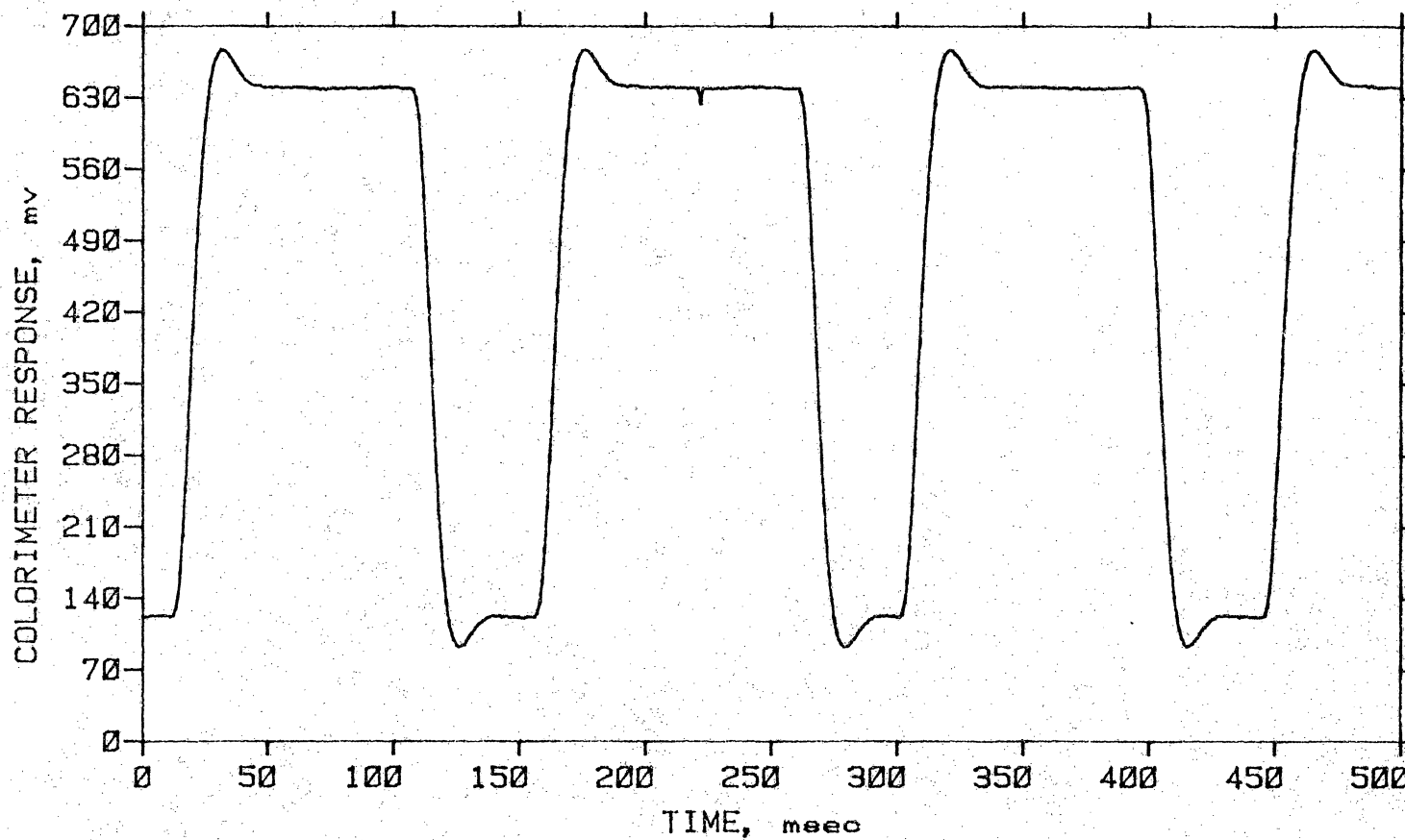


Figure 40. Colorimeter Light Beam Interruption

124

times of the total system, wire and electronics, are about 10 ms. It is important to notice the slight overshoot produced by the filter; thus, it takes about 50 ms to achieve the final output level. Observation of the signal at the output of the transimpedance amplifier indicates that the wire movement requires approximately 5 ms. The figure shows that the response rate of the total colorimeter is more than adequate for digitization rates of 10 points per second or more, which experience has shown to be adequate under most of the situations which are anticipated. Rarely will the maximum voltage excursions, corresponding to no light and maximum light, be encountered in practice. The Figure also shows that the low pass filter adequately filters out all noise due to the chopping process. Once the signal plateau is reached, signal variations are rarely more than ± 1 bit, the minimum error realizable by the digitization process.

3. Colorimeter Performance

The signal at the output of each channel of the colorimeter is proportional to the light transmitted through the reaction-observation tube. To obtain a signal directly proportional to the concentration of the species in the tube, the absorbance will need to be calculated via Equation 3.

$$\text{ABS} = \log I_0 / I \quad (3)$$

I_0 is the light intensity, or colorimeter response, with a blank in the beam. I is the response with the sample in the beam. The computer implementation of this equation is rather time consuming because the ratio I_0 / I is usually only slightly greater than 1, requiring the use of time consuming integer to floating point conversions and floating arithmetic. The floating point logarithmic function requires an order of magnitude more time than a division, resulting in execution times of 20 to 50 milliseconds on an LSI-11 with FIS, far too long to be practical in a real time system with multiple detectors and observation intervals of 100 ms.

Because the colorimeter is a single beam instrument, I_0 or blank values will have to be obtained and stored for use during the actual measurement process. If a fast integer logarithm algorithm could be devised, it would be reasonable to immediately calculate the logarithm of I and I_0 values and then perform the division by subtraction of integers, a relatively fast operation. There would be no need for floating point operations because small fractions would not be encountered. Equation 4 indicates the operations now required.

$$\text{ABS} = \log I - \log I_0 \quad (4)$$

A 12 bit analog to digital converter is used to digitize the colorimeter output; thus, the logarithm

algorithm will have an input range of 0 to 4095. One input unit corresponds to 0.00011⁹; therefore, the algorithm should provide at least four and preferable five significant output digits. Further investigation indicates that base 2 logarithms are evaluated most efficiently by binary computers, after which a simple multiplication will calculate the desired base 10 logarithm. In fact, following the example of Forth, it is possible to perform all internal operations in base 2, converting to base 10 only when output reports are required. This procedure minimizes unnecessary operations, enhancing the throughput of the system considerably.

Most logarithm algorithms evaluate a truncated or modified Taylor series to perform their transformations. This often requires several multiplications and divisions and is excessively time consuming. The fastest method would be obtaining the log value from a table of 4096 entries, using exactly the same procedure as is done manually with logarithm tables. Unfortunately, this requires an excessive amount of memory for the lookup table, making the method impractical.

The algorithm in use normalizes the input value, discards the most significant bit, which is always a 1, and uses the next 8 bits as an index into a 256 word table. The least significant 3 bits are then used to interpolate

between table values, generating a "correction" to be added to the mantissa calculated during normalization. This algorithm calculates logarithms of 12 bit input values resulting in output values accurate to ± 0.3 units in the fifth decimal place in about 300 us. This is several orders of magnitude faster than floating point series evaluation methods and requires a reasonable 256 words of memory for the lookup table. A floating division using the LSI-11 FIS instruction set can require up to 232 us; thus, it is advantageous to calculate the integer logarithm of the I values as they are obtained, and then subtract the previously calculated and stored logarithms of I_0 . This is particularly convenient since I_0 must be obtained before conducting the determination anyway.

A single beam colorimeter must be very stable because drift would invalidate calculations made with I_0 values obtained before a significant amount of drift occurred. The colorimeter stability was evaluated by storing readings consisting of the average of 512 conversions at a 100 Hz rate over a period of an hour. Each stored value represents a time period of slightly more than five seconds. Table X reports the average, range, standard deviation, and relative standard deviation of these hour long runs for each channel of the colorimeter. A blank, consisting of distilled water, and two concentrations of

Table X. Colorimeter Stability Studies

CHAN	Water Blank		Average of 512 observations	
	AVE.*	RANGE	STD DEV	REL STD DEV
0	-2	119	16.9	.7.64
1	-4	111	17.6	.3.62
2	-28	142	24.3	.0.848
3	-13	34	6.75	.5.15
4	-5	56	14.2	.2.39
5	6	78	6.77	.1.04
6	0	33	5.86	.6.46
7	15	45	6.79	.0.444
CHAN	500 uM KMnO4		Average of 512 observations	
	AVE.*	RANGE	STD DEV	REL STD DEV
0	3019	209	38.1	.0126
1	3450	160	13.9	.00403
2	3509	128	14.3	.00407
3	3349	35	9.19	.00274
4	3893	66	10.4	.00267
5	3285	37	9.31	.00283
6	3915	75	13.1	.00335
7	3892	51	9.58	.00246
CHAN	200 uM KMnO4		Average of 512 observations	
	AVE.*	RANGE	STD DEV	REL STD DEV
0	1158	134	23.2	.0200
1	1330	127	20.3	.0152
2	1372	125	21.6	.0157
3	1322	35	6.53	.00494
4	1568	36	6.93	.00442
5	1305	48	6.57	.00503
6	1560	33	5.79	.00371
7	1584	37	9.58	.00605

* - Colorimeter response units equal to 0.1 uM KMnO4

KMnO₄ were used in the evaluation. A green light emitting diode with a ± 20 nm bandwidth at 565 nm was used as the source.

It can be seen that the range of values over the one hour period, reported in hundredths of a milliabsorbance unit, are typically below 50. This corresponds to a change in concentration of 5 μM KMnO₄. The useful range of this colorimeter for KMnO₄ is 10 to 500 μM ; therefore, drift is at or below the noise level for channels 3 to 7. The larger drift observed for channels 0 to 2 is probably due to the increased gain required in these channels and operation outside of their optimum control range. After adjustments for subsequent experiments, this drift was considerably reduced.

A considerable variation in response is observed between individual colorimeters. This is probably due to variations in construction and variations in the diameter of the reaction-observation tube. This problem is easily solved by providing individual calibration factors for each colorimeter. It was found that the calibration curve intercepts are rarely greater than ± 10 hundredths of a milliabsorbance unit, nearly an order of magnitude smaller than the drift or noise level; thus, the intercept may be ignored.

Another important colorimeter characteristic is

photometric linearity. Figure 41 shows a typical calibration curve for one of the colorimeters with eight different concentrations of KMnO₄. The correlation coefficient of 0.9998 indicates a very good correspondence between reagent concentration and colorimeter response over a range of 0 to 500 μM KMnO₄. Greater concentrations begin to show increasing negative deviations from Beer's Law, indicating that intra-molecular interactions and stray light effects are becoming significant.

The colorimeter heads are constructed of black plastic and the LED source is chopped and synchronously demodulated; thus, the presence or absence of ambient light makes no detectable change in the colorimeter output signal. The only source of stray light, since the LED sources are nearly monochromatic, is light which may travel through the glass walls of the reaction-observation tube rather than straight through the absorbing species in the center of the tube. Even this appears to make no difference when a 10 to 500 μM concentration range of KMnO₄ is being used. In fact, this is a good linear range for KMnO₄ in any spectrometer.

Comparison of the operation of the LED colorimeter with moderate cost single and dual beam spectrophotometers indicates that the LED colorimeter is nearly equal or superior in noise, drift, and linearity. Naturally, it has

Slope 8.066 E 0 Intercept 1.658 E 1 Corr. Coef. 9.998 E -1

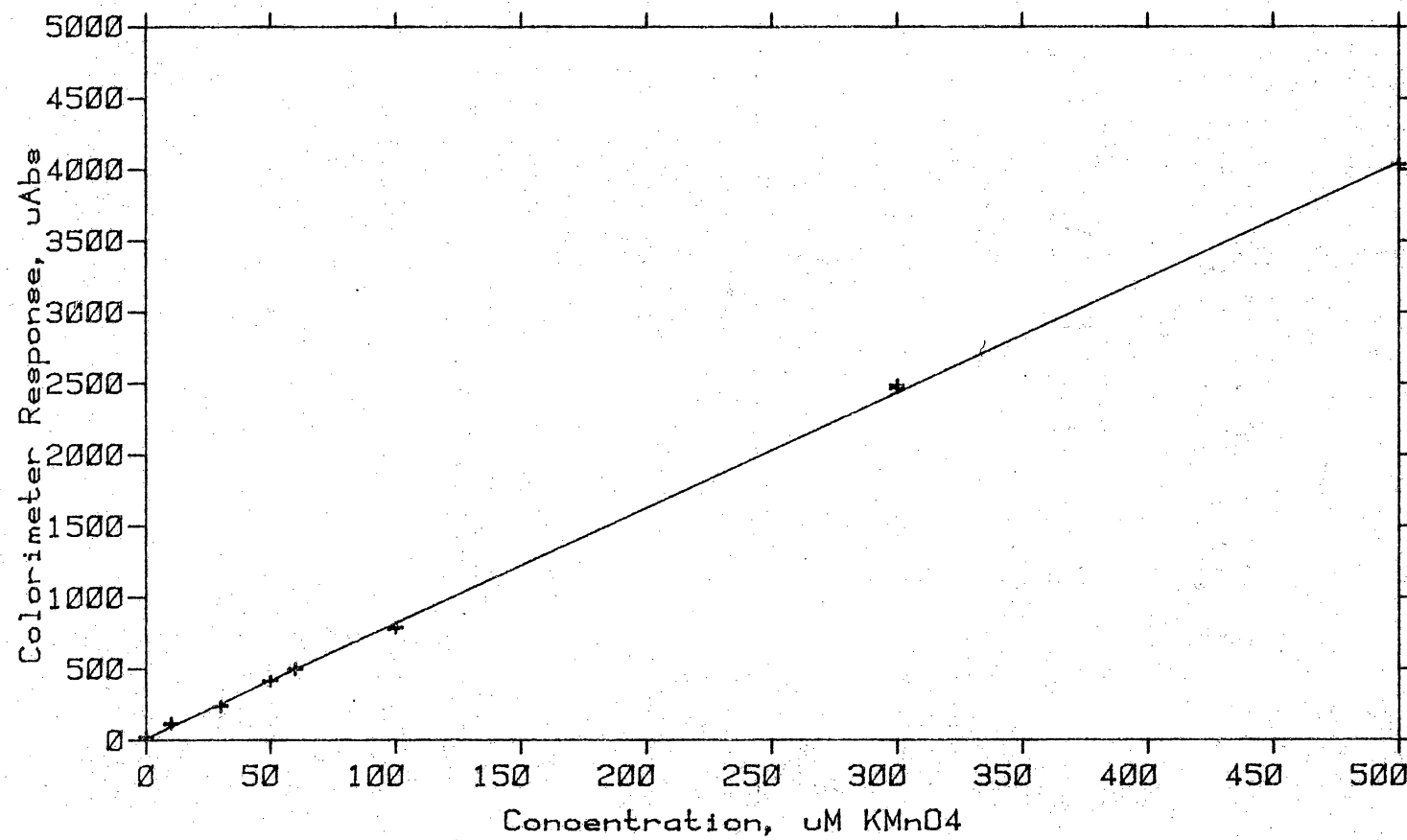


Figure 41. Colorimeter Calibration Curve, KMnO_4

a limited wavelength selection and fixed bandpass. Its 1 mm path length cell results in a significant decrease in sensitivity when compared to longer path lengths.

D. Data Acquisition and Processing System

Software and hardware are subject to even more synergistic effects than previously discussed for the relationship of electronics and chemistry. Increasingly, software is becoming one of the more expensive parts of an instrumentation project (27). Therefore, it is very important to select hardware and software systems which allow easy and convenient development. The software should aid the user rather than continuously requiring him to circumvent its limitations, as often occurs when traditional software constructs are used. In particular, the area of real time programming has been poorly served by most existing high level languages and operating systems, which were really designed with the goal of providing batch type mathematical capabilities like those available in large computing systems. Our experience with several computers and software systems has shown that assembly language methods must be used whenever one's application is not exactly anticipated by the authors of available software systems. This situation is unfortunate because an assembly language program requires at least five times the effort to develop as does a similar program in a higher level language, assuming the higher level language is capable of performing the job. Therefore, a mixture of

high level and assembly language constructs will lead to the optimum result which is providing a high quality software system which does its intended job in a minimum amount of time.

1. Forth Programming System

These problems were recognized by Charles Moore at the National Radio Astronomy Observatory in Green Bank, West Virginia in the early 1970's (28). He developed a programming system which he called Forth, because he considered it a fourth generation language. Machine language is considered the first generation, assembly language the second, and FORTRAN, BASIC, and PASCAL are representatives of third generation languages. Forth is different from traditional languages and operating systems because it combines the functions of both a language and operating system into a single construct. This approach is remarkably terse because it minimizes duplication of instruction sequences via its back-linked dictionary structure. Basic operations are reentrantly programmed and loaded into memory once, after which they are available for use by other operators which are sequences of these basic operations. These operators may be viewed as subroutines whose arguments are passed to each other on a parameter stack. Most Forth words, or operators, act upon values obtained from the parameter stack, leaving the result on

the stack also. This stack structure allows the use of Post-fix or reverse Polish notation, like that of Hewlett-Packard calculators, rather than the infix notation of traditional languages. Infix notation is difficult to parse into machine executable form, thus requiring extensive programs for the conversion.

The most important feature of Forth is its extensibility, i.e., new words or operators can be made by combining previously existing ones. The programmer is not limited to constructs supplied by a vendor, but can develop his own which are more useful in his application. Quantum mechanicians should recognize this feature as one which allows considerable simplification of complex mathematical expressions into a sequence of a few constants and operators.

Examining the structure of a Forth word more closely allows one to understand how assembly and higher level constructs may be easily mixed to achieve optimum program throughput and development effort. High level Forth words are called colon definitions because they start with a :. Each colon definition contains an initial identifying field which contains the first several letters of the word's name. A back-link points to the previous definition in the dictionary allowing dictionary searches to start with the last definition entered and proceed through the dictionary.

until the word is found or the end of the dictionary is encountered, which results in an error. This procedure causes only the last definition of a word to be found, allowing a word to be redefined. These redefinitions may occur during development and debugging of the word's function, or when additional features are being added to the word's operation without changing the word's name.

The next major field in a colon definition is a list of the addresses of previously defined words which make up the function of the word. The execution of a colon definition consists of executing the instructions at each of the addresses making up definition, and returning to the definition to find the address of the next instructions. The addresses may point to other colon definitions, which then perform similar operations, or to code definitions which contain actual machine instructions rather than a list of addresses. Colon definitions are identified by a special construct in their parameter fields which indicates that a list of addresses rather than machine instructions follow.

Code definitions are the most primitive operators of the Forth system, and actually execute the machine instructions which perform the functions of the Forth words. Code definitions have identification and back link fields similar to colon definitions, but contain only

machine instructions in their parameter fields.

The compilation or assembling of colon and code definitions may occur at any time in a Forth system, in contrast to traditional operating systems which require lengthy editing, compiling, linking, and loading steps. In this aspect Forth is similar to BASIC. However, a Forth word is compiled only once, not interpreted every time it is executed, giving Forth a distinct speed advantage. Turnaround time during debugging is also reduced to a matter of seconds to minutes, rather than tens of minutes as in many operating systems, allowing the programmer to generate much more working code in the same amount of time.

A real time computer system is often required to keep track of several relatively independent operations at the same time. Interaction between these operations vary from none to fairly involved timing sequences. To service these operations properly, modular software to complement the already available modular hardware of computer systems is needed. One approach is to dedicate logic or individual microprocessors to each task. This is inefficient since many of the tasks do not require the power available in a separate processor. Forth has solved this problem by allowing multiple tasks to exist in memory. Each task has a vocabulary of words which are specific to its application as well as a link to the basic Forth vocabulary. This

allows the task to use the resources of Forth without duplicating the common code and colon definitions; thus, saving a considerable amount of memory. Each task is allocated its own dictionary, parameter stack, return stack, and task table area. Values which are unique to a particular task are kept in its task table; thus, tasks may use common routines without having to save values from other tasks.

The computer's time is allocated to tasks on a round robin priority scheme. Each task maintains a pointer to the next task in the loop. When a task releases the computer due to the need to wait for an input/output operation or execution of a word which releases the computer, the status of the next task is examined. If the task's status indicates it is ready for execution, several registers are restored and execution of that task proceeds. If the task is not ready, the next one in the loop is examined. Aside from the fact that the programmer must remember to release the computer periodically during a CPU bound operation, this primitive mechanism is very efficient and has proved satisfactory over a wide range of situations.

The consequence of this structure is that a number of tasks may be present in one computer system with a minimum of interaction between them. Unless the programmer uses

all the available time of the processor, changes in the operation of one task do not affect the operation of other tasks. Because tasks can easily communicate, synchronization is more easily implemented than in traditional operating systems where the goal is usually complete isolation of tasks from each other.

Input/output operations may be done directly via code and colon definitions or through the task structure when multiple transfers are required. Direct input/output is useful when hardware timing is not critical and the minimum program development time is necessary. When multiple transfers requiring time for hardware operations between them are anticipated, it is best to set up a task to handle the operation. The first step is to set up the task table values to point to the location in memory to or from which the transfer is to occur, and a count for the number of transfers to take place. An interrupt service routine is written to perform each transfer when the hardware device signals it is ready by asserting its interrupt line. When the operation is done, the task's status is set so that it is again executed when it is tested in the round robin loop. During the transfer time, the task is ignored because it is not ready. This situation is analogous to a programmed simulation of a hardware Direct Memory Access (DMA) transfer, where registers are loaded with a memory

address and count of transfers to be made. The hardware supervises the transfer, just as the interrupt service routine does during the programmed transfer. A DMA peripheral interrupts the computer when the transfer is complete, just as the status of the task going to ready signals that the next step in the task's program may be carried out. The difference between DMA and non-DMA tasks is apparent only in the interrupt service routine.

This task mechanism may also be used to implement variable time delays using a relatively simple fixed period clock rather than a more expensive real time clock. The task is set up with a count of the number of fixed period clock interrupts which should occur to produce the desired interval. When the interrupts have occurred, the task status is set to ready, and the next high level operation is executed.

Forth will result in much faster program development, which translates into reduced cost or increased capability. Forth will require minimal memory and mass storage for programs; however, data will require the same amount of storage in any system. Forth will allow the generation of operator interaction routines which are human oriented rather than forcing the operator to adapt to computer's requirements. Forth will allow the programmer to do almost anything he could in assembly language, and do it more

efficiently. The language will not need to be circumvented at every point.

Forth is available for many computer systems and can be written for others in a matter of months so that availability of Forth for a particular system does not influence the hardware selection. Inexpensive, reliable, well designed hardware is naturally desirable. Relatively easy interfacing or the availability of basic interfaces to the computer is necessary to avoid prolonged hardware developments. Digital Equipment Corporation's LSI-11 computer was chosen because it meets all the above criteria. Very importantly, the LSI-11 has an excellent instruction set, resulting in some of the most efficient implementations of Forth.

2. Operator Interaction

With the facilities and concepts of Forth available, improved computer-operator interaction should be implementable. Two levels of interaction are conceivable. The highest level of interaction requires the operator to initiate all operations of the system at the console by invoking the proper words and supplying the needed parameters. These words, descriptions of their functions, and necessary parameters are obtained from the system's operation manual by the user. This level of interaction provides the greatest versatility but requires considerable

knowledge and understanding of the system by the operator. For completely automatic operation, these words and parameters can be combined into a single definition which performs a complete, preprogrammed analysis without requiring multiple operator entries.

At this level the operator may generate definitions which provide any degree of interaction desired. The complete, preprogrammed mode is useful when an analysis method is completely developed. During the development of the method; however, the operator may want to try different parameters or sequences of operation; thus, interaction at a much more detailed level is desired. The operator performing development work is probably quite familiar with the system and would be considerably irritated by lengthy sequences of pedestrian and childish questions utilized by most traditional software to provide the versatility required. Therefore, operator initiated actions at multiple levels of sophistication, as just described, are a welcome improvement in the state of the art.

Another level is possible for persons who may need to develop methods and change operational parameters but are not intimately familiar with the system or do not want to spend a lot of time studying the operation manual. This level can be implemented by programming an extensive series of operator prompts, questions, and opportunities for the

operator to signal the computer to proceed to the next preprogrammed step. These routines can be viewed as an interpreter which operates between the computer and operator. It first determines the operator's wishes through a series of questions, and then implements them by translating them into the parameters and words of the higher level of interaction previously discussed. Thus, it is possible for the operator to choose the level of interaction required by loading or not loading the extra software which provides the prompting level after the basic system is loaded.

This prompting level of software is not implemented for this instrument due to lack of time and the fact that only experienced personnel are expected to use the instrument. The nature of Forth and care exercised in developing the highly interactive level of software indicate that very little modification of the basic system would be required to add the prompting level. It is conceivable that the prompting level software could exist in several versions to more closely supply the needs of different determinations performed with the same or slightly modified hardware configurations.

An automated operator's manual may be provided in the form of a Forth documentation dictionary. Such a dictionary contains descriptions and required parameters

for all the words in the software dictionary resident in the memory of the computer. In addition, operating procedures, comments, cautions, and other useful information could be included in the documentation dictionary. Maintaining this dictionary on-line, with commands available to the operator for searching and displaying the entries, provides a facility superior to the "HELP" files of traditional software systems.

Operator interaction with the on-line documentation dictionaries takes the following form. Entering the word HELP at the keyboard causes a short description of the HELP facility and its use to be printed. The operator may display the contents of the documentation dictionary by typing HELP WORD where WORD is a character string representing the name of the definition or procedure for which information is desired.

The software documentation in Appendix B was produced by listing all the entries of the documentation dictionary for the Multicomponent Continuous Flow Kinetic Analysis instrument. Due to the large volume of information in the documentation dictionary, it must be stored on large capacity mass storage devices. It is not practical to keep more than a very limited subset of the documentation dictionary in memory; thus, the printed dictionary, requiring manual searching of the alphabetized entries, is

a means of providing the required information in systems without mass storage. The printed dictionary is less convenient than the on-line system and requires reprinting when changes or additions are made, but is an organized, versatile means of providing the information needed for operating the instrument.

The form of a documentation dictionary entry is relatively unstructured after the first line, which contains the name of the entry, the block number where the source code for the entry may be found, the vocabulary to which the entry belongs, and a very short description of the entry. Subsequent lines for actual Forth definitions should contain an example of the definition's use and a description of its function and parameters. Other types of entries may take any form after the first line.

This free format allows the inclusion of documentation dictionary entries which provide general information, direct the operator to other entries supplies additional information, or identify errors and suggest diagnostic procedures. The usefulness of the documentation dictionary, be it on-line or printed, is determined by the contents of its entries and the ability of the system designer to provide concise, clear descriptions and to anticipate the user's needs.

The philosophy of providing several levels of

software interaction and "HELP" files has been developed through personal experience with a number of systems and has recently been the subject of a paper by Ziesler (29), who proposed similar ideas.

A rudimentary record management system was implemented to aid in organizing and identifying data records corresponding to the experimental runs conducted with the instrument. An operator assigned run number and the current date and time of day are stored in the data buffer, along with an operator supplied 40 character buffer giving descriptive information about the run, before starting the data acquisition. Consequently, all runs in a group of similar experiments are assigned sequential run numbers and data buffers are stored on disk in sequential locations. These run numbers also correspond to the run numbers recorded in the operator's laboratory notebook, allowing convenient retrieval of the stored data for a run. The type of experiment determines the other information stored with the run data. All data buffers include the colorimeter and flowmeter calibration factors. Other information includes reagent concentrations, timing information, control status information and addresses of subsections of the data.

This information can be used to monitor the performance of the instrument over a period of time. The

analysis of standard materials periodically would allow the easy implementation of a quality assurance program.

Additional fields in the data buffer should be allocated to permit the storage of post run comments by the operator about the validity of the data. Anticipated governmental regulations may require detailed records on all analyses conducted; thus, it may be necessary to substantiate the reasons for rejecting specific runs to non-scientific personnel.

One of the results of the use of the record management system is that tabulated experimental results may not exhibit sequential run numbers. This is apparent in many of the tables in this work. Obviously, an instrumental failure requires the rejection of the data for the run involved. Such failures include running out of reagents, leaks, the inability to maintain flow control over the period of a run and data storage errors. All of these problems were experienced during this study.

Computerized systems allow the rapid generation of huge volumes of data. It is not possible to present all the data in a form useable by human beings; thus, representative data must be selected for presentation. Another reason for nonsequential run numbers is the need to tabulate results in an order other than the order in which data was taken. Occasionally it was desirable to obtain

more intermediate data points in a sequence, or to take data in a random sequence to assure that systematic errors were not being observed.

V. INSTRUMENT EVALUATION

A. Dilution Stability

Before reliable use of the total instrument is possible, an evaluation of the mixing accuracy and overall instrument stability must be made. The questions to be answered are: 1. What are the typical error values to be expected when operating in dilution mode? 2. What is the overall stability or expected variation in output signal under optimum conditions? To answer these questions a series of dilution runs of four minutes duration were conducted with KMnO₄ under varying conditions to generate the information needed to suspect the optimum conditions and performance characteristics.

Initial results suggested that performance could be improved by minor changes in the flow control algorithm. In addition, readjustment of the colorimeter electronics was necessary because several channels had drifted away from the optimum range for efficient source stabilization. These changes resulted in significantly improved performance, which is reported here.

The basic experiment consists of a continuous flow dilution of an intensely colored sample solution, such as KMnO₄, by a non-absorbing reagent. Various flow rates in the sample and reagent channels are maintained by the flow controlling portion of the instrument while the detector

portion records the response of the colorimeters over a period of time. The reagents and samples chosen are such that no chemical reaction occurs; thus, dilution is the only process responsible for any changes in the observed output parameters. Previous experiments have determined that KMnO₄ responds linearly in the concentration range to be observed. After careful calibration of both the flowmeters and the colorimeters, the observed colorimeter response should reflect the dilution ratio determined by the individual flow rates.

Information obtained from the 12 runs regarding instrument stability is summarized in Table XI. Plots of the raw data from the first seven colorimeters were used to generate an evaluation of the total system's stability during the four minute observation period. The eighth colorimeter developed excessive drift during the test; thus, it was not included in the calculations because it could not be calibrated satisfactorily. Later electrical adjustments corrected this problem. The average of the relative standard deviations for the colorimeters is also reported. These figures represent the lowest possible noise levels or error limits which could be expected of the total instrumental system.

Earlier studies have indicated that the noise level, or the relative standard deviation, of the colorimeter

Table XI. Instrument Stability Evaluation

Run #	Average Flow Rates, ml/min			First 7 Colorimeters		
	KMnO ₄	Buffer	Total	Ave.*	SDV	RSDV
1	5.43	--	5.56	500	1.63	.003
2	--	5.42	5.35	0	1.44	.1.4
3	5.44	5.45	10.92	256	5.31	.021
4	6.37	5.44	11.88	275	3.41	.013
5	7.52	5.43	13.17	293	2.50	.009
6	7.38	4.71	12.32	307	2.17	.007
7	3.97	3.93	8.11	256	4.37	.017
8	3.93	5.48	9.59	212	1.76	.009
9	4.47	7.04	11.67	200	1.94	.010
10	4.36	8.45	13.31	182	2.90	.016
11	4.55	9.89	14.64	165	1.94	.012
12	5.85	7.82	13.97	222	2.23	.010

* - Colorimeter response units equal to 1 uM KMnO₄.

alone is around 0.2 percent at a concentration of 500 μM KMnO₄. At a concentration of 200 μM , the relative standard deviation is less than 0.5 percent. Relative standard deviations of up to 2.1 percent are observed in Table XI, several times that which would be expected from the colorimeters alone. The increase can be attributed to instability in the flow rate of the reagents being mixed.

As is expected, the colorimeter response is very sensitive to variations in flow rate. Theoretically, the relative standard deviation of the colorimeter signal should be equal to or less than the sum of the relative standard deviations of the measured flow rates because the response observed is proportional to the flow rate of the absorbing species divided by the total flow. Under most conditions the relative standard deviations of the colorimeter response (1 second averaging periods) and the flowmeter response (16 second averaging periods) are nearly equal. Considering the shorter averaging period of the colorimeter, significantly larger relative standard deviations might be expected. The fact that larger variations are not seen indicates that the flowmeter sensing process is where a large part of the flowmeter noise is introduced and that the actual flow rate does not change rapidly, but very slowly as pressures and liquid levels change.

These results suggest that additional averaging of the flowmeter signal would be in order since the noise of the signal is causing the flow to be adjusted when it shouldn't be. This averaging should only be done when the flow rate is near the flow setpoint to minimize the time required to make large changes in flow rates. Thus, it appears as if two regions of control are needed, the first with less averaging to allow rapid changes in flow rate, and the second with more averaging to prevent adjustment of the flow rate when it shouldn't be.

Rather than actually changing the number of points averaged, two parameters in the flow control algorithm were made changeable. The first parameter restricts the range of deviation from the average value in the buffer which is allowed to be entered in the buffer. Reducing this parameter reduces the effect of a flow value differing greatly from the average on the values for the next 16 seconds. Characteristically, flowmeter values greatly different from the average value are due to noise in the measuring circuit and often appear for only one or two measurement periods, after which the signals return to more normal values.

The second parameter determines the deviation from the setpoint which causes valve movement. Increasing this value decreases the movement of the valve, resulting in

slower adjustment of the flow rate and less oscillations about the flow goal value. An unfortunate side effect of making this change is that the system will tend never to reach the flow goal exactly. Typically, the actual flow rate will be slightly lower than the goal. This is not really a problem since the actual flow rate as determined by the flowmeter is used in subsequent calculations, rather than the actual flow goal value.

Satisfactory flow stability is experienced when the improved flow control algorithm is used, as plots of raw data and the relative standard deviations listed in Table XI show. No significant trends are identifiable, other than the expected fact that lower relative standard deviations are observed as the colorimeter outputs approach full scale. Generally, colorimeter signal relative standard deviations of less than two percent are encountered. Figure 42 shows a plot of the first seven colorimeter channels (superimposed) for a period of four minutes. A relatively stable output is observed. It can be seen from Figure 43 that relatively minor changes in flow produce corresponding changes in the response, particularly near the end of the run.

The accuracy of the overall instrument can be evaluated by comparing the dilution predicted by the ratio of the measured flow rates, averaged over the observation

Run 6 of 145 58 10 17 27 FEB 1981
7.5/4.8 500 uM KMnO4 DILUTION Block 2750

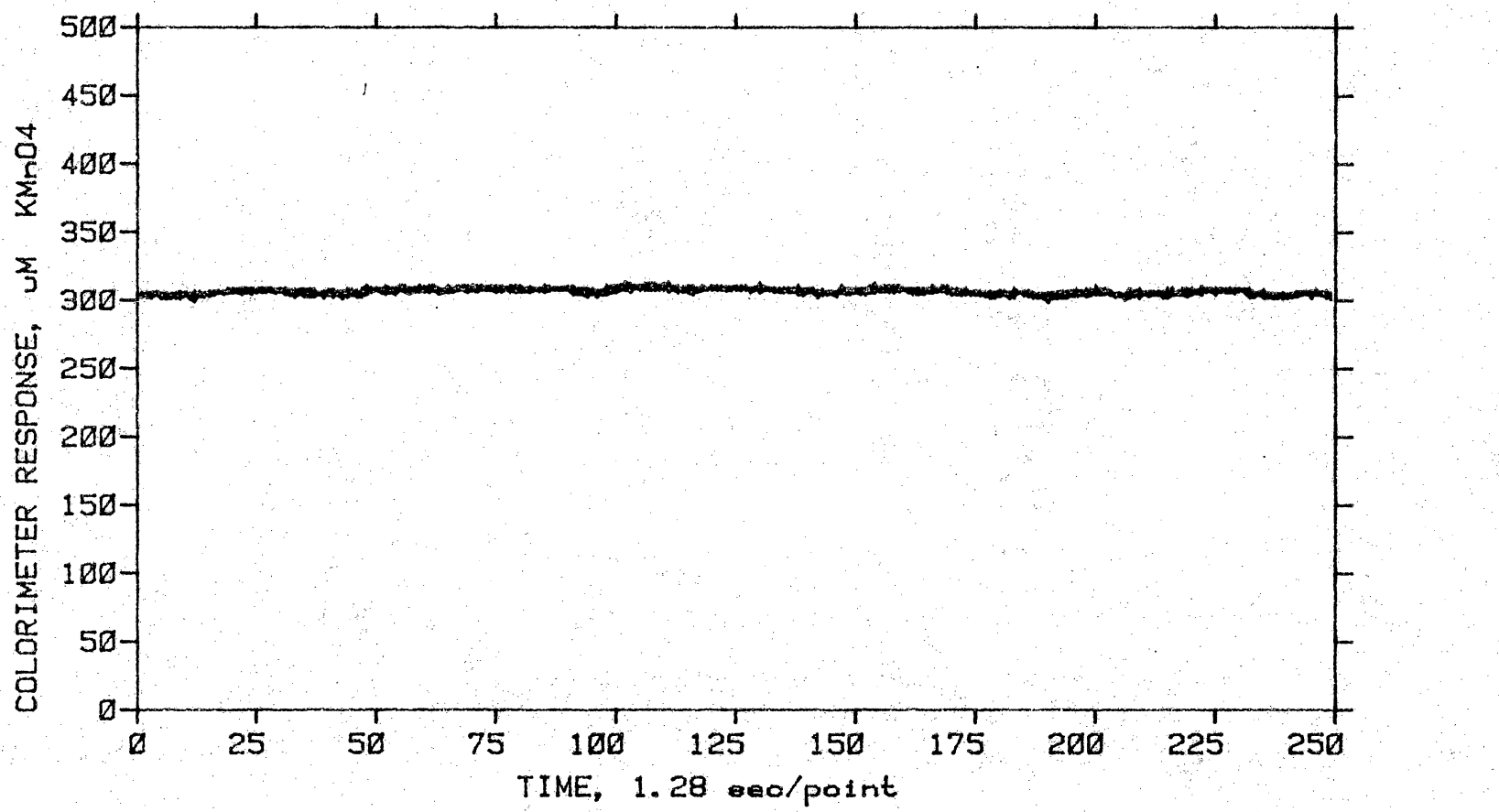


Figure 42. Dilution Stability Colorimeter Response

Run 6 of 145 58 10 17 27 FEB 1981

7.5/4.8 500 UM KMNO4 DILUTION Block 2750

FM1 ----- FM2 ----- BALANCE -----

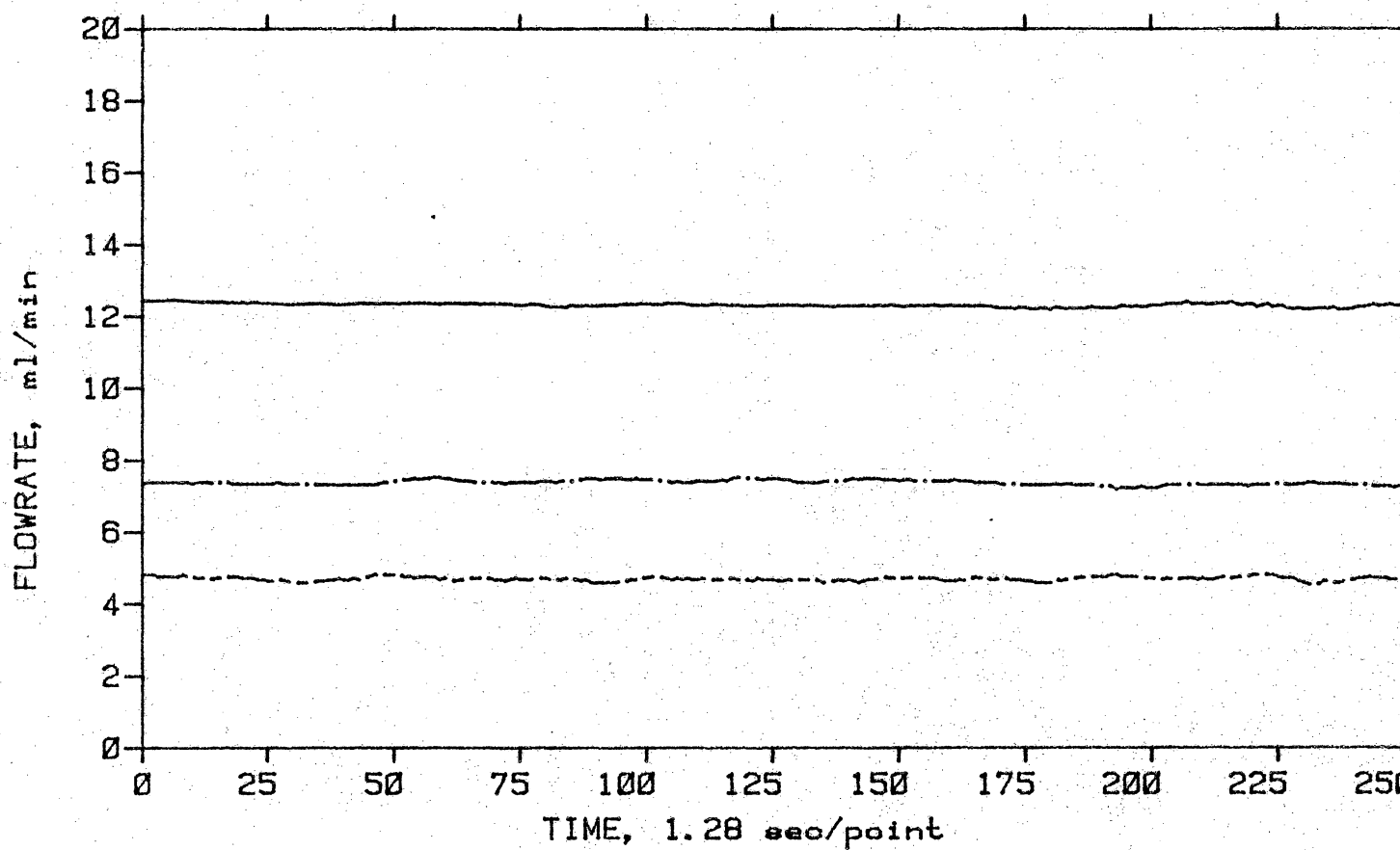


Figure 43. Dilution Stability Flowmeter Response

period, to the response of the colorimeters. Table XII indicates the fraction of the full scale colorimeter value which should be expected on the basis of the flow soil values, actual measured and averaged flow values, and the average of the actual observed values for the first seven colorimeters, reported as a fraction of the full scale value.

In many cases the observed colorimeter value is within two standard deviations of the fraction of full scale predicted from the measured flow rates, a satisfactory result. Larger errors are observed as the colorimeter output value decreases, as would be expected. Errors of less than two percent can be expected under optimum conditions.

Table XII. Dilution Accuracy Evaluation

Run#	Flow Goals, ml/min			Measured Fraction of Full Scale	SDV	Error %
	KMn	Buf	Ratio			
1	5.5	--	--	--	1.000	.003
2	--	5.5	--	--	.000	.003
3	5.5	5.5	.500	.500	.512	.011
4	6.5	5.5	.542	.539	.550	.007
5	7.5	5.5	.577	.581	.586	.005
6	7.5	4.8	.610	.610	.614	.004
7	4.0	4.0	.500	.500	.512	.009
8	4.0	5.5	.421	.418	.424	.004
9	4.5	7.0	.391	.388	.400	.004
10	4.5	8.5	.346	.354	.364	.006
11	4.5	10.0	.310	.315	.330	.004
12	6.0	8.0	.429	.428	.444	.005

B. Flow Injection Analysis

The configuration of this instrument is very similar to that of flow injection analysis instrumentation; thus, its performance under flow injection conditions is of interest. A simple flow injection configuration was assembled, consisting of a carrier reagent source and flow controlling element. This was followed by a chromatographic sampling valve which allowed the injection of sample pluss into the flowing carrier stream. Finally, the reaction-observation tube, with its eight detectors, served as a colorimetric detector for flow injection analysis. In this configuration, only one reagent stream is used and no mixer is necessary. Evaluation of the instrument's flow injection performance was done with a non-absorbing buffer solution as a carrier. The sample solution injected into the carrier stream consisted of the carrier with various concentrations of KMnO₄ added. The colorimeters employed green LEDs, emitting radiation at 565 nm.

The instrumental configuration is different from conventional flow injection instrumentation in several ways. First, the carrier reagent is propelled through the system by pressure from an inert gas rather than by some type of pump. Although many types of pumps have been used

successfully for flow injection analysis, only syringe pumps provide compressible pulseless flow. Also, pressurized flow is much less expensive than most satisfactory pumps. Pressurized flow is not without its problems, however. The flow rate is sensitive to reagent reservoir level and resistance to flow by components of the system. It is necessary to control the flow of the liquid, not just regulate the pressure of the gas. In this respect, positive displacement pumps have the advantage.

The other major difference is in the detector. Eight detectors are evenly spaced along the reaction-observation tube. This allows the dispersion of the sample plus to be studied easily. The current observation tube has an inside diameter of 1 mm, considerably larger than the 0.5 mm which results in the minimum amount of dispersion. This is a compromise between reducing dispersion or colorimeter sensitivity by reducing the absorption path length.

Experience indicates that dispersion is not excessive at the first colorimeter, which is the detector corresponding to the detector of a conventional flow injection system. The effect of dispersion during transit of the tube is important if the rest of the detectors are to be used to follow the progress of a reaction taking place in the tube.

The questions to be answered are then: 1. What is

the effect of dispersion on the peak height, shape, and area? 2. What is the response of the system to a range of reagent concentrations and how linear is that response? 3. What is the effect of flow rate on peak area? The primary point here is the error introduced in peak area due to small changes in flow rate. To answer these questions, 76 runs consisting of an injection of a sample plus into the flowing carrier stream and subsequent data recordings were done. Various flow rates, sample loop sizes and sample concentrations were used.

Figures 44 to 46 show the observed response of the eight colorimeters to 100 μl injections of 500 μM KMnO₄ at flow rates of 9, 6, and 3 ml/min. It is clear that dispersion increases as the sample plus travels down the observation tube and as the flow rate decreases. Only in the last two colorimeters of the 3 ml/min run does the signal not return completely to baseline in the 40 second observation time. In all cases the signal eventually does return to baseline. It is obvious that increasing dispersion, due to decreasing flow rate or increasing distance from the injection point, decreases the peak height and increases peak tailing considerably.

Table XIII displays the peak area for each colorimeter at various flow rates. Injections of 100 μl of 500 μM KMnO₄ were used to generate this data. It is clear

Run 47 of 837 56 7 22 25 JAN 1981

500 PPM KMNO4 9 ML/MIN LOOP A

Block 3620

COLORIMETER RESPONSE, Absorbance

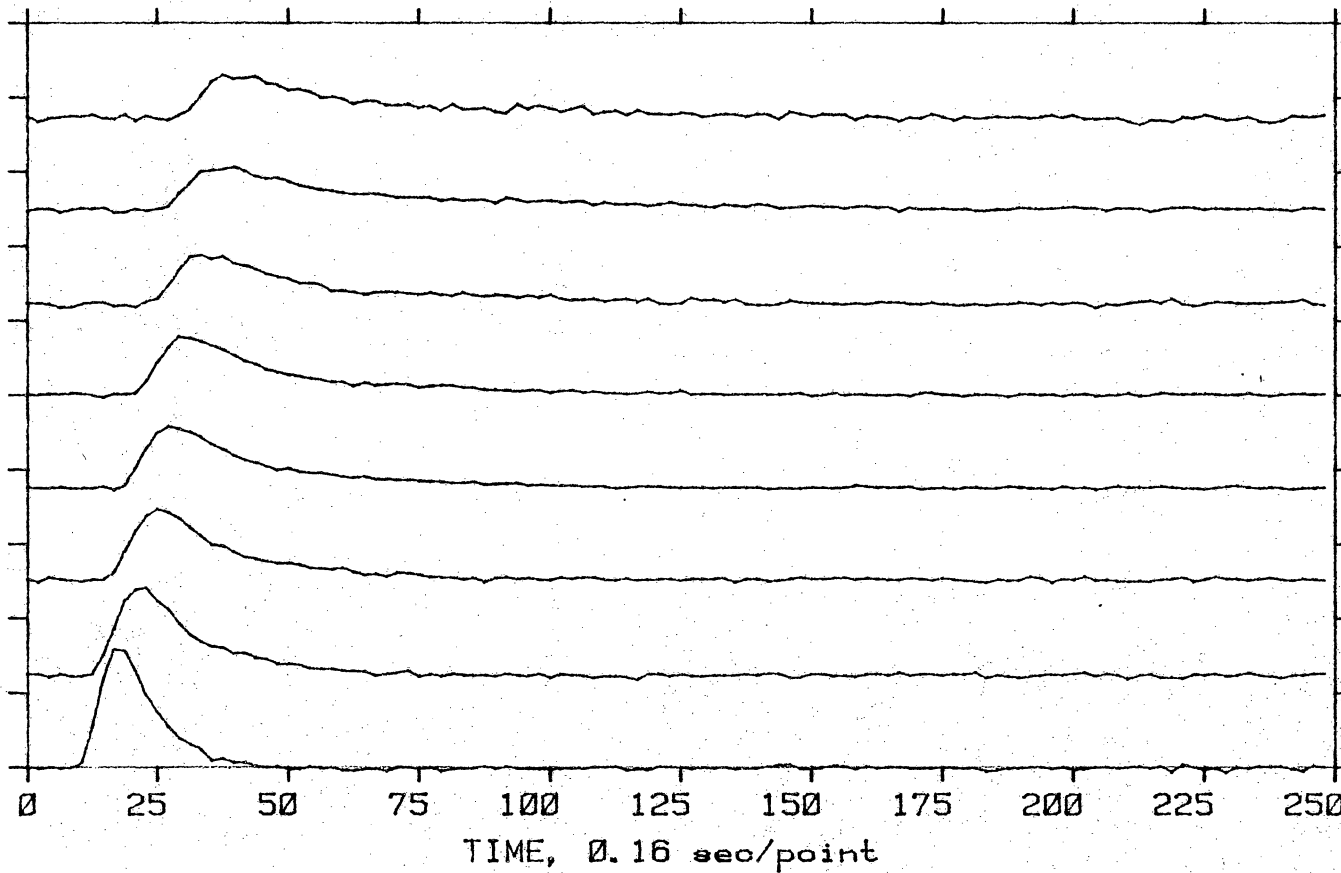


Figure 44. Colorimeter Response to KMnO₄, 9 ml/min

Run 50 of 199 46 14 22 25 JAN 1981

500 PPM KMNO4 6 ML/MIN LOOP A

Block 3650

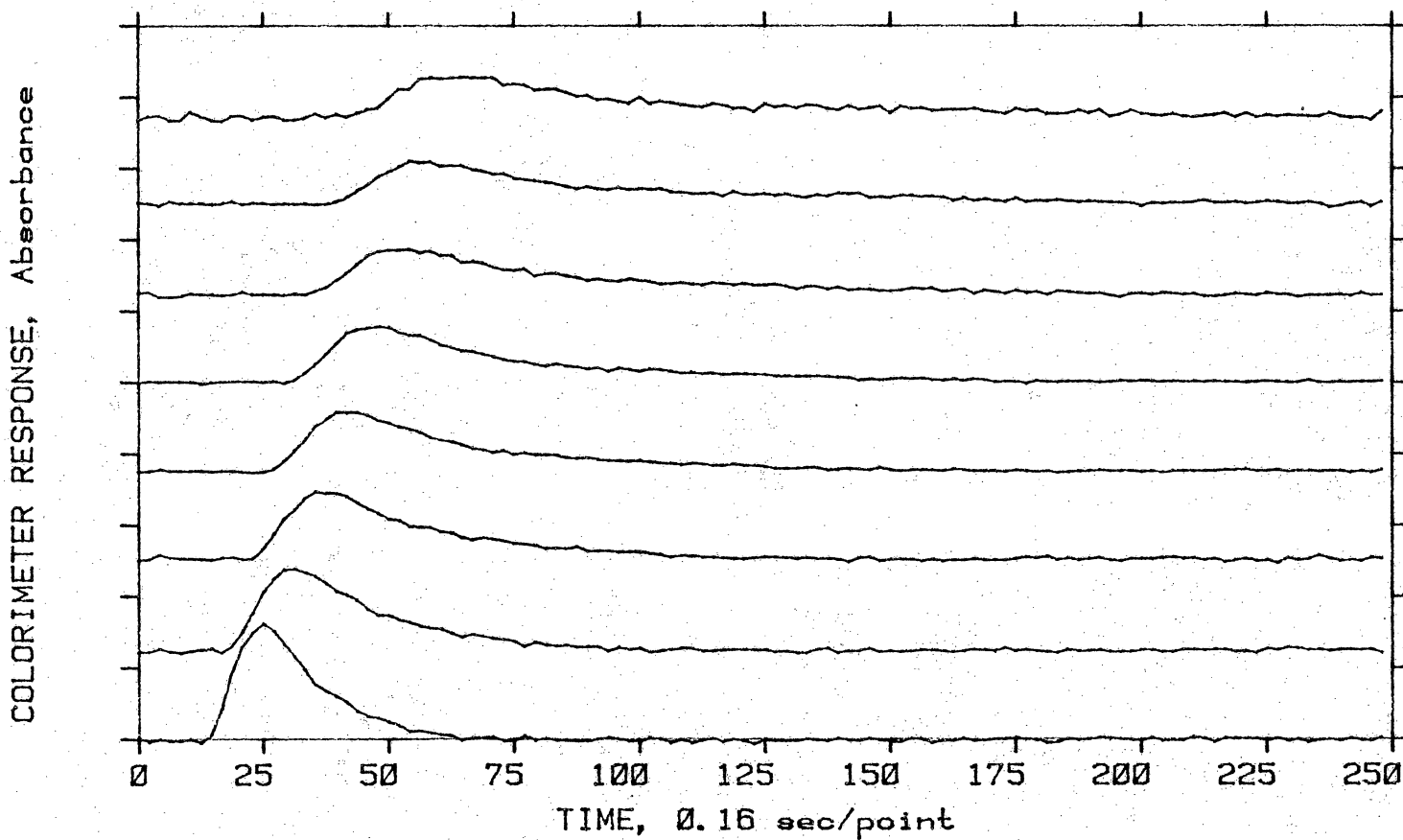


Figure 45. Colorimeter Response to KMnO₄, 6 ml/min

Run 53 of 128 24 23 22 25 JAN 1981
500 PPM KMNO4 3 ML/MIN LOOP A Block 3700

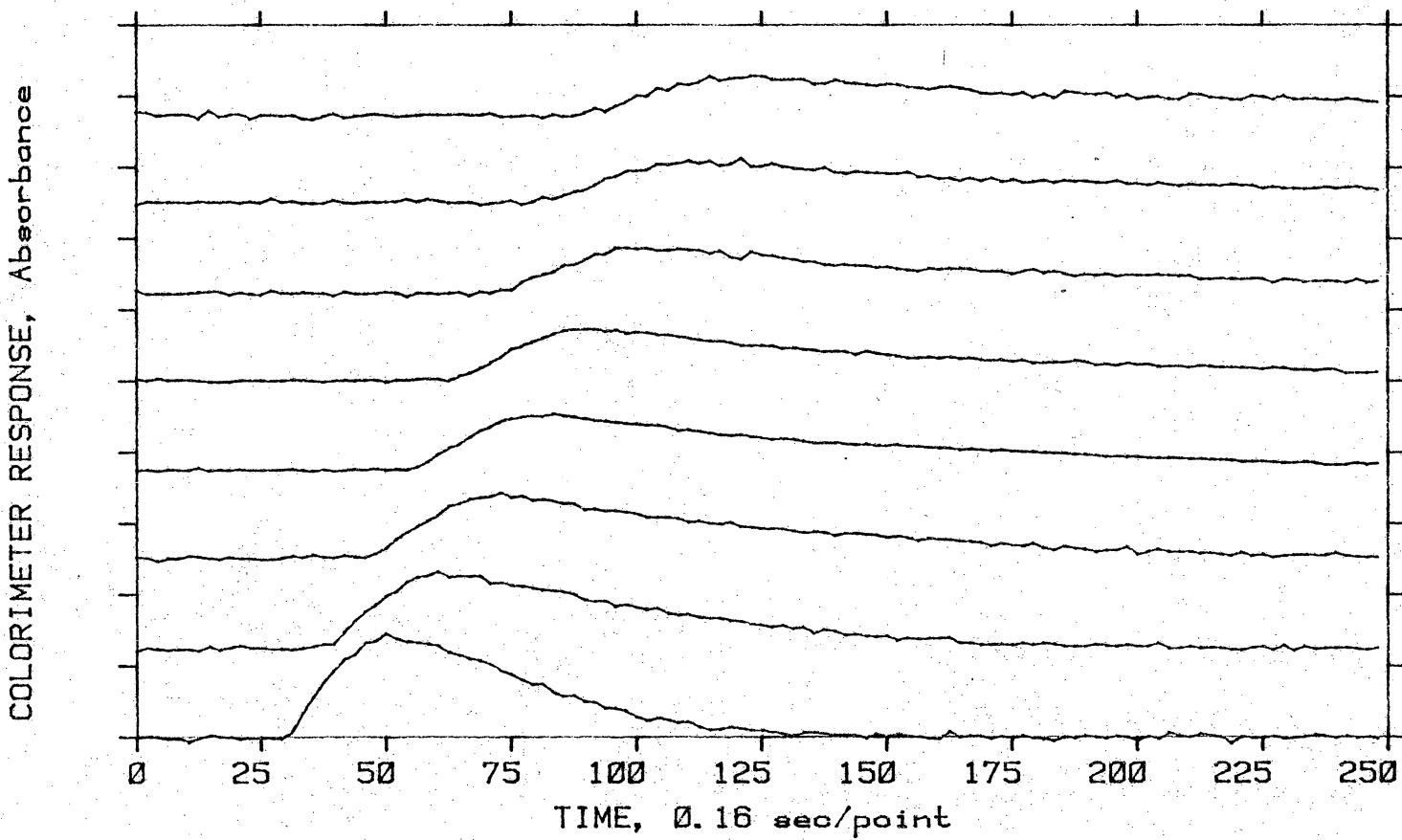


Figure 46. Colorimeter Response to KMnO₄, 3 ml/min

Table XIII. Peak Areas, 100 μl injections of
500 μM KMnO₄

Run#	47	48	50	51	52	53	54	55
Flow, ml/min	9	8	6	5	4	3	2	1
Channel								
0	17.9	18.8	31.1	38.1	51.2	68.6	110.8	91.0
1	19.6	25.2	33.3	39.1	51.0	74.1	100.7	91.4
2	20.2	20.5	26.7	39.2	44.4	67.7	107.3	93.8
3	20.8	22.7	29.9	36.6	46.9	68.4	102.5	89.7
4	20.6	23.8	32.0	36.2	47.0	64.4	102.4	91.2
5	23.7	22.9	31.3	38.0	46.7	62.1	103.3	89.1
6	25.1	23.1	28.8	34.2	43.3	66.1	95.6	92.2
7	23.1	26.5	36.3	35.3	43.0	60.0	106.6	93.7
Average	21.4	22.9	31.2	37.1	46.7	66.4	103.7	91.5
SDV	2.4	2.4	2.9	1.8	3.1	4.4	4.6	1.7
RSDV	.11	.11	.09	.05	.07	.07	.04	.02

from the table that, aside from fairly large relative standard deviations, no consistent trends are observed. For all practical purposes, the area under the peak is equal for all the colorimeters, even if dispersion varies greatly, at a constant flow rate. The integration window was closed before the signal returned completely to baseline for several of the final colorimeters at the low flow rates; however, no significant trends toward decreasing area are observed. Under more severe tailing conditions, a decrease is observed; thus, the area contained in the extreme trailing part of the peak is quite small, as would be expected.

It is also reasonable to expect that equal areas would be observed under varying dispersion conditions. The area should be proportional to the amount of material injected. It should not change if a linear detector is used, even if the material is dispersed in the carrier stream. The amount of material passing the detector does not change, just the amount of time it takes for the material to pass changes. Obviously, if the area does not change, but the dispersion does, the peak height must change. A steadily decreasing peak height is observed with increasing dispersion.

A point of minor interest is the variation of peak area with flow rate. Theoretical studies (30) indicate

that dispersion is inversely proportional to flow rate. It has been established that area is not dependent on dispersion, but Figure 47 shows that, over the limited flow rate range of 9 to 3 ml/min, the peak area is inversely proportional to the flow rate. Examining Figures 44 to 46 it is apparent that the sample plus spends more time being observed by the detector at lower flow rates, even though the peak amplitude of the plus is not as great. An integration method which sums periodically sampled amplitudes will obviously result in larger areas if peak amplitude does not decrease proportionally, as it does not according to the Figures. Assume no dispersion, i.e., the sample plus appears as a constant amplitude pulse with sharp edges. Area would then be given by the amplitude multiplied by the time. The area under these conditions would be inversely proportional to the flow rate because more time is required for a sample plus of a given size to pass the detector. Some reduction in height is experienced under flow injection conditions, but it is only a factor of about 1/3 under the flow rate range examined. The important point to be obtained from this investigation is that the area is affected by the flow rate; thus, constant flow rates are required for consistent results with this method.

Table XIV reports peak areas determined under a

Slope 2.135 E 0 Intercept -4.389 E 1 Corr. Coef. 9.987 E -1
500 μ M KMnO₄ 100 μ l Sample Loop Average of all detectors

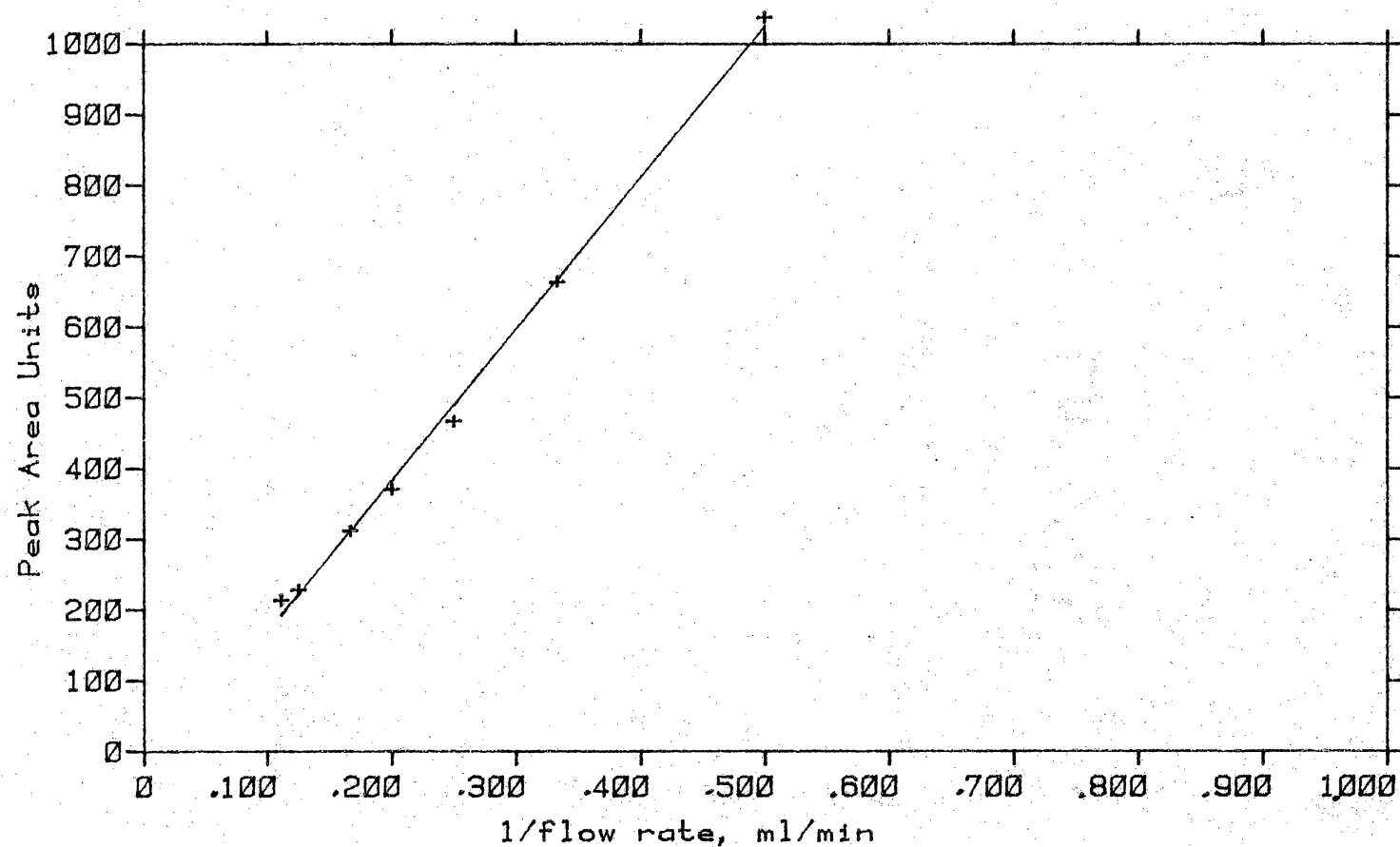


Figure 47. FIA Mode Calibration Curve, Flow Rate

Table XIV. Peak Areas, 100 μ l injections into a
2 ml/min carrier stream

Run#	62	63	64	65	66	67	68	69	61	60
Conc., μ M	0	60	100	200	300	400	500	600	1000	2000
Channel										
0	1.7	3.0	7.5	17.3	25.5	32.2	45.2	58.5	92.4	178.9
1	1.2	4.0	10.7	15.7	29.4	30.1	45.5	55.7	92.1	172.7
2	4.0	4.3	9.2	17.3	26.3	29.1	41.1	52.4	95.7	183.6
3	1.4	5.2	7.7	19.4	26.1	30.1	47.2	57.2	93.3	181.0
4	0.4	3.1	6.4	19.6	26.0	30.3	46.4	58.3	99.2	187.3
5	0.4	5.2	8.2	19.5	27.5	31.2	46.7	54.2	98.6	190.8
6	0.0	3.1	6.4	13.4	25.0	29.4	42.7	57.7	104.3	196.9
7	6.2	3.1	9.4	13.2	28.0	32.7	47.8	57.2	103.8	194.4
Ave.	1.9	3.9	8.2	17.4	26.7	30.6	45.3	56.4	97.4	185.7
SDV	2.1	.9	1.5	2.2	1.5	1.3	2.3	2.1	4.9	8.2
RSDV	1.11	.24	.18	.13	.05	.04	.05	.04	.05	.04

constant flow rate of 2 ml/min and 100 μ l injections of various concentrations of KMnO₄, reported in μ M. Again, in the concentration range of 0 to 600 μ M KMnO₄, no clear trends are apparent. At concentrations above 600 μ M, where diversion does not reduce the observed concentration of the sample plus to values below 600 μ M, it appears that negative deviations from linearity result in slightly low area values for the first few colorimeters.

Considerable variation is observed between colorimeter channels, as in Table XIII. At concentrations greater than 100 μ M, the relative standard deviation is less than 20 percent, declining to about 5 percent at 300 μ M and above. Therefore, the optimum concentration range for this configuration is 300 to 600 μ M, with the range of 100 to 1000 being usable. Figure 48 shows that peak area exhibits very good linearity with concentration, even over the extended range of 0 to 2000 μ M.

Slope 9.404 E -1 Intercept -1.177 E 1 Corr. Coef. 9.988 E -1
Flow Rate 2 ml/min 100 ul Sample Loop Average of all detectors

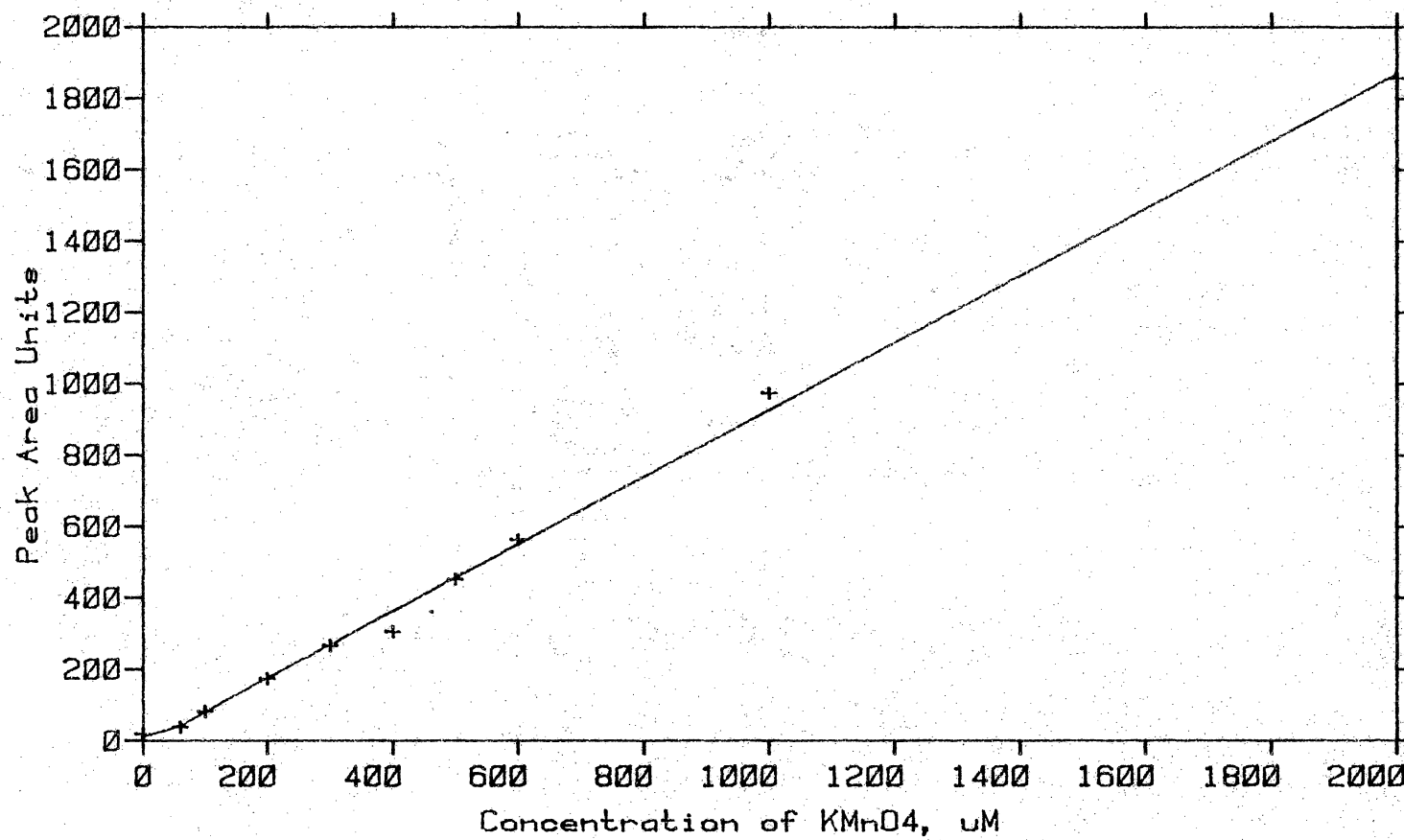


Figure 48. FIA Mode Calibration Curve, Peak Area

C. Flow Injection with a Reaction

Many of the more useful Flow Injection methods mix a reagent with the carrier stream containing the sample plus, allowing a reaction to occur, before the detector is reached. In this manner, various chemical reactions can occur, resulting in the appearance or disappearance of color which can be measured conveniently by a simple colorimeter. The Multicomponent Continuous Flow Kinetic Instrument is easily configured to perform determinations of this type.

One of the chemical systems chosen for evaluation of this mode of operation is the same one that was used for the mixing efficiency evaluation, the neutralization of NaOH by HCl. Methyl Red indicator is added to the base which is injected into a carrier stream consisting of a neutral buffer of NaCl. The sample plus, of base and indicator, in the carrier stream reacts with a slight excess of acid in the mixer and then flows down the observation-reaction tube. The red form of Methyl Red appears in the mixer when the solution becomes slightly acidic. The area under the peaks, detected by the colorimeter, can be used to prepare a calibration curve to allow determination of various concentrations of the indicator. The base must be completely neutralized by the

acid before the red color can appear. Because of the binary nature of indicators, the actual concentrations of base and acid have no effect as long as the acid is in excess.

Table XV indicates the peak area observed when 100 μ l injections of base and indicator are made in a 6 ml/min neutral carrier stream which is subsequently mixed with a 6 ml/min acid stream. Selected runs are reported from the total of 34 conducted at various relative concentrations of Methyl Red indicator in base. As in Table XIV, where no reaction occurred, no significant trends in the area is observed.

Trends in the relative standard deviation of the peak areas of a particular run correspond to those of Table XIV, with comparable values. It is clear that low relative concentrations result in higher deviations or greater noise in the observed areas, as would be expected. Examining run to run statistics compiled in the last several lines of the Table, it is apparent that the relative standard deviations of the average peak areas for the 4 to 7 runs made at each relative concentration are beginning to approach values of one percent at the higher concentrations. Relative standard deviations of less than one percent are typical of good flow injection analysis systems.

These results indicate that the instrument is capable

Table XV. Peak Area, 100 μ l injections of indicator into a 6 ml/min carrier stream with a subsequent reaction

Run#	23	21	6	30	32
Rel. Conc.	.111	.167	.333	.667	1.000
Channel					
0	1674	2851	4654	8637	13023
1	1671	2555	5052	8846	13503
2	1618	2685	4858	8371	12775
3	1583	2810	4694	8740	13466
4	1444	2420	5056	8405	12813
5	1615	2168	4870	8551	12859
6	1399	2558	4640	8558	13374
7	1467	2630	4647	8401	12878
Average	1567	2584	4809	8564	13090
SDV	114	219	177	171	310
RSDV	.073	.085	.037	.020	.024
Average of average areas					
	1622	2406	4885	8455	13160
RSDV of average areas					
	.053	.047	.038	.016	.005
Average of channel 0 peak heights					
	176	258	525	877	1349
RSDV of channel 0 peak heights					
	.086	.039	.049	.026	.008

of good flow injection analysis operation in the higher concentration portion of the test range. These concentrations are probably higher than one would routinely encounter; thus, a reduction in colorimeter noise or an increase in colorimeter sensitivity is desirable. This problem is not unexpected because the colorimeter path length is one tenth that of most instruments.

One of the final lines of Table XV lists the average peak amplitude of channel 0 at the various relative concentrations. The colorimeter was calibrated with blank or I_0 values obtained when non-absorbing material was in the tube. Full scale, or values of 1000, were obtained when a solution of relative concentration of .333 (0.5 ml Methyl Red stock in 100 ml 0.1 M NaOH) was neutralized by a very slight excess of acid. Significant dispersion has not yet occurred at colorimeter 0 because a peak amplitude of 525 is observed. A value of 500 is expected because the base has been diluted 1:1 by the reaction with an equal flow of acid in the mixer.

Figure 49 shows the calibration curve prepared from the peak areas in Table XV. The average of the average peak areas are plotted vs. relative concentration. A good linear response is obtained, with the point at .667 being about one standard deviation low and the point at .333, one standard deviation high.

Slope 1.265 E 0 Intercept 3.585 E 1 Corr. Coef. 9.990 E -1
Flow Rate 6 ml/min each 100 ul Sample Loop Average of all detectors

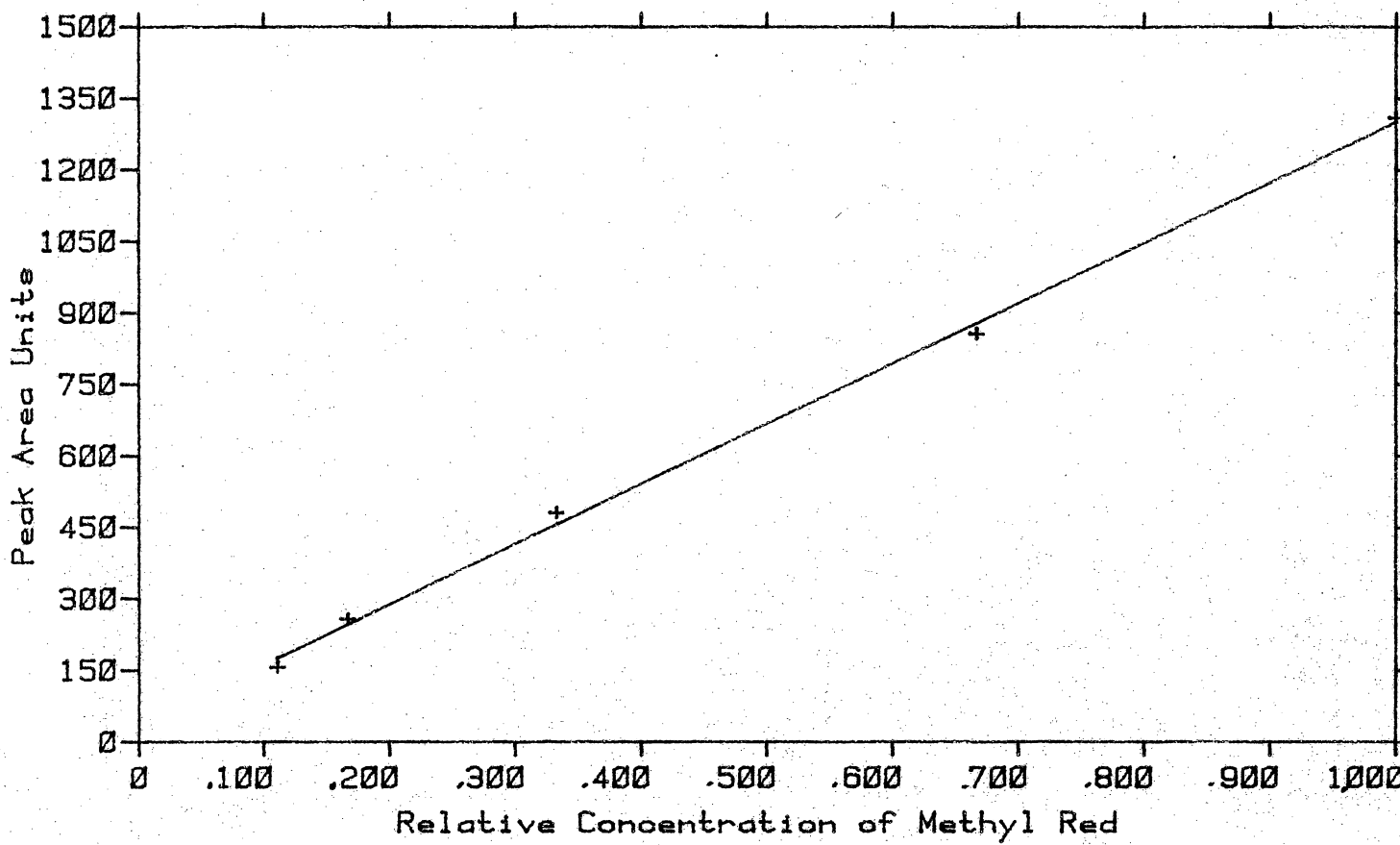


Figure 49. FIA Mode Calibration Curve, Methyl Red Area

Figure 50 shows the peak amplitude response of colorimeter 0 plotted vs. relative concentration. Good linearity is experienced at low relative concentrations. This may be due to the fact that the .111 and .167 solutions were prepared by dilution from the .333 solution, while the .667 and 1.000 solutions were separate preparations.

A more interesting system is the reaction of KMnO₄ with Fe(_{aq})²⁺. The flow injection characteristics of KMnO₄ without a reaction have been investigated in the previous section. Table VIII of the mixer section shows that this reaction results in good mixing at flow rates greater than 5 ml/min and that the relative standard deviations of the colorimeter values are less than two percent. In contrast to the acid-base indicator system, a continuous response is obtained. The observed response to KMnO₄ at 565 nm should be diminished in proportion to the concentration of Fe(_{aq})²⁺ reacting with the KMnO₄ sample plus at the mixer.

In practice, a 2.5 mM solution of Fe(II) in acid combines with the carrier stream, consisting of the buffer solution without Fe, at the mixer. 100 μ l injections of various concentrations of KMnO₄ in the same buffer solution are made by the sampling valve in the carrier stream.

According to a conventional titration, 1.90 ml of Fe(_{aq})²⁺ is required to neutralize 1.00 ml of 500 μ M KMnO₄.

Slope 1.290 E 0 Intercept 4.900 E 1 Corr. Coef. 9.980 E -1
Flow Rate 6 ml/min each 100 ul Sample Loop Average Chan 0 Height

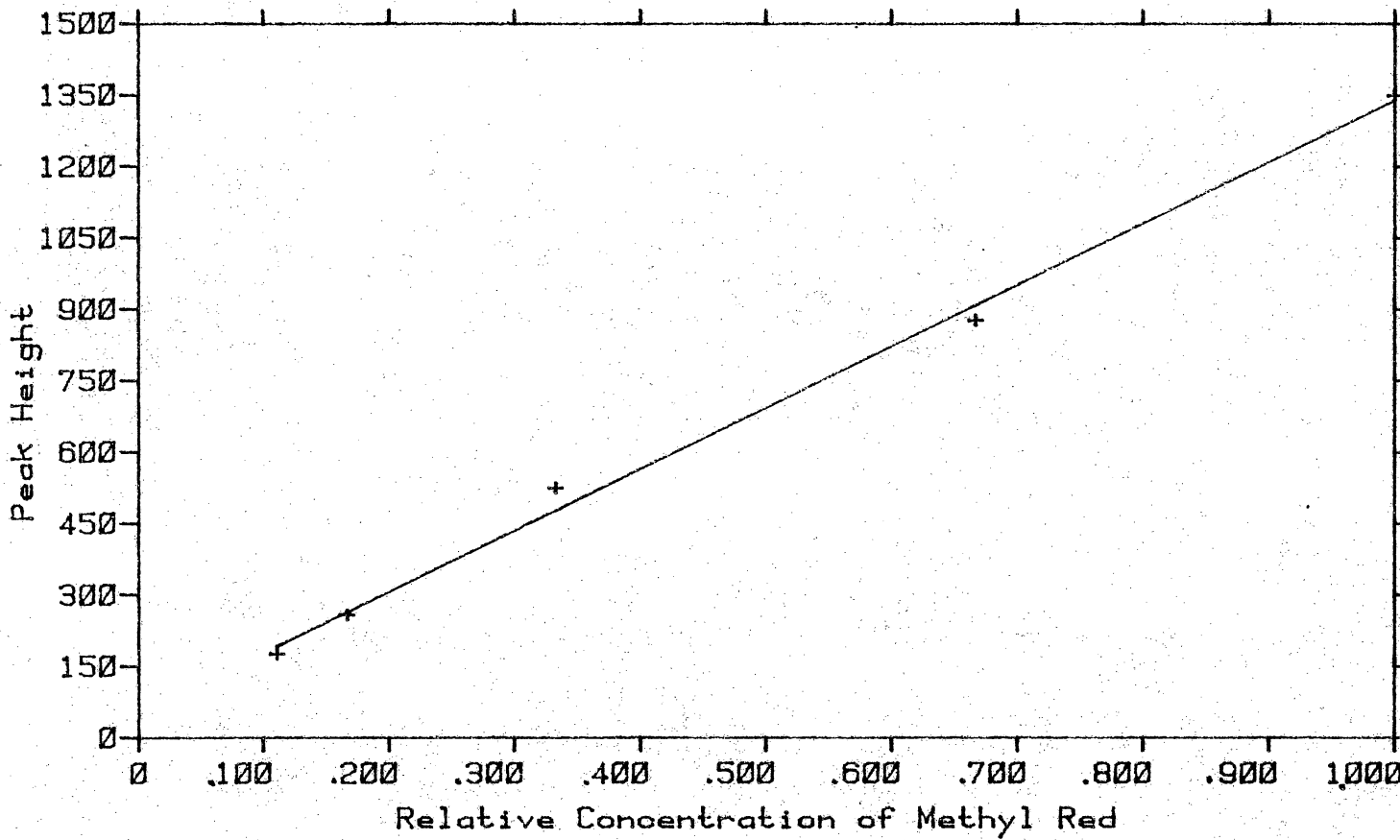


Figure 50. FIA Mode Calibration Curve, Methyl Red Peak Height

Therefore, the $\text{Fe}(\text{aq})^{++}$ is equivalent to 263 μM KMnO_4 . With equal flow rates for both channels, the $\text{Fe}(\text{aq})^{++}$ reagent stream will be diluted by the carrier stream, resulting in a 132 μEqV $\text{Fe}(\text{aq})^{++}$ concentration in the mixer. Likewise, the KMnO_4 sample plus will be diluted by the reagent stream. One would expect to observe a response proportional to the KMnO_4 sample concentration minus the quantity neutralized by the $\text{Fe}(\text{aq})^{++}$.

Figure 51 shows the peak response of the first colorimeter to various sample concentrations of KMnO_4 . It is quite obvious that the presence of the $\text{Fe}(\text{aq})^{++}$ has displaced the X axis intercept from the origin to practically 500 μM KMnO_4 . After the KMnO_4 concentration is greater than the $\text{Fe}(\text{aq})^{++}$, a good linear response is observed. A similar response is obtained from the peak areas of the first colorimeter.

Table XVI compiles peak areas of the colorimeter signals for runs representative of the various KMnO_4 concentrations. The most outstanding feature of this Table is that the peak area consistently decreases for successive colorimeters. Previous tests have shown that mixing is adequate and that all colorimeters agree when the same reaction is conducted in a non flow injection mode. Careful tests show that this is not an artifact, in fact, the values look suspiciously like some type of rate

Slope 3.444 E 0 Intercept -1.571 E 3 Corr. Coef. 9.995 E -1
Flow Rate 6 ml/min each 100 μ l Sample Loop Chan 0 Peak Height

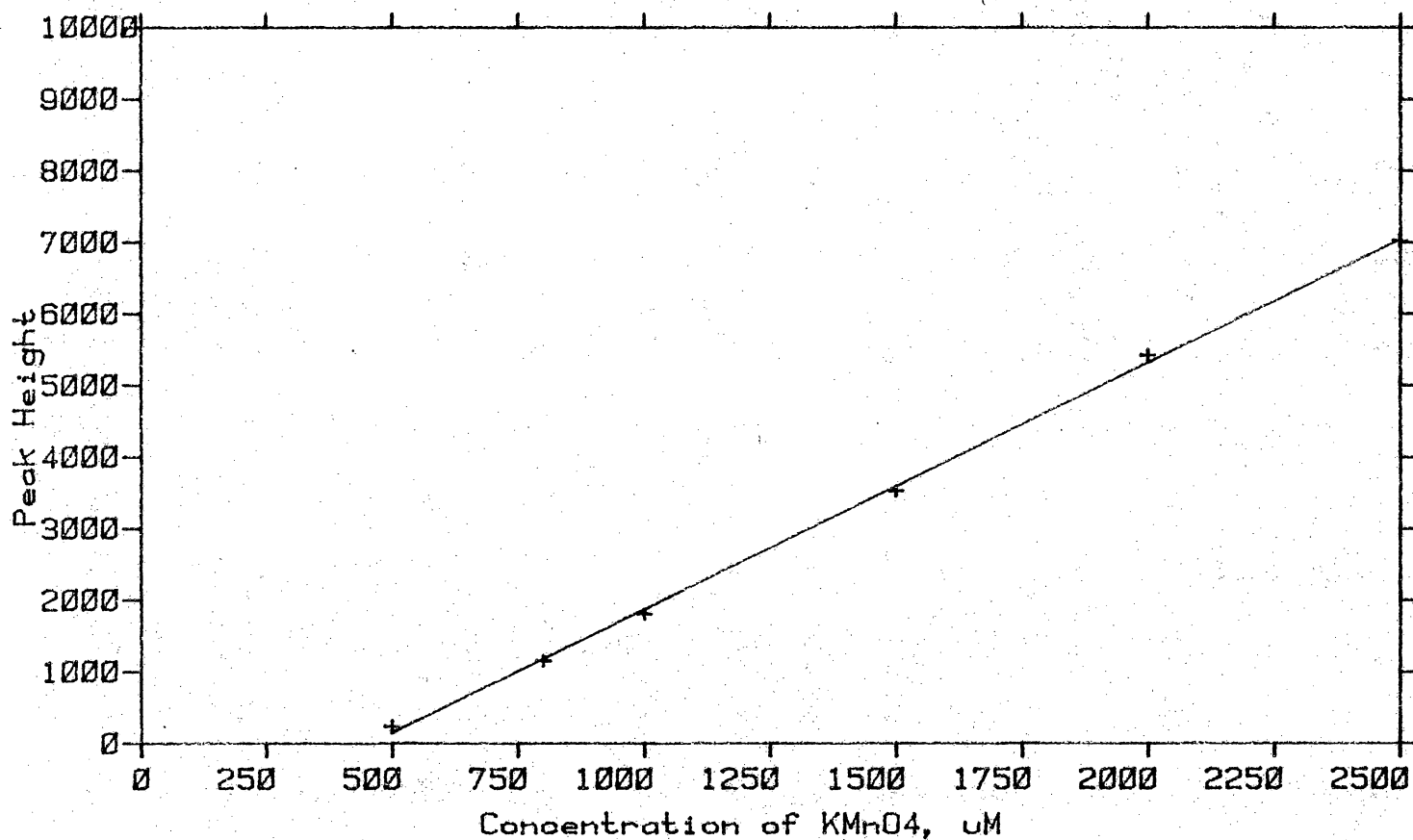


Figure 51. FIA Mode Calibration Curve, KMnO₄ Peak Height

Table XVI. Peak Area, 100 μl injections of KMnO₄
into a 6 ml/min carrier stream with a
subsequent reaction with Fe(asc)⁺⁺

Run#	104	109	114	118	121	127
Conc., μM	500	800	1000	1500	2000	2500
Channel						
0	940	11244	19661	46058	74271	106609
1	983	9665	15634	42313	69586	99941
2	1854	7823	13345	38671	65009	96608
3	1280	7636	12861	35104	62007	93955
4	910	7311	12681	33504	58738	90088
5	1154	6356	12209	28638	53589	84127
6	1255	6358	11191	25489	48334	76983
7	252	5122	10359	24413	44607	73384
Average	1016	7689	13492	34274	59517	90211
SDV	594	1958	2939	7840	10272	11425
RSDV	.585	.255	.218	.229	.173	.127

process. Figure 52 confirms this fact. Plotting the logarithm of the peak area vs. colorimeter number, which corresponds to time, results in a good linear decay line.

Naturally, the interpretation of this observation is very important if kinetics are to be done in this mode of operation. The kinetics of the KMnO₄ - Fe(^{aq})²⁺ reaction are known to be fast (16) and the mixer is known to perform adequately. Thus, a significant problem exists. Carefully reviewing the characteristics of flow injection peaks and the chemical configuration of this system points to the answer. The system consists of a Fe(^{aq})²⁺ reagent stream mixing with a carrier which may contain a 100 μ l plus of KMnO₄. The Fe(^{aq})²⁺ neutralizes an equivalent amount of KMnO₄ in the mixer, but the system is designed to operate with an excess of KMnO₄ so that an absorbing species is present. A decrease in response compared to the situation where no Fe(^{aq})²⁺ is present will be observed.

After leaving the turbulent conditions in the mixer, the flow in the observation tube is laminar. The plus of KMnO₄ moves down the tube while undergoing the process of dispersion. The plus spreads along the axis of the tube, with the center of the plus traveling faster than the sides. This, of course, effects the peak height detected by the colorimeters considerably; but, very importantly, it has been shown that the area is not significantly effected.

Slope -4.089 E 1 Intercept 4.667 E 3 Corr. Coef. -9.944 E -1
Flow Rate 6 ml/min each 100 ul Sample Loop Run 118

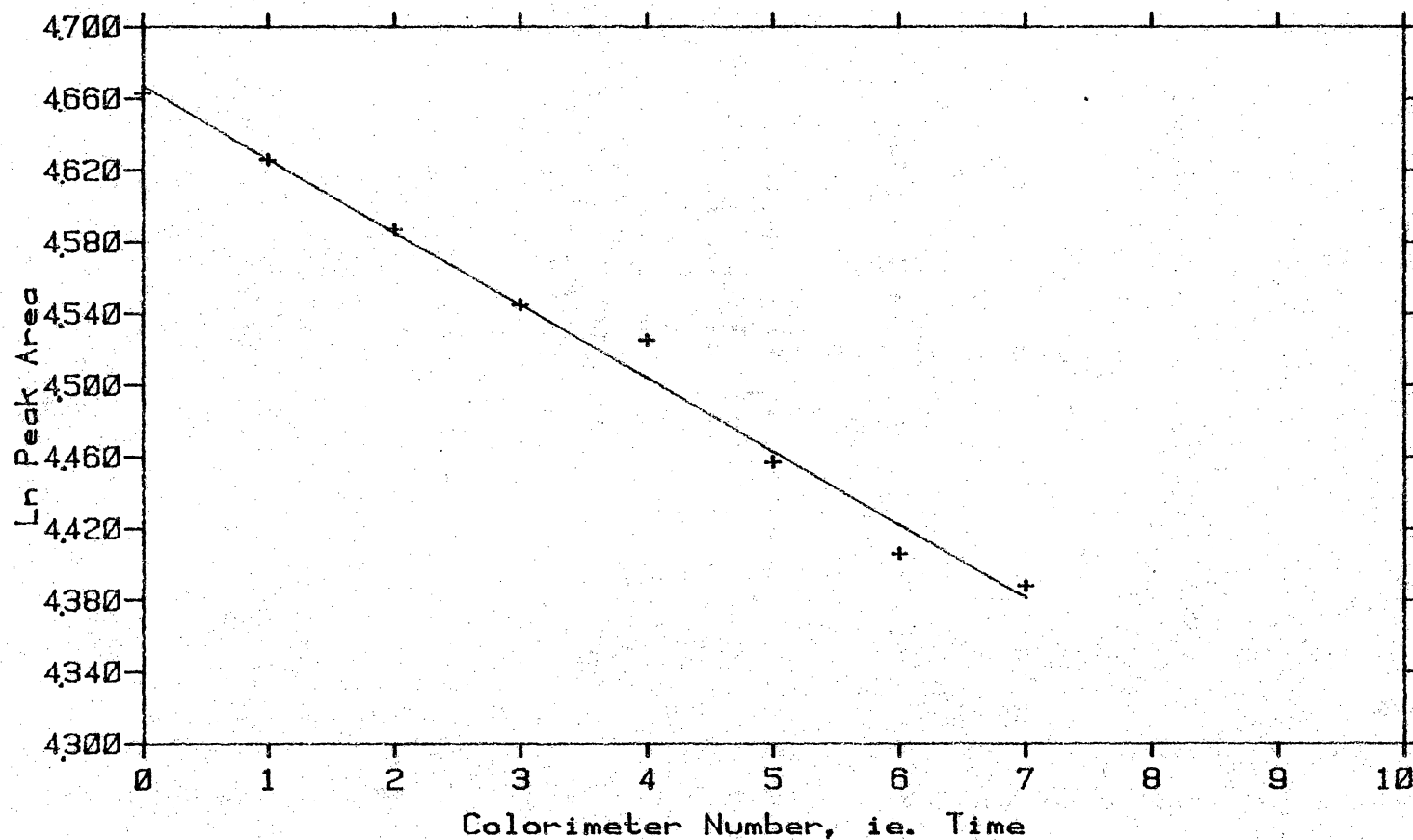


Figure 52. FIA Diffusion Rate

The process of dispersion consists of convection, the mixing of the molecules within the sample plus, and diffusion. Although the plus maintains its envelope as it travels, there is obviously some diffusion of molecules between the contents of the plus and the carrier around it. Because the flow is non-turbulent, the rate of this diffusion is low and not much mixing occurs between the molecules of the plus and surrounding carrier solution.

The plus in this system contains unneutralized KMnO₄, while the carrier contains Fe(Se)⁺⁺. The unexpected rate, which was observed, is probably the diffusion of Fe(Se)⁺⁺ into, and KMnO₄ out of the plus. The amount of KMnO₄ gradually disappears as this process occurs. Naturally, for analytical purposes, this situation is to be avoided. The next section will investigate a modification which solves the problem for this chemical system.

As the theory of flow injection analysis has only recently become commonly understood, and various points are still being investigated and contended, this instrumental system could be used to study the diffusion process. Undoubtedly, this situation has been encountered by many users of flow injection, but not many people have the multiple detector facilities which make the study of the process much easier.

Initial studies result in first order rate constants

of .63 sec⁻¹ at flows of 9 ml/min in both channels, .54 at 8 ml/min, and .51 at 6 ml/min. Additional studies are required, but one would expect to observe less disappearance of KMnO₄ if the time elapsed between colorimeters was less, as is the case with increasing flow rates. One would not expect the rate of diffusion to change with flow rate unless the increased turbulence, due to increased flow, caused an increased amount of mixing.

The rate constants above were obtained by plotting Ln(peak area) vs. time. The time interval between colorimeters was obtained from a previously obtained flow-time calibration curve. The uncertainty in the rate constants is probably greater than several percent; thus, it is unlikely that significant differences have been observed.

The diffusion effect is a serious problem when the chemical and instrumental systems can not be rearranged to avoid it, as illustrated in the next section. Vanderslice (31) indicates that an extension of his current flow injection theory (30) will be able to treat diffusion and first order rate constants. He feels that this instrument, and the chemical reactions studied, are potential experimental systems which can be used to test the results of his theoretical calculations (31). With a good theoretical framework, it may be possible to utilize

systems where diffusion is significant. It is apparent that further investigation in this area is needed, and will produce a better understanding of flow injection analysis.

The same KMnO₄ - Fe(_{aq})⁺⁺ reaction was carried out in a slightly different configuration to eliminate the diffusion effect just discussed. The reagent stream now consists of 500 μM KMnO₄ which reacts with the 100 μl pluses of Fe(_{aq})⁺⁺, which are injected into the carrier stream. A number of concentrations of Fe(_{aq})⁺⁺ were used, the most concentrated being about 3.2 mM Fe(_{aq})⁺⁺. A conventional titration indicates that 1.30 ml of 500 μM KMnO₄ are required to neutralize 1.00 ml of the Fe(_{aq})⁺⁺ solution.

At the mixer, a solution of 250 μM KMnO₄ (1:1 dilution by the carrier stream) will react with a plus of Fe(_{aq})⁺⁺ which is capable of neutralizing a 325 μM KMnO₄ sample (1:1 dilution of the Fe(_{aq})⁺⁺ plus by the reagent stream). As Figure 53 shows, the normal "baseline" colorimeter value of about 250 μM shows a flat valley for colorimeter 0, indicating that all of the Fe(_{aq})⁺⁺ of the sample plus has not reacted with the KMnO₄ of the reagent stream. Subsequent colorimeters show the normal flow injection peak shape (inverted) because dispersion has reduced the concentration of the plus by the time it reaches these colorimeters. At lower concentrations of Fe(_{aq})⁺⁺, normal flow injection peak shapes are observed. This

Run 152 of 876 7 16 15 3 MAR 1981
6/6 FS FE - KMNO4

Block 4120

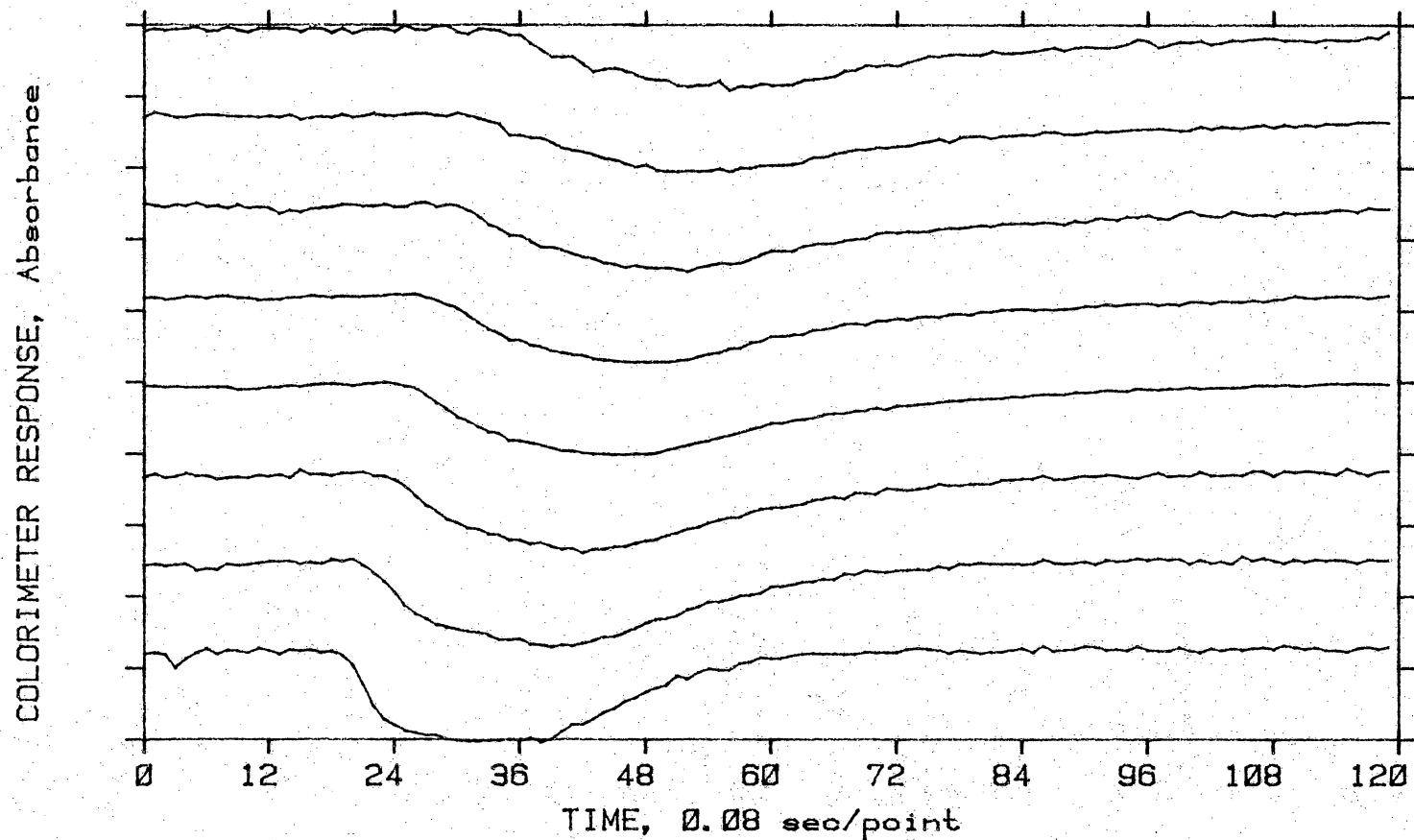


Figure 53. Multiple Colorimeter Response to KMnO₄

indicates that all the $\text{Fe}(\text{aq})^{2+}$ in the sample plus has reacted in the mixer and the only processes occurring in the reaction-observation tube are those of dispersion.

Notice that this configuration actually results in valleys rather than the traditional peaks of flow injection analysis. Since the disappearance of absorption rather than its appearance is of interest, one can shift the traditional zero value baseline to the 250 μM level of the unreacted KMnO_4 . This results in negative peak areas after integration. Changing the sign of the output results in the more traditional positive areas, from which a calibration curve can be prepared. Figure 54 shows the resulting calibration curve. The most concentrated $\text{Fe}(\text{aq})^{2+}$ values are not included when calculating the least squares fit because of the saturation mentioned earlier.

Table XVII shows the data from which this plot was prepared. Peak areas for representative runs at each relative concentration are shown. Relative concentration 1.0 is the slight excess of $\text{Fe}(\text{aq})^{2+}$ discussed earlier. It is apparent that a slight trend toward decreasing area occurs at the lower concentrations; however, higher concentrations show an opposite effect at succeeding colorimeters. This is due to the saturation experienced by the first colorimeters at the higher concentrations. The size of this trend is about the magnitude of the noise

Slope 3.857 E 0 Intercept 2.558 E 2 Corr. Coef. 9.934 E -1
Flow Rate 6 ml/min each 100 μ l Sample Loop Average of all Detectors

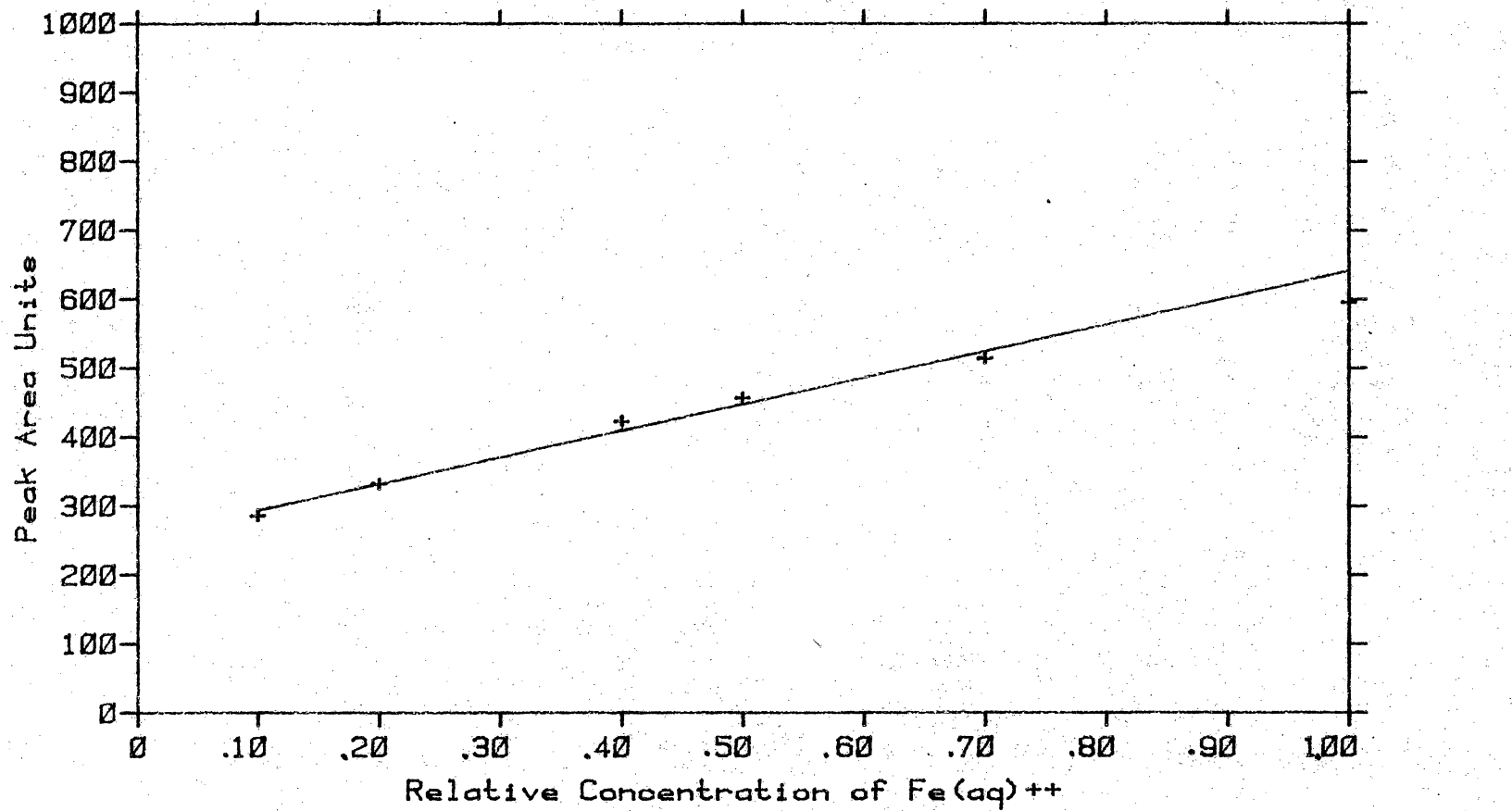


Figure 54. FIA Mode Calibration Curve, KMnO₄ - $\text{Fe}(\text{aq})^{++}$

Table XVII. Peak Area, 100 μ l injections of Fe(III) into a 6 ml/min carrier stream with a subsequent reaction with 500 μ M KMnO₄

Run#	156	161	166	168	175	154
Rel. Conc.	0.1	0.2	0.4	0.5	0.7	1.0
Channel						
0	31761	35332	41703	44974	50704	56448
1	30532	33802	41637	43720	50939	59428
2	29512	34951	41973	44198	50977	61203
3	27974	32157	41903	46036	51148	59192
4	27068	32304	42091	45780	50667	58444
5	28027	33850	42366	49071	53559	62529
6	27217	31262	41490	46808	51169	58827
7	26947	32280	45467	45055	51985	59573
Average	28630	33242	42329	45705	51394	59455
SDV	1783	1458	1298	1683	966	1814
RSDV	.062	.044	.030	.037	.019	.031

level for the measurement. In addition, a very small part of the tail of the larger concentration peaks are lost because of data buffer limitations. Thus, it appears that the peak area can be regarded as constant, as it should be.

D. Single Component Continuous Flow Kinetics

It was felt that a simple, preferably first order, kinetic system should be investigated as a test case before work on the more involved and instrumentally demanding multicomponent system was started. This allowed experience in the operation and characteristics of the instrument to be gained with a minimum of effort. It would also indicate the level of performance which may be expected of the instrument. This exercise proved to be very valuable, leading to the identification and solution of a number of problems as well as pointing out the limitations and optimum operating ranges of the instrument.

A chemical test reaction involving KMnO₄ was desirable both because of its high absorptivity, and previous sections of this thesis reporting on work involving the KMnO₄ - Fe(aq)⁺⁺ system. These investigations led to a series of four papers from J. R. Sutter's laboratory which studied the kinetics of permanganate oxidation reactions with various ions (32-35). The reaction with ferrocyanide ion appeared to be ideal because none of the other reactants or products absorb in the same spectral region as KMnO₄. Unfortunately, the rate of the reaction was too fast (2.64 E 4 l/M-s at 15 C) to be useful in this continuous flow instrument (33). In the

present system it proved impossible to adjust the concentrations of the reactants to produce a slow enough second order reaction so that changes in absorption could be observed in other than the first colorimeter. If the KMnO₄ concentration was reduced to a point yielding usable reaction rates, the sensitivity limits of the colorimeters prevented the observation of a significant signal. If the ferrocyanide concentration was reduced, the reaction rate could be reduced, but then not enough ferrocyanide was present to react with a significant amount of KMnO₄. Without an increase in sensitivity or a large decrease in the observable time interval between colorimeters, the ferrocyanide reaction could not be observed under second order conditions. Pseudo-first order conditions are clearly out of the question. The reaction with tris(1,10-phenanthroline)iron(II) has a slightly greater second order rate constant and also generates products which have interfering absorbances (34). The reaction with bromide ion has similar rate constants and consists of multicomponent reactions (35).

The reaction of permanganate with iodide has a lower second order rate constant (59 l/M-s at 35°C) and has been previously studied under pseudo-first order conditions (32). The rate equation is complex and has a second order component involving the MnO₄⁻ and I⁻ concentrations. A

siginificant third order term exists which adds Ht to the expression. Fortunately, for the purposes of testing the present instrument, apparent pseudo-first order and second order rate constants are given for a number of concentration, temperature and pH conditions. This information was used to establish the proper operating conditions for the instrument, resulting in pseudo-first order kinetics.

The purpose of these experiments is not to generate new or improved kinetic data, but to evaluate the operation of the instrument. Because of this fact, the normal rigorous control of reaction conditions, such as temperature control, may be relaxed slightly. Fresh reagents were carefully prepared by weight before each group of runs. The ratio of the initial absorbance of KMnO₄ to that at time t are the only parameters associated with the KMnO₄ which are involved in the calculations for first order kinetics; thus, the exact initial concentration of KMnO₄ is not required. Temperature control by means of an ambient air bath was remarkably effective.

Reactions were carried out at approximately 25 C and at a pH of 6.1, maintained by phosphate buffers. Literature rate constants are only given at 35 C for this pH; thus, an adjustment for temperature was needed to compare the observed data with the literature values.

Appendix D shows the details of this calculation. Because of a lack of temperature dependency data for all the pH's, some minor approximations were required. It is unlikely that they will seriously affect the results of the calculation. The result of the correction calculations yields an estimated apparent second order rate constant of 52.8 ± 1.6 at a temperature of 25 C.

One product of the reaction, I_3^- , absorbs significantly over the visible spectrum, causing a measurement problem because the measured absorbance is now due to the decreasing concentration of MnO_4^- and the increasing concentration of I_3^- . The absorbance value at infinite time is no longer zero and must be determined to achieve the correct rate constants. Unfortunately, absorbance values at completion of the reaction are not necessarily available in the continuous flow kinetic instrument because of the limited observation time determined by the length of the reaction tube and rate of the reaction. Fast reactions may be completed by the last several colorimeters; however, the more normal and desirable situation occurs when the residence time in the tube is less than several half lives of the reaction. Measurement errors are minimized under these circumstances.

In the case of this experimental test system, infinite time values can be obtained by stopping the flow

very rapidly after obtaining colorimeter readings under constant flow conditions. Because the reaction is rapid, the absorbance observed changes very little after the first few seconds of static conditions. Notice that in the case of Run 10 in Figure 55, the reaction is nearly complete as it reaches the last colorimeter on the top line of the plot.

Figure 56 shows a plot of $\ln(A_i - A_\infty)$ vs. colorimeter number for Run 10, where operating conditions are good. Error ranges for several of the colorimeters were calculated on the basis of the standard deviations of the observed raw absorbance values and are shown in the Figure. The error ranges are relatively small and consistent except when the reaction is nearly complete at the end of the tube.

Table XVIII lists data obtained from eight runs at varying reagent concentrations and flow rates. Runs 10 to 12 are the best, because KMnO₄ concentrations are in a low error region of the colorimeter response curve and observation of three to four half lives of the reaction is possible. The pseudo-first order rate in Runs 13 to 15 is greater due to the doubling of the KI concentration. In Runs 13 and 14, four half lives correspond to three or four colorimeters, after which errors become large because of colorimeter sensitivity limitations and the fact that the

Run 10 of 772 54 38 15 18 MAR 1981

500 UM KMNO4 .08 M KI 6/6

Block 4144

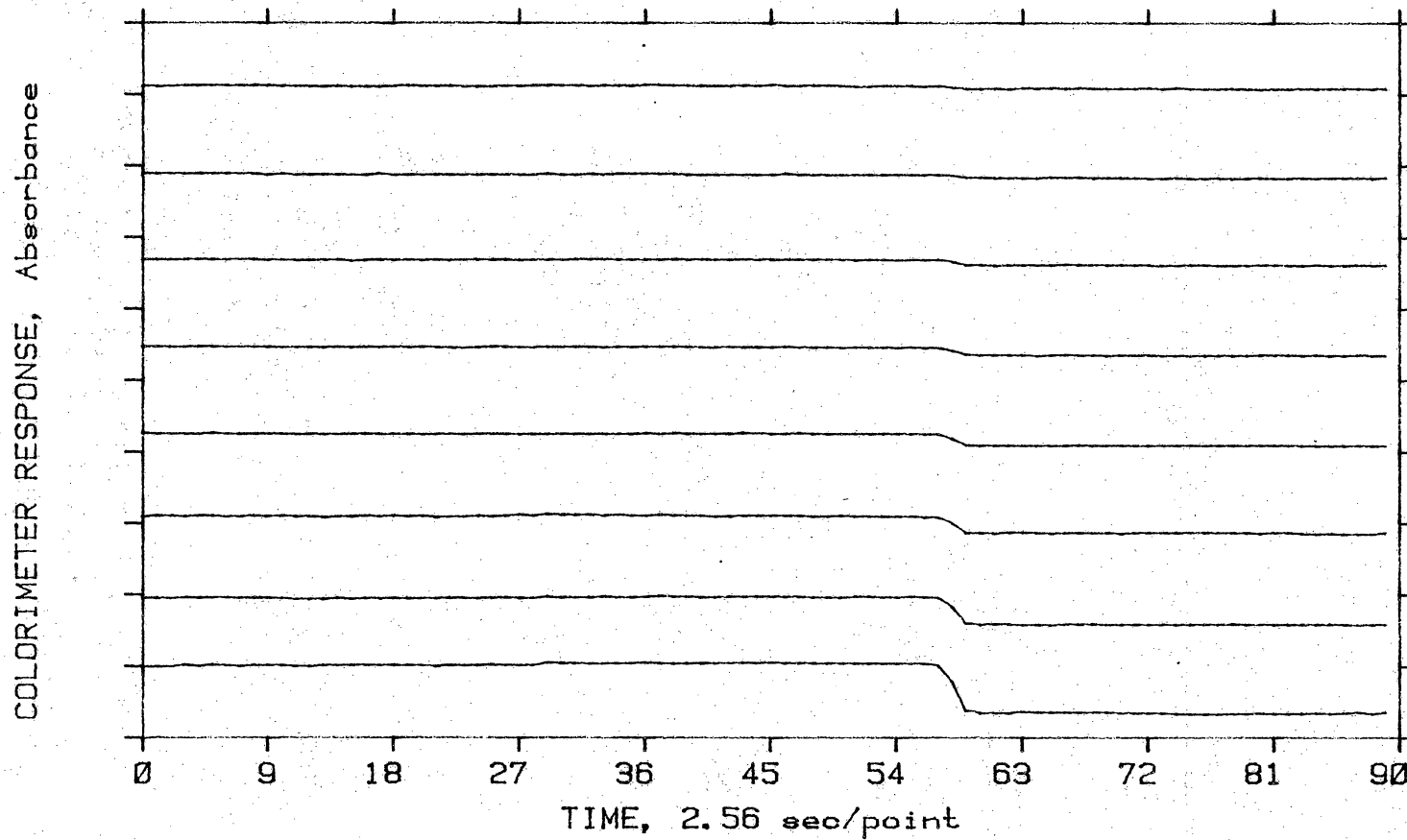


Figure 55. Colorimeter Response vs. Time for KMnO₄ - KI

Slope -3.926 E -1 Intercept 4.736 E 0 Corr. Coef. -9.967 E -1
Flow Rate 6 ml/min each 500 uM KMnO₄ 0.08 M KI RUN # 10

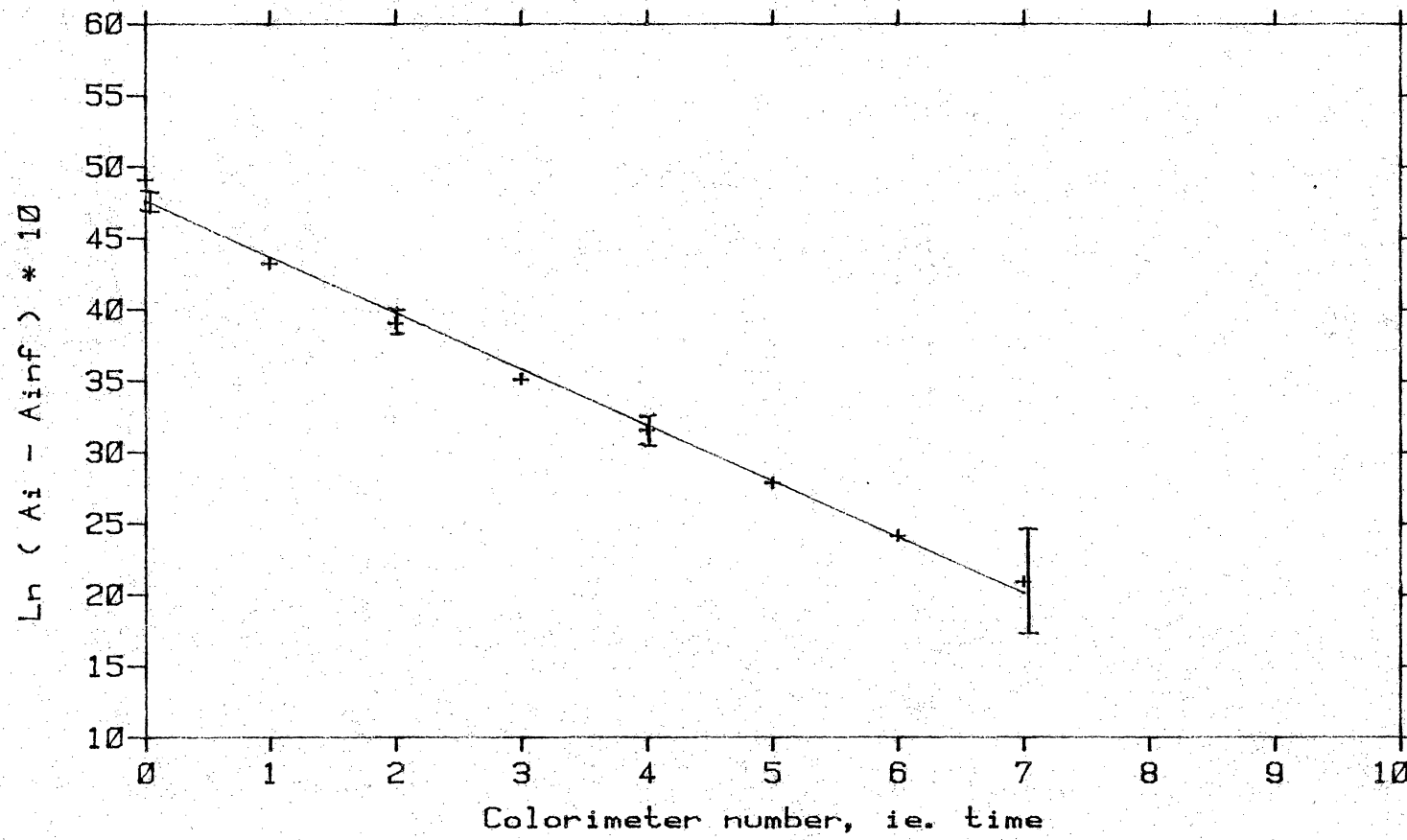


Figure 56. Single Component Kinetic Plot for KMnO₄ - KI

Table XVIII. KMnO₄ - KI Reaction Summary

Run#	Total Flow ml/min	seconds/colorimeter	rate/colorimeter	rate (k) 1/sec	T 1/2 sec
10	11.94	.185	.379	2.15	.322
11	14.69	.146	.387	2.65	.262
12	13.41	.164	.295	1.80	.385
13	12.30	.180	.712	3.96	.175
14	16.22	.124	.662	5.34	.130
15	16.53	.120	.414	3.45	.201
16	12.51	.177	.422	2.38	.291
17	15.87	.129	.416	3.22	.215
18	16.16	.125	.274	2.19	.316

Run#	Flow of KMnO ₄ ml/min	Conc. of KMnO ₄ uM	Conc. of KI mM	Excess KI before Rx.	k ₂ = k/I-
10	5.74	6.07	243.	41.1	52.3
11	5.92	8.96	199.	48.2	55.0
12	7.92	5.45	296.	32.6	55.2
13	6.02	5.95	251.	79.5	49.8
14	6.04	10.07	187.	100.0	53.4
15	9.92	6.01	311.	60.4	57.1
16	6.02	5.95	161.	39.8	59.8
17	6.05	9.87	122.	49.6	65.9
18	9.95	5.95	200.	29.9	73.2

Average of Runs 10 to 15 53.8 ± 2.6

Average of Runs 10 to 18 57.9 ± 7.2

Literature value corrected for temperature 52.8 ± 1.6

reaction is essentially complete early in the reaction tube. Changing the flow rates in Run 15 restored operation to a more optimum regimen and resulted in good linearity and lower noise levels. Runs 16 to 18 were conducted with lower KMnO₄ concentrations; again, the error in observed values is larger than in previous runs. Even so, good linearity is observed, except for Run 17 where the KMnO₄ concentration is the lowest and considerable scatter in the plotted data points is observed.

Calculation of the pseudo-first order rate constants was done by applying a least squares fit to data points spanning at least three half lives of the reaction. This included all eight colorimeters in all runs except 13 and 14 where only the first four points were used. Greater uncertainty in these values would be expected because fewer points are available.

An average apparent second order rate constant of 53.8±2.6 was observed for the first 6 runs. Including Runs 16 to 18, where noise levels were considerably higher, results in a constant of 57.9±7.2. The average of Runs 10 to 15 is practically identical to the estimated value, an extremely satisfying result, considering the many possible sources of error and approximations made. Even with all the runs included, the error ranges overlap with those of the temperature corrected literature values, suggesting

that there is not much difference in the values.

An attempt to calculate rate constants without knowledge of the absorption at infinite time via the Guszenheim method was made (36). Intervals of four and five colorimeters were used, corresponding to two or three half lives. The resulting data points were not in good linear agreement. Significantly larger rate constants were obtained than were calculated earlier. It is clear that the method is not suitable for use with the limited number of data points available in this instrument.

Swimbourne (37) has developed a similar method which allows calculation of a first order rate constant and an infinite time value which best fits the earlier data points. This method can be used to determine if the measured infinite time values are consistent with previous data points.

Table XIX lists the results obtained from this procedure. The averages of the runs are slightly higher than those in Table XVIII, but agree quite well. The scatter of the points is significantly greater than in Table XVIII. Again, more points than the four pairs available for the above calculations are required for good performance. Runs 13 and 14, where the reaction was completed in the first four points, produced erroneous values with this procedure and were not included in the

Table XIX. Time Interval Data Treatment Results

Run#	Slope 1/sec	Rate 1/M-s	k_2'	Intercept 1/M-s	Pred. A_∞	Ave A_∞
10	4.56	2.05	49.9	-238	66.8	65.2
11	4.42	2.54	52.7	-182	53.3	57.1
12	3.50	1.91	58.6	-220	88.1	88.9
13	5.05	2.25	28.3 *	-256	63.2	66.1
14	5.62	3.48	34.8 *	-239	51.8	48.0
15	4.99	3.34	55.5	-350	87.8	90.5
16	5.45	2.39	60.1	-199	44.7	44.2
17	4.47	2.90	58.5	-115	33.2	36.4
18	3.27	2.37	79.3	-144	36.6	58.6
Average of Runs 10-12,15				54.2 ± 3.7		
Average of Runs 10-12,15-18				59.2 ± 9.6		
Corrected literature value				52.8 ± 1.6		

* - Reaction complete in the first four points.

averages.

Absorbances at infinite time were calculated by the method and compared to the average absorbance at infinite time which was measured directly. Agreement within experimental error was observed, even for Runs 13 and 14. The Swinbourne method confirmed that the observed infinite time values were consistent with the data points earlier in the run. The method results in only a slight increase in uncertainty over traditional methods which require infinite time values.

E. Flow Injection Kinetics

The operation of the multicomponent continuous flow kinetic instrument in the flow injection mode is of considerable interest, as indicated in earlier sections. Therefore, the experiments of the single component continuous flow kinetic section were repeated in flow injection mode to determine the characteristics of the instrument in this mode.

The instrumental configuration is similar to the previous section. The reagent stream consists of 0.08 M KI in a phosphate buffer. KMnO₄ in the same phosphate buffer is injected into a carrier stream of pure phosphate buffer by a chromatographic sampling valve. The two streams react at the mixer and proceed down the reaction-observation tube, passing the colorimeters in sequence.

Data acquisition consists of periodically storing the colorimeter values during the passage of the KMnO₄ peaks. Peak areas are then calculated. It has been shown in earlier sections that peak area is independent of dispersion and linearly related to the concentration of absorbing species in the tube.

Several significant problems exist with this instrumental and chemical configuration. Diffusion is expected to be significant because reactive KMnO₄ peaks are

moving in a carrier consisting of large excesses of KI. A previous section has shown that diffusion can be assigned a first order rate constant; thus, the rate observed should consist of a first order term due to the reaction (k_1) plus another first order term due to diffusion (k_d). There is no reliable way to directly measure the absorbance at infinite time in the flow injection configuration. Even if the flow could be stopped and the area of a peak determined after the reaction was complete, diffusion would render the results invalid. Diffusion, as well as the actual reaction, produces an absorbing product which complicates the calculations considerably, forcing the use of estimates of infinite time values. The data resulting will be sufficient to show that method is potentially useful, especially if instrumental performance is improved.

Table XX shows rate constants calculated by Swinbourne's method (37). Seven of the sixteen runs conducted are listed. Instrumental noise is significant because of the low absorbances encountered due to the extra dilution effect of the carrier on the KMnO₄ sample. Assigning the four pairs of points available for calculations is a severe limitation. Included in the Table is a column reporting the correlation coefficient of the least squares fit of the four points of a run. It can be seen that reasonable results are obtained when this value is about

Table XX. Flow Injection Kinetic Results using
Swinbourne's method

Run#	k ₁ , 1/sec	C. Coef.	ρ_{red}	KI, M	k ₂ , 1/M-s
20	2.33	.98	318	.040	58.2
23	1.09	.92	223	.040	27.2
24	1.49	.85	32	.047	31.7
25	2.79	.977	268	.047	59.3
31	1.19	.987	149	.032	37.1
35	1.81	.908	279	.040	45.3
36	1.80	.911	313	.040	45.0

0.98 or greater. Values of the second order rate constant for the reaction compare remarkably well with those obtained experimentally in the previous section (53.8 ± 2.6), when the correlation coefficient is above 0.98. Predicted absorbance at infinite time values also appear to be reasonable at high values of the correlation coefficient.

Table XXI lists values calculated by the normal $\ln(A_i - A_\infty)$ vs. time procedure. Predicted absorbance at infinite time values were obtained from Table XX. In cases where Table XX does not provide a reasonable value, values from a run obtained under similar conditions were used. This procedure must be used very cautiously because the Swinbourne procedure results in an infinite time value which would produce the best fit to the data. Values were calculated for the pseudo-first order rate constant and the second order rate constant. Correlation coefficients are included to indicate the quality of the least squares fit. Based on previous experience, values of less than 0.99 indicate a rather poor linear fit with this type of data. Improved agreement between the rate constants is observed, as would be expected from the increase in data points fitted and the absorbance at infinite time estimation procedure. Even so, the second order rate constants are within ± 15 percent of the previously determined

Table XXI. Flow Injection Kinetic Results using Predicted A_∞ 's

Run#	A_∞ used	k_1 , 1/sec	C. Coef.	KI, M	k_2 , 1/M-sec	pred. k_1 1/sec	dif.
20	318	2.25	.988	.040	56.2	2.16	.09
23	318	1.71	.959 (6)	.040	42.8	2.16	-.45
24	268	2.75	.986 (6)	.047	58.4	2.54	.21
25	268	2.90	.994	.047	61.6	2.54	.36
31	149	1.40	.960 (7)	.032	43.7	1.73	-.33
35	279	1.88	.988	.040	46.9	2.16	-.28
36	313	1.86	.980	.040	46.5	2.16	-.30

experimental value for runs with good correlation coefficients.

The last two columns of the Table give a pseudo-first order rate constant predicted on the basis of the previous experimental results. The difference observed between this value and the flow injection values can be attributed to experimental error and diffusion. It is obvious that no consistent trend is present in the difference values listed. Experimental error is too large to draw any conclusions. From previous results, a diffusion value of around 0.5 might be expected. Note that Run 25, which has a relatively good correlation coefficient, gives a difference value of 0.34. Runs with poor correlation coefficients, leading to doubts about the validity of the data, give negative difference values.

It is clear that the multicomponent continuous flow kinetic instrument has potential as a kinetic detector for flow injection analysis. Efforts should be directed towards improving the performance of the instrument by increasing the number of colorimeters and reducing their noise level. Instruments of this type are needed to develop analysis systems for enzyme kinetics in agricultural and nutritional laboratories (38).

F. Multicomponent Continuous Flow Kinetics

Multicomponent Kinetic Analysis has been the object of much research and development in the last 20 years (1,39-42). It is particularly useful when the separation of the species of interest from a mixture for subsequent single component determination is difficult or time consuming (42). Maserum and coworkers (41,42) have developed and refined chemical and data handling techniques for multicomponent metal ion analysis using stopped flow instrumentation. Excellent results for three or four component mixtures have been obtained via regression analysis involving a large number of data points taken periodically during the complete reaction. The data handling method essentially applies least squares analysis to the method of proportional equations. Extensive investigations of experimental and computational errors have resulted in procedures and recommendations for optimum analysis (42).

The intent of this study is to determine the feasibility of applying these methods to continuous flow analysis. Multicomponent kinetic analysis involving continuous flow apparatus is not apparent in the literature. The excessive reagent consumption of early continuous flow methods, along with warnings about slit

width error and the requirement of turbulent flow conditions caused development efforts to be channeled into stopped and pulsed flow methods, where these problems are not experienced in the same way (43,44).

As indicated in earlier sections of this work, advances in electronic technology and an improved understanding of the theory supporting flow injection operation, at lower than turbulent flow velocities, have given continuous flow methods a new vitality. Such methods have the advantage of continuous operation, i.e., the periodic taking of discrete samples is not required. Therefore, automatic operation is achieved with less effort and essentially continuous monitoring is possible. Complicated mechanical apparatus can be avoided.

It is also possible to reduce the sample requirements to an absolute minimum by employing flow injection sampling techniques, as discussed in an earlier section of this work. In fact, the greatest utility of the continuous flow instrument is as a kinetic flow injection detector. Currently, most kinetic flow injection analysis has been done by stopping the flow to allow kinetic measurements to be made. Work is just beginning on continuous flow injection kinetic analysis and the supporting theory (31).

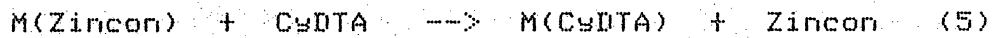
Simple graphical methods of data handling will be used for this study because of the limited number of data

points available from the eight colorimeters. The use of the improved data handling procedures is only a matter of implementation because colorimeter position along the reaction-observation tube can be correlated with the time since mixing. Because the goal of this study is analysis, the correlation of the concentrations of the species in the mixing cell, as determined by kinetic analysis, and the concentrations calculated from the mixing of the reagents will be of primary importance. Previous sections of this work indicate that good single component kinetic results are obtainable. This section will investigate multicomponent systems. The number of components determinable, accuracy of determination, and instrumental limitations are of primary interest.

The metal(Zincon) - CyDTA ligand exchange reaction used by Ridder and Mærskum (42) was chosen for investigation because of a number of favorable factors. Zincon is 2-carboxy-2'-hydroxy-5'-sulfoformazylbenzene and CyDTA is trans-1,2-diaminocyclohexane,N,N,N',N'-tetracetate. The metal-Zincon complexes absorb strongly at 630 nm with few interferences; thus, an orange-red LED will provide an excellent light source for the colorimeter. The rate of the zinc-Zincon reaction is very convenient for the continuous flow instrument. The mercury-Zincon reaction is significantly more rapid than the zinc-Zincon

reaction, allowing the use of the graphical data handling method. Other common metal ions react too fast or slow to be observed. Alkali metal ions do not form observable complexes. The reactions are all pH sensitive and the mercury reaction is influenced by chloride ion; therefore, buffering was necessary to hold these parameters constant. Reaction rates were listed for a pH of 8.5 but temperatures were not given. Rather than adjust the pH to 8.5, work was carried out at 9.2, the value of a standard borate buffer. Because zinc ion must be kept in acid solution to prevent precipitation, and CyDTA is also an acid, the buffer capacity was exceeded at 0.02 M Na₂B₄O₇ and 0.02 M NaCl employed by Ridder (42). Inconsistent rates were observed with this buffer so the concentration of Na₂B₄O₇ was increased to 0.1 M. A pH of 9.2 was maintained in this buffer and consistent results were obtained.

The reaction being observed is the dissociation of the intensely colored metal-Zincon complex and formation of a non-absorbing complex of metal-CyDTA according to Equation 5.



Zincon has been used as a sensitive colorimetric reagent for metal ion detection (45). It forms intensely absorbing blue complexes with metal ions such as zinc, cadmium, and mercury. Ridder and Maserum (42) are the only researchers

reporting on the kinetics of this system. Their purpose was also instrumental evaluation; therefore, specific mechanistic studies are not available. To assure that all metal ions in the system are in complexed form, Zincon is in an excess of at least six times. Reaction rates are first order in metal-Zincon complex concentration.

Likewise, to assure that all metal ions are complexed after the dissociation of the metal-Zincon complex, CyDTA is present at about twice the Zincon concentration. Reaction rates are independent of the CyDTA concentration.

The mercury-Zincon reaction is so rapid that the reaction is complete before the mixture reached the second colorimeter in the original configuration, preventing the accurate calculation of mercury-Zincon reaction rates. The flow rate could not be increased enough to remedy this problem; therefore, it was necessary to change the spacing of the colorimeters at the beginning of the tube so that sufficient data points would be available for accurate calculations. Table XXII gives the distance from the mixer to the center of each colorimeter. Also listed are the times elapsed from mixing at each colorimeter for several flow rates. This configuration is analogous to acquiring data points at a rate proportional to the reaction rate of current interest, as recommended by Ridder (42). This results in the most efficient use of the limited number of

Table XXII. Colorimeter Spacings and Time Intervals

Colorimeter	Distance, mm.	Time, ms. at flow rate of 12.45 ml/min.	Time, ms. at flow rate of 15.55 ml/min.
0	25	55	42
1	45	100	75
2	65	144	109
3	110	244	184
4	190	421	318
5	350	776	585
6	510	1131	853
7	590	1309	987

colorimeters available.

The differing reaction rates and unequally spaced colorimeter configuration allows processing of data in the following manner. First, the infinite time absorbance due to non-complexed Zincon at the end of the reaction is subtracted from the observed absorbances. In this study the infinite time values were obtained by stopping the flow and allowing the reaction to proceed to completion. This value can also be calculated, given the absorbancy of Zincon and its concentration at the end of the reaction, determined from the initial reagent concentrations and dilution factors. Calculated and observed values are in good agreement in most cases. Minor differences are due to occasional inaccurate flow values because of flowmeter stability problems. Experimental observations were used in this study to reduce the chance for error. Stopping the flow would be unacceptable in a non-experimental continuous flow application.

The mercury-Zincon reaction is fast compared to zinc-Zincon; thus, the absorbance in the last four colorimeters can be totally attributed to the zinc-Zincon reaction. The rate and intercept of the zinc-Zincon reaction can be obtained by a least squares fit to these data points. This information can be used to calculate the absorbance due to zinc-Zincon in the earlier data points of

the multicomponent reaction. Subtracting the zinc-Zincon absorbance and applying a least squares fit to the first three resultant values gives the mercury-Zincon rate and intercept. This procedure has been applied to a typical run shown in Figure 57.

The conditions employed result in a least squares fit over one to two half lives of the zinc-Zincon reaction with typical relative standard deviations of around one percent in the data values. Good results are obtained, even with only four points available. Relative standard deviations of the three mercury-Zincon points increase from comparable values for the first point to between 10 and 50 percent for the third point. This is due to the rapidity of the reaction, which is complete by the third or fourth colorimeter. Therefore, the agreement of the calculated and determined mercury-Zincon concentrations is surprisingly good. This problem can be corrected by fitting more points earlier in the reaction. Suggestions for accomplishing this will be given in the Discussion section.

In the case of the two component (zinc and mercury) system investigated, the total observed absorbance is made of additive contributions from Zincon, zinc-Zincon and mercury-Zincon. Each of these components has a different absorbancy at 630 nm. Zincon's absorbancy is approximately

Zn Rate, 1/sec 01.184 Detm'd Zn Conc, μM 15.2
Hg Rate, 1/sec 23.969 Detm'd Hg Conc, μM 41.0
Total Flow Rate, ml/min 15.49 Flow Ratio .505 Run # 116

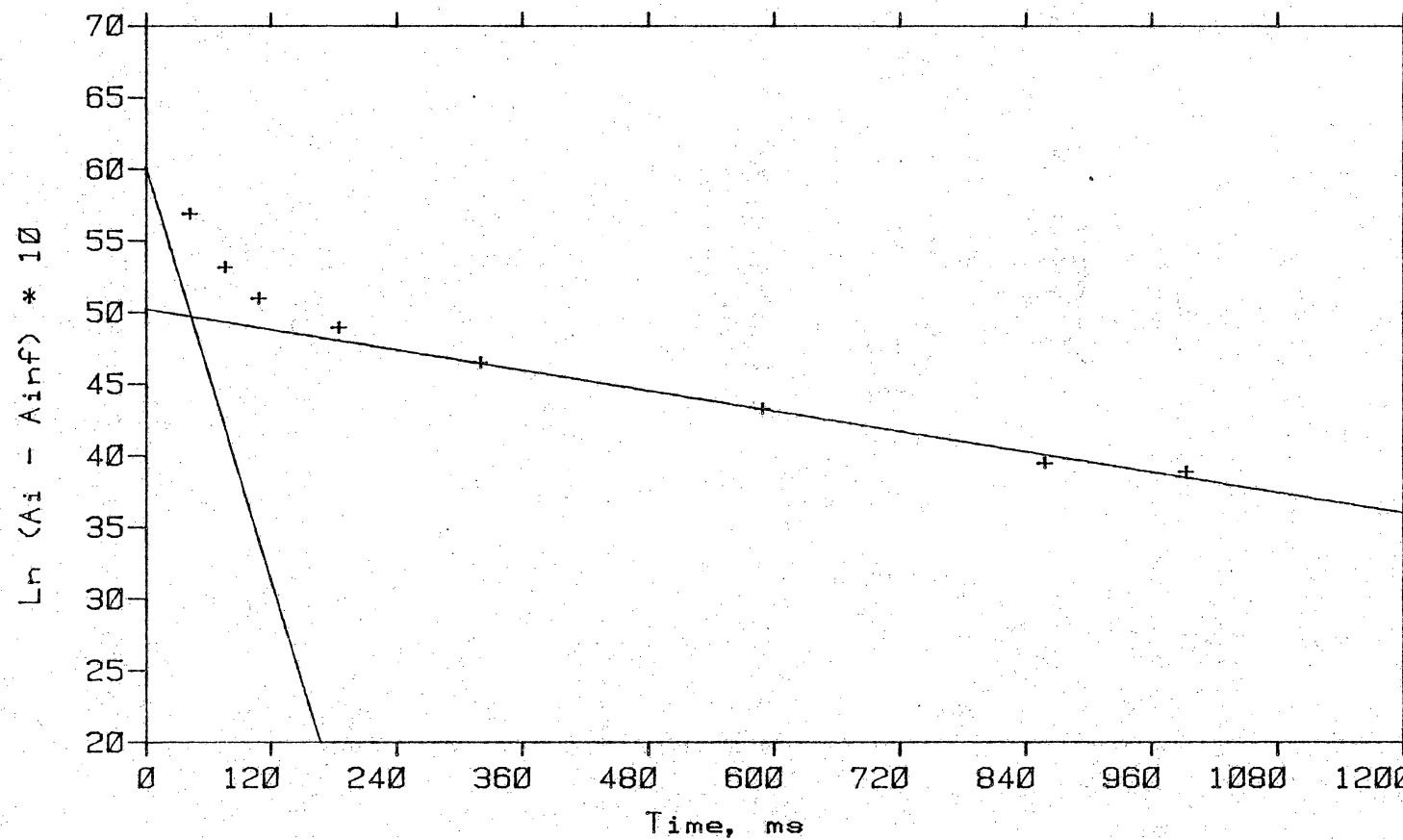


Figure 57. Multicomponent Kinetic Plot

2 percent of zinc-Zincon's or mercury-Zincon's, which differ by about 10 percent. This situation is different from the more commonly encountered multicomponent kinetic analysis where the change in a detected parameter is due to the appearance or disappearance of a common product or reactant. This complicates the calculations only slightly, as long as the absorbances are additive and no synergistic effects occur.

A number of instrumental and chemical characteristics become important at this point. The colorimeter section discussed the fact that absorbances calculated in the normal way are not useful because of path length and colorimeter variations. It is possible to multiply the observed absorbances by an individually determined colorimeter factor, resulting in consistent, linear responses from all colorimeters. In the case of this system, the colorimeter factor was determined with a solution of 1.53×10^{-4} M zinc-Zincon in the tube. It was found that a similar mercury-Zincon solution gave a slightly higher but consistent response, as was expected. Pure Zincon gave consistent values which were about 2 percent of the zinc-Zincon values. Therefore, using the graphical data handling procedure discussed earlier, a correction factor relating the concentration calculated from the intercept of the fitted line will be required.

The best agreement of calculated and determined single component zinc-Zincon concentrations was achieved with a factor of 0.976. This indicates an average error of 2.4 percent because the calibration of the colorimeters with zinc-Zincon should result in a factor of 1.00. Three major sources of error are present. First, and perhaps the largest source of error, is the flow rate measurement in the sample and reagent channels. Relative standard deviations of the flow values are typically one percent; therefore, the flow ratio used to calculate the concentration in the mixer has a relative standard deviation of two percent. Suggestions for improvement of the flow measurements are made in the Discussion section. The second source of error is in colorimeter subsystem. Typical relative standard deviations of less than 0.4 percent over a 20 to 40 second period indicate that the colorimeter and actual flow rates are very stable over the observation period. It is possible that deviations from Beer's Law could cause a calibration error. Thus, it is necessary to make sure that good linearity is obtained in the concentration range to be observed. The final source of error is the kinetic analysis procedure. In the case of zinc-Zincon, only four data points were available for a least squares fit. This means that minor errors in the observed value from a single colorimeter have more effect

on the calculated values than would be the case if more points were available. These points extend over about one half-life of the reaction, which is adequate for good analysis. Considering these potential problems, an average error of 2.4 percent is remarkably good.

The average correction factor for single component mercury-Zincon concentration measurements was 1.06. The ratio of mercury-Zincon absorbance to that of zinc-Zincon, determined from static colorimetric measurements, is 1.26. This is an average error of -16 percent. In light of the fact that the reaction is nearly complete at the third colorimeter, the quite steep slope of the line fitted to three points may be skewed to lower than correct values because the third colorimeter's response may have to be negative for the fit to give the correct results. It is apparent that the mercury determination suffers badly from instrumental limitations. The surprising fact is that the error is not greater. Again, solutions to these problems will be presented in the Discussion section.

Data from a number of single component test runs at several metal ion concentrations are presented in Table XXIII. These reactions were run at approximately 27°C in a 0.1 M $\text{Na}_2\text{B}_4\text{O}_7$ and 0.02 M NaCl buffer. The CuDTA concentration, also in the above buffer, before mixing was 2.00×10^{-2} M. Zincon concentrations were slightly less than

Table XXIII. Single Component Calibration Runs with Hg and Zn

Run#	Hg Rate 1/sec	Concentration, uM Calc.	Concentration, uM Found	Error, %
100	23.2	14.7	15.1	2.7
101	25.2	15.3	16.1	5.2
102	17.5	18.4	19.3	3.8
103	16.6	17.2	18.9	9.9
126	25.0	41.3	37.0	-10.4
127	24.9	44.4	44.0	-0.9
128	26.4	46.0	43.4	-5.7
Average	22.7	Average Error		0.8
Run#	Zn Rate 1/sec	Concentration, uM Calc.	Concentration, uM Found	Error, %
104	1.09	15.0	15.3	2.0
105	1.12	11.9	12.7	6.7
106	1.44	12.2	13.7	12.3
107	1.25	13.0	14.6	12.3
108	1.15	15.1	15.8	4.6
122	1.14	38.0	35.0	-7.9
123	1.17	33.6	32.2	-4.2
124	1.31	41.6	38.8	-6.7
125	1.05	35.1	30.8	-12.3
Average	1.19	Average Error		0.8

8.00 E -4 M, depending on the amount of metal ion solution added to produce the metal-Zincon complex.

The average error reported for these calibration runs is very low because these runs were used to determine the calibration factor discussed earlier. Errors are distributed between plus and minus 10 percent for the mercury runs and 12 percent for the zinc runs. Perhaps the most important characteristic is that errors are positive for low concentrations and negative for higher concentrations. This would indicate a slight negative deviation from Beer's law at the higher concentrations. Colorimeter linearity tests with several concentrations of these reagents indicated that good linearity extended to more than twice these concentrations. A flowmeter drift problem was present during these runs. This could result in erroneous flow ratio values which are used to calculate the concentration of species in the mixer. Such a problem should result in more random errors than are apparent here. Careful work with a wider range of conditions and using instrumentation incorporating some of the improvements suggested will be necessary to identify the source of the errors. Particular attention should be directed to improving the flowmeter response because the stability of the colorimeter response indicates that flow variations are not as great as the flowmeter output implies.

Table XXIV presents data obtained under similar conditions as in the previous table; however, a two component system with zinc and mercury was employed. The correction factors determined with the single component systems were used when calculating the concentrations reported. Average reaction rates are in good agreement when comparing the single and dual component systems.

A consistent low response was observed for zinc ion in the dual component system. However, the range of the error values is much less than observed in the single component zinc runs. A possible source of this error is the data analysis procedure. If the mercury is not completely reacted by the fifth colorimeter, it will influence the least squares fit for the zinc component. This situation would result in high zinc values, which is not consistent with the observed results. It is more probable that the negative deviation at high zinc concentrations has resulted in an incorrect zinc correction factor. Recalculation of all the zinc values with the predicted correction factor of 1.00 adds 2.4 to all the zinc errors, making the positive errors larger and the negative errors smaller in magnitude. Better results are obtained for the dual component tests, with most errors being less than two percent.

The average mercury error in the dual component tests

Table XXIV. Multicomponent Test Runs with Hg and Zn

Run#	Rate, k 1/sec	Zn Conc., uM		Error %		Hg Conc., uM		Error %	
		Zn Calc.	Hg Calc.	Zn Fnd.	Hg Fnd.	Zn Calc.	Hg Calc.	Zn Fnd.	Hg Fnd.
110	1.11	17.7	14.6	13.9	-4.8	14.3	14.9	4.2	
111	1.37	20.6	18.5	17.8	-3.8	18.1	22.6	24.9	
112	1.22	19.4	16.5	16.0	-3.0	16.2	17.0	4.9	
116	1.18	24.0	15.5	14.8	-4.5	45.5	43.5	-4.4	
117	1.21	26.3	14.4	13.9	-3.5	42.3	38.2	-9.7	
118	1.24	24.8	32.4	31.7	-2.2	25.4	24.3	-4.3	
119	1.21	21.8	39.7	38.1	-4.0	31.1	32.2	3.5	
120	1.07	18.4	34.4	32.1	-6.7	27.0	22.7	-15.9	
121	1.16	20.6	40.2	36.8	-8.5	31.5	29.6	-6.0	
Ave	1.20	21.5	Ave Error	-4.6				-3	

is very low, but most of the error values range from -6 to 5 percent. This wider variation is to be expected because of the low number of data points available for the mercury calculation.

It has been shown that single and dual component continuous flow kinetics are possible with the current prototype instrument, using a simple, graphical data handling method. The faster component reacts about twenty times as fast as the slower component and suffers from instrumental limitations. More than two components are not practical with this instrument. It is doubtful that implementation of the suggested improvements would allow three component systems to be analyzed except in very special cases. The improved data handling procedures suggested by Ridder (42) would be required and the range of rate constants would need to be less than 40 to 1. Obviously, many more data points than the current eight would be required.

The range of error values for the zinc component is disappointingly large. Identification of the source of this apparently determinate error should allow steps to be taken which should reduce it by a factor of two or more. Implementation of the instrumental and data handling improvements should produce an instrument with adequate accuracy.

The current instrument must be improved in the areas of flow measurement and number of data points before development in other areas would be justified. The suggested improvements will extend the operational range of the continuous flow method considerably; however, the wide range of stopped flow instrumentation will not be equaled.

V. DISCUSSION

The first major part of this section will examine the components of the current Multicomponent Continuous Flow Kinetic Instrument and suggest potential improvements. The second part will discuss the effect of these improvements on the current instrument's capabilities and suggest some additions or changes to the instrument's operation which would extend its applicability.

Experience has indicated that a great disparity in flow rates between the reagent and sample channels, or a large disparity in the resistance to flow of the reagents due to path obstructions, occasionally require a wider control range than is delivered by the capillary valves. It is often convenient to move operation into the optimum control range of the capillary valves by varying the pressure of the inert gas providing the motive force in the system. More convenient operation would occur if separate gas pressure regulators were provided for each channel. An even greater convenience would exist if the regulators could be adjusted by the computer. This would result in a two stage control system for reagent flows, first at the gas regulator for coarse adjustments, and then at the capillary valve for fine adjustment of the flow rate. Probably the most practical and inexpensive method to

implement this control of the gas regulator is in the same manner as the capillary valve is controlled, as will be discussed.

Considerable improvement can be made in the capillary valve controller. It is desirable to move the valve in smaller increments than are now possible to allow finer control of the flow rates and reduce instability. It is also desirable to move the valve more rapidly than is now possible to reduce the time required to establish a new flow rate. More precise control of the increments of movement than provided by the current reversible DC motors is also required. The ideal positioning device for the capillary valves, and perhaps the gas regulator, if necessary, is a stepping motor. Current stepping motor technology has improved considerably in the last several years, allowing much less expensive and less complicated systems to be easily constructed. The addition of a shaft encoder would allow positive feedback on the exact position of the valves, resulting in more reliable sensing of the physical limits of operation than the current light beam interruption mechanism. The fewer adjustments required for such a system would considerably improve the reliability and ease of construction of the flow controlling subsystem of the instrument.

As other sections have indicated, the electromagnetic

flow meter is subject to severe instabilities because of noise. This is not surprising because of the low signal level, on the order of microvolts, existent in the flow cell. Noise reduction techniques and signal averaging have been used in every step of the circuit, resulting in adequate performance. Because the signal is proportional to the applied magnetic field, perhaps the most productive direction of attack would be to increase the field experienced by the cell. This has been done by adding a second solenoid, allowing a reduction in the usable flow rate by a factor of two. The field could be increased by increasing the solenoid excitation current. This was not done because the present amplifiers were not powerful enough and the solenoids already produce a significant amount of heat. Better design of the flow cell and electromagnet could potentially increase the experienced field by a factor of two to four. Cooling the electromagnet may allow the excitation to be increased by a similar factor. Thus, it may be possible to increase the applied field by a factor of up to ten, if necessary.

Perhaps the most disturbing noise source is the large changes in DC level experienced in the cell. The current input instrumentation amplifier is operated at very high gain (4000) which results in frequent output saturation under changing conditions. To satisfy bias current

requirements, low value resistors to ground were required at this gain value. Although low gain input stages were earlier rejected because of high noise levels, it is possible that an improved design could employ moderate gain in the input stage. This would set the signal, improved due to the increase in magnetic field, out of the noise while reducing the effect of DC level shifts and allowing higher input resistances to be used. Higher input resistances should result in a lower dependence of the flowmeter response on solution conductivities. This currently requires recalibration of the flowmeters for each solution used. Practically, high solution conductivities exist because buffers are used to provide the constant ionic strengths required by the reactions investigated. The high conductivities of the solutions result in reduced cell impedance, considerably reducing noise experienced in the flowmeter system.

In conclusion, noise is the major problem in the flowmeter. Its effect can be reduced by increasing the signal level by increasing the magnetic field or flow velocity. Noise can also be reduced by reducing the cell impedance by increasing the solution conductivity. Reducing the occurrence of amplifier saturation should make a considerable improvement in flowmeter performance when solutions with inadequate conductance are being used.

The complete potential of the electromagnetic flowmeter has not yet been reached. The current implementation is capable of measurements at a flow rate of 5 ml/min to ± 0.1 ml/min, a considerable improvement over designs reported in the literature. Perhaps improved engineering and circuit design could extend this to 1 ml/min and ± 0.01 ml/min. A considerable effort will be required, however.

Although the colorimeter performs quite well, some practical electronic improvements are possible. An approach, similar to that employed in the flowmeters, could be used to demodulate the chopped radiation signal and provide improved signal to noise levels. The analog sample and hold amplifiers could be replaced by a voltage to frequency converter whose output is fed into a digital counter. During the time of no excitation, the counter would count down. It would count up when excitation is applied. In this manner, the photodiode signal will be averaged continuously and noise reduced. This also results in a reduction of the number of analog adjustments needed for the colorimeter. Because the signal is converted to digital form early in the processing chain, analog amplifier offsets and temperature coefficients will be much smaller problems. Although very good multiple channel analog to digital converters were used to digitize the

current colorimeter output signals, it was noticed that adjacent channels did influence the value obtained from the other channels, particularly when the values differed greatly. This is probably due to unavoidable capacitance in the connecting cables and the imperfect switching action of the multiplexer. Digital multiplexing of the counter outputs would eliminate this problem.

The primary reason the colorimeter was implemented in analog form is cost. A digital implementation would not be unreasonably expensive for a single channel, but eight channels were required and sixteen would be better. Inexpensive voltage to frequency converters are just now becoming available with specifications satisfactory for this application. Implementing the feedback required for regulating the modulated source intensity would require a high quality digital to analog converter for each channel, and again, inexpensive models are just becoming available. A considerable increase in software and processing time would also be required because the source reference channel would also need to be processed. Anticipating the need for more colorimeter channels and the potential improved stability of digital signal processing methods, it may be practical to dedicate a small microprocessor system to the colorimeter, rather than trying to include it in the main processor's software load. The colorimeter would then

provide digital values, representing colorimeter absorbances, on request. Although this division of labor is not really necessary, it reduces the number of electrical adjustments and the level of software interaction considerably. These factors may be even more important than the potential reduction of the colorimeter noise level.

It was noticed that the gain of the colorimeter amplifiers had to be reduced considerably for proper operation of the rest of the colorimeter circuits after installation of the 630 nm LEDs. An examination of the LED data sheet (24) indicated that the 630 nm LEDs radiate about 4 times the power of the 565 nm LEDs used with the KMnO₄ systems. In addition, the photodiodes are slightly more sensitive in this region of the spectrum (25). This indicates that the colorimeter noise performance should be improved at this wavelength. Colorimeter noise studies under conditions similar to those of the colorimeter evaluation study were not done, but it was apparent that less variation around the 0 absorbance value occurred when a blank was in the observation tube. Greater signal to noise improvement would be obtained if the gain of the first, rather than last, amplifier stage was reduced. The first stage has a very high gain and introduces the most noise into the system. Reducing the gain in the final

amplifier stages only reduces the overall signal but makes no change in the signal to noise ratio. The final stage of the colorimeter processing electronics was the only one with adjustable gain; thus, it was most easily changed. In any case, colorimeter noise was not a problem when the 630 nm LEDs were used because fairly large absorbances were encountered. The place where improvement was needed the most was in the flow injection kinetic study.

A reduction in the diameter of the reaction-observation tube to about 0.7 mm would reduce the dispersion experienced in flow injection applications. It would also increase the velocity of flow in the tube, allowing faster reactions to be studied. On the other hand, slower reactions would require a longer tube, which might be more convenient if more colorimeters were desired. In any case, the change in tube residence time is not excessive, and is a relatively minor consideration.

No practical solutions, other than reducing the noise level, exist for increasing colorimeter sensitivity with the current configuration. The short path length is already a considerable disadvantage, as discussed in several of the applications sections. It might be possible to connect a number of commercially available low volume cells in series to provide a function equivalent to the reaction-observation tube and colorimeters. The primary

unknown in this approach would be the effect on sample dispersion of the multiple connectors, right angle changes in flow direction in the cells, and changes between tubing and observation cell diameters as the colorimeters are entered and exited. Vanderslice feels that this is not a viable approach because dispersion would no longer be predictable (31).

As indicated in earlier sections, irregularities in the tube diameter and colorimeter construction required individual calibration of each colorimeter. It is doubtful that one could construct the equipment to tolerances which would not require calibration, but a reduction in individual variations would be an improvement.

Although the limited number of source wavelengths available from light emitting diodes has not proved to be a problem for the reactions investigated, a wider selection of wavelengths, particularly in the ultraviolet region, would be welcome. Several solutions to this problem exist. The first employs the proper continuum source, stabilized if necessary, and the appropriate interference filter for each colorimeter. Another solution would use a single source and wavelength isolation apparatus, with light distributed to the individual colorimeters by fiber optic light guides.

The Forth software system has proved very valuable and convenient to use. The multi-programming feature is

especially valuable, allowing the addition of a second terminal to the system for display of operating parameters without the need for any software changes. Previous experience has indicated that it is absolutely essential to have a real-time display of program and operating parameters. The structure of the Forth system allows easy implementation of this function.

As the software section indicated, a number of operator convenience functions would be desirable. Some of these functions, such as the addition of the prompting level of software and implementation of the HELP facility, require more rapid response from mass storage devices than is now available from the one block per second serial communication link existing between a satellite and host in our laboratory computer network. These functions require the storage of large amounts of information organized into sophisticated data structures. This extended capability requires many disk accesses, resulting in unacceptable time delays. For example, it may be faster to look up the function of a definition in a hard copy listing of a moderate sized documentation dictionary than to wait for it to be found and listed via the serial link. In contrast, response on a host is effectively immediate.

Calculation of peak areas for the flow injection applications, although not nearly as large a problem as

chromatography presents, would benefit from more development. The integration window should be open only when a peak is being detected. The varying amounts of dispersion in this instrument will require different integration windows for each channel. Although it can be shown that peak area is not greatly influenced if the window is closed slightly early, when working at high accuracy levels it becomes important. When signal levels are not high, as in the case of this instrument, minor drift and other baseline noise also becomes important, even though a properly operating flow injection system always returns to baseline, by definition.

The need for more colorimeters to generate more data points for use with the least squares data handling procedures has been discussed at many points. It was particularly acute for multicomponent kinetic analysis. Physical space limitations will allow only 32 of the current colorimeters to be placed along the observation tube. Cost considerations would probably prohibit this enhancement.

An alternate approach to obtaining more data points is available, however. It is possible to vary the time between mixing and observation by a specific colorimeter by changing the total flow rate. If the flow rate were to be increased in a series of steps during the conduction of a

run, the number of data points available for least squares calculations would be multiplied by the number of flow steps taken. A number of assumptions must be made for this procedure to work. First, the reagent concentrations must not change during the flow change period. Data handling would be greatly simplified if the ratio of flows in the sample and reagent streams remained exactly the same over the range of flows. This means that much better flow control is necessary. It remains to be seen if the flowmeter improvements suggested earlier are sufficient to allow this mode of operation to be practical. Examination of the data handling techniques will be required to determine if operation with larger uncertainties in the time, rather than the absorbance, parameter affects the calculations adversely.

Flow rate variation can expand the range of reaction rates usable by a factor of two to four. Flowmeter noise limits the low flow value. High flow values are limited by the amount of pressure which can safely be applied to the apparatus. Reagent consumption becomes a problem at high flow rates also.

The flow velocity is inversely proportional to the square of the tube radius; thus, smaller tubes would have a higher flow velocity at a given flow rate in milliliters per minute. It has been indicated earlier that smaller

diameter tubes will reduce the colorimeter response, but this reduction would not be as great as the increase in velocity. Therefore, it would be reasonable to project that a combination of increased pressure and reduced tube diameter might allow the measurement of reactions five to ten times faster than those currently investigated. Perhaps fast reacting components with first order rate constants of 100 rather than the current 20 could be examined. Similar responses might be obtained with slower components having rates of 10 rather than the current 1.

VI. SUMMARY

This study has clearly shown that multicomponent continuous flow kinetic analysis has potential as an analytical technique. Further development of the instrumentation will extend its range of applicability and improve its accuracy.

Perhaps a more important aspect of this research was the advancement of the state of the art in practical, low cost continuous flow sample transport procedures. Again and again, governmental and industrial contacts have emphasized the fact that a critical need exists for simple, reliable, low cost instrumentation which can do a large number of specific determinations rapidly. Continuous flow transport mechanisms show particular promise because of their mechanical simplicity. Developments in flow injection theory show that many concerns about the operation of such systems are unfounded when the proper conditions are employed.

The only practical means of moving the samples and reagents through the analysis system before this study was via mechanical pumps. Quality pumps are expensive, must be depulsed and often are not chemically inert. Reliability is also an occasional problem. These problems were attacked by using inexpensive, pulseless inert gas pressure

to move the reagents. Flow rates can be monitored by an electromagnetic flowmeter, allowing closed loop control of the flow rate via a capillary valve with only one moving part. The versatility of this control system was enhanced by including the computer in the control loop.

Operation with small diameter tubing and at low flow rates considerably reduced the traditionally excessive reagent requirements of continuous flow methods. Sample requirements can be reduced further by inserting a chromatographic sampling valve in the sample stream which now contains a carrier fluid. Very small volumes of sample may be injected into the carrier stream using this technique. Detection of the results of the subsequent reactions can be accomplished in the same manner as in flow injection systems.

Further development of the flowmeter and controller is necessary to improve the reliability and accuracy of the system, but the concept has proved to be viable as a motive force for both kinetic analysis and flow injection analysis. Initial results indicate that continuous kinetic flow injection analysis is possible. Results rivaling the one or two percent relative standard deviation of flow injection methods were not obtained due to instrumental limitations. Vanderslice indicates that research, as well as development, is needed in the area of flow injection.

kinetics (31). The theoretical framework is nearing completion. Chemical and instrumental systems must be selected and evaluated to determine the characteristics and limitations of the technique.

The multiprogrammed Forth Operating System/Language facilitated the development of software for the project and provided excellent computer-operator interaction. The task structure allowed the sharing of computer resources with minimal interaction between tasks. However, information from any particular task was available to all other tasks, if needed. The remarkable terseness of the language allowed two interactive terminal tasks, two flowmeter tasks, a balance task, an eight channel colorimeter task taking 800 points a second, a 1000 Hz day clock task and a logarithmic calculation and data storage task to operate simultaneously and be completely resident in 12 K words of 16 bit memory. The LSI-11 computer employed in the project was connected to a network host computer via a 1 K byte/sec serial line to provide data storage facilities. Program loading was facilitated by storage of the 8 K word Forth operating system and basic utility definitions in read-only memory.

Information, in addition to the raw data, was stored on disk to allow long term evaluation of the instrument's operation in a quality control program. Suggestions and

Procedures for improved operator interaction were developed.

BIBLIOGRAPHY

1. Mark, H. B., Jr., and Rechnitz, G. A., "Kinetics in Analytical Chemistry", Interscience, New York, 1968, pp. 1-4.
2. Betteridge, D., Anal. Chem. 1978, 50, 832A.
3. Blaedel, W. J., and Leessis, R. H., "Automation of the Analytical Process through Continuous Analysis", in "Advances in Analytical Chemistry and Instrumentation", Vol. 5, C. N. Reilley, Ed., Interscience, New York, 1966, pp. 69-72.
4. Reich, R. M., Anal. Chem. 1971, 43, 85A.
5. Roughton, F. J. W., and Millikan, G. A., Proc. Roy. Soc. London, 1940, A155, 262.
6. Wilks, P. A., Jr., Anal. Chem. 1980, 52, 222A.
7. Bibbero, R. J., "Microprocessors in Instruments and Control", Wiley, New York, 1977.
8. McCormick, W. S., and Birkemeier, W. P., Rev. Sci. Instrum. 1969, 40, 346.
9. Baumol, J., Proc. Inst. Soc. Am. 1975, 30, Paper No. 621.
10. Molnar, I., Pittsburgh Conference 1979, Paper No. 034.
11. Fisher & Porter Co., Specification 10A1471-50EB1210.
12. Kolin, A., Rev. Sci. Instrum. 1945, 16, 109.
13. James, W. G., Rev. Sci. Instrum. 1951, 22, 989.
14. Gaskins, J., Biomed. Eng. 1972, 7, 474.
15. Yanof, H. M., J. Appl. Physiol. 1961, 16, 556.
16. Fath, J. P., Proc. Inst. Soc. Am. 1976, 31, Paper 816.
17. Watt, D. G., Phys Med. Biol. 1961, 5, 300.
18. Cushins, V., Rev. Sci. Instrum. 1958, 29, 692.

19. Ballou, D. P., Ph.D. Thesis, University of Michigan, 1971, pp. 81-104.
20. Holmes, L. F., Silzars, A., Cole, D. L., Rich, L. D., and Eyring, E. M., J. Phys. Chem. 1969, 73, 737.
21. Sutter, John R., Personal Communication.
22. Stewart, K. K., Beecher, G. R., and Hare, P. E., Anal. Biochem. 1976, 70, 167.
23. Anfalt, T., Granelli, A., and Strandberg, M., Anal. Chem. 1976, 48, 357.
24. General Instrument Corp., MV50152 Solid State Lamp Product Description.
25. EG&G Inc. Electro-optics Division, Application Note D3011B-1, 1975.
26. Chappell, A., Ed., "Optoelectronics: Theory and Practice", McGraw-Hill, New York, 1978, p. 185.
27. Dessa, R. E., and Starling, M. K., Am. Lab. 1980, 12, 21.
28. Moore, C. H., Astron. Astrophys. Suppl. 1974, 15, 497.
29. Ziesler, E., Anal. Chim. Acta 1980, 122, 315.
30. Vanderslice, J. T., Stewart, K. K., Rosenfeld, A. G., and Hiss, D. J., Talanta, 1981, 28, 11.
31. Vanderslice, J. T., Personal Communication.
32. Kirschenbaum, L. J. and Sutter, J. R., J. Phys. Chem. 1966, 70, 3863.
33. Rawoff, M. A. and Sutter, J. R., J. Phys. Chem. 1967, 71, 2767.
34. Hicks, K. W. and Sutter, J. R., J. Phys. Chem. 1971, 75, 1107.
35. Lawani, S. A. and Sutter, J. R., J. Phys. Chem. 1973, 77, 1547.

36. Frost, A. A., and Pearson, R. G., "Kinetics and Mechanism", John Wiley & Sons, Inc., New York, 1961, pp. 49-50.
37. Swinbourne, E. S., J. Chem. Soc., 1960, 2371.
38. Stewart, K. K., Personal Communication.
39. Garmon, R. G., and Reilley, C. N., Anal. Chem., 1962, 34, 600.
40. Crouch, S. R., in "Spectroscopy and Kinetics", Mattson, J. S., Mark, H. B., and MacDonald, H. C., Eds., Chap. 3, Marcel Dekker, New York, 1973, pp. 107-207.
41. Willis, B. G., Woodruff, W. H., Friesinger, J. R., Maserum, D. W., and Pardue, H. L., Anal. Chem., 1970, 42, 1350.
42. Ridder, G. M., and Maserum, D. W., "Simultaneous Kinetic Analysis", in "Essays in Analytical Chemistry", Wanninen, E., Ed., Pergamon, New York, 1977, pp. 515-528.
43. Caldin, E. F., "Fast Reactions in Solution", Wiley, New York, 1964, pp. 29-49.
44. Owens, G. D., and Maserum, D. W., Anal. Chem., 1980, 52, 91A.
45. Rush, R. M., and Yoe, J. H., Anal. Chem., 1954, 26, 1345.

APPENDIX A

SOFTWARE SOURCE LISTINGS

BLOCK 1500 832

```

0 (                                - VALVE MOTOR CONTROL * 1 )
1 172070 C PCSR
2
3 CODE OP1    2 S)+ MOV  2 177774 * BIC 2 ASL 2 ASL 2 ASL
4     1 PCSR 2 + * MOV  1 )+ 10 * BIT 0=, NOT, IF,
5     1 ) 70 * BIC 1 ) 2 BIS 1 ) 30 * BIC THEN, NEXT
6 CODE OP2    2 S)+ MOV  2 177774 * BIC
7     1 PCSR 2 + * MOV  1 )+ 1 * BIT 0=, NOT, IF,
10    1 ) 7 * BIC 1 ) 2 BIS 1 ) 3 * BIC THEN, NEXT
11
12 CODE CL1    2 S)+ MOV  2 177774 * BIC 2 ASL 2 ASL 2 ASL
13     2 40 * BIS 1 PCSR 2 + * MOV  1 )+ 20 * BIT 0=, IF,
14     1 ) 70 * BIC 1 ) 2 BIS 1 ) 30 * BIC THEN, 'NEXT
15 CODE CL2    2 S)+ MOV  2 177774 * BIC
16     2 4 * BIS 1 PCSR 2 + * MOV  1 )+ 2 * BIT 0=, IF,
17     1 ) 7 * BIC 1 ) 2 BIS 1 ) 3 * BIC THEN, NEXT

```

BLOCK 1501 833

```

0 (                                - VALVE MOTOR CONTROL * 2 )
1
2 : C1 BEGIN 0 STOP 2 CL1 PCSR 2 + @ 20 AND END ;
3 : 01 BEGIN 0 STOP 2 OP1 PCSR 2 + @ 10 AND 0= END ;
4
5 : C2 BEGIN 0 STOP 2 CL2 PCSR 2 + @ 2 AND END ;
6 : 02 BEGIN 0 STOP 2 OP2 PCSR 2 + @ 1 AND 0= END ;
7
10   1 V VM2EN 1 V VM1EN      ( 0 TO ENABLE MOVEMENT )
11
12 : CL2E VM2EN @ 0= IF CL2 ELSE DROP THEN ;
13 : CL1E VM1EN @ 0= IF CL1 ELSE DROP THEN ;
14 : OP2E VM2EN @ 0= IF OP2 ELSE DROP THEN ;
15 : OP1E VM1EN @ 0= IF OP1 ELSE DROP THEN ;
16
17

```

BLOCK 1502 834

```

0 (                                - ELECTRONIC BALANCE TASK )
1
2 172070 C BCSR    204 C BIVEC
3 CODE RISR    T ) CLR      R -> 0 MOV  R -> 1 MOV
4     R -> 2 MOV R -> 3 MOV 2 ' IDA 2+@T) MOV
5     2 )+ 100000 * BIC 1 ' VOFF 2 + @ * MOV 1 T ADD 0 CLR
6     2 INC    BEGIN, 1 2 I) 170000 * BIC 1 2 I) 0 BIS
7     3 2 ) MOV B 3 ROR B 3 ROR B 3 ROR B 3 ROR B
10    3 177760 * BIC 3 12 * CMP 0>, NOT, IF, 3 CLR THEN,
11    1 )+ 3 MOV B 0 10000 * ADD 0 100000 * CMP 0=, END,
12    3 R )+ MOV 2 R )+ MOV
13    1 R )+ MOV 0 R )+ MOV T R )+ MOV RTI
14
15 BIVEC BIVEC 102 BCSR BCSR 300 TASK BALANCE
16 ' BISR BALANCE 2 -
17

```

BLOCK 1503 835

```

0 (                                BALANCE FLOW CALCULATOR & AVERAGER )
1
2 : BFAADR BALANCE 24 + @ 40 + ;    : B0IF BALANCE 52 + ;
3 : BFLNG BALANCE 54 + ;           : BFPTTR BALANCE 56 + ;
4 : BAADR BFAADR 400 + ;          : BAPTR BALANCE 60 + ;
5 : BAFLN BALANCE 76 + ;          : BAVALU BALANCE 50 + ;
6 : BCVAL BALANCE 72 + ;
7
10 : BCDIF BFPTTR @ 2 + DUP BFLNG @ > IF DROP 0 THEN
11     BFAADR + @ - 2* DUP 41 23420 */ + B0IF ! ;
12
13 : BSVAL BAVALU @ 1 DUP BFPTTR @ BFAADR + ! BCDIF 2 BFPTTR + !
14     BFPTTR @ BFLNG @ > IF BFPTTR OSET THEN ;
15
16 : BASVAL BCVAL @ BAPTR @ ! 2 BAPTR + ! BAADR BAFLN @ +
17     BAPTR @ > NOT IF BAADR BAPTR ! THEN ;

```

BLOCK 1504 836

```

0 (                                - ELECTRONIC BALANCE ROUTINES -
1
2 DECM    1 V PTAB 10 , 100 , 1000 , 10000 , 0 , 0 , OCTAL
3        4 V OTAB 0 , 7 , 3 , 6 ,
4
5 : BCONV 0 5 0 DO BALANCE 100 + I2 OTAB + @ + B@
6     I2 PTAB + @ M* DROP + LOOP ;
7
10 : BACTU      BALANCE ACTIVATE 36 4 * 1 - 2* BFLNG !
11     30 2* BAFLN ! BAADR BAPTR ! BFPTTR OSET 12 BASE !
12     BEGIN BCONV VSEL ! 1 ERR ! -1 STOP 0 END ;
13
14 : BASUM 0 . BAFLN @ 0 DO I BAADR + @ DSEXT D+ 2 +LOOP
15     BAFLN @ 2 / M/ BAVALU ! ;
16
17 : BAVGR BASVAL BASUM ;

```

BLOCK 1505 837

```

0 (                                PLATINIZING ROUTINE )
1 ( MILLSEC TDELAY )
2 : TDELAY TICKS 20 ROT M+ BEGIN 0 STOP 2DUP TICKS 20
3     D< END 2DROP ;
4
5 176760 C DACO
6
7 : PLAT      BEGIN 1000 DACO ! 20000 TDELAY -1000 DACO !
10     20000 TDELAY 0 END ;
11
12
13
14
15
16
17

```

BLOCK 1506 838

0
1
2
3
4
5
6
7
10
11
12
13
14
15
16
17

BLOCK 1507 839

0 (- STORE DATA)
 1
 2 140000 C AZZ 120000 C AXX 0 V OPTL 7774 C TOPLIM
 3 130000 C AYY 0 V OPTN 0 V OPTM
 4 : OINIT OPTL OSET OPTM OSET OPTN OSET ; OINIT
 5 : STVL OPTL @ AXX +! OPTL @ TOPLIM < IF 2 OPTL +! THEN ;
 6 : STVM OPTM @ AZZ +! OPTM @ TOPLIM < IF 2 OPTM +! THEN ;
 7 : STVN OPTN @ AYY +! OPTN @ TOPLIM < IF 2 OPTN +! THEN ;
 10 (ADDR B# *BLKS WDTD - WRITE DATA TO DISK
 11 STARTING WITH BLOCK NUMBER B# . BUFFER STARTS AT ADDR)
 12
 13 : WDTD SWAP BLK ! 0 DO DUP BLK @ BUFFER 1000 MOVE UPDATE
 14 BLK 1+! 2000 + LOOP DROP ;
 15 (B# *BLKS ADDR RIFD - READ DATA FROM DISK)
 16 : RIFD -ROT SWAP BLK ! 0 DO DUP BLK @ BLOCK SWAP 1000 MOVE
 17 BLK 1+! 2000 + LOOP DROP ;

BLOCK 1510 840

0 (- FLOW METER ISR , FM1 , FM2)
 1
 2 172030 C FM1CSR 114 C FM1IV 172050 C FM2CSR 124 C FM2IV
 3
 4 CODE FMISR R-> 0 MOV 0 ' IDA 2+@T) MOV
 5 0) 100000 * BIC 0 4 * ADD '(R# 2+@T) 0) MOV
 6
 7 0) CLR T) CLR 0 R)+ MOV T R)+ MOV RTI
 10
 11 FM1IV DUP 102 1 FM1CSR 200 TASK FM1
 12 ' FMISR DUP FM1 6 - ! FM1 2 - !
 13
 14 FM2IV DUP 102 0 FM2CSR 200 TASK FM2
 15 ' FMISR DUP FM2 6 - ! FM2 2 - !
 16
 17

BLOCK 1511 841

```

0 (          - FLOW METER AVERAGING )
1
2 FM1 ! V+7 2 + @ + C FM1G   FM2 ! V+7 2 + @ + C FM2G
3
4 : FMSUM      0. VOFF 2!    V+4 @ 0  DO  PAD I2 + @ DSEXT
5     VOFF D+!  LOOP ;
6 : FMSTO      V+5 @ !  2 V+5 +!  V+5 @ V+4 @ 2* -
7     PAD < NOT IF PAD V+5 ! THEN ;
10 : FMVAL      VOFF 2@ V+4 @ M/ DUP V+6 @ + DUP
11     R# @ - < IF SWAP DROP ELSE DROP V+6 @ -
12     DUP R# @ < IF DROP R# @ THEN THEN ;
13 : FMALIAS NULL ;
14 : FMVSS      FMVAL FMSTO FMSUM
15 STATUS FM1 = IF BAVGR BSVAL THEN FMALIAS ;
16
17

```

BLOCK 1512 842

```

0 (          FLOWMETER CONTROLS
1
2
3 : VALVMOV    DUP ABS 3 MIN SWAP 0< IF
4     ODA @ 0= IF CL2E ELSE CL1E THEN ELSE
5     ODA @ 0= IF OP2E ELSE OP1E THEN THEN ;
6
7 : VALVCONT    HOLD @ 3 < IF 1 HOLD +! ELSE
10     VOFF 2@ V+7 @ V+4 @ M* D- DROP DUP DUP
11     #COL @ - SWAP #COL ! RPT @ * + DUP VSEL ! 400
12     / MINUS DUP P# ! VALVMOV HOLD OSET THEN ;
13
14 : FMOPR      34 V+6 ! 100 V+4 ! V+7 @ PAD ! PAD PAD 2 +
15 V+4 @ 1 - MOVE PAD V+5 ! V+7 @ V+4 @ M* VOFF 2! 7 RPT !
16     BEGIN FMVSS VALVCONT 1 ERR ! 1 STOP 0 END ;
17

```

BLOCK 1513 843

```

0 (          FLOWMETER CALCULATIONS
1 0 0 V FM1OF , 0 0 V FM1SL , 0 0 V FM2OF , 0 0 V FM2SL ,
2
3 ( CALCULATE FLOW RATE FROM METER RESPONSE )
4 ( FMRESPONSE CFR1 FLOWRATE IN .01 ML/MIN )
5 : CFR1      FM1OF 2@ F- FM1SL 2@ F/ ;
6 : CFR2      FM2OF 2@ F- FM2SL 2@ F/ ;
7
10 ( CALCULATE FLOW GOAL VALUE )
11 ( FLOWRATE IN .01 ML/MIN CFG1 FLOWMETER RESPONSE )
12 : CFG1      FM1SL 2@ F* FM1OF 2@ F+ ;
13 : CFG2      FM2SL 2@ F* FM2OF 2@ F+ ; ;
14 ( SET FLOW GOALS INTEGER IN 100THS SFG1 -- SETS FM1G )
15 : SFR1      0 FLOAT CFG1 FIX DROP FM1G ! ;
16 : SFR2      0 FLOAT CFG2 FIX DROP FM2G ! ;
17

```

BLOCK 1514 844

```

0 ( SHORT FLOWMETER CALIBRATION CALCULATIONS )
1
2 0 V FMCPTR 0 V FSCTR 400 V FMCTIM 0 V FMC1V 40 DP+
3 0 V FMC2V 40 DP+! 0 V BLCVAL 40 DP+! 0 V FMCSBF 64 DP+
4 FMCSBF STADD ! 4 V FMCGOAL 0 , 100 , 240 , 400 ,
5 : FMCDIN 'NULL' FMALIAS !
6
7 : FMCSUM STATUS FM1 = IF
10   FM2 100 + 20 FM2 110 + @ M/ DSEXT FMCPTR @ FMC2V + DP+
11   FM1 100 + 20 FM1 110 + @ M/ DSEXT FMCPTR @ FMC1V + DP+
12   BALANCE 52 + @ DSEXT FMCPTR @ BLCVAL + DP+
13   FSCTR 1+! FSCTR @ FMCTIM @ < NOT IF FMCDIN THEN THEN ;
14
15
16 : FMCINST FSCTR OSET 'FMCSUM 2 - ' FMALIAS !
17

```

BLOCK 1515 845

```

0 ( SHORT FLOWMETER CALIBRATION ROUTINES )
1   0 0 V FLFTM ,
2
3 : FMCRPT FMCSBF STADD ! FMCTIM @ DSEXT FLOAT FLFTM 2!
4 SINIT FMCGOAL @ 0 DO I2 2* BLCVAL + 20 FLOAT
5   FLFTM 20 F/ I2 2* FMC1V + 20 FLOAT
6   FLFTM 20 F/ SACC 0 STOP LOOP
7   SCIPD SCSIIC 2DROP FM10F 2! FM1SL 2!
10  SINIT FMCGOAL @ 0 DO I2 2* BLCVAL + 20 FLOAT
11  FLFTM 20 F/ I2 2* FMC2V + 20 FLOAT
12  FLFTM 20 F/ SACC 0 STOP LOOP
13  SCIPD SCSIIC 2DROP FM20F 2! FM2SL 2!
14
15
16
17

```

BLOCK 1516 846

```

0 ( SHORT FLOWMETER CALIBRATION TASK )
1
2
3 340 DUP 102 340 DUP 200 TASK FMCTASK
4
5
6 : FMCSTEP FMCDIN DUP FMCGOAL 2++ @ DUP FM1G ! FM2G !
7   DUP 1+ STOP FMINST 100 + STOP ;
10
11 : FMCSEQ FMCGOAL @ 0 DO I2 2* FMCPTR ! I2 FMCSTEP LOOP
12   FMCRPT ;
13 : FMCAL FMCTASK ACTIVATE FMC1V 20 ERASE FMC2V 20 ERASE
14   BLCVAL 20 ERASE FMCSSEQ BEGIN -10 STOP 0 END ;
15 : FMCNEXT FMCTASK OSET ;
16
17

```

BLOCK 1523 851

```

0
1
2
3 : FPSUM CHOME FM1 100 + 2@ 2DUP 10 D.R. FM1 110 + @ M/
4   DSEXT FLOAT CFR1 FIX BASE @ -ROT 12 BASE ! 10 D.R BASE !
5     FM2 100 + 2@ 2DUP 10 D.R FM2 110 + @ M/
6
7   DSEXT FLOAT CFR2 FIX BASE @ -ROT 12 BASE ! 10 D.R
10  BALANCE 52 + @ 10 .R. BASE ! 3 SPACES TICKS 2@ .TIME OLDCR
11    STPTR @ 120000 + 20 - DUP 7 U.R 10 0 DO DUP I2 + @
12      7 .R LOOP DROP OLDCR ;
13
14 : FMDISA BEGIN FM1 62 + @ 0= NOT IF FM1 62 + OSET
15   FPSUM THEN 0 STOP 0 END ;
16
17

```

BLOCK 1524 852

```

0 ( DUAL FLOWMETER LOAD BLOCK W/ SHORT CALB )
1
2 1640 LOAD 1642 LOAD 1644 LOAD ( FLOATING STATS )
3 1500 LOAD 1501 LOAD
4 1502 LOAD 1503 LOAD 1504 LOAD
5 1510 LOAD 1511 LOAD
6 1512 LOAD 1513 LOAD 1514 LOAD 1515 LOAD 1516 LOAD
7 1525 LOAD
10
11 : STFM2 FM2G ! 40000 FM2CSR ! FM2 ACTIVATE FMOPR ;
12 : STFM1 FM1G ! 40000 FM1CSR ! FM1 ACTIVATE FMOPR ;
13 : STBAL 40000 BCSR ! BACTV ;
14 : STOPOP BCSR OSET FM1CSR OSET FM2CSR OSET ;
15
16
17

```

BLOCK 1525 853

```

0 ( FLOWMETER CONTROLS )
1
2
3 : FLCON 20 DUP FM1 114 + ! FM2 114 + !
4   600 ' VALVCONT 112 + ! ;
5
6
7 : FLCHG 60 DUP FM1 114 + ! FM2 114 + !
10   400 ' VALVCONT 112 + ! ;
11
12
13
14
15
16
17

```

BLOCK 1564 884

```

0 (          8 CHAN ADC TASK    ISR )
1 176770 C ADCSR 130 C ADCIV 172000 C FPCSR 100 C FPCIV
2 ( VSEL = CNT FOR ASHC RPT = # CONVS TO AVG ADDR = # LEFT )
3 CODE ADCISR ( R -) 0 MOV ( R -) 1 MOV ( R -) 2 MOV
4 T )+ T )+ CMP ( 2 T ) DEC ( IDA 2+@T ) 100000 * BIC
5 0 ( ODA 2+@T ) MOV 0 ) 5 * MOV 1 ) 10 * MOV 2 ) 140 * MOV
6 2 T ADD BEGIN NOP BEGIN, 0 ) TST 0<, NOT, END,
7 2 )+ 2 0 I ADD 2 )+ ADC 0 ) INC 1 DEC 0>, NOT, END,
10 2 T ) TST 0>, NOT, IF, R -) 3 MOV ( R -) 5 MOV
11 2 ) 40 * SUB 3 2 MOV 3 40 * SUB 5 10 * MOV
12 BEGIN, 1 2 )+ MOV 0 2 )+ MOV 72 T ) 0 ASHC
13 3 )+ 1 MOV 5 DEC 0>, NOT, END,
14 5 R )+ MOV 3 R )+ MOV 2 40 * SUB 0 20 * MOV
15 BEGIN, 2 )+ CLR 0 DEC 0>, NOT, END, T ) CLR
16 2 T ) 52 T ) MOV THEN, ( ODA 2+@T ) CLR
17 2 R )+ MOV 1 R )+ MOV 0 R )+ MOV T R )+ MOV RTI

```

BLOCK 1565 885

```

0 (          8 CHAN ADC & CALCULATION TASK & ROUTINES )
1
2 ADCIV FPCIV 102 ADCSR FPCSR 300 TASK ADC8
3 ADCISR DUP ADC8 2 - ! ADC8 6 - ! FPCIV 2 + OSET
4
5 340 340 102 340 340 300 TASK ADCAL
6
7 : ADALIAS NULL ;
10
11 : STADC ADC8 ACTIVATE 20 DUP DUP ADC8 ! ADDR ! RPT !
12 -4 VSEL ! 41400 FPCSR !
13 BEGIN ADCAL OSET 100 STOP 0 END -10 STOP ;
14
15 : STACAL ADCAL ACTIVATE BEGIN ADALIAS -11 STOP 0 END ;
16 STACAL
17

```

BLOCK 1566 886

```

0 (          8 CHAN COLORIMETER - BIN LOGS LOAD BLOCK )
1
2 1633 LOAD 1636 LOAD ' CCTL FORGET ( LOAD BINARY LOGS )
3 1564 LOAD 1565 LOAD ( ADC TASK )
4
5
6
7 1567 LOAD 1570 LOAD 1571 LOAD
10
11
12
13 COLORIMETER.LOADED
14
15
16
17

```

BLOCK 1567 887

```

0 (          8 CHAN COLORIMETER      ROUTINES )
1
2   0 V IOBUF 40 DP+!  0 V IBUF 40 DP+!
3   0 V ABSBUF 20 DP+!  0 V ABSCB 20 DP+!  0 V CABB 20 DP+!
4   23420 ABSCB !  ABSCB DUP 2 + 7 MOVE
5
6 : GETIO 10 0 DO I2 ADC8 100 ++ @  BLOG
7     I2 2* IOBUF + 2! LOOP ;
10
11 : GETI 10 0 DO I2 ADC8 100 ++ @  BLOG
12     I2 2* IBUF + 2! LOOP ;
13
14 DECM 5000. E 0 V ABSMAX , 10000. E 0 V F1OK , OCTAL
15 : ABSCAL 10 0 DO ABSMAX 2@ I2 ABSBUF + @ 0 FLOAT F/
16   F1OK 2@ F* FIX DROP I2 ABSCB + ! LOOP ;
17

```

BLOCK 1570 888

```

0 (          8 CHAN COLORIMETER      ROUTINES )
1
2 : CABS 10 0 DO I2 2* IOBUF + 2@ I2 2* IBUF + 2@ D-
3     DROP 72627 40000 */ I2 ABSBUF + ! LOOP ;
4
5 : DABS CR 10 0 DO ABSBUF I2 + @ 7 .R LOOP ;
6 : DCABS CR 10 0 DO ABSBUF I2 + @ ABSCB I2 + @
7     23420 */ DUP CABB I2 + ! 7 .R LOOP ;
10
11
12
13
14
15 : GF GETI CABS DABS DCABS ;
16
17

```

BLOCK 1571 889

```

0 (          8 CHAN COLORIMETER      ROUTINES )
1
2   0 V CFLAG 0 V STPTR 40000 C STPMX
3 : STINIT STPTR OSET ;
4 : STTABF GETI CABS ABSBUF 120000 STPTR @ + 10 MOVE
5   1 CFLAG ! ;
6 : STABF STPMX STPTR @ - 0> IF STTABF 20 STPTR +! THEN ;
7
10 : CPP STPTR @ 120000 + 20 - DUP 7 U.R 10 0 DO DUP I2 +
11   @ 7 .R LOOP DROP CR ;
12 : STABS BEGIN 0 STOP CFLAG @ 0= NOT IF
13   CFLAG ! OSET CPP THEN 0 END ;
14
15 : STABF 2 - ' ADALIAS !
16
17

```

BLOCK 1621 913

```

0 ( LEIGHTON FLOATING POINT LOG OPERATIONS ) DECM
1
2 : UNIT 1E0 F- 2DUP 2E0 F+ F/ 2DUP 2DUP F* 2DUP 2DUP 2DUP
3 : 11 0 FLOAT F/ 1.9 DO I 0 FLOAT 1/X F+ F* -2 +LOOP 2E0 F* ;
4 : FRACTION 127 AND 16384 + SWAP 65535 AND SWAP ;
5 : CHARAC 2DUP SWAP DROP 32640 AND 128 / 0
6 : 128 0 D- FLOAT 29207 16433 F* 2SWAP ;
7 : 1LN CHARAC FRACTION UNIT F+ ;
10 : LN 2DUP 0. F> IF 1LN ELSE 2DROP 0. THEN ;
11 : LOG10 LN 10 0 FLOAT LN F/ ;
12 : LOG2 LN 2E0 LN F/ ;
13
14
15 OCTAL
16
17

```

BLOCK 1622 914

```

0 ( LEIGHTON FLOATING POINT EXP OPERATIONS ) DECM
1 : TANHX/2 2E0 F/ 2DUP 2DUP F* 2DUP 0. 1 5 DO
2 : I 0 FLOAT F+ F/ -2 +LOOP ;
3 : 1+T/1-T 1E0 2OVER F+ 2SWAP 1E0 2SWAP F- F/ ; OCTAL
4 : 2**N 200 * 40177 + 177777 SWAP ;
5 : X<2**-16 2DUP SWAP DROP 4000 < ; DECIMAL
6 : X<1 2DUP 1E0 F< ;
7 : 2EXP TANHX/2 1+T/1-T ;
10 : X>1 29207 16433 F/ 1E0 F/MOD DROP DUP 127 > IF
11 : DROP 2DROP 10 QEXX ELSE 2**N 2SWAP 29207 16433
12 : F* 2EXP F* THEN ;
13 : 1EXP X<2**-16 IF 1E0 F+ ELSE X<1 IF 2EXP
14 : ELSE X>1 THEN THEN ;
15 : -EXP FABS 1EXP 1/X ;
16 : EXP 2DUP 0. F< IF -EXP ELSE 1EXP THEN ;
17 : 10*** 23512 16350 F/ EXP ; OCTAL

```

BLOCK 1633 923

```

0 ( DH FORTH      BINARY LOGARITHMS - LOOKUP & CALCULATION )
1   0 V CTABL 1000 DP+
2
3 ( VALUE BLOG    DBL. LOG - TAKE LOG -2- OF VALUE )
4 CODE BLOG        0 S) MOV 2 17 * MOV
5   BEGIN,          0 ASL 1N, NOT, IF, SWAP 2 SOB THEN,
6   S) 2 MOV S-) 0 MOV 0 ASL 0 SWAB 0 177400 * BIC
7   0 ASL
10 0 CTABL * ADD 1 0)+ MOV 2 S) MOV S) 1 MOV
11   S-) 2 MOV 0 0) MOV 1 0 SUB
12 0 S) + MOV 2 CLR
13   1 ASR 0 100 * BIT 0=, NOT, IF, 2 1 ADD THEN,
14   1 ASR 0 40 * BIT 0=, NOT, IF, 2 1 ADD THEN,
15   1 ASR 0 20 * BIT 0=, NOT, IF, 2 1 ADD THEN, 2 NEG
16 2 S) + ADD 0 S)+ MOV 1 CLR 0 ASR 1 ROR 0 ASR 1 ROR
17   1 2 SUB 0 SBC S-) 1 MOV S-) 0 MOV NEXT

```

BLOCK 1634 924

```

0 ( DH FORTH      FLOATING LOGARITHM CALCULATIONS )
1   200000. FLOAT V F200K , 0 V CNTR
2   1.342520342 E 0 V C0 , .5607625 E 0 V C1 , -.35 E 0 V C2 ,
3
4 : P8(X) 2DUP 2DUP C2 2@ F* C1 2@ F+ F* C0 2@ 2SWAP F- F* ;
5
6 ( DBL. C&M CHARAC N.FRACTION CNTR )
7 CODE C&M 0 S)+ MOV 1 S) MOV 2 37 * MOV
10 BEGIN, 1 ASL 0 ROL 1V, NOT, IF, SWAP 2 SOB THEN,
11 S) 2 MOV S-) 0 MOV 1 CLR 0 ROL
12 0 ASL 1 ROL 0 ASL 1 ROL 0 ASL 1 ROL S-) 1 MOV NEXT
13
14
15 1.66 E 0 V MULT , 1.52 E 0 , , 1.40 E 0 , , 1.30 E 0 , ,
16 1.20 E 0 , , 1.14 E 0 , , 1.06 E 0 , , 1.02 E 0 , ,
17

```

BLOCK 1635 925

```

0 ( DH FORTH      FLOATING LOGARITHM CALCULATIONS )
1
2   .70372345 E 0 V LMULT , .56454377 E 0 , ,
3   .45340032 E 0 , , .35316517 E 0 , ,
4   .24464741 E 0 , , .17674055 E 0 , ,
5   .10214261 E 0 , , .026565575 E 0 , ,
6
7 : FBMLU C&M 2* 2* DUP CNTR ! MULT + 2@ ROT 0 FLOAT
10   F200K 2@ F/ F* ;
11
12 : FBLOG   FBMLU 1E0 F- P8(X)
13   CNTR @ LMULT + 2@ F-
14   ROT 0 FLOAT F+ ;
15 DECM
16 : FLOG10 FBLOG .30102999 E 0 F* ;
17 OCTAL

```

BLOCK 1636 926

```
0 ( BH FORTH      BINARY LOGARITHMS - DECM CONV., TBL. INIT.)
1
2 DECM    16384. FLOAT V F16K , .30103 E 0 U F.301 ,
3 ( VALUE DLOG LOG - TAKE LOG -10- OF VALUES UP TO 1892 )
4 : DLOG BLOG 8 M/ 30103 20480 */ ;
5 ( VALUE FDLOG FLOG - RETURN FLOATING DLOG IN BASE 10 )
6 : FDLOG BLOG FLOAT F16K 2@ F/ F.301 2@ F* ;
7 OCTAL
8 : CCTL ; SCR @ 1- DUP 1- LOAD LOAD ( LOAD FLOATING LOGS)
9 DECM
10 ( CCT - CALCULATE COEFFICIENT TABLE FOR BINARY LOGS )
11 : CCT CTABL 257 ERASE 512 256 DO I 0 2DUP FBLOG
12     F16K 2@ F* FIX >R >R DROP BLOG R> R> I-
13     I 256 - DUP 0< NOT IF 2* CTABL + ! ELSE 2DROP
14     THEN 0 STOP LOOP CTABL 512 + OSET ; OCTAL
15 CR : CCT CR ;S ' CCTL FORGET
```

BLOCK 2000 1024

```

0 ( DSE ROUTINES )
1
2 0 V DSEAD 0 V STPTR 10000 C STPMX 0 V CFLAG
3 : DSESTR 42 WORD HERE COUNT 40 MIN DSEAD @ 20 + SWAP BMOVE ;
4
5 : DSEINIT DUP DSEAD ! ! DSEAD @ 20 + 60 BLANKS DSESTR
6 PSHDT DSEAD @ 2 + ! DSEAD @ 4 + 2! FPCSR @ DSEAD @ 10 + !
7 ' RPT 2 + @ ADC8 + @ DSEAD @ 12 + ! 0 140 DSEAD @ 14 + 2!
10 ABSCH DSEAD @ 100 + 10 MOVE
11 FM1SL 20 DSEAD @ 120 + 2! FM1OF 20 DSEAD @ 124 + 2!
12 FM2SL 20 DSEAD @ 130 + 2! FM2OF 20 DSEAD @ 134 + 2!
13 140 STPTR !
14 ( B# SDSEDATA -- STORE 4 BLOCKS ON DISK AT B# )
15 : SDSEDATA DSEAD @ SWAP 4 WDTD ;
16 ( LENGTH START SADDR - STORE LENGTH & START BYTE ADDR )
17 : SADDR DSEAD @ 16 + ! DSEAD @ 14 + ! ;

```

BLOCK 2001 1025

```

0 ( DSE ROUTINES )
1
2
3 : STTABF GETI CABS ABSBUF DSEAD @ STPTR @ + 10 MOVE
4 DSEAD @ STPTR @ + DUP DUP BALANCE 52 + @ SWAP 16 +
5 FM2 100 + 2@ FM2 110 + @ M/ SWAP 14 +
6 FM1 100 + 2@ FM1 110 + @ M/ SWAP 12 + ! 1 CFLAG !
7
10 : STABF STPMX STPTR @ - 0> IF STTABF 20 STPTR +! THEN ;
11
12 : CPP STPTR @ DSEAD @ + 20 - DUP 7 U.R 10 0 DO DUP I2 +
@ 7 .R LOOP DROP CR ;
13 : STABS BEGIN 0 STOP CFLAG @ 0= NOT IF
14 CFLAG OSET CPP THEN 0 END ;
15
16 ;S ' STABF 2 - ' ADALIAS !
17

```

BLOCK 2002 1026

```

0 ( DSE EXPERIMENT LOAD BLOCK )
1
2 ( FLOWMETER ) 1524 LOAD
3
4 ( COLORIMETER ) 1633 LOAD 1636 LOAD / CCTL FORGET
5 1564 LOAD 1565 LOAD 1567 LOAD
6 1570 LOAD 1571 LOAD
7
10 STADC CR @ 200 DUP DUP ADC8 2! ADC8 52 + ! -7 ADC8 72 + !
11 ( DATA STORAGE ) 1507 LOAD
12 ( DSE ROUTINES ) 2000 LOAD 2001 LOAD
13 ( FMDISA ) 1523 LOAD
14 DECM 2.8 E -1 FM1SL 2! 2.3 E -1 FM2SL 2! OCTAL
15 -1 AXX DSEINIT DUMMY
16 ' STABF 2 - ' ADALIAS ! 100 STFM1 100 STFM2 STBAL
17

```

BLOCK 2003 1027

```

0 ( DSE CALCULATIONS )
1 2025 LOAD 0 V CHARBF 200 DP+! 0 V ABCBF 20 DP+!
2 ( RUN # CONVERSIONS PER POINT CHAN# MEAN MIN MAX
3   SDEV RSDEV READY TO PLOT )
4 : LCHBF SCR @ BLOCK 202 + CHARBF 100 MOVE ; LCHBF 2005 LOAD
5 ( B# DSEIIIS - DISPLAY DSE DATA )
6 : DSEIIIS CR CR VOFF ! CHARBF 6 TYPE 0. VWQ 3 .R
7   5 SPACES 2. VDQ .TIME 6. VWQ .DATE 3 SPACES
10   12. VWQ 5 .R CHARBF 14 + 32 TYPE CR
11   20. 40 VTYPE CR 120. VDQ FM1SL 2! 124. VDQ FM1OF 2!
12   130. VDQ FM2SL 2! 134. VDQ FM2OF 2! ABCBF 100. 20 MFYM ;
13
14 2004 LOAD ( NEW BUFS )
15 ( B# DISPLAY - DISPLAY DATA FROM B# )
16 : DISPLAY VSEL OSET STINIT DSEDIS CR 140. 14. VWQ 140 - 40
17 / DLINS ( SUMMARY ) CR CR ;

```

BLOCK 2004 1028

```

0 ( DSE OUTPUT TO TERMINAL AND ACCUMULATE STATISTICS )
1 ( VALUE CHAN# CALcab - CALC CORRECTED ABS VALUE )
2 : CALcab 2* ABCBF + @ 23420 */ ;
3
4 ( VADDR DSELIN - DISPLAY DATA LINE AT VADDR )
5 : DSELIN 2 DUP 10 0 DO 2 DUP VWQ I CALcab DUP 6 .R
6   I 100 * SBBF + STADD ! 0 FLOAT 2 DUP SACC 2 M+ LOOP 2DROP
7 2 DUP 2 DUP 20 M+ VWQ 0 FLOAT CFR1 2 DUP FIX DROP 10 .R
10 1000 SBBF + STADD ! 2 DUP SACC 22 M+
11 VWQ DSEXT FLOAT CFR2 2 DUP FIX DROP 6 .R 1100 SBBF + STADD !
12 2 DUP SACC 24 M+ VWQ DUP DSEXT FLOAT 2 DUP 1200 SBBF + STADD !
13   SACC 6 .R CR ;
14
15 ( VADDR #L DLINS - DISPLAY LINES )
16 : DLINS 0 DO 2 DUP I 40 * M+ DSELIN LOOP 2DROP ;
17

```

BLOCK 2005 1029

```

0 ( STATS FOR DSE )
1
2 0 V SBBF 1300 DP+! ( 10 TABLES OF 100 -8- BYTES )
3 1640 LOAD 1642 LOAD 1644 LOAD 1647 LOAD ( FLOATING STATS )
4 SBBF STADD ! SBBF V SBBFA
5 : STINIT 13 0 DO I 100 * SBBF + STADD ! SINIT LOOP ;
6 : EI.FR >R 2SWAP DUP 100000 AND >R FFAIJ FIX >R >R
7 SWAP DUP >R - SWAP R> R> R> R> ROT R> FDCNV ;
10 : SUMLIN 4 .R SXI 20 SCNT @ 0 FLOAT F/ FIX 7 D.R
11 SXMIN 2@ FIX 7 D.R SXMAX 2@ FIX 7 D.R
12 SCIPN SCIV 2DROP 2 DUP FIX 10 D.R
13 SMEAN 2DROP F/ 2 1 20 EI.FR CR ;
14
15 : SUMMARY CR CR CHARBF 46 + 60 TYPE CR
16 13 0 DO I 100 * SBBFA @ + STADD ! I SUMLIN LOOP ;
17

```

BLOCK 2006 1030

```

0 ( DSE      ACCUMULATE STATISTICS ONLY )
1 ( VALUE CHAN# CALCAB - CALC CORRECTED ABS VALUE )
2 : CALCAB 2* ABCBF + @ 23420 */ ;
3
4 ( VADDR DSELIN - ACCUMULATE STATISTICS ON LINE AT VADDR )
5 : DSELIN 2DUP 10 0 DO 2DUP VW@ I CALCAB
6   I 100 * SBBF + STADD ! 0 FLOAT 2DUP SACC 2 M+ LOOP 2DROP
7   2DUP 2DUP 20 M+ VW@ DSEXT FLOAT CFR1
10  1000 SBBF + STADD ! 2DUP SACC
11  22 M+ VW@ DSEXT FLOAT CFR2           1100 SBBF + STADD !
12  2DUP SACC 24 M+ VW@ DSEXT FLOAT 2DUP 1200 SBBF + STADD !
13   SACC 0 STOP ;
14
15 ( VADDR #L DLINS - DISPLAY LINES )
16 : DLINS 0 DO 2DUP I 40 * M+ DSELIN LOOP 2DROP ;
17

```

BLOCK 2007 1031

```

0 ( DSE      OUTPUT PROCESSED DATA TO FILE IN V+1 )
1 ( VALUE CHAN# CALCAB - CALC CORRECTED ABS VALUE )
2 : CALCAB 2* ABCBF + @ 23420 */ ;
3   O V OCTR ( OUTPUT COUNTER )
4 ( VADDR DSELIN - GENERATE OUTPUT BUFFERS FROM LINE AT VADDR )
5 : DSELIN 2DUP 10 0 DO 2DUP VW@ I CALCAB OCTR @ I 2000
6   * + 0 1 VSEL ! VW! VSEL OSET 2 M+ LOOP 2DROP 2DUP 2DUP
7   20 M+ VW@ DSEXT FLOAT CFR1 FIX DROP OCTR @ 20000 + 0 1 VSEL !
10  VW! VSEL OSET 22 M+ VW@ DSEXT FLOAT CFR2 FIX DROP
11  OCTR @ 22000 + 0 1 VSEL ! VW! VSEL OSET 24 M+ VW@ OCTR
12  OCTR @ 24000 + 0 1 VSEL ! VW! VSEL OSET 2 OCTR +!
13   0 STOP ;
14
15 ( VADDR #L DLINS - DISPLAY LINES )
16 : DLINS OCTR OSET 0 DO 2DUP I 40 * M+ DSELIN LOOP 2DROP ;
17

```

BLOCK 2010 1032

```

0 ( PLOT ROUTINES OF DSE DATA )
1
2 ( LOAD PLOTTER ) 1507 LOAD 1671 LOAD          O V BKNUM
3
4 ( #PLOTS PRAWD - DO #PLOTS OF DATA, BKNUM HAS 1ST BLK # )
5 : PRAWD 0 DO I BKNUM @ + BLOCK AXX 400 MOVE
6   AXX BYADD ! BXADD OSET XYOTP LOOP ;
7
10
11
12
13
14
15
16
17

```

BLOCK 2020 1040

```

0 (      FIA EXPERIMENT LOAD BLOCK  )
1
2 ( FLOWMETER )      1524 LOAD
3
4 ( COLORIMETER )   1633 LOAD 1636 LOAD " CCTL FORGET
5                   1564 LOAD 1565 LOAD 1567 LOAD
6                   1570 LOAD 1571 LOAD
7 STADC CR
10 ( DATA STORAGE ) 1507 LOAD      2023 LOAD LOADS
11 ( FIA ROUTINES )  2021 LOAD 2022 LOAD
12 ( FMDISA )        1523 LOAD
13    DECM 2.8 E -1 FM1SL 2! 2.3 E -1 FM2SL 2! OCTAL
14    -1 AXX FIAINIT DUMMY !
15    ' STABF 2 - ' ADALIAS ! 100 STFM1 100 STFM2 STBAL
16    40 ' FPSUM 250 + !
17

```

BLOCK 2021 1041

```

0 (      FIA ROUTINES )
1
2 0 V DSEAD 0 V STPTR 20000 C STPMX 0 V CFLAG
3
4 : DSESTR 42 WORD HERE COUNT 40 MIN DSEAD @ 20 + SWAP BMOVE ;
5
6 : FIAINIT DUP DSEAD ! ! DSEAD @ 20 + 60 BLANKS DSESTR
7 PSHDT DSEAD @ 2 + ! DSEAD @ 4 + 2! FPCSR @ DSEAD @ 10 +
10 ' RPT 2 + @ ADC8 + @ DSEAD @ 12 + ! 0 140 DSEAD @ 14 + 2!
11 ABSC8 DSEAD @ 100 + 10 MOVE
12 FM1SL 2@ DSEAD @ 120 + 2! FM1OF 2@ DSEAD @ 124 + 2!
13 FM2SL 2@ DSEAD @ 130 + 2! FM2OF 2@ DSEAD @ 134 + 2!
14 140 STPTR ! INJECT ;
15 ( B# SFIADATA -- STORE 10 -8- BLOCKS ON DISK AT B# --)
16 : SFIADATA DSEAD @ SWAP 10 WDTD ; 
17

```

BLOCK 2022 1042

```

0 (      FIA ROUTINES )
1
2 167774 C PINP
3 : STTABF GETI CAB5 ABSBUF DSEAD @ STPTR @ + 10 MOVE
4 DSEAD @ STPTR @ + DUP DUP DUP BALANCE 52 + @ SWAP 24 + !
5 FM2 100 + 2@ FM2 110 + @ M/ SWAP 22 + !
6 FM1 100 + 2@ FM1 110 + @ M/ SWAP 20 + !
7 PINP @ SWAP 26 + ! 1 CFLAG ! ;
10
11 : STABF STPMX STPTR @ - 0> IF STTABF 40 STPTR +! THEN ;
12
13 : CPP STPTR @ DSEAD @ + 40 - DUP 7 U.R 10 0 DO DUP I2 +
14 @ 7 .R LOOP DROP CR ;
15 : STABS BEGIN O STOP CFLAG @ 0= NOT IF
16 CFLAG OSET CPP THEN O END ;
17

```

BLOCK 2023 1043

```

0 (          FIA INJECTION VALVE CONTROL )
1
2 : 167770 C PICSR      ( PARALLEL INPUT CSR )
3 : INJECT 1 PICSR ! ;
4 : LOADS PICSR OSET ;
5
6
7
10
11
12
13
14
15
16
17

```

BLOCK 2024 1044

```

0 (          FIA ANALYSIS ROUTINES )
1 1507 LOAD 2025 LOAD 0 V CHARBF 200 DP+! 0 V ABCBF 20 DP+
2 ( RUN #           CONVERSIONS PER POINT   BASELINE PERIOD
3   INTEGRATION WINDOW
4   400 V INTLEN 10 V BASEPD
5 : LCHBF SCR @ BLOCK 202 + CHARBF 100 MOVE ; LCHBF
6 : FIADIS CR CR VOFF ! CHARBF 6 TYPE .0. VW@ 3.R
7   5 SPACES 2. VD@ .TIME 6. VW@ .DATE 3 SPACES
10   12. VW@ 5 .R CHARBF 14 + 32 TYPE CR
11  20. 40 UTYPE CR 120. VD@ FM1SL 2! 124. VD@ FM1OF 2!
12  130. VD@ FM2SL 2! 134. VD@ FM2OF 2! ABCBF 100. 20 MFVM
13 CHARBF 46 + 21 TYPE BASEPD @ 6 .R CHARBF 76 + 24 TYPE
14 INTLEN @ 6 .R CR ; 2026 LOAD 2027 LOAD 2030 LOAD
15 : FIABRP CHANBF ABSCOR INTEG BASEADJ INTEG PAGE ;
16 ( STB# EDB# FIARPT )
17 : FIARPT 4 + SWAP 12 BASE ! DO I FIABRP 4 +LOOP CR ;

```

BLOCK 2025 1045

```

0 (          FLOWMETER CALCULATIONS )
1 0 0 V FM1OF , 0 0 V FM1SL , 0 0 V FM2OF , 0 0 V FM2SL ,
2
3 ( CALCULATE FLOW RATE FROM METER RESPONSE )
4 ( FMRESPONSE CFR1 FLOWRATE IN .01 ML/MIN )
5 : CFR1 FM1OF 20 F- FM1SL 20 F/ ;
6 : CFR2 FM2OF 20 F- FM2SL 20 F/ ;
7
10 ( CALCULATE FLOW GOAL VALUE )
11 ( FLOWRATE IN .01 ML/MIN CFG1 FLOWMETER RESPONSE )
12 : CFG1 FM1SL 20 F* FM1OF 20 F+ ;
13 : CFG2 FM2SL 20 F* FM2OF 20 F+ ; ;S
14
15
16
17

```

BLOCK 2026 1046

```

0 ( FIA ANALYSIS ROUTINES )
1 0 0 V BASUM , 0 V BASCOR 0 V ABUFF 40 DP+!
2 0 V BBUFF 40 DP+!
3
4 ( B# CHANBF - START AT B# AND MAKE 8 BUFFERS IN AXX )
5 : CHANBF TOPPAGE FIADIS AXX 10000 ERASE
6 140. 375 0 DO 2DUP
7 10 0 DO 2DUP I2 M+ VW0 AXX I 1000 * + J2 + ! LOOP 2DROP
10 40 M+ LOOP 2DROP CR CR ;
11
12 : BASEADJ 10 0 DO I 1000 * AXX + DUP 0. BASUM 2!
13 10 0 DO DUP I2 + @ DSEXT BASUM D+! LOOP DROP
14 BASUM 20 10 M/ MINUS BASCOR !
15 400 0 DO DUP I2 + DUP @ BASCOR @ + SWAP ! LOOP DROP
16 LOOP ;
17

```

BLOCK 2027 1047

```

0 ( FIA ROUTINES )
1
2 1650 LOAD ( INTEGER STATS ) DECM
3 ( # ADDR NORM )
4 : NORM DUP >R SWAP 2* 2* + 20 FLOAT R> 20 FLOAT
5 F/ 1000 0 FLOAT FIX 7 D.R ; OCTAL
6 : ISUM DUP DUP >R 4 .R SXI 20 2DUP 10 D.R R> 2* 2* DUP >R
7 ABUFF + 2! DUP ABUFF NORM SXMIN 20 12 D.R SXMAX 20
10 2DUP 10 D.R R> BBUFF + 2! BBUFF NORM CR ;
11
12 : INTEG CR CR ABUFF 10 0 DO I 1000 * AXX + SINIT
13 400 0 DO DUP I2 + @ DUP SACC LOOP DROP I ISUM LOOP CR ;
14
15 : CALCAB 2* ABCBF + @ 23420 */ ;
16 : ARSCOR 10 0 DO I 1000 * AXX +
17 DO DUP I2 + DUP @ J CALCAB SWAP ! LOOP DROP LOOP ;

```

BLOCK 2030 1048

```

0 ( FIA FLOATING STATS )
1
2 0 V FSTAB 140 DP+! ( FLOATING STATS ) 1651 LOAD
3
4 : FPSTAT STADD @ FSTAB STADD ! SINIT
5 10 0 DO I2 2* ABUFF + 20 FLOAT
6 2DUP SACC LOOP CR SCIPD SMEAN G. CR
7 SCIV G. CR SRELIV G. CR 2DROP 2DROP 2DROP STADD ! ;
10
11
12
13
14
15
16
17

```

BLOCK 2050 1064

```

0 ( MULTICOMPONENT KINETIC CALCULATIONS LOAD BLOCK )
1
2 2003 LOAD ( LOAD DSE PGMS )
3 1640 LOAD 1642 LOAD 1644 LOAD ( LOAD FLOATING STATISTICS )
4 2051 LOAD 2052 LOAD 2053 LOAD ( ARRAYS, LEAST SQU, BUFFERS )
5 1621 LOAD 1622 LOAD ( LEIGHTON LOG & EXP )
6 2055 LOAD 2056 LOAD ( KINETIC CALCS )
7 2057 LOAD ( UTILITY CALCS )
10 146 LOAD 63 LOAD 1660 LOAD ( LOAD HP DIGITAL PLOTTER )
11 1661 LOAD 1662 LOAD 1663 LOAD 1664 LOAD
12 1604 LOAD 1665 LOAD 1666 LOAD 1667 LOAD 1670 LOAD
13 2065 LOAD 2066 LOAD 2067 LOAD ( PLOTTING UTILITIES )
14 2070 LOAD 2071 LOAD ( CONC REPORT )
15
16
17

```

BLOCK 2051 1065

```

0 ( MULTICOMPONENT KINETIC CALCULATIONS ) DECM
1
2 0 V RUNID 64 DP+! 0 V ABST 20 DP+! 0 V ABSINF 20 DP+!
3 0 0 V FRATIO , 0 0 V CONZN , 0 0 V CONHG , 0 0 V CONZIN ,
4 0 0 V CONCYD , 0 0 V RATZN , 0 0 V RATHG , 0 0 V INTZN ,
5 0 0 V INTHG , 0 V STBUF 64 DP+! STBUF STADD !
6 25 V COLOFF 45 , 65 , 110 , 190 , 350 , 510 , 590 ,
7 0 V ABSDEF 16 DP+! 0 V ABSZN 32 DP+! 0 V ABSHG 32 DP+!
10 10. FLDAT 1/X 2DUP V ZNCF , V HGCF ,
11
12 : CTATC 2* COLOFF + @ >R ABST 20 + @ -1409 MK
13 3529000. D+ 80 M/ R> MK 5000. D+ 10000 M/ ;
14
15
16
17 OCTAL

```

BLOCK 2052 1066

```

0 ( FLOATING LEAST SQUARES FOR MULTICOMPONENT KINETICS )
1
2 0 V XBUFA 0 V YBUFA 0 V NYBUFA 0 V LSPTS
3
4 : LSFIT SINIT LSPTS @ 0 DO
5 XBUFA @ I2 2* + 2@ YBUFA @ I2 2* + 2@ SACC LOOP
6 SCIFD SCSIC SCCOEF 2! SINTER 2! SLOPE 2! ;
7
10
11
12 : CALCPT 2* 2* XBUFA @ + 2@ SLOPE 2@ F* SINTER 2@ FT+ ;
13
14 : CALCLINE LSPTS @ 0 DO I CALCPT I 2* 2* NYBUFA @ + 2! LOOP ;
15
16 : CLSL LSFIT CALCLINE ;
17

```

BLOCK 2053 1067

```

0 ( FLOATING & INTEGER BUFFER DISPLAY )
1
2 O V XBUF 60 DP+! O V YBUF 60 DP+! O V NYBUF 60 DP+!
3 XBUF XBUFA ! YBUF YBUFA ! NYBUF NYBUFA !
4 O V BFFTS 14 V BFLIM
5 : CBF BFFTS OSSET ;
6 : EBF CBF XBUFA @ BFLIM @ 2* ERASE YBUFA @ BFLIM
7 @ 2* ERASE NYBUFA @ BFLIM @ 2* ERASE ;
10 : IBFL CR BFFTS @ O DO I 4 .R I2 2* DUP DUP
11 XBUFA @ + 2@ 16 D.R YBUFA @ + 2@ 16 D.R NYBUFA @ +
12 2@ 16 D.R CR LOOP ;
13
14 : FBFL CR BFFTS @ O DO I 4 .R I2 2* DUP DUP
15 XBUFA @ + 2@ 4 1 16 EI.FR YBUFA @ + 2@ 4 1 16 EI.FR
16 NYBUFA @ + 2@ 4 1 16 EI.FR CR LOOP ;
17 SCR @ 1+ LOAD

```

BLOCK 2054 1068

```

0 ( FLOATING AND INTEGER BUFFER ENTRY )
1
2 ( BUFFER IS FULL ) O V BFULM 40 DP+!
3 : TBFULM SCR @ BLOCK 202 + BFULM 20 MOVE ; TBFULM
4 : TFULL BFFTS @ BFLIM @ < NOT IF BFULM 16 TYPE CR 0
5 ELSE 1 THEN ;
6
7 : FBFE TFULL IF BFFTS @ 2* 2* YBUFA @ + 2!
8 BFFTS @ 2* 2* XBUFA @ + 2! BFFTS 1+! THEN ;
10 : DBFE FBFE ;
12
13 : IBFE TFULL IF DSEXT >R >R DSEXT R> R> FBFE THEN ;
14
15 : IFBFE TFULL IF DSEXT FLOAT >R >R DSEXT FLOAT R> R>
16 FBFE THEN ;
17

```

BLOCK 2055 1069

```

0 ( MULTICOMPONENT KINETIC CALCULATIONS )
1
2 : SINVAR EBF 10 BFFTS ! ABST 20 + @ 0 FLOAT 2DUP
3 ABST 22 + @ 0 FLOAT F+ F/ FRATIO 2! 10 O DO I CSTATC 0
4 FLOAT 1750 0 FLOAT F/ I2 2* XBUFA @ + 2! LOOP ;
5
6 : CATS 10 O DO I2 ABST + @ I2 ABSINF + @ - DUP
7 I2 ABSdif + ! DSEXT FLOAT LN I2 2* YBUFA @ + 2! LOOP
8 ABSDIF 10 + @ 10 < NOT IF 4 LSPTS !
11 XBUF 20 + XBUFA ! YBUF 20 + YBUFA ! NYBUF 20 + NYBUFA !
12 LSFIT XBUF XBUFA ! YBUF YBUFA ! NYBUF NYBUFA !
13 ELSE 0. SLOPE 2! 0. SINTER 2! THEN 10 LSPTS !
14 CALCLINE SLOPE 2@ RATZN 2! SINTER 2@ INTZN 2! ;
15
16
17

```

BLOCK 2056 1070

```

0 ( MULTICOMPONENT KINETIC CALCULATIONS )
1
2 : CHGLINE 10 0 DO I2 ABSDIF + @ DSEXT FLOAT
3   I2 2* NYBUFA @ + 2@ 2DUP DO= NOT IF EXP THEN 2DUP
4   I2 2* ABSZN + 2! F- 2DUP I2 2* ABSHG + 2!      LN
5   I2 2* YBUFA @ + 2! LOOP
6   3 LSPTS ! CLSL SLOPE 2@ RATHG 2! SINTER 2@ INTHG 2! ;
7
10 : MKSUM CR CHARBF 200 + 60 TYPE CR
11   10 0 DO I 4 .R I CTATE 7 .R
12   I2 ABSDIF + @ 10 .R I2 2* ABSZN + 2@ FIX 10 D.R
13   I2 2* ABSHG + 2@ FIX 10 D.R CR LOOP
14   CR RATZN 2@ 4 1 16 EI.FR INTZN 2@ EXP 4 1 16 EI.FR CR
15   RATHG 2@ 4 1 16 EI.FR INTHG 2@ EXP 4 1 16 EI.FR CR
16   ;
17 : MKCALC SINVAR CATS CHGLINE BASE @ 12 BASE ! MKSUM BASE ! ;

```

BLOCK 2057 1071

```

0 ( MULTICOMPONENT ANALYSIS UTILITY DEF'S )
1
2 : TDRID RUNID 0. 100 MFVM 60. VD@ CONZN 2!
3   64. VD@ CONHG 2! 70. VD@ CONZIN 2! 74. VD@ CONCYD 2! ;
4
5 : TAITAB 13 0 DO I 100 * SBRFA @ + STADD !
6   SXI 2@ SCNTR @ 0 FLOAT F/ FIX DROP I2 ABST + ! LOOP ;
7 : TAFTAB 13 0 DO I 100 * SBRFA @ + STADD !
10  SXI 2@ SCNTR @ 0 FLOAT F/ FIX DROP I2 ABSINF + ! LOOP ;
11 : CAIFS STINIT 16. VD@ 0 40 DLINS ;
12
13 : MKANAL 12 BASE ! TOPPAGE CR DISPLAY SUMMARY
14   TDRID TAITAB CAIFS SUMMARY TAFTAB MKCALC ;
15
16
17

```

BLOCK 2060 1072

```

0 ( 8KW PROM LOAD BLOCK FOR SATELLITES )
1
2
3 102 SETL/P 117774 364 ! 60000 366 ! 57676 370 !
4   0 372 ! 24562 374 ! 364 376 !
5
6   DECM 1981 AD 0:00 EST 25 APR TODAY !
7   CR PSHDT .TIME .DATE CR OCTAL
10
11 : OPERCONT / CONTEXT 2 + @ OPER + @ CONTEXT ! ;
12 (
13 154 150 102 177554 177550 400 TASK RAY
14 RAY ACTVU )
15 UPIPO CR BH.FORTH..PROM.SATELLITE..V1..25.APR.81.BLOCK.2060
16
17

```

BLOCK 2065 1077

```

0 ( SPECIAL UTILITIES FOR PLOTTER OUTPUT )
1
2 : CVRTO 2@ 1750. FLOAT F* FIX <# *# *# *# 56 !HOLD *#
3      5 OVER - SPAC #> ; ;
4 : OTRTO CVRTO DTYPE ;
5 : CVFLD @ 0 <# *# *# 56 !HOLD *# *# *# 6 OVER - SPAC #> ;
6 : OTFLD CVFLD DTYPE ;
7 : CURAT 2@ 1750. FLOAT F* FIX DARS <# *# *# *#
10     56 !HOLD *# *# *# 6 OVER - SPAC #> ;
11 : OTRAT CURAT DTYPE ;
12 : CVCN 12. FLOAT F* FIX <# *# 56 !HOLD *# *# *#
13     6 OVER - SPAC #> ;
14 : OTCON CVCN DTYPE ;
15 : OTZCON INTZN 2@ EXP ZNCF 2@ F* CVCN DTYPE ;
16 : OTHCON INTHG 2@ EXP HGCF 2@ F* CVCN DTYPE ;
17

```

BLOCK 2066 1078

```

0 ( MULTICOMPONENT KINETIC DATA PLOTTING DEFINITIONS )
1
2 : 0 V PXBUF 312 DP+! 0 V PYBUF 312 DP+!
3
4 : PRAWD 10 NPTS ! NPTS @ 0 DO I2 2* XBUF + 2@
5     1750. FLOAT F* FIX DROP I2 PXBUF + !
6     I2 ABSdif + @ DSEXT FLOAT LN 1750. FLOAT F* FIX
7     DROP I2 PYBUF + ! LOOP PXBUF BXADD ! PYBUF BYADD !
10    60 4 OTASC -1 DPMODE ! 0 2260 3720 15530 XYFXS XYOTP
11    70 3 OTASC DPMODE OSET ;
12
13 : PZNLIN 145 NPTS ! NPTS @ 0 DO XRANG @ 144 / I * DUP
14     PXBUF I2 + ! 0 FLOAT 1750. FLOAT F/ RATZN 2@ F* INTZN
15     2@ F+ 1750. FLOAT F* FIX DROP PYBUF I2 + ! LOOP
16     PXBUF BXADD ! PYBUF BYADD ! 0 2260 3720 15530 XYFXS XYOTP ;
17

```

BLOCK 2067 1079

```

0 ( MULTICOMPONENT KINETIC DATA PLOTTING DEFINITIONS )
1
2
3 : PHGLIN 145 NPTS ! NPTS @ 0 DO XRANG @ 144 / I * DUP
4     PXBUF I2 + ! 0 FLOAT 1750. FLOAT F/ RATHG 2@ F* INTHG
5     2@ F+ 1750. FLOAT F* FIX DROP PYBUF I2 + ! LOOP
6     PXBUF BXADD ! PYBUF BYADD ! 0 2260 3720 15530 XYFXS XYOTP ;
7
10
11
12
13
14
15
16
17

```

BLOCK 2070 1080

```

0 ( MULTICOMPONENT CONCENTRATION REPORT )
1
2 : Calculated Cell Concs. M/1      Determined      Rate
3 Total Flow      Flow Ratio      Zn      Hs      Zircon
4 : CVDTA
5 : 0 V CRHD 300 DP+! 33676 33206 V 1E-6 ,
6 : LCRHEAD SCR @ BLOCK 202 + CRHD 140 MOVE ; LCRHEAD
7 : .EFO 4 1 16 EI.FR ;
10 : CRHDT CRHD + SWAP TYPE ;
11 :
12 :
13 :
14 :
15 :
16 :
17 : ~

```

BLOCK 2071 1081

```

0 ( MULTICOMPONENT CONCENTRATION REPORT )
1
2 : ECCON BASE @ 12 BASE ! CR 76 0 CRHDT CR CR 10 140 CRHDT
3 CONZN 2@ FRATIO 2@ F*.EFO 10 SPACES INTZN 2@ EXP
4 ZNCF 2@ F* 1E-6 2@ F*.EFO
5 6 SPACES RATZN CVRAT TYPE CR
6 10 150 CRHDT CONHG 2@ FRATIO 2@ F*.EFO 10 SPACES
7 INTHG 2@ EXP HGCF 2@ F* 1E-6 2@ F*.EFO
10 6 SPACES RATHG CVRAT TYPE CR
11 10 160 CRHDT CONZIN 2@ FRATIO 2@ F*.EFO CR
12 10 200 CRHDT CONCYD 2@ 1E0 FRATIO 2@ F* F*.EFO CR CR
13 14 100 CRHDT ABST 24 + CVFLD TYPE 14 116 CRHDT
14 FRATIO CVRTO TYPE CR BASE !
15 :
16 : MKANAL MKANAL CCCON ;
17 :

```

BLOCK 2072 1082

```

0 ( DSE CONC STORAGE DEFS )
1
2 : 0 0 V CONZN , 0 0 V CONHG , 0 0 V CONCY , 0 0 V CONZI ,
3
4 ( SCONS - STORE CONC DATA IN DSE BUFFER )
5 : SCONS CONZN 2@ 60 DSEAD @ + 2!
6 : CONHG 2@ 64 DSEAD @ + 2!
7 : CONZI 2@ 70 DSEAD @ + 2!
10 : CONCY 2@ 74 DSEAD @ + 2!
11 :
12 :
13 :
14 : DSEINIT DSEINIT SCONS ;
15 :
16 :
17 :

```

APPENDIX B

DOCUMENTATION DICTIONARY

: .EFD 2070 DSEC output floating number
 flt. .EFO Output floating value

VARBL ABCBF 2003 DSE abs correction values
 ABCBF addr Returns addr of the first location of
 an array containing scaled integers used to correct the
 absorbance values of the corresponding colorimeter channels.

VARBL ABSBUF 1567 CMETER absorbance value buffer
 ABSBUF addr Returns the addr of a buffer holding
 the absorbance values from the 8 colorimeter channels.
 The values are single precision integers representing
 10000 -10- times the base 10 log of I_0 / I .

: ABSCAL 1567 CMETER calc abs calib factors
 ABSCAL Calculate the 8 absorbance correction
 factors for ABSCB from values in ABSBUF and ABSMAX.
 ABSCB = ABSMAX / ABSBUF * 10,000

VARBL ABSCB 1567 CMETER absorbance correction b.
 ABSCB addr Returns the addr of a buffer holding
 single precision integers (scaled by a factor of
 10000 -10-) used as correction multipliers for each of
 the 8 colorimeter channels to account for differences
 in the sensitivity of each of the channels.

: ABSCOR 2027 FIA correct absorbances
 ABSCOR Calculate corrected absorbances for
 the values in the buffers of AXX via CALCALC.

VARBL ARSDIF 2051 DSEC absorbance diff buffer
 ARSDIF addr Returns the addr of a buffer for
 storage of the absorbance difference values.

VARBL ABSHIG 2051 DSEC Hg absorbance buffer
 ABSHIG addr Returns the addr of a buffer for
 storage of absorbance values due to Hg.

VARBL ABSINF 2051 DSEC inf time absorbances
 ABSINF addr Returns the addr of a buffer with
 infinite time absorbance values for colorimeters 0 - 7 in
 words 0 - 7.

VARBL ABSMAX 1567 CMETER abs value for correction
 ABSMAX addr Returns the addr of the floating
 point value representing the correct full scale absorption
 value for use in calculating ABSCB.

VARBL ABST 2051 DSEC absorbance value buffer
ABST addr Returns the addr of a buffer with
absorbance values for colorimeters 0 - 7 in words 0 - 7.
Words 8 - 10 contain flowmeter 1, 2 and balance flow
values in hundredths of a ml/min.

VARBL ABSZN 2051 DSEC Zn absorbance buffer
ABSZN addr Returns the addr of a buffer for
storage of absorbance values due to Zn.

VARBL ABUFF 2026 FIA buffer for area values
ABUFF addr Returns the addr of a buffer of
double precision integers representing the area under the
peak for the colorimeter channels.

:
ADALIAS 1565 CMETER dummy def for later use
ADALIAS A definition which does nothing. NULL
in ADALIAS's Parameter field is replaced with the
address of a definition to los data or perform some
other function if desired.

DOCUM ADC8 1565 CMETER A-I conversion task
ADC8 addr Returns the addr of the STATUS word
of the A-I converter task. This task supervises the
conversion of 8 channels of analog input to digital values
and the averaging of multiple conversions via ADCISR.
Because of the length of ADCISR (requires 500 to 1100 us)
interrupts must be enabled during its execution to allow
other tasks to execute without loss of data.
ADDR of the task table is used as a counter for the
number of conversions to accumulate before transferring the
average to VOFF because it is necessary to reset this counter
to its maximum value in less than 1 fixed period clock period
after the counter has gone to zero to maintain operation.
It is not possible to assure that this can be done in high
level Forth at a 100 Hz rate with the number of other tasks
and operations occurring in the system; particularly if a
CPU intensive operation is undertaken by another task.
STATUS must be used to signal the availability of another
averaged conversion result; thus, ADDR was used as the number
of conversions in a group counter instead of STATUS.
One now has 10 ms times the number of conversions in a group
to act on the "high level interrupt" caused by STATUS going
to zero.

ADC8 TASK TABLE ALLOCATIONS

Offset	Name	Function
0	STATUS	flag indicating averaged values ready
2	ADDR	counter for conversion in a group
52	RFT	value to set ADDR to when it has gone to 0
72	VSEL	nes of number of bits to shift right

100-116 VOFF buffer for 8 chan averaged values
 140-176 buffer for dbl prec accumulated values
 for 8 channels during acquisition

DOCUM ADCAL 1565 CMETER colorimeter calc. task
 ADCAL addr Returns the addr of the STATUS word
 of the ADCAL task which is activated when the high level
 Forth code for ADC8 is executed, ie., when ADC8 has a
 new 8 chan averaged data buffer. Calculations or data
 lossing can be done by ADCAL via ADALIAS.

CODE ADCISR 1564 CMETER A-D conv int. serv. rout
 ADCISR is entered on interrupts from the fixed
 period clock and is responsible for acquiring data from
 the 8 colorimeters via the multiplexed A-D converter and
 accumulating this data until the specified number of
 conversions are made. The accumulated data is then
 normalized and stored in VOFF through V+7 of the ADC8
 task table for use by other tasks.

In more detail, the first operation of ADCISR is to decrement the conversions left counter in ADIR of ADC8. The fixed period flag is cleared and a loop, which does 8 A-D conversions on sequential input channels, is started under flag check control. (Processor interrupts are enabled because of the time required by this routine) As each conversion is completed, the value is added to a double precision accumulation buffer for that channel which is maintained in locations 140 to 177 of the ADC8 task table. If ADDR is 0 after the conversions, the accumulated values are shifted right according to the number in VSEL (negative the desired number of bits to shift) and stored in VOFF to V+7 of the ADC8 task table for external use. The accumulation table is then cleared for the next group of conversions. RPT indicates the number of conversions in a group. STATUS is cleared to signal the completion of the current group of conversions. See ADC8 for more information.

CONST ADCIV 1564 CMETER A-D conv int. vector
 ADCIV addr Returns the addr of the vector for
 the A-D converter.

CONST ADCSR 1564 CMETER A-D converter CSR addr
 ADCSR addr Returns the addr of the analog to
 digital converter CSR used to acquire colorimeter data.

BAADR 1503 EBAL addr of 30 sec buffer
 BAADR addr Returns addr of the beginning of the
 30 second circular buffer for balance readings which is
 maintained in the dictionary area of the task, 400 bytes
 beyond the weight averaging buffer.

: BACTV 1504 EBAL activate balance task
 BACTV Start the execution of the balance task by initializing buffer lengths and pointers for the 6 and 30 second buffers. An endless loop is then started which converts the balance weight value to binary via BCONV and stores it in VSEL of the balance task table at every balance done interrupt. ERR is set to 1 to indicate conversion completed and the balance task is deactivated until another interrupt occurs.

: BAFLN 1503 EBAL averasins buffer length
 BAFLN addr Returns addr of PRMSEL in the balance task table which contains the length of the weight averasins buffer.

DOCUM BALANCE 1502 EBAL electronic balance task
 BALANCE addr Returns the addr of the STATUS word of the task for BALANCE which supervises the transfer of digits from the balance buffer interface through a parallel interface and maintains a number of variables reflecting the current balance reading.

Balance reading updates can occur at 0.5 to 2.5 second intervals, depending on the weight on the balance; thus, an average of the last 6 seconds is maintained to reduce noise. (The timing is controlled by a task with an accurate time base but buffers and variables are in the balance task)

BALANCE TASK TABLE ALLOCATIONS

Offset	Name	Function
50	#COL	average balance value of the last 6 secs
52	RPT	BDIF flow rate in .01 ml/min
54	R#	BFLNG length of wt averasins buffer
56	P#	BFPTR pointer to 30 sec buffer
60	OFFSET	BAPTR pointer to weight averasins buf
62	ERR	conversion done flag when 1
72	VSEL	current balance value
76	PRMSEL	BAFLN averasins buffer length
100	VOFF	BCD digit buffer - through 106 -

A 30 second long circular buffer is also maintained in the balance task area from which the flow rate as measured by the balance in 0.01 sms/min (.01 ml/min) can be calculated.

: BAPTR 1503 EBAL pointer to wt avs buf
 BAPTR addr Returns addr of OFFSET in the balance task table which contains the pointer into the 6 second weight averasins buffer for addition of the next value into the buffer.

VARBL BASCOR 2026 FIA baseline correction
 BASCOR addr Returns the addr of a variable
 containing a baseline correction calculated by BASEAUJ.

: BASUM 1504 EBAL calc 6 second average
 BASUM Accumulate the sum of all the entries
 in the 6 second average circular buffer, divide by the
 number of entries in the buffer and store in BAVALU,
 #COL of the balance task table to provide the average
 weight on the balance in the last 6 seconds.

VARBL BASUM 2026 FIA baseline sum
 BASUM addr Returns the addr of a double
 precision variable used when accumulating baseline sums.

: BASVAL 1503 EBAL store bal value in buff
 BASVAL Obtain the current balance weight value
 from VSEL of the balance task table (stored by RACTV) and
 place it in the proper location of the 6 second averaging
 buffer. Increment and reset the pointer into the buffer
 if necessary.

: BAVALU 1503 EBAL average balance value
 BAVALU addr Returns addr of #COL in the balance
 task table which contains the average value of the balance
 weight averaging buffer containing values of the last 6 secs.

: BAVGR 1504 EBAL combine BASVAL & BASUM
 BAVGR Perform the functions of BASVAL & BASUM

VARBL BBUFF 2026 FIA buffer for peak values
 BBUFF addr Returns the addr of a buffer of
 double precision integers representing the peak values
 found in each colorimeter channel.

: BCDIF 1503 EBAL calculate difference
 BCDIF Calculate the difference in weight
 between the value just entered in the 30 second buffer
 and the value of 30 seconds ago and store it in BDIF.
 RPT of the balance task table. A small correction is
 calculated and added to correct the flow rate because
 the flowmeter time base, which is used to cause entries
 into the 6 and 30 second buffers, is slightly less than
 250 ms, resulting in low values. The flow value is
 multiplied by 2, leaving the result in units of
 .01 gm/min or .01 ml/min in the case of water.

: BCONV 1504 EBAL convert digits to binary
 BCONV a Convert a strings of BCD digits stored
 in the balance task table to binary in the order
 specified by OTAB with the powers of 10 stored in PTAB,
 leaving the converted binary weight value on the stack.

CONST BCSR 1502 EBAL balance CSR addr
 BCSR addr Returns the address of the balance CSR.

: BCVAL 1503 EBAL current balance value
 BCVAL addr Returns addr of VSEL in the balance
 task table which contains the last balance readings.

: BDIF 1503 EBAL balance flow rate
 BDIF addr Returns addr of RPT in the balance
 task table which contains the flow rate in .01 ml/min.

: BFADR 1503 EBAL addr of weight avg buf
 BFADR addr Returns addr of PAD of the balance
 task where the weight averaging buffer starts.

VARBL BFLIM 2053 BUFED buffer length limit
 BFLIM addr Returns the addr of a memory location
 containing the maximum number of points allowed in the
 buffers.

: BFLNG 1503 EBAL length of wt avg buf
 BFLNG addr Returns addr of R# in the balance
 task table which contains the length of the weight averaging
 buffer.

: BFPTR 1503 EBAL pointer into 30 sec buf
 BFPTR addr Returns addr of P# in the balance
 task table which contains the pointer into the 30 second
 buffer for addition of the next weight into the buffer.

VARBL BFPTS 2053 BUFED points in buffer
 BFPTS addr Returns the addr of a memory location
 giving the current number of points in the X & Y buffers.

VARBL BFULM 2054 BUFED error message buffer
 BFULM addr Returns the addr of a buffer
 containing error messages.

CODE BISR 1502 EBAL balance i. serv. routine
 Services the balance interrupts which occur when the balance done line is activated when a new balance reading is available. (between .5 and 2.5 sec) The balance STATUS is cleared, the balance interface flag is cleared, and a number of digits from the balance buffer are read and stored as BCD digits in the balance task table starting at VOFF. The address in the buffer is selected and output just before reading the input port. Input digits are rotated 4 bits, masked, and set to 0 if not less than 10. -10-

CONST BIVEC 1502 EBAL balance i. vector addr
 BIVEC addr Returns the address of the balance interrupt service vector.

VARBL BLCVAL 1514 FMETER buffer for bal calb. val
 BLCVAL addr Returns addr of the beginning of a table containing double precision sums of the balance readiness over the FCMTIM time period at individual flow rates used in preparing the flowmeter calb. curve.

: BSVAL 1503 EBAL store in 30 sec buff
 BSVAL Store average value from 6 sec buffer in a 30 second circular buffer to allow calculation of the flow rate by BCDIF. After calculation of the difference the pointer into the buffer is incremented and reset if necessary.

: C1 1501 VALVE close valve 1 completely
 C1 Start an endless loop using CL1 to close valve #1. When the input bits indicate the valve is closed, exit the loop.

: C2 1501 VALVE close valve 2 completely
 C2 Start an endless loop using CL2 to close valve #2. When the input bits indicate the valve is closed, exit the loop.

VARBL CARB 1567 CMETER corrected abs buffer
 CARB addr Returns the addr of a buffer holding single precision integers (scaled by a factor of 10000 -10-) which represent the corrected absorbance of each of the 8 colorimeter channels.

: CARS 1570 CMETER calculate absorbances
 CARS Calculate the 8 absorbance values and store them in ARSBUF. IRBUF is subtracted from IOBUF and the results converted to base 10 loss.

:
 CAIFS . 2057 DSEC calc Ainf stats
 CAIFS Calc average infinite time absorbances
 for data in the blocks pointed to by YOFF. The word at byte
 16 has the addr of the beginning of the infinite time data.

:
 CALCAB . 2004 DSE calc corrected abs
 a chan# CALCAB b The raw absorbance value, a ,
 is multiplied by the correction factor for chan# and
 the corrected absorbance, b , is left on the stack.

:
 CALCAB . 2027 FIA calc calibrated absorb.
 value chan# CALCAB Calculate a corrected absorbance
 given the value to correct on the stack and the chan#
 which it is obtained from. ABCBF contains scaled correction
 factors for each colorimeter.

:
 CALCLINE . 2052 LSQU calculate line
 CALCLINE Calculate new Y points for a line
 consisting of the number of points in LSPTS. Floating X
 values are in the buffer pointed to by the addr in XBUFA.
 The slope and intercept of the lines are obtained from the
 statistics buffer. Calculated points are stored in a
 buffer pointed to by the addr in NYBUFA.

:
 CALCPT . 2052 LSQU calc a Y point
 pt# CALCPT value. Calculate a floating point value.
 for pt# in the buffer pointed to by the addr in XBUFA
 using values for the slope and intercept from the statistics
 table.

:
 CATS . 2055 DSEC calc abs at colorimeters
 CATS Calc absorbance differences for each
 colorimeter and store in ARSDIF. Store LN of difference
 in YBUF, do least squares on last 4 points & calc line.

:
 CBF . 2053 BUFED clear buffers
 CBF Set BFFTS to 0, effectively emptying
 the buffers.

:
 CCCON . 2071 DSEC calc all concentrations
 CCCON Calculate concentrations of reagents
 in the mixing cell from concentrations supplied in the
 run ID section and the dilution ratio.

:
 CFG1 . 1513 FMETER calc resp from flow rate
 flt.rate CFG1 flt.resp Calculate the flowmeter response

given a flow rate (in .01 ml/min) for flowmeter #1 according to the calibration curve determined by the short calibration procedure. All values are floating point numbers.

: CFG2 1513 FMETER calc resp from flow rate
flt.rate CFG2 flt.resp Calculate the flowmeter response given a flow rate (in .01 ml/min) for flowmeter #2 according to the calibration curve determined by the short calibration procedure. All values are floating point numbers.

VARBL CFLAG 1571 CMETER done flag for storage of

: CFR1 1513 FMETER calc flow rate from resp
flt.resp CFR1 flt.rate Calculate the flow rate in .01 ml/min from the response of flowmeter #1 according to the calibration curve determined by the short calb. procedure. All values are floating point numbers.

: CFR2 1513 FMETER calc flow rate from resp
flt.resp CFR2 flt.rate Calculate the flow rate in .01 ml/min from the response of flowmeter #2 according to the calibration curve determined by the short calb. procedure. All values are floating point numbers.

: CHANBF 2026 FIA setup buffs for FIA rpts
b# CHANBF Setup 8 buffers in AXX from FIA data stored on disk starting at b#. Buffer identification is printed and data transferred from disk to memory buffers.

VARBL CHARBF 2003 DSE storage buffer
CHARBF addr Returns addr of the first location of an array containing ascii strings for table headings.

: CHGLINE 2056 DSEC calc Hs line
CHGLINE Calculate the absorbance due to Zn from the LS fit and store in ABSZN. Subtract this from the ABSNDIF calc'd earlier and store in ABSHG for the absorbance due to Hs.

CODE CL1 1500 VALVE close valve 1
s CL1 Output 2 ls bits of s from the stack to the proper bits of the parallel output port to cause movement of valve #1. The output operation is skipped if bits of the parallel input port indicate the valve is completely closed. If s is 0, no movement

occurs, 1 produces a slight movement, 2 about 1/10th of a turn and 3 about 1/4th of a turn.

:

CL1E 1501 VALVE close valve 1
 a CL1E Transfer a to CL1 if VM1EN is 0,
 causing valve 1 to close slightly, otherwise drop a .

CODE CL2 1500 VALVE close valve 2
 a CL2 See description for CL2

CL2E 1501 VALVE close valve 2
 a CL2E Transfer a to CL2 if VM2EN is 0,
 causing valve 2 to close slightly, otherwise drop a .

CLSL 2052 LSQU calc least squares line
 CLSL Calculate a least squares line by doing
 the LSFIT and CALCLINE operations on the number of points
 indicated by LSPTS.

COLOFF 2051 ISEC colorimeter distances
 COLOFF addr Returns the addr of a buffer which
 contains the distance from the mixer to the colorimeter
 in millimeters.

VARBL CONCY 2072 ISE conc of CyDTA
 CONCY addr Returns the addr of a floating point
 memory location containing the concentration of CyDTA in
 the solution.

VARBL CONCYD 2051 ISEC CyDTA concentration
 CONCYD addr Returns the addr of a floating point
 buffer containing the CyDTA concentration.

VARBL CONHG 2072 ISE conc of Hg
 CONHG addr Returns the addr of a floating point
 memory location containing the concentration of Hg in the
 sample solution.

VARBL CONHG 2051 ISEC Hg concentration
 CONHG addr Returns the addr of a floating point
 buffer containing the Hg concentration.

VARBL CONZI 2072 ISE conc of Zincon
 CONZI addr Returns the addr of a floating point
 memory location containing the concentration of Zincon in
 the solution.

VARBL CONZIN 2051 DSEC Zircon concentration
 CONZIN addr Returns the addr of a floating point
 buffer contains the Zircon concentration.

VARBL CONZN 2072 DSE conc of Zn
 CONZN addr Returns the addr of a floating point
 memory location contains the concentration of Zn in the
 sample solution.

VARBL CONZN 2051 DSEC Zn concentration
 CONZN addr Returns the addr of a floating point
 buffer contains the Zn concentration.

: CPP 1571 CMETER output abs from st buff.
 CPP Output 8 signed values from the output
 storage buffer to the terminal.

VARBL CRHD 2070 DSEC buffer for report header
 CRHD addr Returns the addr of the buffer for
 the multicomponent report header.

: CRHDT 2070 DSEC output header fields
 count offset CRHDT Output count chars from CRHD
 starting offset bytes into the buffer.

: CTATC 2051 DSEC calc time at colorimeter
 chan# CTATC ms Calculate the time from mixing
 in milliseconds at colorimeter channel chan#. The
 flowrate in the calibration equation flow * -14.09 +
 $352.9 = \text{time}$ is obtained from word 10 $\times 10^{-4}$ of ARST.

: DABS 1570 CMETER display absorbances
 DABS Output the 8 absorbance values in ABSBUF

: DBFE 2054 BUFED double buffer entry
 xval, yval, DBFE Redefinition of FBFE for
 double precision integer input.

: DCABS 1570 CMETER display cor. absorbances
 DCABS Calculate the corrected absorbances by
 multiplying ABSBUF by ARSCB, storing the results in
 CABB and also outputting them.

: DISPLAY 2003 DSE display DSE run info.
 b# DISPLAY Calculate and output information from
 the DSE run starting at b#. The statistics tables are
 initialized; the number of data lines indicated by byte 14
 are processed and a summary is output.

: DLINS 2004 DSE display x lines
 vaddr. #1 DLINS Use DSELIN to operate on #1
 lines of 20 bytes starting at vaddr.

DOCUM DSE 2000 DSE Dilution Stability doc
 The purpose of the dilution stability experiment is to evaluate the flow sensing and controlling ability of the instrument. The variation in colorimeter output with time will indicate the stability of the flow controller and the overall noise expected of the system. For example, assume equal flow rates of non-absorbing and absorbing solutions. An absorbance of one half that of the pure absorbing solution should be observed. Accuracy and stability can be determined by how close the colorimeter output comes to half scale.

Operational Procedure

1. Run short calibration procedures on both flowmeters with the solutions they will be controlling. Record slopes and intercepts for later use. Maintain conditions exactly as they will be when using the instrument; don't allow the slightest movement of apparatus. (FMCAL)
2. Run the colorimeter calibration procedure with pure non-absorbing (GETIO) and absorbing (ABSCAL) solutions to determine the correction factors for each colorimeter.
3. Set the desired flow rates in both channels and wait for stabilization. (SFG1 , SFG2)
4. Start data storage via DSEINIT .
5. Store the data buffer on disk for subsequent calculations and plotting. (B# SDSEDATA)

DOCUM	DSE.ARRAY.FORMAT	2000 DSE	DSE array allocations
Byte	Contents	Byte	Contents
0-1	Run #	100-117	colorimeter corrections
2-5	Time	120-123	FM1 Slope floating
6-7	Date	124-127	FM1 Offset
10-11	FP Clock CSR	130-133	FM2 Slope
12-13	* readings avsd	134-137	FM2 Offset
14-15	* bytes in array	140 on	Data entries of 40 bytes
16-17	addr of 2nd section	0-17	8 colorimeter chans
20-57	ascii strings	20-21	FM1 value
60-63	conc of Zn	22-23	FM2 value
64-67	conc of Hs	24-25	Balance value
70-73	conc of Zinc		
74-77	conc of CyDTA		

VARBL DSEAD 2000 DSE DSE storage buf addr
 DSEAD addr Returns addr of the first location of
 an array used for storage of data from the DSE Procedure.

: DSEDIS 2003 DSE display DSE data
 b# DSEDIS Output the identification data from the
 DSE array and set up flowmeter and colorimeter calibration
 variables for later use.

: DSEINIT 2000 DSE init DSE data file
 Run# addr DSEINIT xxxx' Initialize a data array
 for a dilution stability experiment run. Run# is stored in
 the first word of the data array which starts at addr.
 xxxx is an ascii char string (see DSESTR) of up to 32 chars
 which will be stored 20 bytes into the array as identifying
 information. STPTR is set to the first data storage area,
 allowing data to be stored in the buffer until it is full.

: DSELIN 2004 DSE display line at vaddr
 vaddr. DSELIN Display, accumulate, or process
 the DSE data consisting of the 20 bytes following vaddr.
 on the stack. Corrections or calibrations are applied to
 the raw data which is then displayed, accumulated for the
 statistics, or stored in an output buffer for plotting,
 depending if block 2004, 2006, or 2007 is loaded.

: DSESTR 2000 DSE obtain input char string
 DSESTR Enter a character string to be stored
 in the DSE data buffer for identification purposes. The string
 is terminated by a ' and up to 40 -8- chars may be stored.

: EBF 2053 BUFED erase buffers
 EBF Set all locations in the buffers to 0.

VARBL F10K 1567 CMETER floatins const of 10,000

: FBFE 2054 BUFED floatins buffer entry
 fxval, fyval, FBFE Store the floatins point values
 on the stack in the X & Y buffers at the location determined
 by the current value of BFPTS. If the buffer is full,
 output an error message and do not store or drop the
 numbers from the stack.

: FBFL 2053 BUFED fit. pt. buffer list
 FBFL List the contents of the least squares
 buffers in floatins point format. BFPTS contains the
 number of points to be output. XBUFA, YBUFA and NYBUFA
 point to the buffers containing the values to be listed.

DOCUM FIA 2021 FIA Flow Injection doc.
 The purpose of the Flow Injection Analysis experiment is to evaluate and determine the characteristics of the instrument in flow injection mode. Absorbins sample pluss (KMnO4) are injected into a non-absorbins carrier stream whose flowrate is controlled by the flow controller. The response of the 8 detectors, flowmeters, and balance is recorded periodically (intervals of .08 to .64 seconds) and stored for later analysis. Information on dispersion of the sample plus, linearity of area response, and reproduciblity under flow injection conditions may be obtained.

Operational Procedure

1. Run the short calibration procedure on the flowmeter to be used with the solutions to be used.
2. Run the colorimeter calibration procedure with pure non-absorbins (GETIO) and absorbins (ABSCAL) solutions to determined the correction factors for each colorimeter.
3. Set the desired flow rate and wait for stabilization. Be sure the sample loop is filled and the sampling valve is in the proper position.
4. Start data storage via FIAINIT which also causes the sampling valve to insert the sample loop in the carrier stream.
5. When finished, store the data buffer on disk for later calculations and plotting. (B# SFIADATA)

DOCUM	FIA,ARRAY,FORMAT	2021 FIA	FIA array allocations
Byte	Contents	Byte	Contents
0- 1	Run #	100-117	colorimeter corrections
2- 5	Time	120-123	FM1 Slope floating
6- 7	Date	124-127	FM1 Offset
10-11	FP_Clock_CSR	130-133	FM2 Slope
12-13	# readings avsd	134-137	FM2 Offset
14-15	# bytes in array	140 on	Data entries of 20 bytes
16-17	spare	0-17	8 colorimeter channels
20-57	ascii strings	20-21	FM1 value
60-77	spare	22-23	FM2 value
		24-25	Balance value
		26-27	Parallel input port (LSB=1 -> valve is injecting)

: FIABRP 2024 FIA generate FIA report page
 b# FIABRP Output a FIA run report given the starting
 b# . Data is read in, absorbances corrected and areas
 integrated for each colorimeter. A second integration is
 done after correctins for baseline values.

: FIADIS 2024 FIA display FIA data
 b# FIADIS Output the identification data from the

FIA array and set up flowmeter and colorimeter calibration variables for later use.

: FIAINIT 2021 FIA init FIA data file
 Run# addr FIAINIT xxxx Initialize a data array for a flow injection analysis run. Run# is stored in the first word of the data array which starts at addr . xxxx is an ascii char string (see DSESTR) of up to 32 chars which will be stored 20 bytes into the array as identifying information. STPTR is set to the first data storage area, allowing data to be stored in the buffer until it is full. INJECT activates the solid state relay which causes the sampling value to move to the inject position.

: FIARPT 2024 FIA generate FIA reports
 startB# endB# FIARPT Generate reports via FIABRP for buffers starting at startB# and ending at endB#. Buffers are 10 -8- blocks long.

: FLCHG 1525 FMETER set chansins flow param.
 FLCHG Set the limit of differences from the average and the control value divisor to values optimum for chansins flow conditions.

: FLCON 1525 FMETER set constant flow param.
 FLCON Set the limit of differences from the average and the control value divisor to values optimum for constant flow conditions.

VARBL FLFTM 1515 FMETER temp flt storese loc.

DOCUM FM1 1510 FMETER flowmeter 1 task
 FM1 addr Returns the addr of the STATUS word of the FM1 task which supervises the operation of flowmeter #1. The task reads data from the counter via FMISR and is responsible for keeping an average flowmeter value and driving the flow controller valves in proper direction to maintain flow control.

FLOWMETER TASK TABLE ALLOCATIONS

Offset	Name	Function
14	IDA	addr of RTC CSR for flowmeter
16	OIA	0 if xx2 valve controller should be used 1 if xx1 valve controller should be used
50	#COL	last error value for calc of err derivs.
52	RPT	multiplier for derivative
54	R#	number read directly from RTC counter
56	P#	calculated control value for valve
62	ERR	set to 1 when flowmeter operations done
72	VSEL	sum of error & deriv values

100&102	V0FF	sum of last X values. X in V+4
110	V+4	width of averaging window in points
112	V+5	Pointer to next mem loc to store flowmeter values (abs. addr)
114	V+6	limit of differences from average to be stored in averaging buffer
116	V+7	flowmeter soal value
122	HOLD	counter for flowmeter control (valve movement done every 4th interrupt
132	STADD	<u>statistics</u> table address for calibration

CONST FM1CSR 1510 FMETER flowmeter 1 CSR addr
 FM1CSR addr Returns the addr of the CSR for FM1

CONST FM1G 1511 FMETER addr of FM1 soal
 FM1G addr Returns the addr of V+7 in the flowmeter #1 task table which contains the setpoint value.

CONST FM1IV 1510 FMETER flowmeter 1 vector addr
 FM1IV addr Returns the addr of the interrupt vector for FM1

: 1513 FMETER flowmeter 1 calb. offset
 FM1OF addr Returns the addr of a double precision floating point value sivins the offset of the flowmeter #1 calibration curve determined by the short calb. procedure.

: 1513 FMETER flowmeter 1 calb. slope
 FM1SL addr Returns the addr of a double precision floating point value sivins the slope of the flowmeter #1 calibration curve determined by the short calb. procedure.

DOCUM FM2 1510 FMETER flowmeter 2 task
 FM2 addr Returns the addr of the STATUS word of the FM2 task which supervises the operation of flowmeter #2. See FM1 for details.

CONST FM2CSR 1510 FMETER flowmeter 2 CSR addr
 FM2CSR addr Returns the addr fo the CSR for FM2

CONST FM2G 1511 FMETER addr of FM2 soal
 FM2G addr Returns the addr of V+7 in the flowmeter #2 task table which contains the setpoint value.

CONST FM2IV 1510 FMETER flowmeter 2 vector addr
 FM2IV addr Returns the addr of the interrupt
 vector for FM2

: FM2OF 1513 FMETER flowmeter 2 calb. offset
 FM2OF addr Returns the addr of a double precision
 floating point value giving the offset of the flowmeter #2
 calibration curve determined by the short calb. procedure.

: FM2SL 1513 FMETER flowmeter 2 calb. slope
 FM2SL addr Returns the addr of a double precision
 floating point value giving the slope of the flowmeter #2
 calibration curve determined by the short calb. procedure.

: FMALIAS 1511 FMETER dummy def for later use
 FMALIAS A definition which does nothing. NULL
 in FMALIAS's parameter field is replaced with the
 address of a definition to log data or perform some
 other function if desired.

VARBL FMC1V 1514 FMETER buffer for FM1 calb val.
 FMC1V addr Returns addr of the beginning of a
 table containing double precision sums of flowmeter #1
 readings over the FMCTIM time period at individual flow
 rates used in preparing the flowmeter calb. curve.

VARBL FMC2V 1514 FMETER buffer for FM2 calb val.
 FMC2V addr Returns addr of the beginning of a
 table containing double precision sums of flowmeter #2
 readings over the FMCTIM time period at individual flow
 rates used in preparing the flowmeter calb. curve.

: FMCAL 1516 FMETER initiate fm calb. seq.
 FMCAL Activate FMCTASK and start execution
 of the FMCSEQ after clearing the data accumulation
 buffers. After execution of FMCSEQ, an endless loop
 is entered to prevent possible problems with FMCTASK
 if extra FMCNEXTs are done and no soal values are avail.

: FMCDIN 1514 FMETER deinstall logging def
 FMCDIN Replace the address in the parameter
 field of FMALIAS with that of NULL, thus stopping
 any data logging activity by the calibration routines.

VARBL FMCGOAL 1514 FMETER fm soals for calb curve
 FMCGOAL addr Returns addr of the beginning of a
 table containing flow soal values for use in preparing

the flowmeter calb curve by the short calibration procedure.

- : FMCINST 1514 FMETER install losings routines
FMCINST Install FMCSUM in FMALIAS, starting the accumulation of data for preparation of calibration curves.
- : FMCNEXT 1516 FMETER do next step in cal seq.
FMCNEXT Cause the next step in the calibration sequence as defined by FMSEQ and FMCSTEP to be executed by clearing STATUS of FMCTASK.
- VARBL FMCPTR 1514 FMETER ptr to cal buffer
FMCPTR addr Returns addr of a variable which is a pointer into a buffer of accumulated flow values used to calculate the flowmeter calibration curve.
- : FMCRPT 1515 FMETER calculate calb curve
FMCRPT Calculate calibration curves for both flowmeters from the values accumulated in FMCSUM, leaving floating point slopes and offsets in FMxSL and FMxOF. The routine uses SACC of the statistics package to accumulate sums and sums of squares of the average values obtained from FMC1V and FMC2V with BLCVAL supplying the X values at the various flow rates employed by the short calibration procedure. A least squares linear regression calculation is done which yields the slope and offset values which are stored for later use.
- VARBL FMCSBF 1514 FMETER fm calb statistics buf
FMCSBF addr Returns addr of the beginning of a table containing various values used by the statistics routines which calculate the flowmeter calb curve.
- : FMSEQ 1516 FMETER - calb sequence
FMSEQ Supervises the stepping through the flow soal values in FMCGOAL and calculating the slopes and intercepts. Operates under the FMCTASK and uses FMCSTEP to do the individual steps.
- : FMCSTEP 1516 FMETER do next calb step
a FMCSTEP Execute the next step in the short calibration sequence by using a as an offset into FMCGOAL to obtain the next flow soal value which is stored in the flow soal position for both tasks. Execution is suspended until the flow rates stabilize as signaled by the operator clearing STATUS of FMCTASK. FMCINST then installs data accumulatins routines which

operate until FMCTIM is exceeded. Execution is again suspended until clearing of STATUS again indicates that it is time to proceed.

: FMCSUM 1514 FMETER accum calb. values
 FMCSUM If the task is FM1, accumulate flow sums in FMC1V, FMC2V, and BLCVAL for use in calculating the flowmeter calibration curves. If FSCTR is not less than FMCTIM, use FMCDIN to stop the accumulation.

DOCUM FMCTASK 1516 FMETER short calibration task
 FMCTASK addr Returns addr of the STATUS word of a task used to supervise the short flowmeter calibration procedure. When STATUS of this task is set to 0, the next flow value in FMCGOAL is passed to the flowmeters. Data accumulation is started the next time STATUS is set to 0 to allow flow rates to become stable. After data for all the flow rates is accumulated, FMCRPT is executed and the task inactivated until FMCAL restarts it.

VARBL FMCTIM 1514 FMETER number of readings for c
 FMCTIM addr Returns addr of a variable containing the number of readings to be taken at a specific flow rate when executing the short calibration procedure.

: FMDISA 1523 FMETER display FM & CM values
 FMDISA If ERR of FM1 is 1, indicating that calculations are completed, reset ERR and display the flowmeter and colorimeter parameters via FPSUM. FMDISA initiates an endless loop which tests ERR, displays, releases the processor, and then repeats.

CODE FMISR 1510 FMETER flowmeter i. serv. rout.
 ~ The flowmeter interrupt service routine clears the flowmeter flag, stores the value in the interface counter in R# of the flowmeter task table, resets the counter, and clears the flowmeter task STATUS in response to a flowmeter interrupt.

: FMOPR 1512 FMETER set up flowmeter task
 FMOPR Set up variables in the flowmeter task table and begin an endless loop consisting of FMUSS and VALVCONT. ERR is set to 1 when the operations are completed.

: FMSTO 1511 FMETER store in fm sys. buffer
 a FMSTO Store a in the flowmeter averages circular buffer in the location pointed to by V+5, increment V+5, resetting if necessary.

:
 FMSUM 1511 FMETER sum fmeter avgs. buffer
 FMSUM Sum the values (number in V+4) in the
 flowmeter averages circular buffer starting at PAD of
 the task. The double precision sum is stored in VOFF.

:
 FMVAL 1511 FMETER calc value to put in buf
 FMVAL a Calculate a value to be stored in the
 flowmeter averages circular buffer which does not
 differ from the average value of the buffer by more than
 the value in Vt6 of the task table from the raw data
 in R# obtained from the interface counter.

:
 FMVSS 1511 FMETER perform flowmeter calcs
 FMVSS Combines the operations of FMVAL,
 FMSTO, and FMSUM. If FM1 is executing this def,
 the balance buffer update operations are done. FMALIAS
 is done to allow data lossing, etc, if desired.

CONST FPCIV 1564 CMETER fixed period vector
 FPCIV Returns the addr of the fixed period
 clock vector.

CONST FPCSR 1564 CMETER fixed period clock CSR
 FPCSR addr Returns the addr of the fixed period
 clock CSR for use with colorimeter data acquisition.

:
 FPSUM 1523 FMETER display FM & CM values
 FPSUM Output flowmeter and colorimeter values
 for continuous operator monitoring of the operation
 of the system. The flowmeter line consists of the
 accumulated flow value in VOFF of FM1, the flow rate
 in .01 ml/min calculated by CFR1 from the average flow
 response, the accumulated flow value in VOFF of FM2,
 the flow rate in .01 ml/min calculated by CFR2 from
 the average flow response, and the flow rate in .01
 ml/min determined by the electronic balance. The
 current time in ms sec min hrs concludes the line.
 The second line consists of a memory dump of the
 last 8 absorbance values obtained from the colorimeters
 and stored in memory.

VARBL FRATIO 2051 DSEC flow ratio
 FRATIO addr Returns the addr of a double precision
 floating point variable containing the ratio of the flow
 in the sample channel to that in the reagent channel.
 FRATIO = FM1 / (FM1 + FM2)

VARBL FSCTR 1514 FMETER counter for cal routines
 FSCTR addr Returns addr of a variable which counts the number of flowmeter readings taken when accumulating flow values for preparing a calb. curve.

: GETI 1567 CMETER set I values
 GETI Calculate the BLOGs of the 8 colorimeter values in VOFF of the ADC8 task and store them in IBUF

: GETIO 1567 CMETER set IO values
 GETIO Calculate the BLOGs of the 8 colorimeter values in VOFF of the ADC8 task and store them in IOBUF.

: GF 1570 CMETER set I, calc and output
 GF Do the functions of GETI CARS DABS DCARS.

VARBL HGCF 2051 DSEC Hg correction factor
 HGCF addr Returns the addr of a floating point correction factor relating Hg response to actual concs.

VARBL IORUF 1567 CMETER IO value buffer
 IORUF addr Returns the addr of a buffer holding the BLOGs of the IO or blank values from the 8 colorimeter channels. Values are dbl prec scaled integers.

: IBFE 2054 BUFED inteser buffer entry
 x y IBFE Convert x & y to double prec. intesers and use FBFE to store them in the buffers.

: IBFL 2053 BUFED inteser buffer list
 IBFL List the contents of the least squares buffers in double precision format. BFPTS contains the number of points to be output. XBUFA, YBUFA and NYBUFA point to the buffers containing the values to be listed.

VARBL IRUF 1567 CMETER I value buffer
 IRUF addr Returns the addr of a buffer holding the BLOGs of the I or sample values from the 8 colorimeter channels. Values are dbl prec scaled integers.

: IFBFE 2054 BUFED int. to flt. buf. entry
 x y IFBFE Convert x & y to floating point values before using FBFE to store them in the buffers.

:
 INJECT 2023 FIA move valve to inject pos
 INJECT Activate solid state relay (set parallel CSRO)
 which causes the sampling valve to be moved to the inject
 position.

:
 INTEG 2027 FIA integrate channel data
 INTEG Integrate area under peaks whose profiles are
 stored in 8 buffers in AXX by CHANBF. Min & max values are
 also reported via ISUM.

VARBL INTHG 2051 DSEC Hg intercept
 INTHG addr Returns the addr of a floating point
 memory location containing the Hg initial concentration.

VARBL INTZN 2051 DSEC Zn intercept
 INTZN addr Returns the addr of a floating point
 memory location containing the Zn initial concentration.

:
 ISUM 2027 FIA output integration summ.
 chan# ISUM Output values accumulated by INTEG.
 Values are: channel number, area, normalized area, minimum
 value, peak value, normalized peak value.

:
 LCHBF 2003 DSE load CHARBF
 LCHBF Load strings from the block into CHARBF

:
 LCRHEAD 2070 DSEC load header buffer
 LCRHEAD Load header buffer from disk block

:
 LOADS 2023 FIA release valve from inj.
 LOADS Clear CSRO, deactivating the solid state relay
 holding the valve in INJECT position. Activating the
 opposite valve controller returns the sampling valve to
 load the sample loop position. (currently done manually)

:
 LSFIT 2052 LSQU do a least squares fit
 LSFIT Do a least squares fit on the number of
 points indicated by LSPTS in the floating X buffer pointed
 to by the addr in XBUFA and the Y values pointed to by the
 addr in YBUFA. The calculated slope, intercept, and
 correlation coefficients are left in the statistics table
 for later use.

VARBL LSPTS 2052 LSQU number of points of LS.
 LSPTS addr Returns the addr of a memory location
 containing the number of points to operate on during the
 least squares calculations.

: MKANAL 2057 DSEC do calcs & report
 b# MKANAL Do kinetic calculations and output
 a summary report on the data.in b# .

: MKCALC 2056 DSEC multicomps calculations
 MKCALC Do a series of calculations on the
 multicomponent kinetic data.

: MKSUM 2056 DSEC multicomps summary
 MKSUM Output a summary of the multicomponent
 kinetic calculations.

: NORM 2027 FIA calc normalized values
 chan# addr NORM Calculate the ratio of the value pointed
 to by chan# to the first double precision value in the
 buffer pointed to by addr and output it in parts per
 thousand. addr points to the first location in a buffer
 containing values for each channel of data.

VARBL NYBUF 2053 BUFED new Y buffer array
 NYBUF addr Returns the addr of a dbl. prec.
 floating point buffer of 12 -10- Points for use with the
 least squares routines.

VARBL NYBUFA 2052 LSQU new Y buffer address
 NYBUFA addr Returns the addr of a memory location
 containing the address of a dbl. prec. floating point
 buffer containing new Y values for a line.

: 01 1501 VALVE open valve 1 completely
 01 Start an endless loop using OP1 to open valve
 #1. When the input bits indicate the valve is opened,
 exit the loop.

: 02 1501 VALVE open valve 2 completely
 02 Start an endless loop using OP2 to open valve
 #2. When the input bits indicate the valve is opened,
 exit the loop.

CODE OP1 1500 VALVE open valve 1
 a OP1 Output 2 ls bits of a from the stack
 to the proper bits of the parallel output port to
 cause movement of valve #1. The output operation is
 skipped if bits of the parallel input port indicate the
 valve is completely open. If a is 0, no movement
 occurs. 1 produces a slight movement; 2 about 1/10th
 of a turn and 3 about 1/4th of a turn.

: OP1E 1501 VALVE open valve 1
 a OP1E Transfer a to OP1 if VM1EN is 0,
 causing valve 1 to open slightly, otherwise drop a .

CODE OP2 VALVE open valve 2
 a OP2 see description for OP1

: OP2E 1501 VALVE open valve 2
 a OP2E Transfer a to OP2 if VM2EN is 0,
 causing valve 2 to open slightly, otherwise drop a .

VARBL OTAB 1504 EBAL conversion order table
 OTAB addr Returns addr of a table containing
 offsets to use when accessing BCD digits stored in
 the balance task table for conversion to binary.

CONST PCSR 1500 VALVE Parallel csr for valve cont

CONST PICSR 2023 FIA Parallel input CSR addr

CONST PINP 2022 FIA Parallel input buf addr

: PLAT 1505 MESC Platinization pot. rout.
 PLAT Start an endless loop of about 8 seconds
 of a positive 2.5 volt potential followed by 8 seconds
 of a negative 2.5 volt potential developed via DAC0
 for use in platinization of electrodes.

VARBL PTAB 1504 EBAL Power of 10 table
 PTAB addr Returns addr of a table containing 5
 powers of ten for use in converting BCD digits to binary

VARBL RATHG 2051 DSEC Hs rate
 RATHG addr Returns the addr of a floating point
 memory location containing the Hs reaction rate.

VARBL RATZN 2051 DSEC Zn rate
 RATZN addr Returns the addr of a floating point
 memory location containing the Zn reaction rate.

VARBL RUNID 2051 DSEC Run ID buffer
 RUNID addr Returns the addr of a buffer with
 run information. See DSE.ARRAY.FORMAT

: SADDR 2000 DSE set section addresses
 lens start SADDR Set length of the first section of the
 DSE buffer and the start of the section section from lens
 and start on the stack. Values are in bytes from the
 beginning of the buffer and are stored in words starting
 14 & 16 bytes into the buffer for later use.

VARBL SBBF 2005 DSE statistics buffer
 SBBF addr Returns addr of the first location of
 an array containing 10 -8- statistics tables.

VARBL SBBFA 2005 DSE addr of SBBF
 SBBFA addr Returns addr of the address of the
 statistics table. Is used in SUMMARY in place of SBBF so
 that other tasks may use the table of the current task.

: SCONS 2072 DSE store conc. data.
 SCONS Store reasent concentrations in the
 DSE buffer for later use.

: DSSEDATA 2000 DSE store DSE data on disk
 b# DSSEDATA Store 4 blocks of data, starting at the
 address in DSEAD, on disk starting at block b#.

: SFG1 1513 FMETER set flow rate soal, FM1
 a SFG1 Set the flow rate soal value for FM1,
 using CFG1 to calculate the necessary value from the inteser,
 a , on the stack which is in 100ths of a ml/min.

: SFG2 1513 FMETER set flow rate soal, FM2
 a SFG2 Set the flow rate soal value for FM2,
 using CFG2 to calculate the necessary value from the inteser,
 a , on the stack which is in 100ths of a ml/min.

: SFIAIDATA 2021 FIA store FIA data on disk
 b# SFIAIDATA Store 10 -8- blocks of data, starting
 at the address in DSEAD, on disk starting at block b#.

: SINVAR 2055 DSEC ...setup initial variables
 SINVAR Assumes ABST & ABSINF are loaded. Calcs.
 FRATIO, calcs times for XBUF (< via CTATC)

: STABF 1571 CMETER if room, store abs value
 STABF If the storage pointer (STPTR) is not

- greater than the max, (STPMX) use STTABF to store the 8 channel data in the output buffer.
- : STABS 1571 CMETER control output of abs v.
 STABS Endless loop for execution by a terminal task to output absorbance values when CFLAG is a 1 via CPP.
- : STACAL 1565 CMETER start ADCAL task
 STACAL Activate the ADCAL task and start it executing the endless loop which does ADALIAS and waits for another activation.
- : STADC 1565 CMETER start A-D conv & ADC8
 STADC Activate the ADC8 task, set up STATUS, ADDR, RPT, and VSEL with the desired values. Enable the FF clock interrupts and set the rate to 100 Hz. Initiate an endless loop which is executed every time ADC8 is activated. The loop activates ADCAL, and resets ADC8 to wait for another group of conversions to be averaged.
- : STBAL 1524 FMETER start balance operations
 STBAL Enable the balance interrupts and activate the balance task.
- VARBL STRUF 2051 DSEC statistics buffer
 STRUF addr Returns the addr of a buffer used for storage of statistics and least squares values.
- : STFM1 1524 FMETER start FM1 operations
 a STFM1 Use a to set the flow goal value, enable FM1 interrupts and activate the FM1 task, executing the FMOPR definition.
- : STFM2 1524 FMETER start FM2 operations
 a STFM2 Use a to set the flow goal value, enable FM2 interrupts and activate the FM2 task, executing the FMOPR definition.
- : STINIT 1571 CMETER reset storage pointer
 STINIT Set the colorimeter data storage pointer to 0, causing the next points to be at the start of the buffer.
- : STINIT 2005 DSE initialize SBBF
 STINIT Clears all 10 -8- stat tables in SBBF.

STOPOP 1524 FMETER stop flowmeter operation
 STOPOP Stop flowmeter operations by clearing
 the interrupt enables of the balance, FM1, and FM2.

CONST STPMX 1571 CMETER max storage ptr value

VARBL STPTR 1571 CMETER pointer for storage ops.
 STPTR addr Returns the addr of a pointer giving
 the offset into the colorimeter data storage buffer.

STTABF 1571 CMETER store abs values
 STTABF Get I (sample) values, calculate
 absorbances and store the 8 channel data in the output
 buffer at the offset provided by STPTR. Set CFLAG
 to 1 to indicate new values stored.

STTABF 2001 DSE store DSE data
 STTABF Get I (sample) values, calculate
 absorbances and store the first 5 colorimeter channels in
 the output buffer, pointed to by DSEAD, at the offset
 provided by STPTR. The next two locations in the output
 buffer receive the averaged flowmeter 1 and 2 values with the
 last location receiving the flow rate from the balance.
 Finally, CFLAG is set to 1, indicating data has been stored.

STTABF 2022 FIA store FIA data
 STTABF Get I (sample) values, calculate
 absorbances and store the 8 colorimeter channels in the
 output buffer, pointed to by DSEAD, at the offset provided
 by STPTR. Flowmeter, balance, and parallel port values
 are also stored in the buffer.

SUMLIN 2005 DSE output line of summary
 a SUMLIN Outputs information from the statistics
 table pointed to by STADD as channel number a. The mean,
 min, max, and relative standard deviation are calculated and
 printed.

SUMMARY 2005 DSE output stat summary
 SUMMARY Output a summary of the information in
 the stat tables via SUMLIN after printing a header.

TAFTAB 2057 ISEC transfer Ainf to ABSINF
 TAFTAB Transfer data from the statistics table
 of the DSE summary program to ABSINF.

- : TAITAB 2057 DSEC transfer Ai to ABST
TAITAB Transfer data from the statistics table of the DSE summary program to ABST.
- : TBFULM 2054 BUFED load error msg buffer
TBFULM Transfer an error message from the source block to the BFULM buffer.
- : TDELAY 1505 MESC time delay routine
msec TDELAY Delay task execution for approximately msec milliseconds by comparing the initial time plus the delay requested to the current time maintained in TICKS in an endless loop. If the current time is greater than the initial plus delay, exit the loop. A 0 STOP is included in the loop to allow other tasks to execute.
- : TDRID 2057 DSEC transfer data to RUNID
TDRID Transfer data to RUNID buffer from DSE format data in the block pointed to by VOFF.
- : TFULL 2054 BUFED test for buffer full
TFULL flag If BFPTS is less than BFLIM, the flag left is 1 and entry of another point is allowed. If not, the message BUFFER IS FULL is printed but the numbers are not stored and are not dropped from the stack.
- : VALVCONT 1512 FMETER calc valve control value
VALVCONT If HOLD is greater than 3 do the valve control operations, otherwise skip them, resulting in reasonable control system stability. Calculate a control value by subtracting the flow goal from the average flow value, then calculate a change in this flow error before storing the error in #COL of the task table. Multiply this change in error by a factor in RPT and sum with the flow error. Finally divide the sum by 400 -8- and pass this value to VALVMOV to cause correcting action to be taken. This implements a PID control algorithm.
- : VALVMOV 1512 FMETER execute valve movement
a VALVMOV Drive the flow controlling valve, depending on the task in execution, open if a is positive or closed if negative. a is limited to a maximum value of 3 which is then passed to the proper definition for the desired movement.

VARBL VM1EN 1501 VALVE enable valve 1 movement
VM1EN addr Returns addr of a variable controlling
the movement of valve 1 via the CL1E and OP1E defs.
If 0, movement is enabled, otherwise no movement occurs.

VARBL VM2EN 1501 VALVE enable valve 2 movement
VM2EN addr Returns addr of a variable controlling
the movement of valve 2 via the CL2E and OP2E defs.
If 0, movement is enabled, otherwise no movement occurs.

VARBL XBUF 2053 BUFED X buffer array
XBUF addr Returns the addr of a dbl. prec.
floating point buffer of 12 -10- points for use with the
least squares routines.

VARBL XBUFA 2052 LSQU X buffer address
XBUFA addr Returns the addr of a memory location
containing the address of a dbl. prec. floating point
buffer containing the X values for a line.

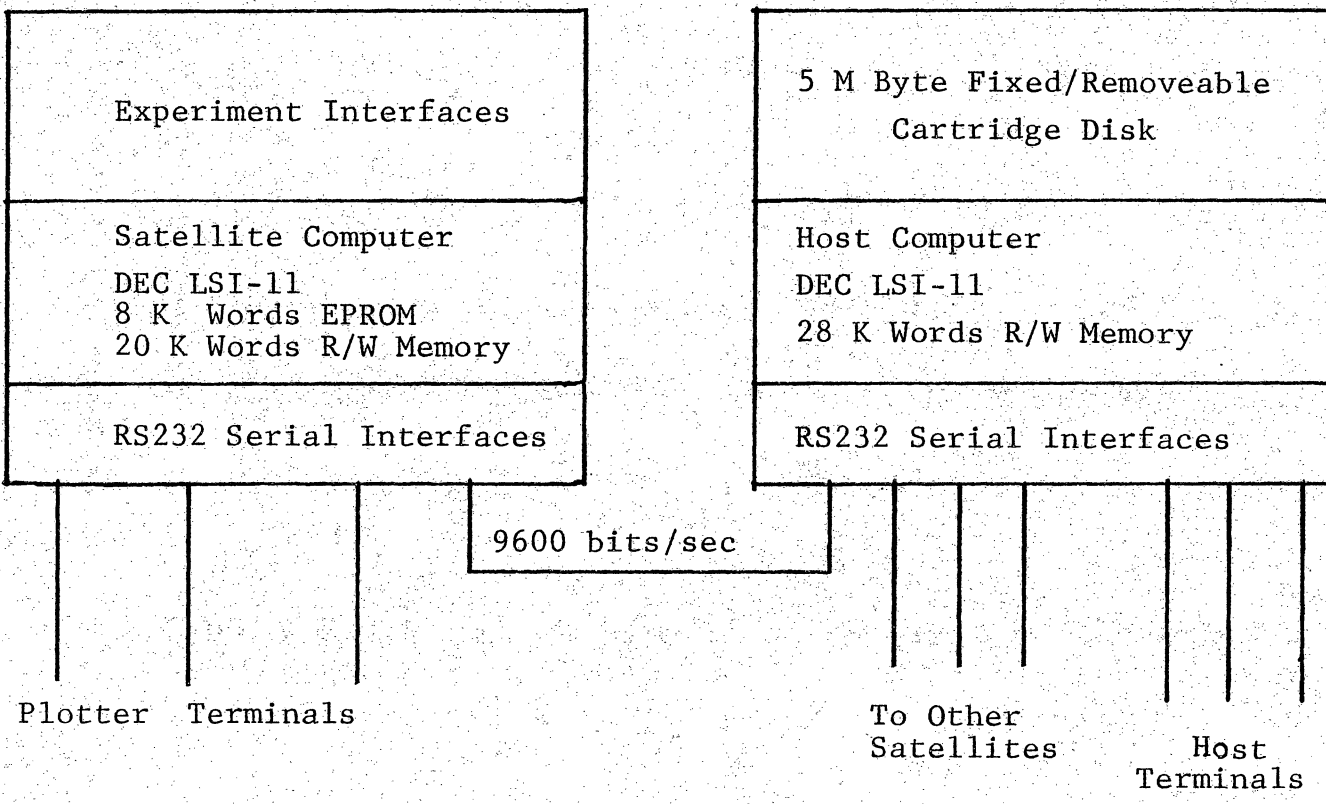
VARBL YBUF 2053 BUFED Y buffer array
YBUF addr Returns the addr of a dbl. prec.
floating point buffer of 12 -10- points for use with the
least squares routines.

VARBL YBUFA 2052 LSQU Y buffer address
YBUFA addr Returns the addr of a memory location
containing the address of a dbl. prec. floating point
buffer containing the Y values for a line.

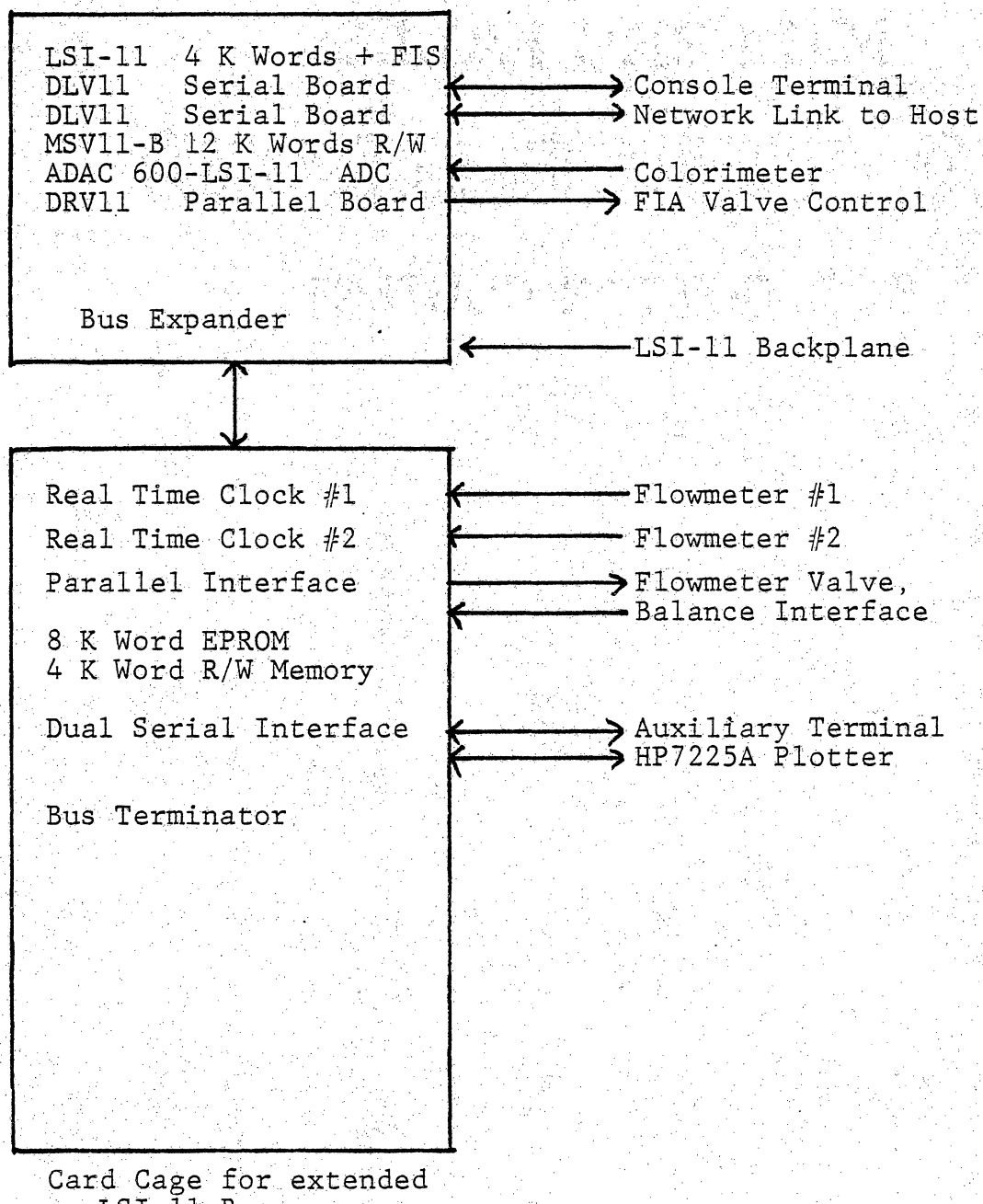
VARBL ZNCF 2051 DSEC Zn correction factor
ZNCF addr Returns the addr of a floating point
correction factor relating Zn response to actual concs.

APPENDIX C

HARDWARE BLOCK DIAGRAMS



Chemistry Computer Laboratory Network Configuration



177776

160000

120000

60000

40000

20000

0

Peripheral Device Addresses

Data Storage Buffers

Applications Programs

Auxiliary Terminal Task Table

Block Editor, Calendar

Extended Basic Forth

Basic Forth

DH Forth Kernel

7 - 1024 byte Disk Buffers

Operator Task Table

Vector Area

Satellite Memory Allocation

APPENDIX D

CALCULATION OF THE KMnO₄ - KI RATE CONSTANT AT 25 C

Rate information for the KMnO₄ - KI system is available at 35°C for a number of pH values in the literature (27). Temperature dependence of the rate is available at pHs of 5.5 and 3.4, but not at the pH of 6.1, which was employed in this study. The rate at this pH value is slow enough to allow observation by the instrument. In addition, rate data is available at a number of concentrations for this pH.

The current tests were conducted at a temperature of 25°C, requiring that the literature values at 35°C be corrected to allow comparison with values observed by the continuous flow instrument. Unfortunately, the temperature dependence of the second order rate constant is not available at a pH of 6.1, but is listed at a pH of 5.5. At a pH of 5.5, the rate at 25°C is about 90.5 percent of the rate at 35°C. It is unlikely that excessive error will be introduced by assuming this relationship holds at a pH of 6.1.

The experimentally observed second order rate constant consists of two terms, the second order rate constant calculated above, and a third order term dependent on H⁺ concentration. Temperature dependence of the third order term is available. At a pH of 6.1 and 35°C, the third order term contributes about 7.1 to the apparent rate constant of 59.3 listed for the same temperature and pH.

Subtraction of this contribution leaves a value of 52.2 for the second order rate constant. Adjusting for a temperature of 25 C results in a predicted value of 47.2. The third order contribution at 25 C can be calculated, resulting in a value of 5.6. An estimated apparent second order rate constant of 52.8 is then predicted. Assigning a similar relative error to the estimated rate constant, a value of 52.8 ± 1.6 is obtained.

**The vita has been removed from
the scanned document**

MULTICOMPONENT CONTINUOUS FLOW

KINETIC ANALYSIS

by

David J. Hooley

(Abstract)

An instrumentation system for Multicomponent Continuous Flow Kinetic Analysis has been designed and constructed. Evaluation of the system shows that it is useful for performing dilutions, flow injection analysis and continuous flow kinetics with relative standard deviations of less than 10 percent.

Modern electronic technology was used to construct a flow controller which was able to regulate the flow of a conductive liquid to ± 0.1 ml/min at flow rates of 2 to 10 ml/min. An inexpensive Light Emitting Diode colorimeter was able to detect KMnO₄ linearly at concentrations of 10 to 600 μ M, with better than 1 percent relative standard deviation at the higher concentrations.

Several concepts of hardware-software and software-operator interaction were introduced and developed. The multi-programmed Forth Programming System provided the instrument with much more capability and ease of use than might have been expected otherwise.

The reaction of KMnO₄ with KI was employed as a single component continuous flow test reaction. Rate constants were in good agreement with literature values obtained by stopped flow methods. The ligand exchange reaction between metal-Zincon complexes and CdDTA, using zinc and mercury, demonstrated the feasibility of the instrument for multicomponent continuous flow kinetic analysis. The implementation of suggested instrumental improvements should extend the range of useable reaction rates and improve the accuracy of the determinations.

The flowmeter and flow controller are potential alternatives to the relatively expensive pumps used for flow injection analysis. Evaluation of the instrument's operation in flow injection mode indicates that it is useful as a convenient continuous flow kinetic detector for flow injection analysis and for testing developments in flow injection theory.